THE
PHYSICAL REVIEW

A Journal of Experimental and Theoretical Physics Established by E. L. Nichols in 1893

VOL. 57, NO. 4 FEBRUARY 15, 1940 SECOND SERIES

Note on p-Wave Anomalies in Proton-Proton Scattering

G. BREIT, C. KITTEL AND H. M. THAXTON*
University of Wisconsin, Madison, Wisconsin

(Received December 12, 1939)

The p-wave effects on Bethe's neutral form of meson theory are calculated for proton energies of 2.0 Mev, 2.4 Mev and 3.0 Mev. The range of nuclear force corresponding to a meson mass of 180 electron masses gives effects of the order of a few percent of the total scattering. These effects do not vanish at the scattering angle of 45°. If present, they call for a slight increase in the range of force derived from s scattering. The comparison of the theoretical and experimental angular distributions indicates, however, that p-wave effects predicted by the above meson theory with a mass of 180 m are too large since they give too much small angle scattering.

IN the analysis of proton-proton scattering data[1-3] it has been assumed that the p-wave anomaly can be represented sufficiently well on the assumption of a central field. In the present note the noncentral forces characteristic of the meson theory are used and it is found that the effects on the angular distribution are not so clearly and unambiguously separable from the s-wave anomaly as on the hypothesis of central fields. In particular, at a scattering angle of 45° there is an effect of the p wave so that observations at this angle cannot be taken as a measure of the s-wave anomaly as before. Up to 2400 kev, however, the effects on the s-wave phase shift, which is derived from experiment, are small and do not affect the main conclusions arrived at on the central field theory.

The phase shifts for ${}^3P_0$, ${}^3P_1$, ${}^3P_2$ are in general different from each other, and the ${}^3P_2$ state interacts with ${}^3F_2$. The latter interaction will be neglected, being presumably of little importance at the lower energies. In the notation of BCP a plane wave modified by the Coulomb field has the asymptotic form

$$\psi^c=[1+\cdots]\exp[ikz+i\eta\ln k(r-z)]-\frac{\eta}{k(r-z)}\exp[ikr-i\eta\ln k(r-z)+2i\sigma_0]+\cdots$$

valid at large distances. The normalization is such as to give unit density for the incident wave. The second term in the above expression represents the scattered wave. For fields which are Coulom-

* Now at the Agricultural and Technical College of North Carolina.
[1] G. Breit, E. U. Condon and R. D. Present, Phys. Rev. **50**, 825 (1936). This is referred to as BCP.
[2] G. Breit, H. M. Thaxton and L. Eisenbud, Phys. Rev. **55**, 1018 (1939). Referred to as BTE. The notation in the present note is the same as in BTE and BCP.
[3] E. Creutz, Phys. Rev. **56**, 893 (1939).

bian at a large distance but are central and non-Coulombian at small distances one has for the scattered part

$$(\rho\psi^c)_{sc}=\sum(2L+1)P_L \sin K_L \exp[i\rho-i\eta \ln 2\rho+2i\sigma_L+iK_L]$$
$$-(\eta/2s^2)\exp[i\rho-i\eta \ln 2\rho-i\eta \ln s^2+2i\sigma_0].$$

Here the K_L are the usual phase shifts in a central field. The last formula can be generalized so as to apply to the collision of two particles with spin. Nonidentical particles will be considered first, and the wave function representing relative motion in the system of the center of mass will be dealt with. The wave function will then be antisymmetrized so as to apply to the collision of two protons. The collision may be considered as consisting statistically of a mixture of four relative spin orientations described by the four two-particle spin functions[4]

$$\check{S}_0,\ S_1,\ S_0,\ S_{-1}.$$

The first of these corresponds to a total spin $=0$, and is antisymmetric; the last three describe states with total spin 1, spin projections 1, 0, -1, and are symmetric. After the wave function is antisymmetrized the s anomaly contains only $\check{S}_0$ and the p anomaly contains only linear combinations of S_1, S_0, S_{-1}. The parts of the s anomaly containing S_1, S_0, S_{-1} will be omitted, therefore, and similarly the part of the p anomaly in $\check{S}_0$ will be dropped. Neglecting all but s- and p-wave phase shifts one obtains [for notation see reference 1],

$$(\rho\psi^c\check{S}_0)_{sc}=[e^{iK_0}\sin K_0-(\eta/2s^2)\exp[-i\eta \ln s^2]]\check{S}_0\exp[i\rho-i\eta \ln 2\rho+2i\sigma_0],$$

$$(\rho\psi^c S_1)_{sc}=\{(12\pi)^{\frac{1}{2}}[2^{-\frac{1}{2}}({}^3P_2)_1 e^{i\delta_2}\sin\delta_2+2^{-\frac{1}{2}}({}^3P_1)_1 e^{i\delta_1}\sin\delta_1]e^{2i(\sigma_1-\sigma_0)}$$
$$-(\eta/2s^2)\exp[-i\eta \ln s^2]S_1\}\exp[i\rho-i\eta \ln 2\rho+2i\sigma_0],$$

$$(\rho\psi^c S_0)_{sc}=\{(12\pi)^{\frac{1}{2}}[(\tfrac{2}{3})^{\frac{1}{2}}({}^3P_2)_0 e^{i\delta_2}\sin\delta_2-3^{-\frac{1}{2}}({}^3P_0)_0 e^{i\delta_0}\sin\delta_0]e^{2i(\sigma_1-\sigma_0)}$$
$$-(\eta/2s^2)\exp[-i\eta \ln s^2]S_0\}\exp[i\rho-i\eta \ln 2\rho+2i\sigma_0],$$

$$(\rho\psi^c S_{-1})_{sc}=\{(12\pi)^{\frac{1}{2}}[2^{-\frac{1}{2}}({}^3P_2)_{-1}e^{i\delta_2}\sin\delta_2-2^{-\frac{1}{2}}({}^3P_1)_{-1}e^{i\delta_1}\sin\delta_1]e^{2i(\sigma_1-\sigma_0)}$$
$$-(\eta/2s^2)\exp[-i\eta \ln s^2]S_{-1}\}\exp[i\rho-i\eta \ln 2\rho+2i\sigma_0].$$

The phase shifts of ${}^3P_0$, ${}^3P_1$, ${}^3P_2$ are here denoted by δ_0, δ_1, δ_2 and the phase shift of ${}^1S_0$ is written as K_0. The functions $({}^3P_j)_m$ are linear combinations of angular $Y_L{}^M$ and spin functions corresponding to angular momentum j and magnetic quantum number m. They are normalized to unity for integrations over angles and summation over spin coordinates. The signs of the linear combinations are such as to correspond to standard forms[5] of angular momentum matrices. The orbital function

$$Y_1{}^0=\left(\frac{3}{4\pi}\right)^{\frac{1}{2}}\cos\theta;\ ({}^3P_2)_2=Y_1{}^1S_1;\ ({}^3P_1)_1=2^{-\frac{1}{2}}(Y_1{}^0S_1-Y_1{}^1S_0);\ ({}^3P_0)_0=3^{-\frac{1}{2}}(Y_1{}^{-1}S_1-Y_1{}^0S_0+Y_1{}^1S_{-1}),$$

and the remaining functions are determined by the above conventions. To obtain the expressions $(\rho\psi^c\check{S}_0)_{sc}$, $(\rho\psi^c S_1)_{sc}$, etc. the waves $(\rho\psi^c\check{S}_0)$, $(\rho\psi^c S_1)$, etc., are first expressed as linear combinations of $\check{S}_0$, $({}^3P_j)_m$. The radial factors are then modified so as to correspond to the phase shifts K_0, δ_0, δ_1, δ_2; and so as to have the modified wave asymptotically of the form of incident+scattered wave. These conditions determine the wave function. The asymptotic form of the difference between the wave function and $(\rho\psi^c\check{S}_0)$, $(\rho\psi^c S_1)$, etc. is $(\rho\psi^c\check{S}_0)_{sc}$, $(\rho\psi^c S_1)_{sc}$, etc. Antisymmetrizing the wave function in

[4] The problem is similar to that in C. Kittel and G. Breit, Phys. Rev. **56**, 744 (1939). For proton-proton scattering the ${}^1P$ state drops out and there is interference with the Coulomb wave.

[5] E. U. Condon and G. H. Shortley, *Theory of Atomic Spectra* (Cambridge University Press, 1935).

the two protons and taking the mean of the scattered intensity of the four cases $\check{S}_0$, S_1, S_0, S_{-1} one obtains

$$\mathfrak{M}(\Delta\mathfrak{R})_1=\sum_i g_i\Big\{-\frac{18}{\eta}P_1\Big(\frac{\cos\alpha_1}{\mathbf{s}^2}-\frac{\cos\beta_1}{\mathbf{c}^2}\Big)\sin\delta_i\cos\delta_i+\Big[\frac{108}{\eta^2}P_1^2+\frac{18}{\eta}P_1\Big(\frac{\sin\alpha_1}{\mathbf{s}^2}-\frac{\sin\beta_1}{\mathbf{c}^2}\Big)\Big]\sin^2\delta_i\Big\}$$
$$+\frac{12}{\eta^2}\Big[-\frac{3}{4}(\sin\delta_1-\sin\delta_2)^2-\frac{1}{3}(\sin\delta_0-\sin\delta_2)^2-3\sin\delta_1\sin\delta_2\sin^2\frac{\delta_1-\delta_2}{2}$$
$$-\frac{4}{3}\sin\delta_0\sin\delta_2\sin^2\frac{\delta_0-\delta_2}{2}\Big](3\cos^2\theta-1). \quad (1)$$

Here $(\Delta\mathfrak{R})_1$ is the change in the ratio to Mott's scattering due to the phase shifts δ_0, δ_1, δ_2, while

$$\mathfrak{M}=\mathbf{s}^{-4}+\mathbf{c}^{-4}-\mathbf{s}^{-2}\mathbf{c}^{-2}\cos(\eta\ln\mathbf{s}^2\mathbf{c}^{-2}),$$

which is proportional to the scattering expected on Mott's theory. The statistical weights g_i are $g_0=1/9$, $g_1=1/3$, $g_2=5/9$. The sum containing the g_i in Eq. (1) represents the interference of the p-wave anomaly with the Coulomb wave together with a part in P_1^2 which is part of the direct scattering due to p waves. For $\delta_0=\delta_1=\delta_2$ this sum represents the whole effect, and is in agreement then with the formula for a central field. The part of $\mathfrak{M}(\Delta\mathfrak{R})_1$ with the angular dependence $3\cos^2\theta-1$ is absent on the central field theory and complicates the analysis of experimental data if it is appreciable.

Using the form of neutral meson theory proposed by Bethe,[6] the effects of $(\Delta\mathfrak{R})_1$ have been estimated. Numerical calculations made for the case of a "cut-off" in which the specific nuclear potential is zero inside the cut-off gave values of δ_0, δ_1, δ_2 as in Table I. The cut-off distance was such that the exponential factor at the cut-off radius had the value

$$e^{-0.32}$$

This corresponds to a cut-off radius of $0.32\,\hbar/\mu c=0.70\times10^{-13}$ cm with $\mu\sim180$ m. Substitution into Eq. (1) gives values of $(\Delta\mathfrak{R})_1$ as in Table II. Using values for $\mathfrak{R}$ computed for a square potential well with radius e^2/mc^2 and depth 10.5 Mev as an approximation to the experimental data one obtains values of 100 percent $(\Delta\mathfrak{R})_1/\mathfrak{R}$ as in Table III.

TABLE I. *Values of p-wave phase shift.*

E IN MEV	δ_0	δ_1	δ_2
2.0	−2.07°	1.21°	−0.61°
2.4	−2.66°	1.53°	−0.79°
3.0	−3.57°	2.10°	−1.06°

TABLE II. *Contribution to the ratio of scattering to Mott's value due to p scattering.*

E IN MEV	$\Theta=15°$	20°	25°	30°	35°	40°	45°
2.0	0.032	0.058	0.091	0.132	0.175	0.217	0.234
2.4	0.050	0.094	0.156	0.232	0.326	0.416	0.455
3.0	0.080	0.161	0.286	0.466	0.701	0.941	1.051

TABLE III. *Percentage change in scattering due to p-wave anomaly.*

E IN MEV	$\Theta=15°$	20°	25°	30°	35°	40°	45°
2.0	3.4%	3.1%	2.0%	1.4%	1.0%	0.81%	0.74%
2.4	4.6	3.8	2.5	1.8	1.3	1.13	1.06
3.0	6.0	4.6	3.3	2.5	2.1	1.82	1.74

TABLE IV. *Comparison of observed and computed scattering. Percentage of observed minus computed scattering.*

E IN MEV	$\Theta=$	15°	20°	25°	30°	35°	40°	45°
2.392	Pure s	4.2%	−0.5%	0.4%	0.4%	−0.4%	0.7%	−0.7%
	Meson p	0.5%	−2.9%	−1.0%	−0.1%	−0.3%	0.9%	−0.6%
2.105	Pure s	3.3%	1.7%	0.3%	−0.6%	2.0%	−2.3%	0.9%
	Meson p	0.2%	−0.3%	−0.5%	−0.9%	2.1%	−2.0%	0.9%
1.830	Pure s	2.3%	0.2%	0.6%	0.4%	−1.0%	−0.2%	0.9%
	Meson p	−0.2%	−1.7%	−0.2%	0.2%	−0.9%	0.2%	1.3%

The evaluation of the s-wave phase shift K_0 from experimental data made by BTE from the observations[7] of Herb, Kerst, Parkinson and Plain consisted in determining the mean K_0 from

[6] H. A. Bethe, Phys. Rev. **55**, 1261 (1939).

[7] R. G. Herb, D. W. Kerst, D. B. Parkinson and G. J. Plain, Phys. Rev. **55**, 998 (1939).

$\Theta=30°$, 35°, 40°, 45°. At 2.4 Mev the s-wave scattering is too high at these angles by the average amount of 1.3 percent. According to Table VI of BTE the value of K_0 is too high by $1.3\times0.26°=0.3(4)°$. According to Table XIX of BTE a decrease of K_0 at 2.6 Mev by 0.4° without changing K_0 at 0.8 Mev gives a decrease in the constant α of the potential $Ae^{-\alpha r^2}$ by 1.8 nuclear units. The above effects correspond, therefore, to a decrease of α from 21.6 to about 20. By itself this effect is not serious since the previously adopted value was $\alpha=16$. If, however, the observations or their interpretation contain another error of about the same amount and in the same direction the range of force arrived at by BTE would be definitely too small. The data of Herb, Kerst, Parkinson, and Plain will now be examined for the presence of the p wave. It will be seen that the calculated p anomaly is too large.

Assuming the above p-wave effects one obtains a change in the comparison of observed and expected angular distribution as in Table IV. In the table there is listed the difference between the observed and computed scattering expressed as a percentage of the observed scattering. The first line for each energy is taken from Table XI of BTE in which the details of the treatment of the data of Herb, Kerst, Parkinson and Plain are explained. The second line for each energy has been obtained by subtracting from the observed ratio to Mott's value the contribution to that ratio corresponding to Table II, attributing the result to s scattering, computing the average K_0 for $\Theta=30°$, 35°, 40°, 45° and then computing the expected ratio to Mott using this K_0. These p-wave corrections are more accurate for 2.39 Mev. For 2.10 Mev the corrections were interpolated, and for 1.83 Mev they were extrapolated graphically.

The apparent agreement between theory and experiment is improved at $\Theta=15°$ as a result of making the p-wave correction. For $\Theta=20°$, however, the p-wave correction spoils the agreement, giving too high values for the theoretically expected scattering. The apparent improvement for $\Theta=15°$ is probably accidental because the geometrical corrections have not been applied to the experimental values in the calculations for the above Table IV.[8] These corrections cannot be made with certainty on account of the uncertain structure of the incident proton beam. The probable value of the error introduced by imperfect geometry is $+2.(5)$ percent at $\Theta=15°$, while for $\Theta=20°$ the error is probably $\sim+0.2$ percent at 2.4 Mev and perhaps $+0.6$ percent at 1.83 Mev. Applying these corrections to the experimental values the numbers in the column $\Theta=15°$ for "Meson p" in Table IV become consistently negative. The application of the probable geometrical corrections gives therefore approximately the same amount of disagreement between theory and experiment at $\Theta=15°$ and $\Theta=20°$. The meson theory in the above form predicts in both cases ~2 percent more scattering than is observed.

The above interpretation is also indicated by the data at 860 kev and 1200 kev. For these energies the expected scattering at $\Theta=15°$ is insensitive to the s-wave phase shift K_0 while the effect of p-wave scattering is considerably smaller than at higher energies. The experimental values (without geometrical corrections) are too high by 4 percent as compared with s-wave calculations in both cases indicating, therefore, that the geometrical correction should be made at $\Theta=15°$. In more detail this situation is as follows. The phase shifts δ for 860 kev can be estimated from the approximate rule of proportionality to $E^{\frac{1}{2}}$. This estimate gives

$$\delta_0=-0.60°;\ \delta_1=+0.36°;\ \delta_2=-0.18°.\ (860\text{ kev}).$$

The contribution to $\mathfrak{R}$ due to these phase shifts is $\sim10^{-4}$ at $\Theta=45°$ and is negligible in a total of 4. The value of K_0 determined in Table XI of BTE may be left unchanged, therefore, at this energy. The effect of δ_0, δ_1, δ_2 at $\Theta=15°$ is to contribute ~0.005 to the theoretical $\mathfrak{R}$ so that the theoretically expected $\mathfrak{R}$ becomes $0.723+0.005=0.728$ which should be compared with the experimental 0.752. The theoretical value is thus 3 percent lower than the experimental.

Since the p-wave phase shift does not remove the discrepancy between theory and experiment for $\Theta=15°$ at 860 kev and 1200 kev it is necessary to assume that the geometrical corrections are real and it is therefore very probable that the above calculations with the meson potential give too much small angle scattering. The dependence of the s-wave phase shift on energy also does not

[8] These corrections are discussed on pp. 1036–41 of BTE.

agree with the meson potential corresponding to a meson mass of ~180 m. It indicates a smaller range and a larger meson mass of ~300 m. The p-wave phase shifts are roughly proportional to the cube of the range of force. Using the smaller range of force suggested by the s wave, the p-wave phase shifts are decreased by roughly a factor 4, and their effects become practically negligible. With such a view the interpretation of the experiments is self-consistent, but objections could be raised to the use of the large meson mass. It is also impossible to exclude by means of the experimental material p-wave effects of the order of $\frac{1}{3}$ of those dealt with in Table IV. The only definite conclusion is that the p-wave effects for $\mu\sim180$ m are too large and that the K_0, E curve is not affected by as large amounts as correspond to Table III.

Appendix

Approximate formulae and computational details

The potentials used have been derived by Bethe on the neutral meson type of theory. They are

$$V(^3P_0)=Ce^{-x}(2x^{-3}+2x^{-2}+x^{-1}),$$
$$V(^3P_1)=-Ce^{-x}(x^{-3}+x^{-2}),$$
$$V(^3P_2)=\tfrac{1}{5}Ce^{-x}(x^{-3}+x^{-2}+2x^{-1}),$$

with $C=14.5$ Mev, $x=r\mu c/\hbar$, $\mu=$meson mass. The potentials $V(^3P_0)$, $V(^3P_1)$ correspond exactly to using Bethe's form of the interaction energy while $V(^3P_2)$ is obtained as a mean over spin coordinates. Using Taylor's first-order approximation one obtains for the phase shifts

$$\delta_0=-(2CC_1^2/E)a^5[12\theta_0+40B_1a+180B_2a^2+1008B_3a^3+\cdots],$$

$$\delta_1=(2CC_1^2/E)a^5[3\theta_1+8B_1a+30B_2a^2+144B_3a^3+\cdots],$$

$$\delta_2=-(2CC_1^2-5E)a^5[15\theta_2+56B_1a+270B_2a^2+1584B_3a^3+\cdots].$$

Here

$$\theta_0=e^{-x_0}(1+x_0+5x_0^2/12+x_0^3/12)\leqq1,$$

$$\theta_1=e^{-x_0}(1+x_0+x_0^2/3)\leqq1,$$

$$\theta_2=e^{-x_0}(1+x_0+7x_0^2/15+2x_0^3/15)\leqq1,$$

$$a=\frac{\rho}{x}=(ME/2)^{\frac{1}{2}}/\mu c;\quad \rho=Mv/\hbar,$$

$E=$proton energy, $M=$proton mass, $v=$proton velocity,
$x_0=$value of x for the cut-off,
$F_1=C_1\rho^2\Phi_1=$regular Coulomb function.

The coefficients B_1, B_2, $\cdots$ are defined by

$$\Phi_1^2=1+B_1\rho+B_2\rho^2+\cdots.$$

In the above formulae the coefficients of B_1a, B_2a^2 come out to be products of e^{-x_0} and long polynomials in x_0. For the small x_0 used here these products can be replaced by unity. The contributions to $\int F_1^2\,Vdr$ due to the region inside the cut-off are small and are omitted in the above formulae. For order of magnitude estimates the terms in B_1a may be omitted.

The numerical work has been done by the method previously described.[4] Some of it was checked also by direct numerical integration of the differential equation. The sensitivity to the method of cut-off ("straight" or "zero") was tested by using integrations up to $r=4e^2/mc^2$ for $E=2.4$ Mev. The results checked to 0.01° for δ_0 and δ_2. For δ_1 the "straight" cut-off gave 1.40° and the "zero" cut-off gave 1.50°. An accuracy of 0.01° was not obtained until the integrations were extended to $r=5e^2/mc^2$. The values used correspond to the "zero" cut-off with $x_0=0.32$.

Financial assistance from the Wisconsin Alumni Research Foundation and the WPA project in natural sciences at the University of Wisconsin is gratefully acknowledged.

The Meson Theory of Nuclear Forces

I. General Theory*

H. A. BETHE
Cornell University, Ithaca, New York

(Received November 20, 1939)

In this paper, the meson theory of nuclear forces is presented in a simplified way. As in Yukawa's first paper, the forces between two nuclear particles are derived directly from the field equations and the Hamiltonian of the meson field (§2,3), without quantization of the field. The charge dependence of the forces is discussed (§4) and it is found that only two assumptions are in agreement with experimental facts, notably the equality of the forces between two like and two unlike nuclear particles in the singlet state. These assumptions are either (1) that nuclear particles interact only with neutral mesons (neutral theory) or (2) that they interact equally strongly with neutral, positive and negative mesons (symmetrical theory). It is then shown (§5) that the part of the force which does not depend on the spin of the nuclear particle does not fulfill any useful function in the theory. Accordingly, the hypothesis is made that this part is absent so that there is only a spin-dependent interaction (single force hypothesis). Finally (§6), it is pointed out that the interaction must be cut off at small distances in order to obtain finite eigenvalues for the deuteron. Such a cutting off is to be expected from the general theory, particularly because of the possibility of the simultaneous emission of two or more mesons. The cut-off is to be expected at a distance r_0 of about one-third the range of the nuclear forces.

§1. INTRODUCTION

YUKAWA[1] first pointed out that nuclear forces can be explained by assuming that particles of mass about 200 times the electron mass (mesons) exist and can be emitted and absorbed by nuclear particles (neutrons and protons). With such an assumption a force between nuclear particles of the right range ($\sim 2\times 10^{-13}$ cm) and the right shape (rapid decrease at large distances) was obtained. If the mesons were assumed to be charged (positive or negative) the resulting force between nuclear particles turned out to be of the "exchange" type which had been found successful in the interpretation of empirical facts in nuclear physics. The mesons must obey Bose statistics because they are emitted in the transformation of a neutron into a proton (or vice versa) both of which obey Fermi statistics; their spin could be either zero or one to be reconcilable with their emission in the neutron-proton transformation; zero was chosen by Yukawa for simplicity.

It was suggested by Yukawa that the mesons are intermediate stages in the β-decay. A positive β-decay, e.g., would follow the scheme:

Proton → Neutron + Positive Meson (virtual state) → Neutron + Positive Electron + Neutrino.

In the intermediate state energy is not conserved, in agreement with other dispersion processes. Because of the comparatively high mass of the meson the shape of the β-spectrum is practically the same as in the Fermi theory.

Theories similar to Yukawa's were suggested almost simultaneously by Wentzel[2] and by Stückelberg.[3]

A new impulse was given to these theories by the discovery in cosmic radiation of a particle of mass intermediate between electron and proton. Evidence was obtained by Anderson and Neddermeyer[4] for the occurrence of two kinds of particles in cosmic rays characterized by different losses of energy, *viz.* (1) the shower particles which behaved in every respect as required by theory for electrons, and (2) the particles occurring singly which apparently lost energy only by ionization. These particles of the second type could therefore certainly not be electrons. Anderson and Neddermeyer also showed that

* A second part, on the theory of the deuteron, is in course of publication in *The Physical Review*. Section numbers from §7 on, equation numbers from (36) on, and references from 35 on refer to that second part.

[1] H. Yukawa, Proc. Phys. Math. Soc. Japan **17**, 48 (1935); H. Yukawa and S. Sakata, *ibid.* **19**, 1084 (1938).

[2] G. Wentzel, Zeits. f. Physik **104**, 34 (1936); **105**, 738 (1937).

[3] E. C. G. Stückelberg, Phys. Rev. **52**, 41 (1937); Nature **137**, 1032 (1936).

[4] S. H. Neddermeyer and C. D. Anderson, Phys. Rev. **51**, 884 (1937).

the particles could not be protons because their ionization was too small. This conclusion was confirmed by Street and Stevenson[5] who showed that single cosmic-ray particles of fairly low momentum ($H\rho \sim 10^6$) could penetrate large thicknesses of lead which could not possibly be penetrated by protons of the given momentum (nor by electrons).

Since its discovery, the medium heavy particle has been observed directly in the cloud chamber by several authors and its mass μ has been determined from the curvature and the ionization produced,[6] from curvature and energy loss in solid plates,[7] or from curvature and range.[8] The most reliable measurements give

$$\mu = 150 - 220 \text{ electron masses.} \qquad (1)$$

It was natural to identify these cosmic-ray particles with the particles in Yukawa's theory of nuclear forces. Yukawa's theory was therefore more closely investigated by several authors. It was found that the theory in its original form (charged mesons of zero spin) gave the wrong sign for the interaction in the deuteron, i.e., repulsion instead of attraction in the ^3S state.[9] This could be remedied by assuming spin "one" corresponding to a vector wave function of the meson. This vector theory was developed simultaneously by Yukawa, Sakata *et al.*,[10] by Heitler, Froehlich and Kemmer[11,12] and by Bhabha.[13]

With a vector wave function for the mesons two distinct forces between two nuclear particles are obtained of which one (U) does not and one (V) does depend on the relative spin directions of the two interacting nuclear particles. If the interaction is due only to charged mesons the forces are of the exchange type. The first force (U) is simply a Heisenberg force and is attractive in the ^3S (ground) state of the deuteron, repulsive in the ^1S state. The second force, V, differs from the first by a factor $\boldsymbol{\sigma}_1 \cdot \boldsymbol{\sigma}_2$ where $\boldsymbol{\sigma}_1$ and $\boldsymbol{\sigma}_2$ are the spin operators of the two interacting nuclear particles; it is attractive in both the ^1S and ^3S state of the deuteron (like a Majorana force) and three times as strong in ^1S as in ^3S. By choosing a suitable linear combination we can obtain the empirical positions of the ^1S and ^3S state on this theory.

Any theory involving charged mesons only, will give no force between like nuclear particles (two protons or two neutrons) in first approximation (i.e., with emission and absorption of one meson). In the second approximation there will be a strong repulsion at very small distances.[11] This is in contradiction with experiments on proton-proton scattering[14] which show[15] that the force between two protons is strongly attractive and very nearly equal to that between neutron and proton in the singlet state. A force between two like particles in the first approximation can only be obtained with neutral mesons. While such particles have not yet been observed in cosmic rays it seems not unreasonable to assume their existence from reasons of symmetry. Kemmer[16] has developed a theory of nuclear forces in which neutral and charged mesons occur in a symmetrical way and which explains in a natural way the equality of the forces between like and unlike nuclear particles. An alternative way of explaining this equality is to assume interaction with neutral mesons only; then the charge of the nuclear particle (i.e., whether it is a neutron or a proton) becomes entirely irrelevant and the equality of forces follows immediately. This alternative will be discussed in the present paper.

In the papers quoted the method of second

[5] J. C. Street and E. C. Stevenson, Phys. Rev. **51**, 1005 (1937).
[6] J. C. Street and E. C. Stevenson, Phys. Rev. **51**, 1005 (1937); E. J. Williams and E. Pickup, Nature **141**, 634 (1938); P. Ehrenfest, Comptes rendus **206**, 428 (1938); D. R. Corson and R. B. Brode, Phys. Rev. **53**, 773 (1938).
[7] S. H. Neddermeyer and C. D. Anderson, Rev. Mod. Phys. **11**, 191 (1939); J. G. Wilson, quoted by P. M. S. Blackett and B. Rossi, Rev. Mod. Phys. **11**, 278 (1939).
[8] A. J. Ruhlig and H. R. Crane, Phys. Rev. **53**, 266 (1938); H. Maier-Leibnitz, Zeits. f. Physik **112**, 569 (1938); Y. Nishina, M. Takeuchi and T. Ichimiya, Phys. Rev. **55**, 585 (1939).
[9] W. E. Lamb and L. I. Schiff, Phys. Rev. **53**, 651 (1938).
[10] H. Yukawa, S. Sakata and M. Taketani, Proc. Phys. Math. Soc. Japan **20**, 319 (1938); H. Yukawa, S. Sakata, M. Kobayasi and M. Taketani, *ibid.* **20**, 720 (1938).
[11] H. Froehlich, W. Heitler and N. Kemmer, Proc. Roy. Soc. **166**, 154 (1938).
[12] N. Kemmer, Proc. Roy. Soc. **166**, 127 (1938).
[13] H. J. Bhabha, Nature **141**, 117 (1938); Proc. Roy. Soc. **166**, 501 (1938).
[14] M. A. Tuve, N. P. Heydenburg and L. R. Hafstad, Phys. Rev. **50**, 806 (1936); **51**, 1023 (1937); **53**, 239 (1938); **55**, 603 (1939). R. G. Herb, D. W. Kerst, D. B. Parkinson and G. J. Plain, *ibid.* **55**, 998 (1939).
[15] G. Breit, E. U. Condon and R. D. Present, Phys. Rev. **50**, 825 (1936); G. Breit, H. M. Thaxton and L. Eisenbud, Phys. Rev. **55**, 1018 (1939); G. Breit, L. E. Hoisington, S. S. Share and H. M. Thaxton, Phys. Rev. **55**, 1103 (1939).
[16] N. Kemmer, Proc. Camb. Phil. Soc. **34**, 354 (1938).

quantization was used to derive the force between nuclear particles. Stückelberg[17] and especially Møller and Rosenfeld[18] have shown that this is not necessary and that the interaction in the first approximation can be obtained from a purely classical treatment of the meson field by use of contact transformations. We shall here follow the same procedure without actually putting the contact transformation in evidence: This will lead to a derivation which is even simpler but not as rigorous and far-reaching as that of Møller and Rosenfeld. A similar derivation was given by Yukawa[1] in his first and fourth paper.

Considerable discussion has been devoted to the question of naming the new particle. Heavy quantum,[1] heavy electron,[11] barytron,[19] or baryteron,[20] mesotron[21] and meson[22] have been used in the literature, besides the name yukon (after Yukawa) used in conversation. It seems to us that the only name definitely to be avoided is "heavy electron." If there is any truth in the current theories then the new particle differs from an electron as much as any particle can: It has a different mass, a different spin and different statistics. Even a proton could be more rightfully called "heavy electron" because it has at least the same spin and statistics. If we have to assume a neutral modification of the meson as well as charged ones it becomes even more awkward to use the name "heavy electron" for the charged modification: It would mean that very similar particles are called by different names (heavy electron and "neutretto") and very different particles by similar names (electron and heavy electron; neutrino, neutretto and neutron). The use of the name "heavy electron" is even dangerous because it leads easily to misconceptions.[23] As long as this name is avoided it is not important which name is actually chosen. However, it seems more characteristic for the particle that it has "medium weight" than that it is "heavier" than an electron. Linguistic reasons[22] then decide in favor of meson over mesotron.

§2. General Theory

In this section we shall derive the general expression for the interaction between nuclear particles. By "nuclear particle" we shall generally understand a neutron or a proton; a short common name for these two modifications of the nuclear particle would be highly desirable. Our results will in no way go beyond those previously obtained;[1, 11–13, 16–18] in the derivation we shall only attempt simplicity rather than rigor and completeness. The nuclear particle will be treated nonrelativisitically;[24] the meson must, of course, be treated relativisitically. The meson field is not quantized; therefore the interaction between nuclear particles is only obtained to the order g^2 (for the significance of g see below) while terms of order g^4, etc. are neglected. To show the analogy with the electromagnetic field, all quantities describing the meson field are denoted by the same letters as the corresponding electromagnetic quantities, *viz.* φ, $\mathbf{A}$, $\mathbf{E}$, $\mathbf{H}$. This will not give rise to confusion because we do not consider actual electromagnetic fields in this paper. In this section we shall only consider *neutral* mesons; theories involving charged mesons will be discussed in §4.

The meson field will be described by a four-vector potential φ, $\mathbf{A}$ which satisfies the usual condition

$$\operatorname{div}\mathbf{A}+\partial\varphi/c\partial t=0 \tag{2}$$

and by a six-vector (antisymmetric tensor) $\mathbf{E}$, $\mathbf{H}$. *In the absence of nuclear particles* $\mathbf{E}$ and $\mathbf{H}$ can be derived directly from the potentials:

$$\mathbf{E}=-\operatorname{grad}\varphi-\partial\mathbf{A}/c\partial t, \tag{3a}$$

$$\mathbf{H}=\operatorname{curl}\mathbf{A}. \tag{3b}$$

Likewise in the absence of nuclear particles, the "field intensities" $\mathbf{E}$ and $\mathbf{H}$ satisfy the relations

$$\operatorname{div}\mathbf{E}+\kappa^2\varphi=0, \tag{4a}$$

$$\operatorname{curl}\mathbf{H}-\partial\mathbf{E}/c\partial t+\kappa^2\mathbf{A}=0, \tag{4b}$$

where κ is a constant of the dimensions of a reciprocal length. (4a,b) correspond to one set of Maxwell equations modified by the κ^2 term. The other set follows from (3a,b), *viz.*:

$$\operatorname{div}\mathbf{H}=0, \tag{5a}$$

$$\operatorname{curl}\mathbf{E}+\partial\mathbf{H}/c\partial t=0. \tag{5b}$$

[17] E. C. G. Stückelberg, Phys. Rev. **54**, 889 (1938).
[18] C. Møller and L. Rosenfeld, to be published in Kgl. Dansk. Vidensk. Proc.
[19] L. W. Nordheim and G. Nordheim, Phys. Rev. **54**, 254 (1938).
[20] F. J. Belinfante, Nature **143**, 201 (1939).
[21] C. D. Anderson and S. H. Neddermeyer, Nature **142**, 878 (1938); R. A. Millikan, Phys. Rev. **55**, 105 (1939).
[22] H. J. Bhabha, Nature **143**, 276 (1939).
[23] G. E. M. Jauncey, Phys. Rev. **52**, 1261 (1937); **53**, 106, 197, 265, 669 (1938); S. H. Neddermeyer, Phys. Rev. **53**, 102 (1938).
[24] A short report of a relativistic treatment was given by E. Feenberg, Phys. Rev. **55**, 602 (1939).

If we consider the meson as a particle, the ten quantities φ, **A**, **E**, **H** are the components of its wave function and correspond to the four components of the Dirac wave function of the electron. **E** and **H** may be eliminated from (4), using (3) and (2); then we obtain

$$\nabla^2\varphi-\partial^2\varphi/c^2\partial t^2-\kappa^2\varphi=0, \tag{6a}$$

$$\nabla^2\mathbf{A}-\partial^2\mathbf{A}/c^2\partial t^2-\kappa^2\mathbf{A}=0, \tag{6b}$$

which are the Klein-Gordon equations of a free particle of mass

$$\mu=\hbar\kappa/c, \tag{7}$$

so that

$$\kappa=\mu c/\hbar \tag{7a}$$

is the reciprocal Compton wave-length of the meson (times 2π). If we identify the meson of our theory with the particle observed in cosmic rays, we have $\mu\sim 180m$ where m is the electron mass. For the numerical calculations in the theory of the deuteron it will be convenient (cf. Eq. (39a)) to use

$$\mu=177m, \tag{8}$$

which is within the limits of error of the experimental determination (1). Then we have

$$\kappa=4.58\times 10^{12}\ \text{cm}^{-1}, \tag{8a}$$

$$1/\kappa=2.18_5\times 10^{-13}\ \text{cm}, \tag{8b}$$

$1/\kappa$ is the "range" of the nuclear forces (cf. Eq. (19)).

In the presence of a nuclear particle, (4) is replaced by

$$\text{div}\,\mathbf{E}+\kappa^2\varphi=4\pi\rho, \tag{9a}$$

$$\text{curl}\,\mathbf{H}-\partial\mathbf{E}/c\partial t+\kappa^2\mathbf{A}=4\pi\mathbf{j}/c, \tag{9b}$$

where

$$\rho=g\psi^*\psi, \tag{10a}$$

$$\mathbf{j}/c=g\psi^*\alpha\psi. \tag{10b}$$

ψ is the wave function of the nuclear particle, α the Dirac operator and g a constant. g has the same significance for the interaction of a heavy particle with the meson field as the charge e for the interaction of a charged particle with the electromagnetic field. Eqs. (9) are relativistically invariant, left and right sides being the components of a four vector.

Equations (3) are modified by the addition of an antisymmetrical tensor involving the nuclear particle, *viz.*

$$\mathbf{E}+\text{grad}\,\varphi+\partial\mathbf{A}/c\partial t=4\pi\mathbf{N}/\kappa, \tag{11a}$$

$$\mathbf{H}-\text{curl}\,\mathbf{A}=4\pi\mathbf{M}/\kappa, \tag{11b}$$

$$\mathbf{N}=if\psi^*\beta\alpha\psi, \tag{12a}$$

$$\mathbf{M}=f\psi^*\beta\sigma\psi. \tag{12b}$$

The constant g is independent of f. The right-hand side of (11b) represents the spin density. **M** and ρ are "static" quantities, i.e., they are large for nuclear particles at rest, while **j** and **N** vanish in this case and are generally of the order v/c compared with ρ and **M** where v is the velocity of the nuclear particle. In a theory in which the nuclear particles are treated non-relativisitically, **j** and **N** may be neglected.

Combining (9) and (11), we obtain (cf. 2)

$$\nabla^2\varphi-\frac{1}{c^2}\frac{\partial^2\varphi}{\partial t^2}-\kappa^2\varphi=-4\pi\rho+\frac{4\pi}{\kappa}\,\text{div}\,\mathbf{N}, \tag{13a}$$

$$\nabla^2\mathbf{A}-\frac{1}{c^2}\frac{\partial^2\mathbf{A}}{\partial t^2}-\kappa^2\mathbf{A}=-\frac{4\pi\mathbf{j}}{c}+\frac{4\pi}{\kappa}\left(\text{curl}\,\mathbf{M}-\frac{1}{c}\frac{\partial\mathbf{N}}{\partial t}\right). \tag{13b}$$

In a nonrelativistic approximation for the nuclear particles, **N** and **j** should be neglected and ρ, **M** considered independent of the time. Then the solution of (13) is

$$\varphi(\mathbf{r})=\int d\tau'\frac{\rho(\mathbf{r}')}{|\mathbf{r}-\mathbf{r}'|}\exp\left[-\kappa|\mathbf{r}-\mathbf{r}'|\right], \tag{14a}$$

$$\mathbf{A}(\mathbf{r})=-\frac{1}{\kappa}\int d\tau'\frac{\text{curl}\,\mathbf{M}(\mathbf{r}')}{|\mathbf{r}-\mathbf{r}'|}\times\exp\left[-\kappa|\mathbf{r}-\mathbf{r}'|\right]. \tag{14b}$$

The divergence condition (2) is fulfilled. If the wave function ψ of the nuclear particle is concentrated in a small space (small compared with r) around the origin ("point charge") we may write

$$\varphi(\mathbf{r})=(g/r)e^{-\kappa r}, \tag{15a}$$

$$\mathbf{A}(\mathbf{r})=-\frac{f}{\kappa}\,\text{curl}\left(\mathbf{s}\frac{e^{-\kappa r}}{r}\right). \tag{15b}$$

where

$$\mathbf{s}=\int\psi^*\beta\sigma\psi d\tau'\approx\int\psi^*\sigma\psi d\tau' \tag{16}$$

is the spin of the nuclear particle.

If a nuclear particle is subject to a meson field the potential energy is

$$E_{\text{pot}}=\int d\tau\left(\rho\varphi-\frac{1}{c}\mathbf{j}\cdot\mathbf{A}+\frac{1}{\kappa}\mathbf{M}\cdot\mathbf{H}-\frac{1}{\kappa}\mathbf{N}\cdot\mathbf{E}\right). \tag{17}$$

The general form of this potential energy follows from the field equations (9), (11) and from considerations of relativistic invariance. The sign of the first two terms is the same as in electrodynamics; in general, the sign can only be derived from the Hamiltonian of the field which will be discussed in the next section.

We shall now assume that the meson potential (15) is produced by a nuclear particle 1 located at the origin and acts on a particle 2 located at $\mathbf{r}$. Then we have, neglecting relativistic terms and using (11b):

$$E_{\text{pot}}=\frac{g_1g_2}{r}e^{-\kappa r}-\frac{f_1f_2}{\kappa^2}\mathbf{s}_2\cdot\text{curl curl}\left(\mathbf{s}_1\frac{e^{-\kappa r}}{r}\right)+\frac{4\pi}{\kappa^2}f_1f_2\,\mathbf{s}_1\cdot\mathbf{s}_2\delta(\mathbf{r}), \tag{18}$$

δ being Dirac's singular function. Evaluating the curl curl, we obtain:

$$-\text{curl curl}\left(\mathbf{s}_1\frac{e^{-\kappa r}}{r}\right)=-\text{grad div}\left(\mathbf{s}_1\frac{e^{-\kappa r}}{r}\right)+\mathbf{s}_1\nabla^2\left(\frac{e^{-\kappa r}}{r}\right)=-\text{grad}\left(\mathbf{s}_1\cdot\text{grad}\frac{e^{-\kappa r}}{r}\right)+\kappa^2\mathbf{s}_1\frac{e^{-\kappa r}}{r}-4\pi\mathbf{s}_1\delta(\mathbf{r}). \tag{18a}$$

The last term of (18a) cancels the last term of (18). The first term can be transformed in a straightforward way. The final result is

$$E_{\text{pot}}=U+V, \tag{19}$$

$$U=g_1g_2e^{-\kappa r}/r, \tag{19a}$$

$$V=V_1+V_2, \tag{19b}$$

$$V_1=(2/3)f_1f_2\,\mathbf{s}_1\cdot\mathbf{s}_2\,e^{-\kappa r}/r, \tag{19c}$$

$$V_2=f_1f_2\frac{e^{-\kappa r}}{r}\left(\frac{1}{\kappa^2r^2}+\frac{1}{\kappa r}+\frac{1}{3}\right)\times\left(-3\frac{\mathbf{s}_1\cdot\mathbf{r}\,\mathbf{s}_2\cdot\mathbf{r}}{r^2}+\mathbf{s}_1\cdot\mathbf{s}_2\right). \tag{19d}$$

The interaction U (19a) arises from the term $\rho\varphi$ in (17); it does not depend on the spins of the nuclear particles and is repulsive for two nuclear particles of the same kind ($g_1=g_2$). Thus it behaves in every respect like the Coulomb force in electrodynamics from which it differs only by the exponential factor $e^{-\kappa r}$. This factor provides the rapid decrease of the force at large distances which is required by experiment. $1/\kappa$ is the range of the force (cf. (8b)).

The interaction V is spin-dependent and comes from the term $\mathbf{M}\cdot\mathbf{H}$ in (17). V can conveniently be split into two parts of which the first does not depend on the direction of the vector $\mathbf{r}$ between the two particles (relative to the spin $\mathbf{s}$) while the second does depend on it and gives zero when averaged over all directions of $\mathbf{r}$. V_2 diverges as $1/r^3$ at the origin while U and V_1 behave as $1/r$. V_1 and V_2 are quantitatively related to each other, both depending on the value of f; U is independent of V (depending on g). For like particles ($f_1=f_2$), V_1 is repulsive when the spins are parallel (triplet), attractive for opposite spins (singlet).

§3. Sign of the Interaction

In this section we shall discuss the Hamiltonian of the meson field mainly in order to determine the sign of the potential energy of nuclear particles in the field which had been assumed arbitrarily in (17). The Hamiltonian of the *electromagnetic* field interacting with matter is

$$\mathcal{H}_{\text{elec}}=\int d\tau\{(E^2+H^2)/8\pi-\mathbf{A}\cdot\mathbf{j}/c\}. \tag{20}$$

The occurrence of the term $\mathbf{A}\cdot\mathbf{j}$ without its relativistic partner $\rho\varphi$ should be noted. With the help of the field equations, the Hamiltonian can be expressed in terms of the potentials rather than the field intensities; it then takes the form

$$\mathcal{H}_{\text{elec}}=\int d\tau\left\{\frac{1}{8\pi}\left[\text{grad}^2\,\mathbf{A}+\frac{1}{c^2}\left(\frac{\partial\mathbf{A}}{\partial t}\right)^2-\text{grad}^2\,\varphi-\frac{1}{c^2}\left(\frac{\partial\varphi}{\partial t}\right)^2\right]+\rho\varphi-\frac{\mathbf{A}\cdot\mathbf{j}}{c}\right\}. \tag{21}$$

This form is more symmetrical than (20) and suitable for immediate derivation of the field

equations. It has essentially been used by Fermi in his formulation of quantum electrodynamics.[25] It has the disadvantage of being more complicated than (20) and of making it less evident that the Hamiltonian is positive definite (see below).

The Hamiltonian of the meson field expressed in the field intensities has the form

$$\mathcal{H}=\int d\tau\left\{\frac{1}{8\pi}[\mathbf{E}^2+\mathbf{H}^2+\kappa^2(\mathbf{A}^2+\varphi^2)]-\mathbf{A}\cdot\mathbf{j}/c - \mathbf{N}\cdot\mathbf{E}/\kappa\right\}. \quad (22)$$

With the help of the field equations this can be transformed into a form analogous to (21):

$$\mathcal{H}=\int d\tau\left\{\frac{1}{8\pi}\left[\operatorname{grad}^2\mathbf{A}+\frac{1}{c^2}\left(\frac{\partial\mathbf{A}}{\partial t}\right)^2+\kappa^2\mathbf{A}^2 - \operatorname{grad}^2\varphi-\frac{1}{c^2}\left(\frac{\partial\varphi}{\partial t}\right)^2-\kappa^2\varphi^2\right]+\rho\varphi-\frac{\mathbf{A}\cdot\mathbf{j}}{c} + \frac{1}{\kappa}(\mathbf{A}\cdot\operatorname{curl}\mathbf{M}-\varphi\operatorname{div}\mathbf{N})+\frac{2\pi}{\kappa^2}(\mathbf{M}^2-\mathbf{N}^2)\right\}. \quad (23)$$

We introduce the momenta conjugate to $\mathbf{A}$ and φ as follows:

$$\mathbf{P}=\frac{1}{4\pi c^2}\frac{\partial\mathbf{A}}{\partial t}-\frac{1}{\kappa c}\mathbf{N}, \quad (23a)$$

$$p=\frac{1}{4\pi c^2}\frac{\partial\varphi}{\partial t}. \quad (23b)$$

Then the field equations (13a,b) follow by the usual method.

To deduce the potential entering the wave equation for the nuclear particles it is convenient to transform the second last bracket in (23) by an integration by parts into

$$\int d\tau(\mathbf{M}\cdot\operatorname{curl}\mathbf{A}+\mathbf{N}\cdot\operatorname{grad}\varphi)/\kappa. \quad (23c)$$

The Dirac equation of the nuclear particle is obtained by taking the derivative of the Hamiltonian (including its "material" part) with respect to ψ^*. Remembering the definition of $\mathbf{M}$ and $\mathbf{N}$ we find

$$W\psi=\beta Mc\,\psi+\boldsymbol{\alpha}\cdot\mathbf{p}\,\psi + \left[\varphi-\boldsymbol{\alpha}\cdot\mathbf{A}+\frac{1}{\kappa}\beta\boldsymbol{\sigma}\cdot\left(\operatorname{curl}\mathbf{A}+\frac{4\pi}{\kappa}\mathbf{M}\right) + \frac{i\beta\boldsymbol{\alpha}}{\kappa}\cdot\left(\operatorname{grad}\varphi+\frac{1}{c}\frac{\partial\mathbf{A}}{\partial t}-\frac{4\pi}{\kappa}\mathbf{N}\right)\right]\psi, \quad (24a)$$

where W is the energy. With the use of (11) this simplifies to

$$W\psi=[\beta Mc+\boldsymbol{\alpha}\cdot\mathbf{p}+\varphi-\boldsymbol{\alpha}\cdot\mathbf{A} + \beta(\boldsymbol{\sigma}\cdot\mathbf{H}-i\boldsymbol{\alpha}\cdot\mathbf{E})/\kappa]\psi. \quad (24)$$

Multiplying by ψ^* from the left and integrating over space, this yields the expression (17) for the potential energy of the nuclear particle.

It may be noted that the terms representing the interaction between field and matter in (22) (i.e., the two last terms) are again unsymmetrical relativistically, just as in electrodynamics (cf. (20)). Only the "small" material quantities, $\mathbf{j}$ and $\mathbf{N}$, appear but not the "large" quantities, ρ and $\mathbf{M}$. The alternative form (23) of the interaction which involves the potentials is again symmetrical.

In (22), there is no term containing the material quantities $\mathbf{M}$ and $\mathbf{N}$ quadratically. The transformation from (22) to (23) brings such terms into the Hamiltonian but in such a way that they disappear again in the wave equation (24) and therefore in the potential energy (17) and in the final interaction energy (19). In this respect, our formulation agrees with that of Yukawa, Sakata and Taketani, and differs from that of Froehlich, Heitler and Kemmer.

The form (22) shows most clearly that the Hamiltonian is positive definite for fields not containing matter (i.e., no nuclear particles). From (23) this result follows only when the divergence condition (2) is taken into account. *The positive definite character of the Hamiltonian for the field alone determines essentially the sign of the interaction between two particles.* This point will be considered in more detail in another paper.[26]

[25] E. Fermi, Rev. Mod. Phys. **4**, 87 (1932).

[26] H. A. Bethe, to appear shortly in *The Physical Review*.

§4. Charge Dependence of the Nuclear Forces

A. Neutral mesons only

Thus far we have tacitly assumed that the mesons constituting the field are electrically neutral. Only then can we speak of the meson field "associated with a proton" (or a neutron) because the nature (charge) of the nuclear particle does not change by emitting or absorbing a neutral meson. The only freedom we have in this "neutral theory" is to choose values for the "mesonic charges" f and g of neutron and proton which may be different for the two kinds of particles. We denote the respective values of f, g for proton and neutron by $f_P g_P$ and $f_N g_N$. To determine the relative values of these constants we use general experimental facts of nuclear physics.

(1) Nuclear forces are symmetrical in neutrons and protons,[27] i.e., the forces between two protons are the same as those between two neutrons (except for the electrostatic force). This identity refers to the magnitude as well as the spin dependence of the forces. Therefore we must have (cf. (19))

$$g_N^2 = g_P^2, \tag{25a}$$

$$f_N^2 = f_P^2, \tag{25b}$$

which permits the solutions

$$g_N = \pm g_P, \tag{26a}$$

$$f_N = \pm f_P. \tag{26b}$$

(2) The force between a neutron and a proton in the ^1S state is practically identical[15] with that between two protons in this state, as revealed by the scattering of slow neutrons and slow protons by protons, respectively. This fact shows that the positive sign must be chosen[28] in both (26a) and (26b), *viz.*

$$g_N = g_P, \tag{27a}$$

$$f_N = f_P. \tag{27b}$$

In the neutral theory, therefore, neutron and proton are completely equivalent and indistinguishable as far as the associated meson fields are concerned. The expressions $g_1 g_2$ and $f_1 f_2$ in (19) can be replaced by g^2 and f^2 whatever the interacting particles. The interaction thus obtained will be denoted by W_n in the following. It is an ordinary (nonexchange) interaction which, however, does depend on spin. In the language customary in nuclear theory, it would be a mixture of a Wigner and a Bartlett force.*

B. Charged mesons only

The emission of a charged meson will be accompanied by a change of charge of the emitting nuclear particle. Thus a neutron (N) can only emit a negative (M^-) or absorb a positive (M^+) meson and will thereby be transformed into a proton (P). In the second approximation of the Schrödinger perturbation scheme, i.e., when we consider the emission of one meson by a nuclear particle and its reabsorption by another, this will lead to *forces between a neutron and a proton*. The scheme of the interaction between a particle 1 which is originally a neutron and a particle 2 originally a proton is:

Either $N_1 \rightarrow P_1 + M^-$, $P_2 + M^- = N_2$,

or $P_2 \rightarrow N_2 + M^+$, $N_1 + M^+ = P_1$.

It is obvious that in this way *no force will be obtained between two nuclear particles of the same kind*, i.e., two neutrons or two protons. These statements are also valid in the approximation of the field theory which is completely equivalent to the second order Schrödinger approximation since both theories give the interaction terms of order g^2 (or f^2).

The force between two nuclear particles obtained with charged mesons may be written

$$W_{ch} = W'(Q_1 Q_2^* + Q_1^* Q_2). \tag{28}$$

Here Q is an operator transforming a neutron into a proton and Q^* the reverse operator. If particle 1 is originally a neutron, 2 a proton, $Q_1 Q_2^*$ will interchange the charges of the two particles while $Q_2 Q_1^*$ is zero. If both nuclear particles have the same charge, the operator in (28) will be zero. W' will be identical in form with the interaction due to neutral mesons but

[27] H. A. Bethe and R. F. Bacher, Rev. Mod. Phys. **8**, 133 (1936).

[28] The equality of neutron-proton and proton-proton interaction in the ^1S state by itself shows only that (cf. (19a,c))

$$g_N g_P - 2 f_N f_P = g_P^2 - 2 f_P^2. \tag{27c}$$

Only in conjunction with (26a,b) the two equations (27a,b) can be deduced separately.

* Cf. reference 27, p. 105.

the g and f will now be the quantities which refer to the strength of the *charged* meson field associated with a nuclear particle. It is important that in the formulae (19) for the various parts of W' we must now put $|g|^2$ and $|f|^2$ for g_1g_2 and f_1f_2. This is because g_1 refers to one transformation of the nuclear particle and g_2 to the reverse transformation; from general principles of quantum theory (reality of the Hamiltonian[29]) we must then have $g_2=g_1^*$, $f_2=f_1^*$ (the asterisk denotes complex conjugate). Further, if g represents the interaction between nuclear particles and mesons of *one* charge, there will be a contribution W_{ch} from mesons of each sign of charge. The total nuclear potential due to charged mesons is therefore $2W_{ch}$.

(28) represents an exchange force of the Heisenberg type. It is most convenient to write the wave function of a system of two nuclear particles in terms of five coordinates for each particle, *viz.*

$$\Psi(\mathbf{r}_1, m_{s1}, m_{\tau 1}; \mathbf{r}_2, m_{s2}, m_{\tau 2}).$$

Here $\mathbf{r}$ represents the three space coordinates, m_s the spin and m_τ the charge coordinate. m_s and m_τ can each assume the two values $+\frac{1}{2}$ and $-\frac{1}{2}$. These are the values of the spin component in a given direction in the case of m_s, while $m_\tau=+\frac{1}{2}$ means that the particle is a proton, $m_\tau=-\frac{1}{2}$ that it is a neutron. Now the operator $Q_1Q_2^*+Q_1^*Q_2$ will interchange $m_{\tau 1}$ and $m_{\tau 2}$ provided one of the two particles is a proton, the other a neutron, but irrespective of which is which. (If both particles are of the same kind, the operator is zero, as mentioned before.) Now it is easy to show that Ψ will be either symmetrical or antisymmetrical in the charge coordinates $m_{\tau 1}m_{\tau 2}$; therefore the operator $Q_1Q_2^*+Q_1^*Q_2$ will be equivalent to a factor $+1$ or -1, respectively.

The symmetry with respect to the charge is related to that with respect to space coordinates and spin by the Pauli principle. This principle requires that Ψ be antisymmetrical with respect to interchange of *all* coordinates, *viz.* $\mathbf{r}$, m_s and m_τ. Now the symmetry of Ψ with respect to $\mathbf{r}$ and m_s is as follows:*

Ψ is symmetrical with respect to $\mathbf{r}$ if the orbital momentum L of the system is even, antisymmetrical in $\mathbf{r}$, if L is odd.

Ψ is symmetrical in m_s if the total spin s is one, i.e., if the system is in a triplet state antisymmetrical in m_s if $s=0$ (singlet state).

Therefore, according to the Pauli principle,

Ψ is symmetrical in m_τ for singlet states of even L and for triplet states of odd L,

Ψ is antisymmetrical in m_τ for triplet states of even L and for singlet states of odd L.

In particular, the ground state (^3S) of the deuteron is antisymmetrical, the virtual ^1S state symmetrical in the charge coordinate. For two particles of the *same* kind, we have of course $m_{\tau 1}=m_{\tau 2}$ so that only the states symmetrical in m_τ are permitted.

Summarizing, we find that the interaction caused by the charged meson field is:

$$\begin{cases} 0, & \text{if the two interacting nuclear particles are of the same kind;} \\ +2W', & \text{if they are of opposite kinds (proton and neutron) and if the wave function is symmetrical in the charge coordinate } m_\tau \text{ (e.g. in the } {}^1S \text{ state);} \\ -2W', & \text{if they are proton and neutron and the wave function is antisymmetrical in the charge (e.g. in the } {}^3S \text{ state).} \end{cases} \tag{29}$$

Considering in particular the spin-independent part U (cf. (19a)) of the interaction, this means (W' positive!) a repulsion in the ^1S state (symmetrical in m_τ), an attraction in the ^3S state (antisymmetrical).

C. Symmetrical theory

The theory involving charged mesons only was found to contradict experiment by giving no force between two like nuclear particles. This can be remedied by using neutral as well as charged mesons. In this case, the argument 1

[29] The Hamiltonian operator of the interaction between charged meson field and two nuclear particles 1, 2 will be

$$\mathfrak{H}=g[\varphi(r_1)Q_1+\varphi(r_2)Q_2]+g^*[\varphi^*(r_1)Q_1^*+\varphi^*(r_2)Q_2^*] + \text{terms depending on spin}$$

where φ^* is the operator of emission of a positive meson, φ the operator of absorption. The same formalism as in §2 leads then to the interaction

$$W=gg^*(e^{-\varkappa r}/r)(Q_1Q_2^*+Q_1^*Q_2)+\text{spin terms.}$$

* Cf. reference 27, p. 107.

given in Section A will still be valid, i.e., the f and g values for the interaction with neutral mesons must be either equal for proton and neutron, or equal and opposite. In contrast to A, however, the solution $g_N=g_P$, $f_N=f_P$ is to be ruled out: This solution would make the interaction caused by neutral mesons *alone*, equal for like and for unlike nuclear particles. Since for unlike particles the charged mesons give an additional contribution while for like particles they do not, the *total* interaction could not be the same for like and unlike particles in the ^1S state, in contrast to evidence 2 quoted in Section A. Therefore we must now choose the negative sign in (26), putting

$$g_N{}^0=-g_P{}^0, \tag{30a}$$

$$f_N{}^0=-f_P{}^0, \tag{30b}$$

the superscript 0 signifying the fact that these quantities refer to the interaction with neutral mesons (M^0).

Then we find that the interaction due to neutral mesons alone is

$$\begin{aligned} &+W_n, \text{ if the interacting nuclear particles} \\ &\qquad \text{are alike} \\ &-W_n, \text{ if they are unlike.} \end{aligned} \tag{31}$$

The total interaction in the ^1S state (due to neutral and charged mesons) is therefore

$$\begin{aligned} &W_n \text{ for like particles} \\ &-W_n+2W' \text{ for unlike particles.} \end{aligned} \tag{31a}$$

Since these two interactions are experimentally equal, we find

$$W'=W_n.$$

In other words, the absolute values of g and f must be the same for the interactions with neutral, positive and negative mesons:

$$\begin{aligned} |g^+|=|g^-|=|g^0|=|g|, \\ |f^+|=|f^-|=|f^0|=|f|. \end{aligned} \tag{32}$$

This theory is therefore symmetrical in all the three kinds of mesons. It was first investigated by Kemmer[16] using a more elegant method.

With this symmetrical theory, we find for the total interaction energy (cf. (29), (31))

$$\begin{aligned} &W=+W_n \text{ for all states symmetrical} \\ &\qquad \text{in the charge coordinate,} \\ &W=-3W_n \text{ for all states antisymmetrical} \\ &\qquad \text{in the charge coordinate.} \end{aligned} \tag{33}$$

TABLE I. *Summary of the sign of various interactions.*

INTERACTION (CF. (EQ. 19))	NEUTRAL THEORY	SYMMETRICAL THEORY
U	Always repulsive	Repulsive for states symmetrical in the charge Attractive for states antisymmetrical in the charge
V_1	Repulsive for triplet states Attractive for singlet states	Repulsive for odd L Attractive for even L
V_2	Zero for singlet states Attractive for triplet states if total spin S and vector r from one particle to the other are parallel Repulsive when S perpendicular to r	Zero for singlet states Repulsive for triplet states of even L (attractive for odd L) when S and r are parallel Attractive for even L (repulsive for odd L) when S and r are perpendicular

This result may be written in the form

$$W=W_n\,\tau_1\cdot\tau_2, \tag{33a}$$

where τ_1, τ_2 are the isotopic spin operators[16] of the two nuclea r particles. $\tau_1\cdot\tau_2$ has the value $+1$ for states symmetrical in m_r and -3 for antisymmetrical states, just as for the ordinary spin $\sigma_1\cdot\sigma_2=+1$ for triplet states and -3 for singlets. As has been pointed out before, W_n is given by (19) with $g_1=g_2=g$ and $f_1=f_2=f$.

We see from (33) that the symmetrical theory gives the same interaction as the neutral theory for the ^1S state (and all symmetrical states), but the opposite sign, and three times the magnitude, for the ^3S state (and all antisymmetrical states). The potential in the symmetrical theory is a mixture of exchange and ordinary force which resembles qualitatively an exchange force; the spin-independent part (19a) is similar to a Heisenberg, the spin-dependent part (19c) to a Majorana force.

D. Summary of the sign of the various interactions

A summary of the sign of the various interactions is given in Table I. The statements about U and V_1 follow from the foregoing formulae and discussions considering that $\sigma_1\cdot\sigma_2=+1$ for triplets and -3 for singlets. V_2 will be discussed in detail in §8, 9.

§5. The Single Force Hypothesis

The spin-independent interaction U (cf. (19a)) alone cannot explain the known experimental facts about two-particle systems. For this force is repulsive in the neutral theory, and therefore also in the symmetrical theory for the ^1S state (cf. §4C) whereas experimentally there is an attractive potential in the ^1S state. Moreover, the potentials in ^1S and ^3S states are experimentally different.

Therefore the spin-dependent interaction V (19b,c,d) must certainly be present, i.e., f must be different from zero. We shall show in this section that it is possible with *V alone*, to explain qualitatively all known facts about nuclear two-body systems and also the saturation of nuclear forces. In the quantitative discussion in Part II we shall show that the interaction U is actually harmful in many cases. Therefore we make the hypothesis:

The spin-dependent interaction V is the sole nuclear force (Single Force Hypothesis, S. F. H.).

It is obvious that this hypothesis means an enormous simplification in concept (though not in mathematics) compared with the older nuclear theory with its four different kinds of forces (Wigner, Bartlett, Majorana and Heisenberg) to which another force, not spherically symmetrical, had to be added by Schwinger in order to explain the quadrupole moment of the deuteron.

With the single-force hypothesis, the interaction between two nuclear particles becomes explicitly (cf. (19))

$$V = V_1 + V_2, \tag{34}$$

where for the neutral theory

$$V_1 = \tfrac{2}{3} f^2 \boldsymbol{\sigma}_1 \cdot \boldsymbol{\sigma}_2 e^{-\kappa r}/r, \tag{34a}$$

$$V_2 = f^2 \left(-3 \frac{\boldsymbol{\sigma}_1 \cdot \mathbf{r}\, \boldsymbol{\sigma}_2 \cdot \mathbf{r}}{r^2} + \boldsymbol{\sigma}_1 \cdot \boldsymbol{\sigma}_2 \right) \frac{e^{-\kappa r}}{r} \times \left(\frac{1}{\kappa^2 r^2} + \frac{1}{\kappa r} + \frac{1}{3} \right), \tag{34b}$$

while in the symmetrical theory these expressions must be multiplied by $\boldsymbol{\tau}_1 \cdot \boldsymbol{\tau}_2$. (We have used in (34) the spin *operators* $\boldsymbol{\sigma}$ rather than the average value $\mathbf{s}$ of the spin; this is convenient for later use in the wave equation.)

We shall now show that this force is actually capable of explaining all the empirical facts about two-body systems. For any singlet state, V_2 is identically zero. This can be seen either by direct evaluation, or from the fact that the average of the first parenthesis over all orientations of the spin must be zero, and that for a singlet state this average is equal to the actual value. In V_1, the factor $\boldsymbol{\sigma}_1 \cdot \boldsymbol{\sigma}_2$ is equal to -3. In the neutral theory, we therefore get an attractive potential V_1 for any singlet state. The same is the case in the symmetrical theory for the ^1S state since in this case $\boldsymbol{\tau}_1 \cdot \boldsymbol{\tau}_2 = 1$. This result is in agreement with the experimental evidence which shows attraction in the ^1S state both for the deuteron and the double proton.

Regarding the ground state of the deuteron which is essentially a ^3S state, the two alternative theories differ. In the neutral theory, the central force V_1 will be repulsive since $\boldsymbol{\sigma}_1 \cdot \boldsymbol{\sigma}_2 = +1$ for triplets. In the symmetrical theory, $\boldsymbol{\tau}_1 \cdot \boldsymbol{\tau}_2 = -3$ for this state (cf. §4C) so that $\boldsymbol{\sigma}_1 \cdot \boldsymbol{\sigma}_2\, \boldsymbol{\tau}_1 \cdot \boldsymbol{\tau}_2$ has the same value as for the ^1S state, *viz.* -3. Therefore V_1 will be attractive and equal to its value for ^1S.

Whichever theory is used, the potential V_2 ("tensor interaction") will mix the ^3S state with a $^3D_1$ state. This will cause the ground state of the deuteron to have a quadrupole moment in agreement with the observations of Kellogg, Rabi, Ramsey and Zacharias. In addition, V_2 will lower the triplet state (second-order perturbation of a lowest state). In the case of the symmetrical theory, this will automatically make the ^3S state lower than the ^1S because the two states would coincide if V_2 were neglected. This result agrees with experiment according to which the triplet state is the ground state while the ^1S state is unstable and close to zero energy. In the neutral theory a greater lowering effect of V_2 is required, first to offset the repulsive action of V_1, then to make up for the attraction in the ^1S state, and finally to depress the triplet state below the singlet. However, owing to its divergence with $1/r^3$, the interaction V_2 becomes very large (cf. §6) and can therefore easily make the triplet lower than the singlet even in the neutral theory. That this is actually the case will be shown by the detailed calculations in §12, 13.

We have thus shown that the position of the

deuteron levels can be explained by the potential V, the singlet level being determined exclusively by the central force V_1 while for the triplet the most important force is the tensor interaction V_2. It is not necessary to lower the triplet (and raise the singlet) by means of the spin-independent force U (cf. (19a)) as has been believed;[11, 13, 16] on the contrary, the use of the tensor interaction for this purpose has the advantage of giving a quadrupole moment at the same time.

A very important requirement for any nuclear theory is the saturation of the nuclear forces for heavy nuclei.[30] A necessary (though not sufficient) condition for saturation is that the average of the interaction over all directions of the spins $\boldsymbol{\sigma}_1 \cdot \boldsymbol{\sigma}_2$ be zero or repulsive. The average of our potential V is exactly zero which can be seen most easily by averaging over the two possible values, $+\frac{1}{2}$ and $-\frac{1}{2}$, of m_{s1} and m_{s2}. This would probably be also *sufficient* for saturation if we could show in addition that our forces favor a small value of the total spin of the nucleus (in agreement with the experimental behavior of nuclear spins). The central force V_1 will in the neutral theory indeed show such a tendency, being attractive for antiparallel spin of the two interacting particles (singlet) repulsive for parallel spins (triplet state). On the other hand, the tensor interaction V_2 will favor a parallel alignment of the spins provided the vectors $\mathbf{r}$ are also parallel to the resultant spin. This force, if acting alone, would lead to a very oblong rather than a spherical shape of the nucleus, a tendency which is strongly opposed by the marked increase of the kinetic energy of the particles for a non-spherical shape. For lighter nuclei, for which the kinetic energy is most important, the central force V_1 will certainly win out, yielding almost zero spin in agreement with experiment. For very heavy nuclei, however, the kinetic energy will increase more slowly than the potential energy, *viz.* as[31] $A^{11/16}$ as compared with A^2. Therefore there will be the danger of a predominance of V_2 with its consequences of large spin, non-spherical shape and, worst of all, nonsaturation. Whether this will actually occur, and whether it will occur in the range of existing nuclei ($A < 240$) depends entirely on the behavior of the tensor interaction at very small distances. This is because the effect of nonsaturation is a collapse of the nucleus to a small size which then permits every particle to interact with every other. If V_2 has the same sign at small distances as at large ones, and especially if it becomes very large, there will almost certainly be nonsaturation; if V_2 changes sign, the nonsaturation will not set in except at a much higher nuclear mass A; and if V_2 tends to zero, saturation will be preserved. Of course, there is no evidence at the moment on the behavior of V_2 at small distances, but the assumptions leading to saturation are at least not implausible.

In any case, it seems that the addition of a spin-independent force U will not help matters greatly because such a force would only increase the already existing repulsive central force V_1 in the triplet state. The symmetrical theory gives exactly the same result as the neutral one for nuclei containing only protons or only neutrons so that the same danger of nonsaturation exists here. The nuclei containing both neutrons and protons will not so easily show nonsaturation in the symmetrical theory because the force vanishes when averaged over the charge coordinates $m_{\tau 1}$ and $m_{\tau 2}$; on the other hand, it is then more difficult to prove that the total spin tends to be small.

Summarizing we may say that the single force hypothesis is not in contradiction with any known qualitative fact, and that nothing is gained by adding a spin-independent force U.

§6. The Necessity of Cutting Off

The tensor interaction V_2 behaves at small distances as $1/r^3$ and will therefore give rise to infinite negative eigenvalues. This follows most easily from the fact that there are certain states, particularly the ${}^3P_1$ state (cf. §8, 9), for which the tensor interaction is equivalent to a simple attractive central force depending in the same way on r. (In other states, e.g., ${}^3P_0$, the equivalent central force is repulsive. If the sign of the whole interaction were changed, the role of attractive and repulsive states would be interchanged so that there would still be states with

[30] See, e.g., G. Breit and E. Wigner, Phys. Rev. **53**, 998 (1938); H. Volz, Zeits. f. Physik **105**, 537 (1937); E. Feenberg, Phys. Rev. **52**, 667 (1937).

[31] I am indebted to Professor Wigner for this communication and for pointing out the saturation difficulties mentioned in the text.

an attractive $1/r^3$ potential.) Now it is well known that in an attractive $1/r^3$ potential there is no lowest eigenvalue, and this fact is not changed by taking into account the centrifugal force acting in the $^3P_1$ state because this force diverges only as $1/r^2$ and therefore becomes negligible compared with the tensor interaction at small distances.

It has been suggested that the divergence of the potential might not be so serious because the situation might be similar to that found[32] with respect to some terms in the relativistic interaction of two electrons. As Breit[32] has shown, only the first-order perturbation energy caused by these terms has physical significance while the terms should not be included in the potential used for calculating the wave function. If the same were true of the tensor interaction there would be no divergence difficulty: For then the wave function of the $^3P_1$ state would have to be calculated using only the centrifugal force $\sim 1/r^2$ and potentials which diverge only as $1/r$. Then the wave function would behave as r at small distances, and the average value of the tensor interaction taken over this wave function (first-order perturbation energy) would be finite (given by an integral which behaves for small r as $\int r^2 dr\, r^2/r^3$).

However, this solution is impossible. The tensor interaction is genetically entirely different from the relativistic terms in the electron interaction. The former is a "static" interaction[18] and can be derived from the Hamiltonian of the meson field by a contact transformation just as the Coulomb force is derived from the Hamiltonian of the electromagnetic field. The relativistic terms in the electron interaction are dynamic terms and therefore subject to the same uncertainties as, e.g., the self-energy.

Even if the treatment of the tensor interaction as a true potential could not be justified from its derivation it would still be necessary *a posteriori* from its applications. It is obvious that the quadrupole moment of the deuteron could not be explained if the tensor interaction were to be excluded in the calculation of the wave function. But we can say even more: The tensor interaction and the spin-dependent central force V_1 are genetically related, therefore the latter would have to be excluded as well. This would leave only U as a true potential for the calculation of the wave function, and U is repulsive for the singlet state in both the neutral and the symmetrical theory, in contradiction with experiment.

It is therefore necessary to cut off the potential at small distances and to replace it by one which diverges more slowly (less than $1/r^2$) or not at all. Only such a cutting off will make it possible to obtain finite results for the binding energy of a system consisting of two nuclear particles. To my knowledge, *this is the first time that a cutting off is necessary in a purely mechanical problem.*

There are many reasons why the potential (34) will become invalid at small distances. The first, and probably the easiest to take into account, is the relativistic correction, both in the potential ("small" terms $\mathbf{j}$ and $\mathbf{N}$) and in the wave equation. The first of these effects means the taking into account of the retardation, the second the relativistic change of mass. However, it seems very doubtful whether these corrections will give the desired effect. Relativity can only be expected to be important when the potential energy becomes about $2Mc^2$ (factor 2 because there are two particles) but actually the explicit calculations show that the potential must be cut off at a value of about $\frac{1}{4}Mc^2$ in the neutral theory (straight cut-off, cf. §13, Table IV) and at only $0.015Mc^2$ in the symmetrical theory. Moreover, it is not at all certain in which direction the relativistic corrections will act: The relativistic change of mass will certainly act like an increase in the effective potential, i.e., give an effect in the wrong direction. The retardation will probably give an effect in the right direction but whether this will be sufficient to overbalance the effect of the change of mass is doubtful. In the hydrogen problem, as is well known, the change of mass effect predominates.

A more promising reason for cutting off seems to be the interaction of higher order in $f^2/\hbar c$. The unquantized field theory as presented in §2 gives only the terms of order f^2 in the interaction. Terms involving higher powers of f could be calculated by the Schrödinger perturbation theory in conjunction with a quantization of the meson field. The fourth-order terms have been calculated by Yukawa,[1] by Froehlich, Heitler

[32] G. Breit, Phys. Rev. **39**, 616 (1932).

and Kemmer[11] and by Møller and Rosenfeld;[18] they behave at small distances like

$$W^{(4)} \sim \frac{f^2}{r}\frac{f^2}{\hbar c}\frac{1}{(\kappa r)^4} = \frac{f^4}{\mu c^2 r^2}\frac{1}{(\kappa r)^3}, \qquad (35)$$

thus their ratio to the terms of order f^2 is:

$$W^{(4)}/W^{(2)} = (f^2/\hbar c)(\kappa r)^{-2}. \qquad (35a)$$

From the quantitative calculations in §13, (Table IV) we obtain $f^2/\hbar c = 0.08$. Accordingly, the higher order terms can be expected to become important for $\kappa r \sim 0.3$. In view of the fact that numerical factors have been left out, the agreement with the calculated cutting-off distance in the neutral theory, *viz.*, $\kappa r = 0.32$ or 0.40 with two different methods of cutting off, is satisfactory.

The third, and perhaps most important, consideration is that the meson field produced by nuclear particle A in the neighborhood of B, will interfere with the proper field of B. Since the latter is certainly very large, it cannot be expected to obey the linear field equations of §2. Therefore there will not be a linear superposition of the proper field and the external field. This point has been particularly emphasized by Heisenberg.[33] It is like the second point in making use of the nonlinearity of the field equations (higher than quadratic terms in the field energy). However, it differs from both the preceding points in permitting deviations from the simple fields of §2 even for small values of the "external" field, i.e., for large distances of the interacting particles, because the proper field is always large. In other words, it is possible that in this theory we should not speak of a cut-off at all but of a general modification of the interaction potential.

As Heisenberg[33] has shown the interference between external and proper field will be equivalent to an "inertia" of the spin of the nuclear particle. This is exactly what we need in order to reduce our interaction at small distances because the tensor interaction causes a rapid motion of the spin of the nuclear particles.

A last possibility is that all interactions, nuclear as well as electromagnetic, etc., break down at small distances for some reason unknown at present and distinct from the nonlinearity of the field equations discussed above. There is some indication that such a breakdown is required in order to make the self-energy and the proper field of a particle finite. At what distances (or momentum changes, or field strengths) such a breakdown occurs can, of course, not be estimated at present.

Summarizing we may say that there is ample reason for cutting off the interaction between nuclear particles at small distances. A cutting off distance r_0 of the order of one-third of the range of the nuclear forces, $1/\kappa$, would seem plausible. The exact value of r_0, and the way in which the interaction must be cut off cannot at the moment be deduced from first principles but can only be obtained from a quantitative treatment of the two-body problem in conjunction with empirical data on binding energies, scattering, etc.

In the absence of a rational theory of the cutting off, and in order to obtain an idea of the sensitivity of the results to the unknown behavior of the potential at small distances, we shall investigate two alternative ways of cutting off, *viz*: (*A*) The potential is assumed to be zero inside a certain radius r_0 (zero cut-off), (*B*) The potential is assumed to be constant for $r < r_0$ and continuous at r_0 (straight cut-off). In formulae:

$$V(r) = 0 \quad \text{for} \quad r < r_0 \qquad (A)$$

or

$$V(r) = V(r_0) \quad \text{for} \quad r < r_0. \qquad (B)$$

For $r \geqslant r_0$, we assume in either case the validity of the potential (34).

Our theory contains then two[34] unknowns, *viz.*, the strength of the interaction, f, and the cutting-off radius r_0. These two constants will be determined from the binding energy of the deuteron (triplet state) and from the scattering cross section of slow neutrons by protons which gives evidence on the singlet interaction of two particles. When f and r_0 are known, we can calculate further properties of the deuteron, in particular its quadrupole moment, and the agreement or disagreement of such quantities with experiment will provide a test of the theory.

[33] W. Heisenberg, Zeits. f. Physik **113**, 61 (1939).

[34] The constant κ (reciprocal range of the forces) is assumed to be known from the mass of the meson (Eq. (8)). Cf. however, the calculations of L. E. Hoisington, S. S. Share, and G. Breit, Phys. Rev. **56**, 884 (1939), on the proton-proton scattering, which seem to require a larger value for κ, corresponding to $\mu = 326m$.

Multiple Scattering of Fast Electrons

C. W. SHEPPARD AND W. A. FOWLER
Kellogg Radiation Laboratory, California Institute of Technology, Pasadena, California
(Received November 13, 1939)

The scattering of electrons and positrons of energy from 5 to 17 Mev has been measured in lead foils of thickness 0.015 and 0.038 cm, in carbon laminae of thickness 0.132 and 0.381 cm, and in an aluminum foil of thickness 0.118 cm. The scattering has been shown to be in agreement with the multiple scattering theory of Williams in that the distribution in the product of the scattering angle times the energy of the scattered particle is Gaussian in form, and in that the mean scattering angle times energy is independent of certain geometrical aspects of the experimental method of measurement, and of the energy and sign of charge of the scattered particles. For carbon the experimental magnitude of the mean scattering is in satisfactory agreement with theory, but in aluminum and lead the experimental results are only 85 percent and 60 percent, respectively, of the theoretical predictions.

EXPERIMENTAL results of measurements on the multiple scattering of 10-Mev electrons and positrons in a thin lead foil of 0.015 cm thickness have recently been published.[1] A comparison was made with the calculations of Williams[2] on multiple scattering. The result of this comparison revealed the experimental mean angle of scattering to be slightly less than one-half the theoretical mean angle. In the light of this discrepancy further measurements have been made upon foils of different thickness and atomic number. The results to be discussed in this paper supersede the preliminary values previously published.[3]

The Experimental Material

Approximately 52,000 cloud-chamber pictures were examined, 17,000 of these being selected from those taken during the gamma-ray measurements on $B+H^1$ made in this laboratory,[4] and the remainder from the gamma-ray measurements on $Li+H^1$.[5] In these gamma-ray measurements thin scatterers were placed in the center of the chamber and the recoil electrons and pairs produced by the gamma-rays were measured. Large numbers of recoils and pairs originating in the chamber walls and surroundings were found which traversed the foil, and thus supplied material for the study of scattering.

Measurements were made on the scattering in four different foils. The thickness and superficial density of these and the original foil are included in Table I. The carbon employed was Acheson graphite. In the cloud-chamber photographs taken with the thicker lead foil there were two groups of pictures. In the first group the scatterer had been made somewhat smaller than the light beam which illuminated the chamber. For this reason an appreciable fraction of tracks missed the scatterer, were nevertheless photographed and produced deviations in the experimental results requiring correction. This group was used only in the study of single scattering where the results were not subject to any correction from this cause. In all the other sets of photographs, this difficulty did not arise.

The Theory of Multiple Scattering

The theory of multiple scattering has been given by Williams[2] and others. Williams considers the projection of the angle of scattering on a plane in order to facilitate comparison of the theoretical calculations with the results of cloud-chamber measurements. The distribution (Fig. 1) of this projected angle α is Gaussian in the multiple scattering region with an abrupt transition at a critical angle α_{ms} to a single scattering tail. The Gaussian portion is given by the expression

$$P_m(\alpha)d\alpha=(2/\pi\alpha_m)\exp\left[-(\alpha/\alpha_m)^2/\pi\right]d\alpha, \quad (1)$$

where α_m is the arithmetic mean angle of the Gaussian part of the curve. The distribution in (1) is obtained by superimposing the small angle

[1] W. A. Fowler, Phys. Rev. **54**, 773 (1938).
[2] E. J. Williams, Proc. Roy. Soc. **A169**, 531 (1939).
[3] C. W. Sheppard and W. A. Fowler, Phys. Rev. **56**, 849 (1939).
[4] Fowler, Gaerttner and Lauritsen, Phys. Rev. **53**, 628 (1938).
[5] Delsasso, Fowler and Lauritsen, Phys. Rev. **51**, 391 (1937).

single scattering upon a Gaussian distribution which is purely multiple scattering. To a good approximation the total scattering curve remains Gaussian out to the tail. The Gaussian distribution due to multiple scattering alone has an arithmetic mean angle $\bar{\alpha}_1$, given by

$$\bar{\alpha}_1 = \delta(\log_e M)^{\frac{1}{2}}, \quad (2)$$

where δ is a natural scattering unit angle given by

$$\delta = 2(Nt)^{\frac{1}{2}}Zr_0/\beta^2\xi \simeq 2(Nt)^{\frac{1}{2}}Zr_0(m_0c^2/W) = 12.7(\sigma/A)^{\frac{1}{2}}Z/W \text{ degrees} \quad (3)$$

and M is a dimensionless quantity giving the mean number of collisions which occur in the multiple scattering process. It is expressible as

$$M = 2\pi Z^{4/3}Nt\hbar^2/1.75^2m_0^2\beta^2c^2 \simeq 1850Z^{4/3}\sigma/A, \quad (4)$$

where N = number of atoms of scatterer per cc,
t = thickness of scatterer,
σ = superficial density in grams/cm^2,
Z = atomic number of scatterer,
A = atomic weight,
$r_0 = e^2/m_0c^2$ = classical electron radius,
βc = velocity of electrons,
$\xi = (1-\beta^2)^{-\frac{1}{2}}$,
W = kinetic plus mass energy of electrons (Mev).

The arithmetic mean $\bar{\alpha}$ of the entire distribution including the tail is

$$\bar{\alpha} = 0.80\bar{\alpha}_1 + 1.45\delta. \quad (5)$$

Williams also defines the quantity φ_2 as the angle of intersection of the multiple scattering curve whose mean angle is $\bar{\alpha}_1$ and the single scattering tail and finds it to be given by

$$\varphi_2 = 5.1\bar{\alpha}_1 - 4.0\delta. \quad (6)$$

The angle α_m described above is then found to be

$$\alpha_m = (\bar{\alpha} - \pi\delta^2/\varphi_2)(1 - \pi\delta^2/2\varphi_2^2)^{-1}. \quad (7)$$

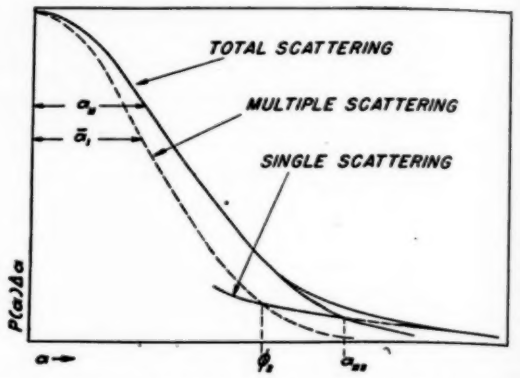

FIG. 1. Theoretical distribution of scattering according to Williams. The curve for purely multiple scattering is Gaussian with an arithmetic mean angle $\bar{\alpha}_1$. It intersects the single scattering curve at φ_2. The total scattering curve is nearly Gaussian merging at φ_2 into a single-scattering tail, taken as the sum of the two dashed curves beyond this point. α_m is the arithmetic mean angle of the Gaussian part of the solid curve. If continued beyond φ_2 it intersects the single scattering at α_{ms}. Single scattering is exaggerated for the sake of clarity.

Formulas (5), (6) and (7) have been taken from a paper by Williams to be published shortly, and are slightly more accurate for the scatterers used in these experiments than those in the previous paper. In Table I we have given the numerical values in units of δ of the above angles for the scatterers used in these experiments. The unit angle δ is given in degrees and is calculated using an effective value of Z corrected for the scattering due to extranuclear electrons, *viz.*, $Z_{eff} = (Z^2+Z)^{\frac{1}{2}}$. The value of W used in these calculations was arrived at by calculating the mean of $1/W$ for the energy spectrum of the electrons and positrons measured. This gave $\langle 1/W\rangle_{Av} = 1/21m_0c^2$ almost exactly for the data used for all scatterers. We have also included the values of M for each foil. Although the "experimental" values for M are somewhat less than those tabulated it is nevertheless clear that since $M \gg 1$ the great bulk of the scattering observed in these experiments is multiple.

TABLE I. *Numerical values of theoretical scattering angles for 10-Mev particles. Thickness t in cm, superficial density σ in g cm^{-2}, unit scattering angle δ in degrees, the last five quantities in units δ, M dimensionless.*

MATERIAL	t	σ	δ	M	$\bar{\alpha}_1$	$\bar{\alpha}$	φ_2	α_m	$\bar{\alpha}_{ms}$
Pb	0.015	0.170	2.80	539	2.51	3.46	8.80	3.17	3.28
Pb	0.038	0.431	4.47	1365	2.68	3.60	9.68	3.33	3.42
Al	0.118	0.319	1.74	666	2.56	3.50	9.08	3.21	3.35
C	0.381	0.605	1.73	1017	2.63	3.56	9.41	3.28	3.42
C	0.132	0.210	1.01	352	2.42	3.39	8.35	3.08	3.28

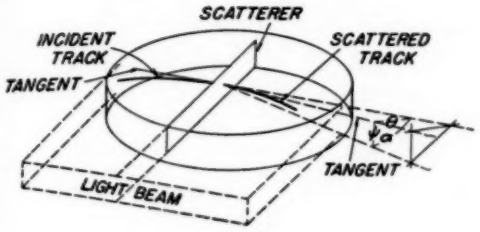

FIG. 2. Geometrical arrangement of the scattering experiment. α is the projection of the angle of scattering θ upon the plane of the cloud chamber. ψ is the vertical component of the scattering.

In Fig. 2 the geometry of the experiment is shown. The chamber is illuminated by a horizontal light beam. All tracks within the light beam are seen, disappearing when they go out of the illuminated portion of the chamber. Setting an arbitrary limit on the length of any track after leaving the scatterer imposes a limit on the vertical angle of scattering, ψ. In most of the work here reported this limit is 3 cm so that since the light beam was 1.6 cm deep we have $-15° \leq \psi \leq 15°$. This limitation does not affect the multiple scattering which is independent of the vertical angle, but changes the observed distribution of the single scattering tail. According to Williams[2] this altered distribution is

$$P_s(\alpha)d\alpha = (2\kappa/\pi\alpha^3)(\beta + \tfrac{1}{2}\sin 2\beta), \qquad (8)$$

where $\kappa = \pi\delta^2$ is the single scattering coefficient, $\tan\beta = \psi_l/\alpha = 15°/\alpha$, and ψ_l is the upward or downward limit imposed on the vertical angle in the experiment.

It is necessary to make this correction in all calculations involving the single scattering including computations of $\bar{\alpha}$. This has been done for the theoretical calculations given in Table I. The corrected $\bar{\alpha}$ Williams denotes by $\bar{\alpha}_{in}$.

MEASUREMENT OF THE SCATTERING

The measurements were made in the same manner as described by Fowler and Oppenheimer.[6] From the data recorded we were able to compute the incident and emergent energy of the scattered electron or positron, the angle of scattering in the plane of the cloud chamber, and the straight line length of path in the scatterer.

In the measurements some of the tracks appearing on the photographs were rejected for the following reasons: (a) primary track too short for accurate energy measurement. (b) track not clear near the scatterer. (c) track visibly distorted in the gas of the chamber. (d) tracks offset at the scatterer more than two millimeters. (e) old tracks too diffuse to permit accurate measurement.

In the measurements on lead all the tracks not rejected were measured irrespective of the length of the emergent track. Since little use was later made of those with a scattered length less than 3 cm these tracks were not measured in the measurements on carbon and aluminum. The later measurements on lead and those on carbon and aluminum contained a record of the direction of scattering with respect to the tangent to the incident track. As should be expected the record gave approximately as many on one side as on the other.

It is difficult to estimate the experimental error but we have endeavored to do so by using a few tracks accidentally measured twice and some material measured by two different observers. We estimate our mean error in the

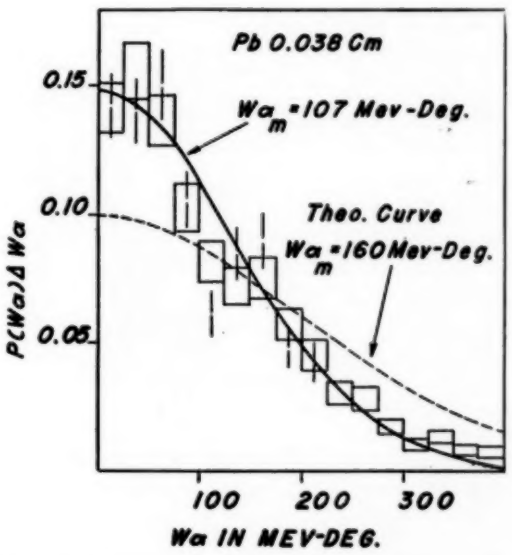

FIG. 3. Comparison of theory and experiment for Pb 0.038 cm thick. Squares represent all tracks with vertical angle of scattering between ±15 degrees. Vertical lines represent tracks of this group with vertical angle between ±7.5 degrees.

[6] W. A. Fowler and J. Oppenheimer, Phys. Rev. **54**, 320 (1938).

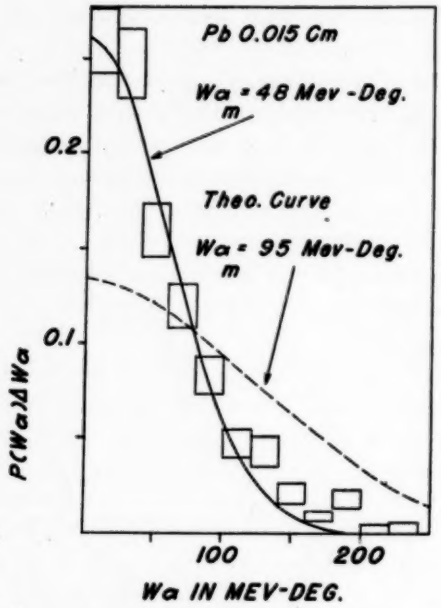

FIG. 4. Comparison of theory and experiment for Pb 0.015 cm thick. (Redrawn from the data of Fowler, reference 1.)

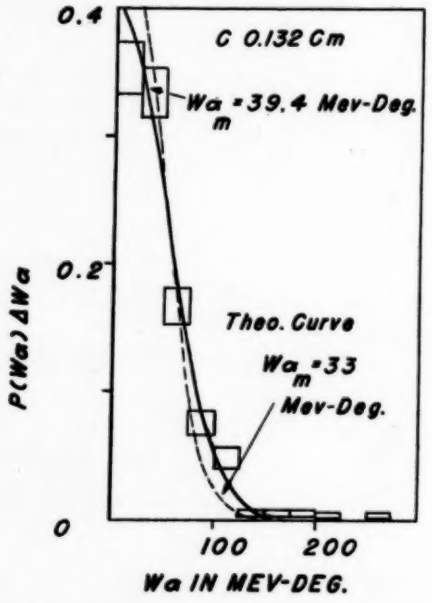

FIG. 5. Comparison of theory and experiment for C 0.132 cm thick.

measurement of the scattering angle not to exceed 1° and in the measurement of energy, 1 Mev.

COMPARISON OF THEORY AND EXPERIMENT

The electrons and positrons measured in these experiments had a rather broad distribution in energy with a maximum at a little over 10 Mev. In comparing the theoretical calculations with the scattering of particles having such a continuous distribution in energy it is profitable to rewrite (1) as follows:

$$P_m(W\alpha)d(W\alpha) = (2/\pi W\alpha_m)\exp\left[-(W\alpha/W\alpha_m)^2/\pi\right]d(W\alpha). \quad (9)$$

In this form the distribution in $W\alpha$ is theoretically independent of the total energy W since to a good approximation α_m is inversely proportional to W.

The experimental distributions in $W\alpha$ for the various foils are shown in Figs. 3, 4, 5, 6 and 7.

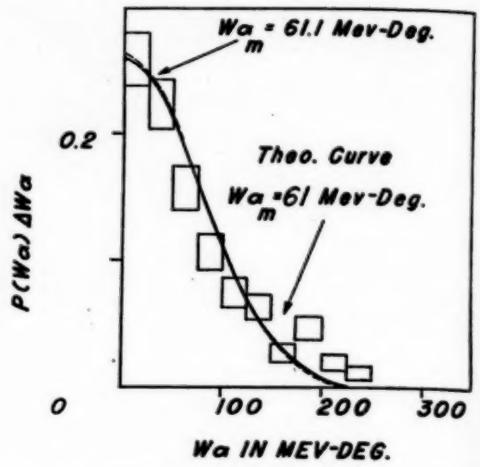

FIG. 6. Comparison of theory and experiment for C 0.381 cm thick.

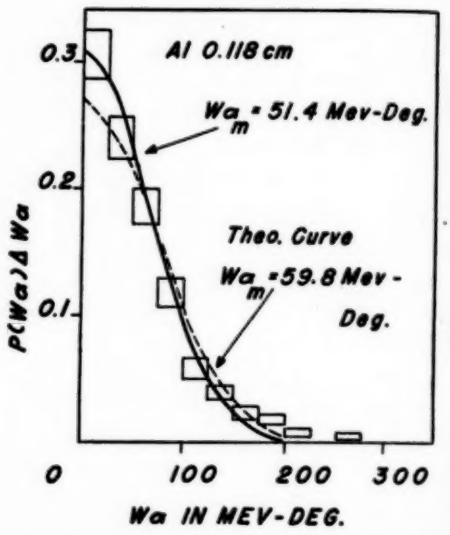

FIG. 7. Comparison of theory and experiment for Al 0.118 cm thick.

In calculating $W\alpha$ for any given track we have used for W the mean of the incident and emergent energy of the track. We have chosen to compare the theoretical and experimental values both for $\langle W\alpha\rangle_{Av}$ and $(W\alpha)_m$ (see Table II) because $\langle W\alpha\rangle_{Av}$ is the easily computed mean of the entire distribution in $W\alpha$ and $(W\alpha)_m$ is directly proportional to the observed width of the Gaussian portion of the total scattering. Theoretically these quantities are equal, respectively, to $W\bar{\alpha}_{in}$ and $W\alpha_m$ since both $\bar{\alpha}_{in}$ and α_m are to a very good approximation inversely proportional to W. Within the statistical fluctuations this is also found to be true experimentally as will be more fully discussed later.

The "corrected" experimental values given in Table II have been found by computing the square root of the difference of the squares of the observed values and the estimated mean error of measurement of $W\alpha$. In this mean error the error in the measurement of W cancels out approximately since as Professor Williams points out, the error in W is less than the mean W. Thus $\Delta W\alpha \backsimeq \bar{W}\Delta\alpha$ which we estimate to be at most equal to 10 Mev-degrees.

For the thickness of the scatterer used in computing $W\bar{\alpha}_{in}$ and $W\alpha_m$ theoretically, a value was obtained by multiplying the measured thickness by the mean of the secants of the angle of incidence of the tracks, this being found by computation from a group of 100 tracks. It was found to be 1.155. It is this corrected and a similarly corrected superficial density which are used throughout this report. No correction was made for the additional scattering path due to the scattering as for average angles of scattering of approximately 5° to 10° this is quite small. In any case it will increase the theoretical values given.

Tests of the Multiple Scattering

(1) Stereoscopic measurements

Although practically all of the measurements were made on only one of the pair of stereoscopic cloud-chamber pictures available it was felt wise to make a stereoscopic check to insure that in no way could tracks get around the scatterer and thus decrease the mean $W\alpha$. For this reason 95 tracks taken from the 0.038-cm Pb group were remeasured in a stereoscopic projector. In this measurement only those tracks were taken which traversed the scatterer within $\frac{1}{4}''$ of its center. For these tracks $(W\alpha)_m$ was found to be 99 Mev-deg. as compared with 102 Mev-degrees for all tracks measured.

(2) The vertical angle of scattering

For the small angles of scattering found experimentally it is approximately true that $\theta^2=\alpha^2+\psi^2$ where θ is the angle of scattering, α is its projection on the horizontal plane and ψ on the vertical plane. Then since $e^{-\theta^2}=e^{-\alpha^2}e^{-\psi^2}$, it is a fundamental requirement of multiple scattering that the form of the distribution with projected scattering angle α be independent of the limits placed on the vertical angle of scattering ψ by the geometry of the scattering experiment. In the measurements on the scattering in the 0.038-cm Pb foil we have determined the distribution in $W\alpha$ for all tracks with emergent length over 6 cm ($\psi_l=\pm 7.5°$) and over 3 cm ($\psi_l=\pm 15°$). Both distributions properly normalized are shown in Fig. 3. Since the mean angle of scattering is 12° the distributions pertain, respectively, to 38 percent and 68 percent of the total number of scatterings and their agreement over the range in $W\alpha$ below 200 Mev-degrees is further evidence that the observed scattering is essentially multiple.

TABLE II. *Comparison of theory and experiment. All values in Mev-degrees. Corrected experimental values represent correction for the broadening of the Gaussian curve due to an error of measurement estimated to be 10 Mev-degrees.*

Material	t in cm	Number of Tracks	Experimental		Corrected Exp.		Theoretical		Ratio of Exp. to Theo.	
			$(W\alpha)_m$	$\langle W\alpha\rangle_{Av}$	$(W\alpha)_m$	$\langle W\alpha\rangle_{Av}$	$W\alpha_m$	$W\bar{\alpha}_{in}$	$(W\alpha)_m$	$\langle W\alpha\rangle_{Av}$
Pb	0.015	362	48.0	55.0	47	54	95	98	0.50	0.55
Pb	0.038	597	107.0	117.0	106	117	160	164	0.66	0.71
Al	0.118	441	51.4	56.6	50	56	60	62	0.83	0.90
C	0.381	252	61.1	71.6	60	71	61	63	0.98	1.13
C	0.132	400	39.4	41.4	38	40	33	35	1.15	1.14

(3) Energy and sign of charge of the scattered particles

It has been previously emphasized that $(W\alpha)_m$ should be independent of the energy W. In Table III $(W\alpha)_m$ is given for two energy ranges of the observed particles. For several scatterers $(W\alpha)_m$ appears to increase definitely with energy but in no case is the difference large compared to the expected statistical fluctuations.

Since the multiple scattering is due principally to small angle single scattering which obeys the relativistic modification of Rutherford's classical scattering formula, it should be independent of the sign of the charge of the scattered particle. We have also given in Table III $(W\alpha)_m$ for both positrons and electrons. Again, the differences do not exceed the expected fluctuations.

Single Scattering

Unfortunately there are too few tracks in the single scattering region to make a satisfactory treatment of the subject possible. An approximate idea, however, could be had in the case of the scattering in the 0.038-cm lead foil. To do this we made use of the group of pictures in which the scatterer was smaller than the light beam. These were not used in the figures given for the multiple scattering. The first interval in $W\alpha$ which is increased by a large number of apparent zero angle scatterings was adjusted to fit a Gaussian curve, and when combined with the other material gave 1590 tracks. The distribution in the tail is shown in Fig. 8. For purposes of comparison the Rutherford single scattering curve has been shown as line B. The curve C represents a smooth joining of this scattering to the observed multiple scattering A. We can only conclude that in order of magnitude the single scattering is not far wrong.

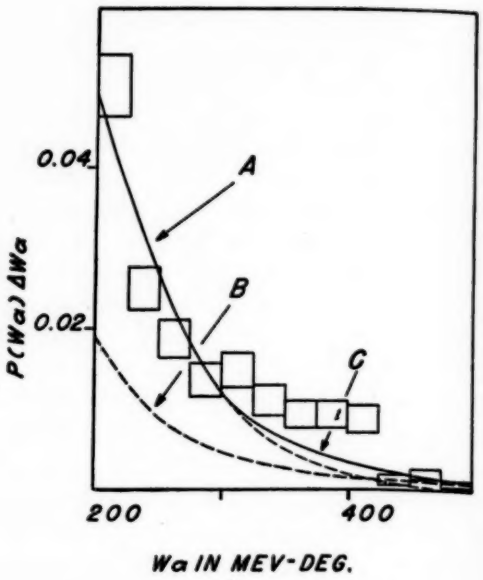

FIG. 8. Single-scattering tail for Pb 0.038 cm thick. A is the Gaussian portion of the total scattering curve. B is the theoretical single-scattering curve. An empirically selected cut-off at 375 Mev-degrees and addition to curve A gives tail C.

TABLE III. *$(W\alpha)_m$ for two energy ranges and for positrons and electrons. Values are corrected for broadening due to estimated error in angle measurement of 1°. All values in Mev-degrees.*

Material	t in cm	Energy Range 0–11 Mev	Energy Range 11–20 Mev	Positrons	Electrons
Pb	0.015	43	44		
Pb	0.038	96	114	114	103
Al	0.118	37	38	36	40
C	0.132	46	56	47	52

The Formation of High Energy Secondaries and Pairs

Although the scattering measurements on 0.038 cm lead were nonstereoscopic, a special examination of this material was also made stereoscopically in a search for high energy secondaries and pairs. We observed 1887 traversals of the lead foil. In six cases secondaries were observed which close examination of the pictures proved to be authentic and to satisfy the conservation of energy. In none of these was momentum conserved. This is to be expected since the number of scatterings after the original secondary production is not small. The total cross section is of the order of 5×10^{-24} cm². This is not in serious disagreement with the theoretical cross section 10^{-23} cm² given by $\sigma\sim2\pi r_0^2Z/W_s$ where W_s is the minimum observable energy for secondaries.

Three cases were found which at first glance seemed to indicate the production of secondary pairs. In one the positron appeared alone. Careful examination of this showed that the

track did not really intersect the primary track. In the other two cases energy was not conserved, and the energy of the pairs was close to 17 Mev which was the energy of the gamma-rays used to produce the recoil electrons. These cases were taken to be pairs produced by gamma-rays with their origin accidentally coincident with the point of traversal of an electron. The null results are in agreement with the low theoretical cross section for the process.

Conclusions

An inspection of Table II indicates that the marked discrepancy originally found between the experimental and theoretical scattering in lead has been confirmed but that a similar discrepancy has not been found in aluminum and carbon scatterers. The scattering in carbon shows a satisfactory agreement with theory. Although the scattering in the thinner carbon absorber is somewhat higher than theory permits, it is to be recalled that all of the experimental factors tend to increase the measured mean angle of scattering and for this reason we do not believe the discrepancy to be serious. For the same reason, however, it must be pointed out that the scattering in aluminum is definitely less than predicted by theory even though the deviation from theory is not nearly so great as in the case of lead.

Our new measurements on the scattering in lead, employing a thicker lead foil, indicate a definite deviation from the theoretical predictions. Although the deviation is somewhat smaller than for the original lead foil we hesitate to ascribe too much importance to this point as the measurements were made by two different observers.

Because of the discrepancy in the case of the scattering in lead we have endeavored to test the dependence of this scattering on various factors at our disposal. We have shown the mean angle of scattering to be independent to a good approximation of the vertical position of the incident track in the chamber, of the vertical angle of scattering and of the energy and sign of charge of the scattered particle. All of these findings as well as the Gaussian form of the scattering curves are readily accounted for by the multiple scattering theory and only in regard to the numerical value of the mean scattering does the theory break down.

Noted added in proof.—The recent work of Crane[7] and his collaborators at Ann Arbor can be compared with the results presented here. For electrons ranging in energy from 2 to 8 Mev they find the experimental scattering to be 0.86 of the theoretical in carbon and 0.65 in lead. For electrons of 0.9 Mev energy scattered in aluminum they find the most probable scattering angle to be only 0.75 of the theoretical value calculated by Bethe, Rose, and Smith.[8] For very thin aluminum, however, their observed mean scattering is 0.90 of the value given by Williams' theory. These results are to be compared with our average ratios for the experimental to the theoretical scattering of 1.13 for carbon, 0.90 for aluminum, and 0.63 for lead (see last column of Table II). Only in the case of the scattering in lead are the experimental results here and at Ann Arbor in sufficient agreement and in sufficient deviation from theory to warrant the assertion that Williams' theoretical calculations are in definite disagreement with the observed scattering.

Two attempts have been made recently to improve and extend Williams' calculations. Wheeler[9] has investigated the high order interference effects of the microcrystalline structure of the scattering material while Goudsmit and Saunderson[10] have proposed a new method of calculating the multiple scattering and have critically examined the effects of screening and of various approximations in Williams' theory. Both investigators report smaller theoretical values for the scattering in lead and it can be concluded that modifications of the existing theoretical calculations can still be made without necessitating a radical revision of our present

---

[7] Oleson, Chao, Halpern and Crane, Phys. Rev. **56**, 482, 1171 (1939); M. M. Slawsky and H. R. Crane, Phys. Rev. **56**, 1203 (1939).

[8] Bethe, Rose, and Smith, Proc. Am. Phil. Soc. **78**, 573 (1938).

[9] J. A. Wheeler, Phys. Rev. **57**, 358 (1940).

[10] S. Goudsmit and J. L. Saunderson, Phys. Rev. **56**, 122 (1939); **57**, 24, 73 (1940). See also A. E. Ruark, Phys. Rev. **57**, 62 (1940).

concepts of the interaction between electrons and nuclei in the elementary scattering process. In addition, we wish to emphasize that the theoretical predictions for secondary production, a process intimately connected with scattering, have been found to be in satisfactory accord with experiment.

In conclusion we wish to express our appreciation to Professors E. J. Williams, J. R. Oppenheimer, and J. A. Wheeler for correspondence and discussions concerning the theoretical aspects of the scattering problem. Our indebtedness to Professor C. C. Lauritsen is also to be acknowledged.

FEBRUARY 15, 1940 PHYSICAL REVIEW VOLUME 57

Scattering and Polarization of Electrons

M. E. Rose*
Sloane Physics Laboratory, Yale University, New Haven, Connecticut
(Received December 6, 1939)

The possibility of accounting for the small polarization of electrons, as observed in the double scattering experiments and the anomalously small scattering of fast electrons ($E \gtrsim 500$ kev) in heavy scattering materials, by the assumption of non-Coulombian forces near the nucleus is investigated. It is assumed that the range of the anomalous forces is of the order of the nuclear (or electron) radius so that for all energies of interest ($E < 2$ Mev), the range is much smaller than the wave-length of the electrons. Consequently, the scattering of only $s_{\frac{1}{2}}$ and $p_{\frac{1}{2}}$ electrons need be considered. Without any further assumptions as to the nature of the forces it is found that the phase shifts due to the deviation from the pure Coulomb field are too small to account for the observed scattering and asymmetry (relative difference between scattering at azimuth 0 and π in double scattering) unless the inside wave functions at the boundary are nearly equal to the irregular part of the outside wave functions. In general this can be the case for either the $s_{\frac{1}{2}}$ or the $p_{\frac{1}{2}}$ wave function so that either the $s_{\frac{1}{2}}$ or the $p_{\frac{1}{2}}$ waves are scattered anomalously with appreciable phase shifts, but not both. The results for the scattering and asymmetry, at 90° in Au, when only one wave is scattered are: For the scattering of $s_{\frac{1}{2}}$ waves the asymmetry has a minimum value which for low energies, 100 to 300 kev, is 5 to 6 times greater than the observations allow; at higher energies, 500 to 1500 kev the scattering intensity has a minimum value of 25 to 40 percent of the Coulomb scattering which is somewhat larger than the observed ratio but is perhaps not beyond the limits of experimental error. The asymmetry corresponding to this minimum scattering is about the same as the asymmetry for the Coulomb field, *viz.* about 5 percent at these energies. Without any measurements at high energies it is difficult to exclude the possibility that the asymmetry may be as large as this. When only $p_{\frac{1}{2}}$ waves are scattered anomalously the correct asymmetry and scattering may be obtained at low energies. At high energies the minimum scattering is 70 to 80 percent of the Coulomb scattering which seems much too large. Therefore in order to obtain an asymmetry and scattering which are not in obvious disagreement with the observations it is necessary to assume either a large range or a specialized form for the non-Coulombian forces. The specialized form must be such that either of the following may take place: (1) At low energies only the $p_{\frac{1}{2}}$ wave is scattered and at high energies only the $s_{\frac{1}{2}}$ wave is scattered. (2) Both waves are scattered at all energies despite the small range of the forces. In the first case it seems necessary to postulate an interaction which has a rather strong energy dependence in the energy region where the scattering begins to depart from the Coulombian value. In the second case it is seen that the interaction must be very large, several times $137mc^2$, and in addition a rather special energy dependence would seem necessary. Insofar as these possibilities do not seem plausible it would appear that the anomalous scattering and asymmetry must be explained on grounds other than the existence of non-Coulombian forces.

Introduction

IT has been shown by Mott[1] on the basis of the relativistic wave equation of Dirac that an initially unpolarized beam of electrons becomes polarized after a large angle scattering by a heavy nucleus. Moreover, according to the theory the polarization should effect an asymmetry about the azimuth if the beam is scattered a second time from a similarly heavy scattering material through a similarly large scattering angle. It is supposed that the effect be observed under conditions insuring single scattering.

* Sterling Fellow.
[1] N. F. Mott, Proc. Roy. Soc. **A135**, 429 (1932).

The intensity of the doubly scattered beam will, for any scattering field, be proportional to $1+\delta^2 \cos\varphi$ where φ is the azimuthal angle, (angle between the two scattering planes). The quantity δ^2 depends on the electron energy and, of course, on the scattering field. The maximum effect, relative difference between scattering at $\varphi=0$ and $\varphi=\pi$, is then $2\delta^2$ which quantity is referred to as the asymmetry of the doubly scattered beam. For scattering in Au and with the assumption of a pure Coulomb field and for both scattering angles equal to 90°, Mott's calculations show an asymmetry which reaches a rather flat maximum of 16 percent at 140 kv energy. With these scattering angles and at energies for which 13 to 16 percent asymmetry would be expected the experiments show that within the experimental error of one percent there is no asymmetry in the scattering in Au.[2]

For the scattering angles in question a deviation from a pure Coulomb field due to screening by the atomic electrons can hardly be expected to be effective. This is in fact shown by the work of Sauter.[3] An attempt to explain the discrepancy as due to the depolarizing action of (1) multiple scattering, (2) inelastic scattering with spin change of the incident electron and/or (3) exchange scattering in which the exchanged electrons have opposite spins gave entirely negative results.[4] Of these three effects the first is the most important and with the largest foil thickness used in the experiments a reduction of the asymmetry by at most 2 percent of the Mott value can be expected. Since all other *known* perturbations which may act in the scattering process are very small compared to the Coulomb field it does not seem fruitful to look in this direction for an appreciable modification of the theoretical results.

In addition to an anomalous polarization and asymmetry, the measurements of the elastic scattering of fast electrons by heavy and medium heavy nuclei also show abnormal effects for the absolute intensity. Up to energies of about 200 kev there is evidence that the scattering in both heavy and light elements is in accord with the expectations based on a pure Coulomb field.[5] For heavy scatterers, in which we are mainly interested, measurements by Dymond[2] of the 90° scattering in Au show agreement within a few percent with the theoretical value for energies up to 160 kev. The energy region in which the scattering is at least approximately Coulombian no doubt extends to somewhat higher energies (say 300 to 400 kev) as is suggested by the measurements of Chadwick and Mercier.[6] However, present evidence is that the scattering is sharply reduced for energies greater than about 500 kev and for scatterers at least as light as Kr. Thus Klarman and Bothe[7] have observed only one-fifth the Mott scattering in Kr and Xe for β-particles of energies between 500 kev and 2.5 Mev scattered at angles greater than 40°. The scattering of 400-kev−1-Mev β-particles in Hg according to Barber and Champion[8] is only about one-sixth the Mott scattering, the factor varying only slightly for different scattering angles. In rough agreement with the results of Klarman and Bothe for the scattering in Xe, Barber and Champion[9] have recently reported an anomalous scattering of 700-kev−1.2-Mev β-particles in I which they found to be about 40 percent of the Mott scattering.[10, 11]

[2] E. G. Dymond, Proc. Roy. Soc. **A136**, 638 (1932); **A145**, 657 (1934). For further references and a critical survey of the experimental work see H. Richter, Ann. d. Physik **28**, 533 (1937). Recently K. Kikuchi, Proc. Phys-Math. Soc. of Japan **12**, 524 (1939) has observed an asymmetry in Au at 75 kev which is in apparent agreement with the theoretical value of 10 percent. Actually, this experiment, if correct, would indicate an asymmetry much *larger* than theory predicts because with the thick (2×10^{-3} cm) targets used the multiple scattering will result in a large depolarization—about 80 percent (cf. reference 4 below). However, while no information was given as to precautions taken against stray electrons, x-rays, etc., it is almost certain that the instrumental asymmetry was not properly taken into account. As Dymond (cf. above) has shown, the instrumental asymmetry due to nonideal geometry can easily be as large as the theoretical asymmetry so that the whole of the Kikuchi effect might be accounted for in this way.

[3] F. Sauter, Ann. d. Physik **18**, 61 (1933).

[4] M. E. Rose and H. A. Bethe, Phys. Rev. **55**, 277 (1939).

[5] We exclude from our consideration small angle scattering where screening or multiple scattering may become of importance.

[6] J. Chadwick and P. H. Mercier, Phil. Mag. **50**, 208 (1925).

[7] H. Klarman and W. Bothe, Zeits. f. Physik **101**, 489 (1936).

[8] A. Barber and F. C. Champion, Proc. Roy. Soc. **A168**, 159 (1938).

[9] F. C. Champion and A. Barber, Phys. Rev. **55**, 111 (1939).

[10] The Mott scattering with which these authors have compared their results is the Rutherford scattering with relativistic corrections but with only first-order corrections in the fine structure constant (times atomic number) taken into account. However, the difference between this and the rigorous expression (see reference 1 and J. H. Bartlett

The existence of these two anomalies, small asymmetry and diminished scattering at high energies, has led to some speculation in regard to a possible failure of the Dirac theory. Such an eventuality does not seem plausible in the energy region under consideration and in the present paper an appeal will be made to a breakdown of the Coulomb field at small distances as a more plausible source of the difficulties. It is essential to note that the asymmetry and the scattering are not independent of each other but both depend on the same pair of scattering amplitudes (see next section). Thus, while it is evident that it is possible to introduce a deviation from the Coulomb field which will result in a small polarization and asymmetry of the twice-scattered beam,[12] it is not at all evident that the same non-Coulombian forces will account for the observed scattering as well. It is obvious that in general such will not be the case. Our purpose here is therefore to determine whether there exists a non-Coulombian interaction at small distances which is consistent with both small asymmetry and diminished scattering at large energies.

Scattering and Polarization

In the following no assumptions will be made other than the existence of a non-Coulombian field of short range. Beyond a distance of the order of the electron (or nuclear) radius the field is to be pure Coulombian. Before we investigate the scattering and polarization in such a field it will first be necessary to recapitulate some of the formalism developed by Mott[1] in the form applicable to scattering in fields which are Coulombian at large distances.

General formalism

The elastic scattering of electrons incident along the z axis with wave number k and scattered in the direction ϑ, φ by a force field which is Coulombian at large distances may be described by the asymptotic form of the third and fourth components of the Dirac wave function:

$$\psi_\nu \sim p_\nu e^{ikz} + S_\nu e^{i(kr + a \log 2kr)}/kr, \qquad a = e^2Z/\hbar v, \quad \nu = 3, 4. \tag{1}$$

Here p_ν are the components of the amplitude of the Dirac plane wave. In particular

$$p_3 = A, \qquad p_4 = B, \tag{2}$$

where A and B are constants related to the direction of the spin axis of the incident electrons and subject to the normalization condition

$$|A|^2 + |B|^2 = 1. \tag{3}$$

The general solution of the scattering problem may be obtained by a superposition of the two waves corresponding to $A=1$, $B=0$ and $A=0$, $B=1$. Mott has shown that in these two cases the asymptotic forms of ψ_3 and ψ_4 are given by

$$\psi_3 \sim e^{ikz} + f(\vartheta) e^{i(kr + a \log 2kr)}/kr, \qquad \psi_4 \sim g(\vartheta) e^{i\varphi} e^{i(kr + a \log 2kr)}/kr, \tag{4a}$$

for $A=1$, $B=0$ and

$$\psi_3 \sim -g(\vartheta) e^{-i\varphi} e^{i(kr + a \log 2kr)}/kr, \qquad \psi_4 \sim e^{ikz} + f(\vartheta) e^{i(kr + a \log 2kr)}/kr, \tag{4b}$$

for $A=0$, $B=1$. It is essential to note that the scattering amplitudes f and g, depending on ϑ alone, are the same functions in both cases.

---

and R. E. Watson, Phys. Rev. **56**, 612 (1939)), is of no great importance in view of the magnitude of the experimental error involved in the measurements.

[11] In contrast to the results described above Stepanowa, Physik. Zeits. Sowjetunion **12**, 550 (1937) finds the scattering of 200-kev−1.1-Mev β-particles in N to be 1.5 times the expected scattering and for 1.5–3 Mev 30 times the theoretical scattering. These results are in contradiction with the measurements of Champion, Proc. Roy. Soc. **A153**, 353 (1936) who found the scattering of 400-kev−1.1-Mev β-particles in N to be normal. Although this discrepancy has not been resolved and further measurements are desirable, we shall proceed on the assumption that the scattering should be in accord with the results of Champion *et al.*

[12] It has been shown by O. Halpern and J. Schwinger, Phys. Rev. **48**, 109 (1935) that the asymmetry can be made small by assuming a repulsion at a distance of the order of the nuclear radius. In a qualitative way this may be understood as an interference effect in which the polarization arising from the spin-orbit interaction in the scattering field at large distances is canceled by the contribution of that arising from small distances. The result of Halpern and Schwinger was based on the use of the Born approximation which is admittedly a poor one for the polarization. For example, for the Coulomb field the Born approximation underestimates the asymmetry by a factor of 6 or so, cf. F. Sauter, reference 3.

Then the scattering cross section per unit solid angle is

$$\Phi = I/k^2 = (|f|^2 + |g|^2)/k^2, \tag{5}$$

and the asymmetry is given by

$$2\delta^2 = 2[i(fg^* - f^*g)]^2/I^2. \tag{6}$$

Since we wish to find the scattering amplitudes f and g it is sufficient to consider the case $A=1$, $B=0$ so that we need consider only the asymptotic forms (4a). It has been shown by Mott that the wave functions with the correct asymptotic behavior are

$$\begin{aligned} \psi_3 &= i\sum_0^\infty [(l+1)e^{i\eta_l}G_l + le^{i\eta_{-l-1}}G_{-l-1}](-)^l P_l, \\ \psi_4 &= i\sum_0^\infty [-e^{i\eta_l}G_l + e^{i\eta_{-l-1}}G_{-l-1}](-)^l P_l^1 e^{i\varphi}, \\ P_l^1 &= \sin\vartheta (d/d\cos\vartheta) P_l. \end{aligned} \tag{7}$$

Here G_l and G_{-l-1} are the radial functions of the third and fourth Dirac components for $j=l+\frac{1}{2}$ and $j=l-\frac{1}{2}$, respectively. These are chosen to have the asymptotic form at large r:

$$G_\kappa \sim (kr)^{-1}\cos(kr + a\log 2kr + \eta_\kappa), \tag{8}$$

where for the Coulomb field the phase η_κ is given by

$$e^{2i\eta_\kappa} = e^{-\pi i\gamma_\kappa}\frac{\kappa+1+ib}{\gamma_\kappa+ia}\frac{\Gamma(\gamma_\kappa - ia)}{\Gamma(\gamma_\kappa+ia)}, \tag{9}$$

$$\gamma_\kappa = ((\kappa+1)^2 - \alpha^2Z^2), \quad b = a(1-v^2/c^2)^{\frac{1}{2}}, \tag{9a}$$

and we have introduced

$$\begin{aligned} \kappa &= l \quad \text{for} \quad j=l+\tfrac{1}{2}, \quad l \geqslant 0, \\ &= -l-1 \quad \text{for} \quad j=l-\tfrac{1}{2}, \quad l \geqslant 1. \end{aligned} \tag{9b}$$

Thus $\kappa=0$ and -2 for the $s_{\frac{1}{2}}$ and $p_{\frac{1}{2}}$ waves, respectively.

From (7) and (8) the asymptotic form of ψ_3 and ψ_4 may be found and a comparison with (4a) gives the amplitudes f and g.

Phase shifts in the non-Coulombian field

We now consider that the scattering field is Coulombian only for distances larger than some radius r_0 and inside r_0 has some other behavior which need not be specified. The only restriction we shall impose on the deviation from the Coulomb field is that the range r_0 shall be much smaller than all wave-lengths in which we shall be interested. For a range of order of the nuclear radius this condition will be well fulfilled for even the most energetic particles used in the scattering experiments (wave-length $\sim\hbar/mc$). It then follows that the only waves which are appreciably perturbed by the anomalous potential are the $s_{\frac{1}{2}}$ and $p_{\frac{1}{2}}$ waves both of which have the same total angular momentum, $j=\frac{1}{2}$. Moreover, since we shall be interested only in scattering angles of $\pi/2$, only the even terms in ψ_3 and the odd terms in ψ_4 (cf. 7) will enter. Therefore in ψ_3 only G_0 will change (to G_0') and in ψ_4 only G_{-2} (to G_{-2}'). In order that the wave functions have the proper asymptotic form (only outgoing spherical waves), we must have at large distances

$$\begin{aligned} G_0' &\sim (kr)^{-1}e^{i\eta_0'}\cos(kr + a\log 2kr + \eta_0 + \eta_0'), \\ G_{-2}' &\sim (kr)^{-1}e^{i\eta_{-2}'}\cos(kr + a\log 2kr + \eta_{-2} + \eta_{-2}'), \end{aligned} \tag{10}$$

where η_0' and η_{-2}' are the phase shifts introduced by the departure from the pure Coulomb field.

The scattering amplitudes may then be determined in terms of the phase shifts and we find for the asymptotic behavior of the wave functions ψ_3 and ψ_4 the form (4a) with f replaced by $f'=f+\phi_f$ and g replaced by $g'=g+\phi_g$ where the additional amplitudes ϕ_f and ϕ_g are given by

$$\phi_f=\frac{\xi_0}{1+i\xi_0}e^{2i\eta_0},\quad \phi_g=-\frac{\xi_{-2}}{1+i\xi_{-2}}e^{2i\eta_{-2}},\quad \xi_\kappa=-\tan\eta_\kappa'. \tag{11}$$

We may now establish the connection between the phase shifts and the force field by the smooth joining of the radial wave functions inside and outside $r=r_0$. Outside r_0 where the field is Coulombian, the wave function is a linear combination of the regular and irregular solutions for the Coulomb field. We write

$$G_\kappa'=(c_\kappa U_\kappa+\bar{c}_\kappa\bar{U}_\kappa)/kr. \tag{12}$$

The regular and irregular solutions times kr are denoted by U_κ and $\bar{U}_\kappa$, respectively. For the asymptotic behavior we choose U_κ and $\bar{U}_\kappa$ so that at large distances

$$\begin{aligned} U_\kappa&\sim\cos(kr+a\log 2kr+\eta_\kappa),\\ \bar{U}_\kappa&\sim\sin(kr+a\log 2kr+\eta_\kappa),\end{aligned} \tag{13}$$

and in order to obtain agreement with (10)

$$c_\kappa=e^{i\eta_\kappa'}\cos\eta_\kappa',\quad \bar{c}_\kappa=-e^{i\eta_\kappa'}\sin\eta_\kappa',\quad \bar{c}_\kappa/c_\kappa=\xi_\kappa. \tag{14}$$

We denote kr times the radial functions inside r_0 by u_κ. In the following we shall refer to the functions u_κ simply as the inside wave functions. Aside from the regularity requirement at the origin so that the integrability condition may be fulfilled no restrictions on the inside wave functions need be made. Joining the inside and outside wave functions at r_0 we have

$$\zeta_\kappa\equiv r_0(d\log u_\kappa/dr)_{r_0}=r_0[d\log(U_\kappa+\xi_\kappa\bar{U}_\kappa)/dr]_{r_0}. \tag{15}$$

The radial functions U_κ and $\bar{U}_\kappa$ may be easily found in terms of solutions of the differential equation for the confluent hypergeometric function. We find

$$U=(kr)^{-\frac{1}{2}}(\chi+\chi^*),\quad \bar{U}=-i(kr)^{-\frac{1}{2}}(\bar{\chi}-\bar{\chi}^*), \tag{16}$$

where χ and $\bar{\chi}$ are the regular and irregular solutions of

$$d^2\chi/dr^2+(k^2+k(2a-i)/r-(\gamma^2-\tfrac{1}{4})/r^2)\chi=0. \tag{16a}$$

The required solutions are

$$\begin{aligned} \chi&=e^{\pi a/2}\Gamma(\gamma+1+ia)(2^{\frac{1}{2}}\Gamma(2\gamma+1))^{-1}e^{i(\eta_\kappa-\pi/4)}M_{-ia-\frac{1}{2},\gamma}(2ikr),\\ \bar{\chi}&=e^{-\pi a/2}2^{-\frac{1}{2}}e^{i(\eta_\kappa+\pi/4)}W_{ia+\frac{1}{2},\gamma}(-2ikr),\end{aligned} \tag{17}$$

where M and W are the confluent hypergeometric functions defined e.g., in Whittaker and Watson.[13]

By virtue of the smallness of the range the arguments of χ and $\bar{\chi}$ at $r=r_0$ are very small and the behavior of these functions at the origin may be used. With

$$\left.\begin{aligned} M&\sim(2ikr)^{\gamma+\frac{1}{2}},\\ W&\sim(\Gamma(2\gamma)/\Gamma(\gamma-ia))(-2ikr)^{-\gamma+\frac{1}{2}}\end{aligned}\right\}kr_0\ll 1, \tag{18}$$

we find from (15), (16), (17) and (18)

$$\xi_\kappa=\sigma_\kappa\frac{\gamma-\zeta_\kappa}{\gamma+\zeta_\kappa}, \tag{19}$$

[13] E. T. Whittaker and G. N. Watson, *Modern Analysis* (Cambridge University Press, Third Edition, 1920), Chapter 16.

where $\gamma=(1-\alpha^2Z^2)^{\frac{1}{2}}$ is the same for both values of κ (cf. 9a and 9b), and

$$\sigma_\kappa=\frac{U_\kappa(r_0)}{\bar{U}_\kappa(r_0)}=\frac{e^{\pi a}|\Gamma(\gamma+ia)|^2}{\Gamma(2\gamma)\Gamma(2\gamma+1)}(\gamma\cot\theta_\kappa-a)(2kr_0)^{2\gamma},\quad e^{2i\theta_\kappa}=(\kappa+1+ib)/(\gamma+ia). \tag{20}$$

From the result (19) for the phase shifts and from Eq. (11) for the additional scattering amplitudes the scattering as well as the asymmetry may be determined in terms of the inside wave functions at the boundary $r=r_0$ (i.e., in terms of ζ_κ). Or more suitably the ζ_κ or ξ_κ can be determined by the condition of small asymmetry (or scattering diminished at high energies and unchanged at low energies) and then the scattering (or asymmetry) can be found from these values of ξ_κ. The question of the consistency of small asymmetry and diminished scattering is considered in the next section.

Scattering intensity and asymmetry

We denote the scattering and asymmetry in the perturbed field by I' and $2\delta'^2$, respectively, the unprimed quantities referring to the Coulomb field. Thus the scattering I' is defined (cf. 5) in terms of the elastic scattering cross section Φ', in the perturbed field, by

$$I'=k^2\Phi'=|f'|^2+|g'|^2, \tag{5a}$$

and the asymmetry $2\delta'^2$ is defined by the intensity of the doubly scattered beam which is now proportional to $1+\delta'^2\cos\varphi$. The relative difference between scattering at the azimuthal angles 0 and π is (cf. 6)

$$2\delta'^2=2[i(f'g'^*-f'^*g')]^2/I'^2. \tag{6a}$$

The scattering amplitudes f' and g' are expressed in terms of the corresponding Coulombian amplitudes, f and g, and the additional amplitudes ϕ_f and ϕ_g (cf. remarks preceding 11). It then follows that

$$I'-I=\Delta I=f\phi_f^*+f^*\phi_f+g\phi_g^*+g^*\phi_g+|\phi_f|^2+|\phi_g|^2, \tag{21}$$

$$\delta' I'-\delta I=i(f\phi_g^*-f^*\phi_g)-i(g\phi_f^*-g^*\phi_f)+i(\phi_f\phi_g^*-\phi_f^*\phi_g), \tag{22}$$

where f and g are defined implicitly in the foregoing and are given explicitly by Mott.[1] Inserting ϕ_f and ϕ_g from (11) and denoting the real and imaginary parts of f and g by the subscripts r and i we have

$$\tfrac{1}{2}\Delta I=\frac{\xi_0}{1+\xi_0^2}(\alpha_1+\alpha_2\xi_0)-\frac{\xi_{-2}}{1+\xi_{-2}^2}(\alpha_3+\alpha_4\xi_{-2}), \tag{21a}$$

where the constants α are

$$\begin{aligned}&\alpha_1=f_r\cos 2\eta_0+f_i\sin 2\eta_0, &&\alpha_2=\tfrac{1}{2}+f_r\sin 2\eta_0-f_i\cos 2\eta_0,\\ &\alpha_3=g_r\cos 2\eta_{-2}+g_i\sin 2\eta_{-2}, &&\alpha_4=-\tfrac{1}{2}+g_r\sin 2\eta_{-2}-g_i\cos 2\eta_{-2},\end{aligned} \tag{21b}$$

and

$$\begin{aligned}\tfrac{1}{2}(I'\delta'-I\delta)=&\frac{\xi_0}{1+\xi_0^2}(\beta_1+\beta_2\xi_0)+\frac{\xi_{-2}}{1+\xi_{-2}^2}(\beta_3+\beta_4\xi_{-2})\\ &+\frac{\xi_0\xi_{-2}}{(1+\xi_0^2)(1+\xi_{-2}^2)}[\beta_5(\xi_0-\xi_{-2})+\beta_6(1+\xi_0\xi_{-2})],\end{aligned} \tag{22a}$$

where the constants β are

$$\begin{aligned}&\beta_1=g_i\cos 2\eta_0-g_r\sin 2\eta_0, &&\beta_3=f_i\cos 2\eta_{-2}-f_r\sin 2\eta_{-2}, &&\beta_5=-\cos 2(\eta_0-\eta_{-2}),\\ &\beta_2=g_i\sin 2\eta_0+g_r\cos 2\eta_0, &&\beta_4=f_i\sin 2\eta_{-2}+f_r\cos 2\eta_{-2}, &&\beta_6=\sin 2(\eta_0-\eta_{-2}).\end{aligned} \tag{22b}$$

The Eqs. (21a) and (22a) must be solved in terms of a prescribed scattering and asymmetry for ξ_0 and ξ_{-2}. The values of ξ_0 and ξ_{-2} must however be consistent with the relations (19) for ξ_κ in terms of the inside and outside wave functions. From (19) we see that in general $\xi_\kappa \sim \sigma_\kappa$ and because of the small range assumed for the non-Coulombian forces, σ_κ is very small compared to unity for all energies of interest: $(kr_0)^{2\gamma} \leqslant 0.1$ for $E \lesssim 5.4$ Mev. Therefore both ξ and ξ_{-2} will in general be small of order $\sigma_\kappa \sim 10^{-2}$. While small phase shifts (or phase shifts near a multiple of π) would obviously give Coulombian scattering at small energies, neither the asymmetry (which must be materially reduced at least at small energies) nor the scattering at higher energies would be in accord with the observations.

In order to avoid this difficulty the phase shifts, or better ξ_0 and ξ_{-2}, must be large (of order unity). From (19) it is seen that this requires a logarithmic derivative of the inside wave function at the boundary differing from $-\gamma/r_0$ by terms of order σ_κ; i.e.,

$$\zeta_\kappa = -\gamma + O(\sigma_\kappa). \tag{23}$$

In general this can be the case for only one of the two waves since the two wave functions are not independent. Thus either

$$\zeta_0 = -\gamma + O(\sigma_0), \quad \zeta_{-2} \sim \sigma_{-2} \ll 1, \tag{23a}$$

and only $s_{\frac{1}{2}}$ waves are scattered appreciably, or

$$\zeta_{-2} = -\gamma + O(\sigma_{-2}), \quad \zeta_0 \sim \sigma_0 \ll 1, \tag{23b}$$

and only $p_{\frac{1}{2}}$ waves are scattered.

These conditions on the wave functions at the boundary simply mean that if one of the phase shifts is not small, the irregular part of the corresponding outside wave function is much larger than the regular part at distances small compared to the wave-length. Therefore, in joining the inside and outside wave functions the former is essentially equal to the irregular part of the latter.

We may now investigate the scattering and asymmetry in the two cases: scattering of $s_{\frac{1}{2}}$ waves or of $p_{\frac{1}{2}}$ waves. If, for example, we consider the scattering of $s_{\frac{1}{2}}$ waves we have only one parameter, ξ_0, which may be chosen so as to give the desired asymmetry at a particular energy. Then for a given choice of the non-Coulombian interaction the energy dependence of ξ_0 would be fixed by (19). However, it is more satisfactory to determine the values of ξ_0 which will give the required asymmetry (or scattering) at each energy and then require that the interaction be chosen so as to give the energy dependence for ξ_0 found in this way. Then with the phase shifts determined the scattering (or asymmetry) may be computed.

The numerical results given below will pertain to scattering at 90° in Au since these are the conditions under which most of the double scattering experiments have been carried out. Since the discrepancies observed in the scattering at angles near 90° are fairly typical of most of the angular distribution and since the calculated scattering is not very sensitive at large angles, the conclusions drawn from the results given below will apply to the scattering at other large angles and for elements of neighboring atomic number. For the observed scattering at large energies the data obtained by Barber and Champion[8] for Hg will apply. Thus we must obtain about 15 percent of the Coulombian scattering for energies of the order 500 kev or more and at smaller energies the scattering must be essentially Coulombian.

The constants α_i and β_i occurring in (21a) and (22a) were computed from numerical results for the Coulomb scattering obtained by Bartlett and Watson.[14] The asymmetry, when only one wave is scattered, is given by

$$\tfrac{1}{2}I(\delta' - \delta) = (\xi_0/1 + \xi_0^2) \times [\beta_1 - \delta'\alpha_1 + (\beta_2 - \delta'\alpha_2)\xi_0] \tag{22c}$$

for the scattering of $s_{\frac{1}{2}}$ waves and a similar expression when only $p_{\frac{1}{2}}$ waves are scattered. The results for the asymmetry and scattering are given below.

Scattering of $s_{\frac{1}{2}}$ waves.—At low energies, $E \lesssim 300$ kev, it is impossible to obtain an asymmetry in agreement with experiment. As may be seen from (22c) the asymmetry as a function of the phase shift parameter ξ_0 has a minimum. This minimum asymmetry at various energies is

E(kev)	100	150	300
$200\delta'^2$	5.64	6.56	3.70

[14] I am indebted to Professor Bartlett for making these results available to me before publication.

which is 5 to 6 times larger than the maximum allowable value. At large energies the phase shift parameter was determined so as to give the minimum scattering (cf. 21a with $\xi_{-2}=0$). This minimum scattering at various energies is

E(kev)	500	750	1000	1500
$(I'/I)_{\min}$	0.26	0.29	0.34	0.38

which is somewhat larger than the observed ratios although perhaps acceptable in view of the large experimental error involved in the measurements. The asymmetry which corresponds to this scattering is about the same as the asymmetry in the pure Coulomb field, *viz.* about 5 percent at these energies. While no measurements of the asymmetry have been made at these large energies, it is somewhat implausible that the polarization at large energies should be any greater than that at the lower energies. However, in the absence of such experimental information it seems difficult to exclude this possibility on *a priori* grounds.

Scattering of $p_{\frac{1}{2}}$ waves.—At low energies it is possible to obtain the correct scattering and asymmetry. For an asymmetry of one percent the scattering is

E(kev)	100	150	300
I'/I	0.94	0.92	0.87

which is in satisfactory agreement with the observations. However, at large energies the *minimum* scattering is much too large:

E(kev)	500	750	1000	1500
$(I'/I)_{\min}$	0.81	0.75	0.72	0.69

Thus it is seen that at low energies the scattering of $p_{\frac{1}{2}}$ waves and at high energies the scattering of $s_{\frac{1}{2}}$ waves yields results for the asymmetry and scattering intensity which are roughly in agreement with experiment. Therefore an explanation of the observations in terms of a deviation from the Coulomb field at small distances requires an interaction which will make the inside wave functions fulfill (23b) at low energies and (23a) at high energies. This would imply that the logarithmic derivatives (at the boundary) of the $s_{\frac{1}{2}}$ and $p_{\frac{1}{2}}$ wave functions vary rather rapidly in some intermediate energy range and are practically constant (equal to 0 or $-\gamma/r_0$) at other energies. Unless one assumes an interaction with a rather special type of energy dependence, this behavior of the wave functions is not to be expected. Excluding the possibility of a comparatively abrupt switch from $s_{\frac{1}{2}}$ scattering to $p_{\frac{1}{2}}$ scattering we may conclude that insofar as the experiments are correct, it is impossible to account for the observed results by assuming a small distance interaction which scatters only one of the two waves. This conclusion is, of course, not surprising since with one parameter it is in general rather difficult to account for a scattering which varies as rapidly with energy as the experiments would seem to indicate and at the same time to account for the absence of polarization as is observed in the double scattering experiments.

Scattering of $s_{\frac{1}{2}}$ and $p_{\frac{1}{2}}$ waves.—If the observed scattering and asymmetry are to be accounted for by a non-Coulombian interaction at small distances it seems plausible from the foregoing to require that both waves must be scattered with appreciable phase shifts. In this section we investigate the conditions which must be imposed on the interaction in order that both waves be scattered.

The scattering of both waves implies that for both $s_{\frac{1}{2}}$ and $p_{\frac{1}{2}}$ electrons the condition

$$\zeta_\kappa = -\gamma(1-2\sigma_\kappa/\xi_\kappa(E)+O(\sigma_\kappa^2)) \qquad (24)$$

must be fulfilled. In order that the correct scattering and asymmetry be obtained the values of ξ_0 and ξ_{-2}, regarded as independent variables, must be those obtained from the simultaneous solution of (21a) and (22a) for prescribed scattering and asymmetry. Thus (24) with the proper values of ξ_κ constitutes the necessary and sufficient condition that a small distance interaction account for the scattering and asymmetry. While it is essential that the small term proportional to σ_κ in (24) be accounted for, the first problem to be considered is the conditions under which the logarithmic derivatives ζ_κ/r_0 can be both equal to $-\gamma/r_0$ within small terms of order σ_κ. In addition to (24) it is necessary that the wave functions be regular at the origin. This requirement together with the requirement of an irregular behavior at the boundary implies that in the distance r_0 the wave functions change appreciably. This means a wave-length comparable with r_0 and hence an interaction inside r_0 which is much larger than mc^2.

The condition that the difference $\zeta_0-\zeta_{-2}$ be small can be expressed in the form

$$\zeta_0-\zeta_{-2}=-2\left[\int_0^{r_0}dr[d\log rV/dr)(u_0u_{-2}/rV)\right]\Big/(u_0u_{-2}/rV)_{r=r_0}, \tag{25}$$

$$\sim O(\sigma_s)\ll 1,$$

wherein we have assumed that the small distance interaction V can be represented by an ordinary scalar potential which is the same for both $s_{\frac{1}{2}}$ and $p_{\frac{1}{2}}$ electrons.

A solution of (25) is in general rather difficult. Certain simple cases which can be investigated do not conform to both (25) and the regularity condition at the origin. Thus (25) may be fulfilled by taking

$$d\log rV/dr=\sigma\rho(r)$$

where ρ is any regular function and of order unity for all $r\leqslant r_0$ while $\sigma\ll 1$. Then V differs from a Coulomb-like potential by terms of order σ. But then the wave-length will be the same as for a pure Coulomb field and the regularity condition cannot be fulfilled. A second example for which the wave functions can be found is the case of a constant potential. For the wave functions which are regular at the origin one finds

$$\zeta_0-\zeta_{-2}=x\cot x-\left(\frac{x^2}{1-x\cot x}-1\right),\qquad x=Vr_0/\hbar c,$$

in which we have used $V\gg mc^2$. Unfortunately there is no value of x for which (25) is satisfied.

It seems that the most plausible solution of (25) is that the interaction V is so large that several oscillations of the wave functions u_0 and u_{-2} may take place in the distance r_0, (large phase shifts!). Then since the phases of the two wave functions will usually be different and since the (variable) wave-lengths will be different, at some points the wave functions will be in phase and at other points out of phase. In this way the integral in (25) may be small by virtue of almost complete interference. The large magnitude of V resulting in many oscillations inside r_0 will allow an irregular behavior at the boundary and a regular behavior at the origin. This then would constitute a necessary though not sufficient condition on the non-Coulombian interaction.

Conditions Influencing the Intensity of the $^3\Pi - {}^1\Sigma$ Cameron Bands of CO

GEORGE E. HANSCHE
Mendenhall Laboratory of Physics, Ohio State University, Columbus, Ohio

(Received December 15, 1939)

Conditions influencing the intensity of the $^3\Pi - {}^1\Sigma$ Cameron bands of CO in emission have been studied in detail in the electrodeless ring discharge. The bands are intense in a large discharge tube at a pressure of about 0.005 mm or less. Under these conditions the mean free time between collisions of CO molecules is 2.5×10^{-6} sec. from which the lifetime of the $^3\Pi$ state is estimated as about ten microseconds. Marked increases of intensity relative to that of other band systems in the same spectral region are produced by increasing the energy of the discharge and by lowering the pressure. This indicates that the excitation function of the Cameron system differs significantly from those of the systems with which it is compared.

THE Cameron bands of CO were originally discovered[1] in a neon discharge with small quantities of carbon, oxygen, and nitrogen as impurities and were definitely ascribed to CO by Hopfield and Birge[2] who obtained them in absorption in pure CO. They were obtained in emission in the pure gas for the first time by Knauss and Cotton[3] who used an electrodeless discharge in a large flask at low pressure. The levels involved in the transition were known to be $^3\Pi \rightarrow {}^1\Sigma$, from analyses of other systems, before the rotational analysis by Gerö[4] verified the designation. The low probability of a transition of this kind accounts for the nonappearance of the bands in emission reported by Hopfield and Birge[2] and by Herzberg.[5] To study in greater detail the conditions influencing the intensity of the Cameron bands in emission, the present work was undertaken.

EXPERIMENTAL

The discharge tube used in the present work was a twelve-liter Pyrex flask with a quartz window attached to a side arm by means of a quartz-to-Pyrex graded seal. Surrounding the flask was a helix of copper tubing which constituted the inductance of the continuous wave oscillator described by Knauss and Cotton,[3] modified to use an FP-3 triode (type 849) with a maximum plate dissipation of 400 watts. The plate voltage was supplied by a 2000-volt d.c. generator, and was controlled by varying the generator field current. Power input to the oscillator was recorded in terms of plate current and plate voltage.

Pure CO gas was obtained by passing the vapor of concentrated formic acid over P_2O_5 which dehydrates the HCOOH molecule, and also removes water vapor. A needle valve made airtight by means of a sylphon bellows was used to control the flow of gas from the generator to the discharge tube. A liquid-air trap, a McLeod gage, a mercury diffusion pump, and a Hyvac backing pump were used in the usual way to control and measure the pressure. A second liquid-air trap was used between the gas generator and the discharge tube. Constant pressure was maintained during each exposure while gas was being pumped through the system.

The effect of using a smaller discharge tube was noted by comparison with spectra obtained with apparatus of Knauss and McCay,[6] in which a cylindrical vessel 6 cm in diameter served as a discharge tube. No definite evidence of Cameron bands was ever obtained from the smaller tube, hence the present experiments were carried out entirely in the large tube.

The effect of changing the frequency of the oscillator could be studied by replacing the $5\frac{1}{2}$-turn helix by one of $2\frac{1}{2}$ turns, the corresponding frequencies being 6000 and 10,500 kilocycles per second, respectively.

[1] W. H. B. Cameron, Phil. Mag. **1**, 405 (1926).
[2] J. J. Hopfield and R. T. Birge, Phys. Rev. **29**, 922 (1927).
[3] H. P. Knauss and J. C. Cotton, Phys. Rev. **38**, 1190 (1931).
[4] L. Gerö, Zeits. f. Physik **109**, 204 (1938).
[5] G. Herzberg, Zeits. f. Physik **52**, 815 (1928).
[6] H. P. Knauss and M. S. McCay, Phys. Rev. **52**, 1143 (1937).

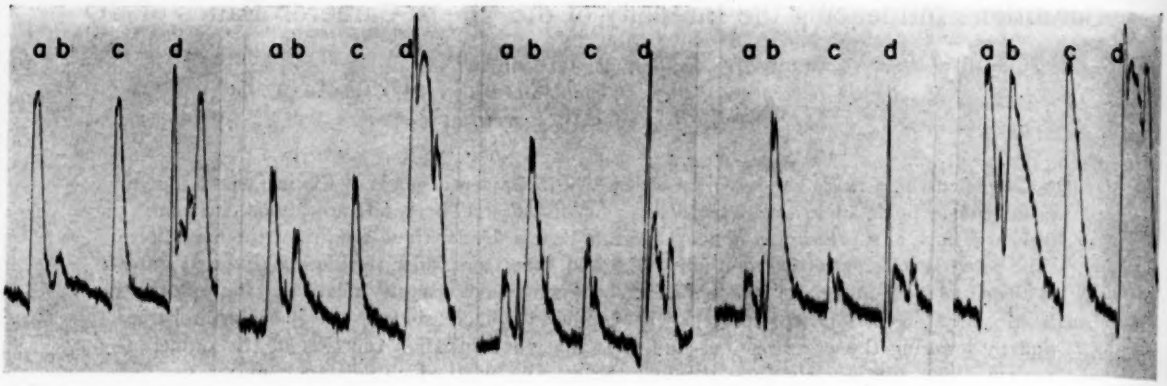

FIG. 1 FIG. 2 FIG. 3 FIG. 4 FIG. 5

FIGS. 1–5. Microphotometer traces of the following CO bands: *a*, (4,12) fourth positive; *b*, (0,1) Cameron; *c*, (5–13) fourth positive; *d* (0,0) first negative (CO^+). For exposure data see Table I.

A Steinheil quartz prism spectrograph of about 40-cm focus produced the spectra in the region 2000 to 3200A on a single 18-cm plate. Eastman ultraviolet sensitizing solution was used to extend the range of Eastman 40 plates to short wave-lengths. A Moll recording microphotometer was employed for comparing intensities.

RESULTS

Variations in the intensity of the Cameron bands in comparison with neighboring band systems were studied in some fifty exposures, planned so as to distinguish between the effects of pressure, power input, and frequency. To illustrate the results, the region 2150–2190A, containing bands of the Cameron, the fourth positive, and the first negative systems has been chosen, since the quartz spectrograph has good dispersion in this region, and the bands included respond to changes of pressure and power input in a way which is typical of the systems to which they belong. Microphotometer traces of this region photographed under a variety of conditions are presented in Figs. 1–5, with exposure data in Table I.

In Figs. 1–4 the power input was kept constant at 10 watts, and the exposure times were chosen on the basis of the visual appearance of the glow to compensate somewhat for the decreased brilliancy at lower pressures. A most striking change in relative intensity of the Cameron bands occurs with a comparatively small change in pressure, namely from 0.003 to 0.002 mm of mercury, as shown in Figs. 2 and 3. At the higher of the two pressures, Fig. 2, the (0,1) Cameron band is considerably less intense than its neighbors, and at the lower pressures, Fig. 3, it is more intense. This marked change in relative intensity within such a small range of pressures was quite unexpected, but was verified by repeated trials.

The effect of increased power input to the oscillator is illustrated by Fig. 5, made with 300 watts input at a pressure of 0.005 mm. By comparison with the other figures, it is apparent that a higher power input increases the relative intensity of the Cameron bands, or from another point of view, produces a given relative intensity at a higher pressure. Thus, the relative intensities obtained in Fig. 5 at 300 watts input could be obtained at 10 watts by reducing the pressure one-half.

Attempts to influence the results by substituting a frequency of 10,500 kilocycles for 6000 kilocycles failed to show any difference in behavior. The exposures illustrated were all made with the $5\frac{1}{2}$-turn helix, at the lower frequency. It was noticed with the aid of a wave

TABLE I. *Exposure data for Figs. 1–5.*

FIG.	TIME (HOURS)	PRESSURE (MM)	ENERGY INPUT (WATTS)	FREQUENCY (KILOCYCLES/SEC.)
1	0.5	0.04	10	5960
2	1.5	0.003	10	6030
3	4.0	0.002	10	6060
4	2.0	0.0005	10	6100
5	0.05	0.005	300	6200

meter that the frequency changed slightly as discharge conditions were changed. The frequency of the oscillator was raised by either lowering the pressure or increasing the input, the observed values associated with the discharges of Figs. 1 and 5 being 5960 and 6200 kilocycles per second, respectively.

Discussion

The occurrence of Cameron bands in a large discharge tube (diameter 35 cm) and their nonoccurrence in smaller tubes (diameter 6 cm and less) can be explained as follows. The upper electronic state, $^3\Pi$, is metastable with respect to the only level below it, the $^1\Sigma$ ground state of the molecule. The transition from a triplet to a singlet state is a violation of the selection rule according to which the resultant spin, and therefore the multiplicity, remains unchanged during a transition. This is not a strict rule; the probability of transitions contrary to this rule is small but not zero. Thus if a CO molecule in the $^3\Pi$ state is given a long enough time before impact, the probability of a radiative transition is greater. In a small tube, impacts with the walls occur before radiation, and at higher pressures, impacts with other molecules; in either case the energy of excitation can be lost without radiation.

An estimate of the lifetime of the excited state may be based on the mean free time between impacts under the discharge conditions at which the Cameron bands are intense. From data on mean free path and molecular velocity at NTP quoted by Loeb,[7] values can be computed for a discharge pressure of 0.005 mm as in Fig. 5, and a temperature of 85°, an estimated discharge temperature based on the observations of Knauss and McCay.[6] Under these conditions, the mean free path is about 1.4 cm, the velocity is 5.6×10^4 cm/sec. and the corresponding mean free time is 2.5×10^{-5} sec. The lifetime of the $^3\Pi$ state is presumably less than this, or of the order of ten microseconds.

It will be noted that the computed mean free path for the conditions under which Cameron bands are intense in the large tube is only half the radius of the small 6-cm discharge tube in which they are missing. This may mean that the assumptions used in computing the mean free path are not quite correct, or that the hypothesis suggested above for the nonappearance of the bands in the small tube is not adequate.

The effect of higher oscillator energies in increasing the relative intensity of the Cameron bands likewise suggests that more is involved than merely the chance of losing excitation energy by impact before radiation can occur. The proportion of molecules excited to the $^3\Pi$ state must vary somehow when the energy of the electron impacts is changed. That is, the excitation function of the Cameron bands, which is simply the way in which the emitted intensity depends on the energy of the exciting electrons, must differ in character from the excitation functions of the fourth positive and the first negative bands. Apparently an increase in average electron energy increases the intensity of the Cameron system much more than that of the other two systems. The present experiments do not yield direct information about the excitation functions of band systems, but merely indicate that there must be significant differences in the forms of the functions for the three band systems in question.

It should be noted that mere change of pressure in the electrodeless discharge could cause a change in the energy distribution of electrons, since at lower pressures the electrons being accelerated in the high frequency field could pick up more energy before impact, on the average. Possibly considerations of this kind, combined with the change in probability of a radiationless escape from the $^3\Pi$ state with changing pressure, can be made to account for the very marked effect of small pressure changes on the relative intensity of the Cameron bands.

The author wishes to express his appreciation to Professor H. P. Knauss for suggestion of the problem, and valuable advice. He is also grateful to Mr. A. T. Owen for undertaking preliminary experiments and to Professor J. B. Green for valuable suggestions.

[7] L. B. Loeb, *The Kinetic Theory of Gases* (McGraw-Hill, New York, Second edition, 1934), p. 651.

The Normal Electron Configuration of Singly Ionized Gadolinium

W. E. ALBERTSON, HENDRIK BRUYNES AND RICHARD HANAU
George Eastman Research Laboratory of Physics, Massachusetts Institute of Technology, Cambridge, Massachusetts
(Received December 16, 1939)

The normal electron configuration of singly ionized gadolinium is established as $4f^7 5d6s$. The quantum numbers of the energy levels are deduced from a study of Zeeman effect patterns obtained with a field of 81,500 gauss.

INTRODUCTION

THE normal electron configuration of gadolinium is known to be $4f^7 5d6s^2$.[1] On ionization, one would expect either the $5d$ or a $6s$ electron to be removed. There is also the possibility of the $4f$ shell becoming relatively more stable on ionization, enabling the capture of an electron to give a configuration of $4f^8 6s$ or $4f^8 5d$. In the cases of samarium[2] and europium,[3] a $6s$ electron is removed on ionization of the neutral atom.

Many violations of the Hund rule for the lowest term of an electron configuration are known for excited electron configurations, but no violation has yet been found among the hundreds of normal electron configurations that are now known. According to the Hund rule, the four most likely normal electron configurations of Gd II should yield the following for the lowest terms:

$4f^7 5d6s - {}^{10}D,\ {}^{8}D,\ {}^{8}D,\ {}^{6}D,$
$4f^7 6s^2 - {}^{8}S,$
$4f^8 6s - {}^{8}F,\ {}^{6}F,$
$4f^8 5d - {}^{8}H,\ {}^{8}G,\ {}^{8}F,\ {}^{8}D,\ {}^{8}P,\ {}^{6}H,\ {}^{6}G,\ {}^{6}F,\ {}^{6}D,\ {}^{6}P.$

Accordingly, the lowest term of Gd II should be one of ^{10}D, ^{8}S, ^{8}F or ^{8}H. It should be noted that $4f^7 5d6s$ (the one expected to be normal by analogy with samarium and europium) is the only one that gives a decet term, namely a lone ^{10}D.

EXPERIMENTAL

The senior author had been engaged for some time in a fruitless attempt to discover the normal electron configuration of Gd II, when the large Bitter magnet[4] was installed in the spectroscopy laboratory of this institute. At the same time Dr. A. S. King at the Mount Wilson Observatory in Pasadena made available to us his most recent furnace temperature classification of lines of the gadolinium spectrum.[5]

Electrodes composed of a silver-gadolinium mixture were prepared by first pressing and then sintering a silver powder-gadolinium salt mixture. We are indebted to Professor John Wulff for their preparation. With these electrodes, Zeeman effect photographs were obtained with

TABLE I. *Calculated and observed Landé g values in* Gd II.

TERM TYPE	J VALUE	g VALUE CAL.	g VALUE OBS.
$a^{10}D^\circ$	2½	2.57	2.57
	3½	2.10	2.10
	4½	1.88	1.88
$z^{10}F$	1½	3.20	3.13
	2½	2.23	2.17
	3½	1.90	1.86
	4½	1.76	1.79

TABLE II. *Energy levels in* Gd II.

TERM TYPE	J VALUE	ENERGY CM^{-1}	TERM TYPE	J VALUE	ENERGY CM^{-1}
$a^{10}D^\circ$	2½	0.00	$z^{10}F$	1½	25,960.08
	3½	261.87		2½	26,211.92
	4½	633.28		3½	26,595.22
	5½	1158.95		4½	27,162.22
	6½	1935.31		5½	27,864.50
				6½	29,353.33
$a^{8}D^\circ$	2½	3082.02	$z^{10}D$	2½	28,629.02
	3½	4483.89		3½	29,242.22
	4½	4852.36		4½	30,027.39
	5½	4841.14		5½	30,101.36
				6½	32,946.23

[1] W. E. Albertson, Phys. Rev. **47**, 370 (1935).
[2] W. E. Albertson, Phys. Rev. **52**, 644 (1937); Astrophys. J. **84**, 26 (1936).
[3] W. E. Albertson, Phys. Rev. **45**, 499 (1934); H. N. Russell and A. S. King, Astrophys. J. **90**, 155 (1939).
[4] F. Bitter, Rev. Sci. Inst. **7**, 479 (1936); G. R. Harrison and F. Bitter, Phys. Rev. **57**, 15 (1940).
[5] A. S. King, unpublished material.

TABLE III. *Multiplets in* Gd II.

WAVE-LENGTH I.A.	WAVE NUMBER CM^{-1}	INTENSITY	COMBINATION
			$a^{10}D^{\circ}-z^{10}F$
3759.011	26,595.21	40	$2\frac{1}{2}-3\frac{1}{2}$
3716.369	26,900.36	80	$3\frac{1}{2}-4\frac{1}{2}$
3671.216	27,231.20	200	$4\frac{1}{2}-5\frac{1}{2}$
3545.794	28,194.41	200	$5\frac{1}{2}-6\frac{1}{2}$
3813.981	26,211.91	200	$2\frac{1}{2}-2\frac{1}{2}$
3796.393	26,333.34	200	$3\frac{1}{2}-3\frac{1}{2}$
3768.405	26,528.93	100	$4\frac{1}{2}-4\frac{1}{2}$
3743.484	26,705.52	200	$5\frac{1}{2}-5\frac{1}{2}$
3646.196	27,418.06	300	$6\frac{1}{2}-6\frac{1}{2}$
3850.981	25,960.07	200	$2\frac{1}{2}-1\frac{1}{2}$
3852.467	25,950.06	150	$3\frac{1}{2}-2\frac{1}{2}$
3850.703	25,961.95	150	$4\frac{1}{2}-3\frac{1}{2}$
3844.584	26,003.27	125	$5\frac{1}{2}-4\frac{1}{2}$
3855.581	25,929.10	20	$6\frac{1}{2}-5\frac{1}{2}$
			$a^{8}D^{\circ}-z^{10}F$
4251.741	23,513.18	300	$2\frac{1}{2}-3\frac{1}{2}$
4408.261	22,678.33	80	$3\frac{1}{2}-4\frac{1}{2}$
4344.313	23,012.15	20	$4\frac{1}{2}-5\frac{1}{2}$
4078.465	24,512.13	150	$5\frac{1}{2}-6\frac{1}{2}$
4322.195	23,129.91	20	$2\frac{1}{2}-2\frac{1}{2}$
4521.303	22,111.34	12	$3\frac{1}{2}-3\frac{1}{2}$
4481.068	22,309.87	100	$4\frac{1}{2}-4\frac{1}{2}$
4342.191	23,023.40	300	$5\frac{1}{2}-5\frac{1}{2}$
4369.775	22,878.07	80	$2\frac{1}{2}-1\frac{1}{2}$
4601.067	21,728.02	100	$3\frac{1}{2}-2\frac{1}{2}$
4597.922	21,742.88	100	$4\frac{1}{2}-3\frac{1}{2}$
4478.812	22,321.11	80	$5\frac{1}{2}-4\frac{1}{2}$

WAVE-LENGTH I.A.	WAVE NUMBER CM^{-1}	INTENSITY	COMBINATION
			$a^{10}D^{\circ}-z^{10}D$
3418.735	29,242.23	150	$2\frac{1}{2}-3\frac{1}{2}$
3358.628	29,765.54	150	$3\frac{1}{2}-4\frac{1}{2}$
3392.534	29,468.06	80	$4\frac{1}{2}-5\frac{1}{2}$
3145.006	31,787.26	100	$5\frac{1}{2}-6\frac{1}{2}$
3491.967	28,628.99	100	$2\frac{1}{2}-2\frac{1}{2}$
3449.628	28,980.36	40	$3\frac{1}{2}-3\frac{1}{2}$
3401.060	29,394.19	20	$4\frac{1}{2}-4\frac{1}{2}$
3454.149	28,942.43	40	$5\frac{1}{2}-5\frac{1}{2}$
3223.740	31,010.95	40	$6\frac{1}{2}-6\frac{1}{2}$
3524.21	28,367.07	80	$3\frac{1}{2}-2\frac{1}{2}$
3494.418	28,608.91	100	$4\frac{1}{2}-3\frac{1}{2}$
3462.99	28,868.54	40	$5\frac{1}{2}-4\frac{1}{2}$
3549.365	28,166.04	200	$6\frac{1}{2}-5\frac{1}{2}$
			$a^{8}D^{\circ}-z^{10}D$
3913.79	25,543.47	6	$3\frac{1}{2}-4\frac{1}{2}$
3959.437	25,249.00	30	$4\frac{1}{2}-5\frac{1}{2}$
3557.062	28,105.09	80	$5\frac{1}{2}-6\frac{1}{2}$
4037.906	24,758.34	125	$3\frac{1}{2}-3\frac{1}{2}$
3971.077	25,174.99	20	$4\frac{1}{2}-4\frac{1}{2}$
3957.681	25,260.20	150	$5\frac{1}{2}-5\frac{1}{2}$
4140.454	24,145.16	12	$3\frac{1}{2}-2\frac{1}{2}$
4098.912	24,389.86	80	$4\frac{1}{2}-3\frac{1}{2}$
3969.28	25,186.39	40	$5\frac{1}{2}-4\frac{1}{2}$

a field of 81,500 gauss at a dispersion of 0.8A/mm throughout the range λλ2400–3900A. Although the gadolinium lines were fairly faint, several lines were completely resolved, with all of their Zeeman effect components showing, enabling the unique determination of both the J values and g values of the levels involved.

RESULTS

A term array was discovered which accounted for all of the low and nearly all of the middle temperature class Gd II lines. All of the low temperature lines were classified in a single multiplet ^{10}DF, of which the ^{10}D was the lowest term in the array. The quantum numbers of this term are established beyond a doubt, the J values by counting the number of components of the resolved patterns, and the L and S values from the excellent agreement between experimental and Landé g values, as is shown in Table I. The fact that all of the fundamental lines of the spectrum are now classified casts serious doubt on the proposition that levels lower than those of the ^{10}D exist. From arguments stated above, it is clear that $4f^{7}5d6s$ is the normal electron configuration of Gd II. Of the other terms from this configuration, fragments of the two ^{8}D terms have been found. The excitation of the $6s$ to a $6p$ electron gives the electron configuration $4f^{7}5d6p$, which yields the triads ^{10}FDP, ^{8}FDP, ^{8}FDP, ^{6}FDP. Of these, the ^{10}F and ^{10}D terms are definitely established, as well as numerous unidentified levels.

The energy levels are given in Table II, and the multiplets in Table III. The wave-length measurements are taken from the M.I.T.-W.P.A. Wavelength Tables.[6] The temperature classifications are from King.[7]

CONCLUSION

In addition to those already acknowledged, we wish to thank Professor G. R. Harrison for the Zeeman effect photographs and for making wave-length data available to us previous to publication.

[6] G. R. Harrison, *Wavelength Tables* (Wiley & Sons, 1939.)

[7] A. S. King, Astrophys. J. **72**, 221 (1930).

The Dielectric Constant of Water Vapor at a Frequency of 42 Megacycles

ANGUS C. TREGIDGA*
California Institute of Technology, Pasadena, California
(Received September 18, 1939)

A heterodyne beat apparatus was constructed for the measurement of the dielectric constant of water vapor at 42 megacycles. One of the oscillators was crystal-controlled, the other having a tuned circuit containing a condenser which could be evacuated and filled with water vapor. A cathode-ray oscilloscope was used to indicate zero beat. Drift of the oscillators was eliminated from the results by plotting readings on a time base and alternating between vacuum and water vapor as rapidly as physical limitations would permit. Air was used as the calibration gas, because it is composed of nonpolar molecules. It should therefore have the same dielectric constant at this frequency as at the lower frequencies at which it has been measured by other observers. The Clausius-Masotti relation was verified for water vapor at constant temperature, and the dielectric constant of water vapor determined at three different temperatures and 760 mm of mercury. The temperatures in question were 71.9°C, 99.8°C, and 147°C, at which the dielectric constant was found to have the values 1.0071, 1.0060, and 1.00475, respectively.

INTRODUCTION

ALL previous investigations of the dielectric constant of water vapor have been made at frequencies less than two megacycles. Although it was not expected that the dielectric constant would be appreciably different at 42 megacycles from the lower frequency value, yet it was thought desirable actually to measure the dielectric constant at this higher frequency. This information is to be used in a research problem on the variation of signal strength between short wave radio stations at Pasadena and Palomar.

EXPERIMENTAL METHOD

The method used in the present research involves the heterodyne beat principle invented by Pungs and Preuner;[1] a signal from a standard oscillator being heterodyned with the note from a test oscillator, which had a frequency very close to that of the standard oscillator. This test oscillator (see Fig. 1) was a symmetrical Hartley arrangement whose tuned circuit contained three condensers in parallel, namely, the gas condenser C_g, the measuring condenser C_m, and the tuning condenser C_t. These were all parallel-plate condensers, the latter two being of the split-stator type, with grounded rotor. The frequency of the test oscillator could be changed by the introduction of water vapor between the plates of the gas condenser, and then this change could be compensated for by a change in the measuring condenser.

The standard oscillator consisted of a crystal oscillator circuit followed by a frequency multiplying arrangement to quadruple the frequency. The crystal used was a Western Electric AT cut crystal rated at 10.58330 megacycles and this frequency was practically independent of temperature variations.

The measuring condenser was of very small capacity, having the range 2.0 to 2.1 micro-microfarads. This was specially constructed so as to be rigid and symmetrical, and was well shielded. It was driven with a National vernier drive, which enabled the setting to be read to one part in 5000, and was calibrated at 42 megacycles in terms of arbitrary capacity units.

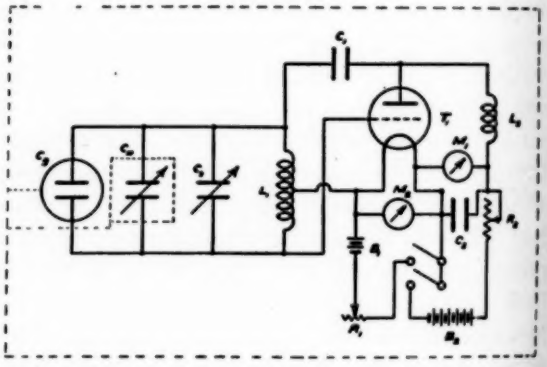

FIG. 1. Circuit of the test oscillator. C_g = gas condenser; C_m = measuring condenser; C_t = tuning condenser.

* Now at Kansas State College, Manhattan, Kansas.
[1] L. Pungs and G. Preuner, Physik. Zeits. 20, 543 (1919).

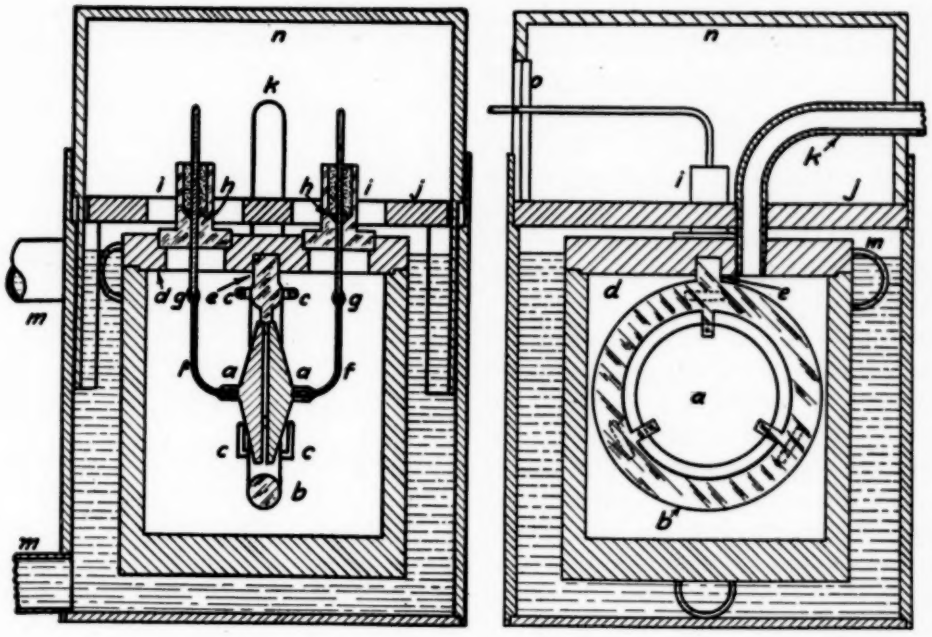

FIG. 2. The gas condenser. *a*, Invar condenser plates. *b*, quartz spacer ring. *f*, flexible leads. *i*, glass bushings. *k*, pipe leading to water vapor system. *m*, oil pipes.

The gas condenser is shown in Fig. 2, which shows mutually perpendicular diametral sections of it. The parallel-plate condenser which formed the nucleus of the arrangement was composed of two Invar plates *a*, 1½ inches in diameter, which were made conical in form to give mechanical strength while keeping the edge effects small. The plates were spaced 0.04 inch apart by the three equidistant quartz pins projecting from the quartz ring *b*. Bronze leaf springs hooked behind the lugs *c* to hold the plates in position. These springs are not shown in the figures.

The cylindrical brass container in which this assembly was mounted was of extremely heavy section, this being necessary in order to prevent distortion on evacuation. The quartz ring hung from the lid of the container by the joint *e* which was made with litharge-glycerine cement. The leads to the condenser were made of very flexible "pigtail" wire. The vacuum seal at this point was made by the glass bushings *i* which were ground plane on their lower surfaces and which fitted snugly into the holes machined to receive them. They were coated with glyptal on the ground surface before assembling and were then baked in situ. The leads were cemented into the bushings with litharge-glycerine cement and the whole outer surface of the container and bushings coated generously with glyptal and allowed to become thoroughly dry. This container was supported from the lid of the oil bath *j* by the brass pipe *k* which was threaded and soldered into both lids. Thus the condenser was doubly shielded electrically in the best manner by this arrangement and was also freed more thoroughly from external mechanical disturbances. The brass pipe also provided the connection to the water vapor system.

The plates of the condenser were at first made of brass, but it was found that small thermal fluctuations produced changes in size of the plates, the resulting capacity changes being by no means negligible. Therefore in the final form Invar plates were used.

The shielding of the oscillator had to be complete, so it was necessary to use dry batteries as the source of power, and to bring no leads or pipes out of the cabinet which were not at ground potential. This made it impossible to heat and stir the oil bath from the inside of the cabinet, so this bath was made in two parts, with the stirring, heating, and temperature regulating being done in the part outside the cabinet. Connection between the two parts of the bath was by

means of two ½-inch brass pipes *m*, the upper one, by which the oil entered, being offset to cause a whirling motion of the oil and consequent rapid temperature equalization. A mercury thermostat was used to control the temperature. The inner bath was fitted with a heavy copper cap *n*, the lower portion of which was beneath the level of the oil, and the whole bath was covered with a layer of felt in order that the bushings and leads should be at the temperature of the oil.

The water vapor used in the experiment was generated in a small bulb, which was evacuated and partly filled with liquid water. This bulb was situated in a thermostated water bath and could be connected through an electrically heated copper pipe to the gas condenser. The heating of the pipe ensured that the bulb was the coolest part of the water vapor system, and hence that the pressure of the vapor was that of saturated water vapor at the temperature of the bath. A $\frac{1}{10}$th-degree thermometer was used to determine this temperature. Connections were such that the condenser could readily be evacuated without evacuating the bulb.

The two oscillators were loosely coupled to the grid of a detector tube, the coupling condensers consisting merely of a few inches of insulated wire twisted together. The beat note generated in this mixer tube was then amplified and impressed on the plates of an RCA oscilloscope. This made it possible to determine the position of zero beat with very great precision, for under these conditions the pattern on the screen was a motionless straight line which would jump up and down as drift started to take place.

At the high frequency at which these measurements were made the total capacity of the resonating circuits had to be small, and hence stray capacities were of far greater importance than at a lower frequency. It was not permissible to measure these stray capacities at zero frequency and assume them to be the same as those existing at 42 megacycles because at this high frequency wires grounded at one end may have an appreciable capacity to ground, which they do not possess at zero frequency. It would therefore be very difficult to make an absolute determination of the dielectric constant at this frequency. A relative measurement was therefore made using air as the calibrating gas. Many

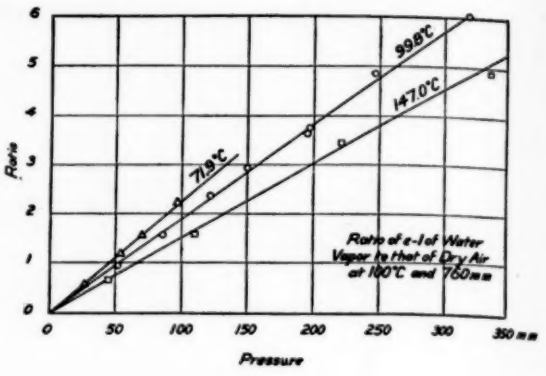

FIG. 3.

measurements have been made on air at lower frequencies, and since it is composed of nonpolar molecules, its dielectric constant should have the same value at 42 megacycles as at lower frequencies. This assumption is substantiated by the fact that the refractive index of air as measured spectroscopically at frequencies in the infra-red region, leads to a value of the dielectric constant in this region which is the same as the value observed directly at lower frequencies.[2]

The method of taking readings was designed to remove the effects of drift as completely as possible. This meant alternating between vacuum and water vapor as rapidly as the physical limitations would permit. Before starting a run it was necessary to wait for the establishment of thermal equilibrium throughout the system and to adjust the various voltages until the drift was as small as it could be made. Then the stopcock was turned so as to evacuate the gas condenser and readings of the measuring condenser setting for zero beat were taken every minute for 8 minutes or so, after which the gas condenser was connected with the bulb and readings taken for 8 minutes or so under this condition, and then the bulb was evacuated again, and so forth. Runs were of about an hour's duration. These readings were plotted on a time base, and the resulting curve corrected with the calibration curve of the measuring condenser to give a curve showing the difference, in arbitrary capacity units, between zero beat settings under the two conditions of the gas condenser, namely, vacuum and water vapor. The mean value of this last curve was taken as the correct value under the conditions of the run.

[2] D. Bender, Phys. Rev. **54**, 179 (1938).

The calibration runs were taken with air in exactly the same manner, the air being dried and freed from carbon dioxide by passing through sulphuric acid, sodium hydroxide, calcium chloride, and phosphorous pentoxide. Seven such calibration runs were made, and the mean of these was used to give the ratios plotted in Fig. 3, which is a plot of the ratio of the quantity $(\epsilon-1)$ for water vapor to that for dry air at 76 cm of mercury and 100 degrees centigrade.

Conclusions

According to the theory given by Clausius and Masotti, the quantity $(\epsilon-1)$ should vary linearly with the density of the gas for nonpolar molecules. The results given in Fig. 3 show that this relation is also true for water vapor at constant temperature since the isothermal curves are all straight lines.

Assuming a value of 1.000425 for the dielectric constant of air at 76 cm and 100 degrees centigrade,[3] the slopes of the lines in Fig. 3 correspond to values of the dielectric constant of water vapor of 1.0071 at 76 cm and 71.9°C; 1.0060 at 76 cm and 99.8°C; 1.00475 at 76 cm and 147°C. Of these, the value at 99.8°C is the most reliable, as more points were taken to determine it. The value found by Sanger[4] was $1+(0.600+3507/T)$ (density) and the present results agree with this within the limits of accuracy of the experiment.

Acknowledgment

The author wishes to express his gratitude to Dr. S. S. Mackeown who directed the research; to Dr. I. S. Bowen for his many helpful suggestions during the progress of the investigation; and to the California Institute of Technology for the use of its research facilities.

[3] H. E. Watson, Proc. Roy. Soc. **A143**, 558 (1934).
[4] R. Sanger, Helv. Phys. Acta **1**, 359 (1928).

FEBRUARY 15, 1940 PHYSICAL REVIEW VOLUME 57

The Thermionic Constants of Tungsten as a Function of Crystallographic Direction

M. H. Nichols*
George Eastman Research Laboratory of Physics, Massachusetts Institute of Technology, Cambridge, Massachusetts
(Received November 10, 1939)

A method is described for recrystallizing tungsten wire into long single crystals occupying the whole cross section of the wire and so oriented that one of the face diagonals is parallel to the axis of the wire. The temperature dependence of the emission associated with the different crystal directions has been investigated for one such specimen and fitted to the empirical equation $i_0=A^*T^2\exp(e\varphi_0/kT)$. The values of φ_0 range from 4.35 volts for the (111) crystal direction to 4.65 volts for the (110) crystal direction. The values of A^* range from 125 for the (112) and (001) directions to 15 for the (110) direction. A possible explanation for the low values of A^* is suggested. These results show that the values of φ_0 and A^* obtained from the usual measurements on polycrystalline wire are characteristic of a weighted average of the properties of the various crystal surfaces occurring and have, therefore, only empirical value, indicating that all attempts to relate observed to theoretical values of emission constants have so far no great significance.

Introduction

THE work of Johnson and Shockley[1] and later of Nelson[2] and Martin[3] has shown that the high field thermionic emission from pure and caesiated tungsten surfaces depends upon the crystallographic direction normal to the emitting surface. Up to the present, all quantitative measurements of the thermionic constants of metallic surfaces have been made on polycrystalline specimens. Thus the results obtained are characteristic only of a weighted average of the properties of the various crystal faces exposed, making the interpretation of the results exceedingly complex.

* Now National Research Fellow at Princeton University.
[1] R. P. Johnson and W. Schockley, Phys. Rev. **49**, 439 (1936).
[2] R. B. Nelson, M.I.T. Doctor's Thesis. (Soon to be published.)
[3] S. T. Martin, Phys. Rev. **56**, 947 (1939).

Martin's[3] work with a system consisting of a small sphere, essentially a single tungsten crystal, surrounded by a concentric spherical fluorescent screen is of particular interest because it shows that of all the possible crystallographic directions normal to the surface of the sphere, the only ones possessing important characteristic thermionic properties are the (001), (110), (111), and (112) crystal directions. It has been known for some time that on account of the pure tensile stress experienced by the crystal grains near the center of a tungsten wire as it is drawn through the dies, these grains show a preferred orientation; namely, that in which one of the (110) directions coincides with the wire axis. Nelson[2] has shown that it is possible to recrystallize tungsten wire, polycrystalline as it comes from the dies, in such a way that crystals occupying the whole cross section of the wire are produced with this preferred orientation. This orientation makes all the crystal directions which have Miller indices of the form (hhk), which includes all the directions found to be thermionically important by Martin, normal to the surface of a smooth wire.

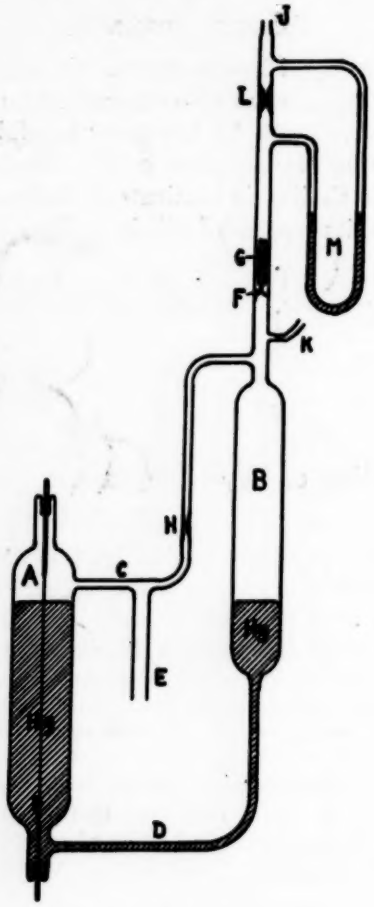

FIG. 1. Crystal growing apparatus.

With Nelson's method for obtaining a properly oriented "seed" crystal, long single crystals have been produced in pure tungsten wire by a method to be described here. Quantitative thermionic measurements upon one such crystal have yielded values of the thermionic constants for the different crystal directions normal to the surface of this wire.

PRODUCTION OF SINGLE CRYSTAL WIRES RETAINING THE PREFERRED ORIENTATION

For a number of years single crystal tungsten wire has been produced by the firms of Julius Pintsch and others. In general, the method consists of passing a polycrystalline tungsten wire, including suitable fluxing agents, through a steep temperature gradient. This process yields single crystals, meters long, which occupy the whole cross section of the wire. Unfortunately, they contain relatively large amounts of impurity from the fluxing agent. This fact, together with the random orientation of the crystals, makes these commercial products unsuited for experimental use. The procedure set forth in the following is simply to extend a "seed" crystal, produced with the proper orientation by Nelson's method, by passing it through a steep temperature gradient.

Two Pyrex tubes *A* and *B* (of Fig. 1) of about the same diameter are mounted with interconnecting tubes *C* and *D*. The tube *E* leads to the vacuum system. A raw polycrystalline tungsten wire (G.E. No. 218, five-mil), having been ground and polished to remove the die marks,[4] is mounted with suitable springs in tube *A*. The thin-walled glass tube *F* seals *B* from the mercury manometer and the capillary leak *L*. A mercury distilling apparatus is connected at *K*. After the tubes have been evacuated and baked, mercury is distilled in until the levels are somewhat as indicated in the drawing. The still is

[4] R. P. Johnson, A. B. White, and R. B. Nelson, Rev. Sci. Inst. 9, 253 (1938).

then sealed off. Tank hydrogen, from which the water vapor, oxygen, and hydrocarbon vapors have been removed by passing through hot copper shot and then through a trap filled with glass beads and immersed in liquid air, is admitted through the fore vacuum end of the system until atmospheric pressure is reached. Liquid air is kept on the traps at all subsequent times. The system is flushed with hydrogen several times before the final charging.

Up to this time, the raw wire has not been heated above 1000°K, and has retained its polycrystalline nature. In order to produce a crystal seed possessing the proper orientation relative to the axis of the wire and lying just above the mercury surface in tube *A*, Nelson's[2] heat treatment process is used. The temperature of the wire is raised to 1000°K by passage of an alternating current and raised in steps of about 100° each half-hour thereafter until the temperature is about 2600°K. The presence of the hydrogen cools the surface of the hot wire so that a temperature gradient exists between the center and the surface of the wire. From a measurement of the power dissipated by a five-mil wire at 2000°K in an atmosphere of hydrogen, it has been calculated that the center of the wire is about one degree hotter than the surface. In such a small wire this slight temperature difference represents a considerable gradient which is favorable to the growth of crystals in the radial direction. Under these conditions, crystals start from parent grains near the center of the wire and grow rapidly toward the cooler outer portions. Thus crystals are obtained which occupy the whole cross section of the wire and retain the preferred orientation of their parents.

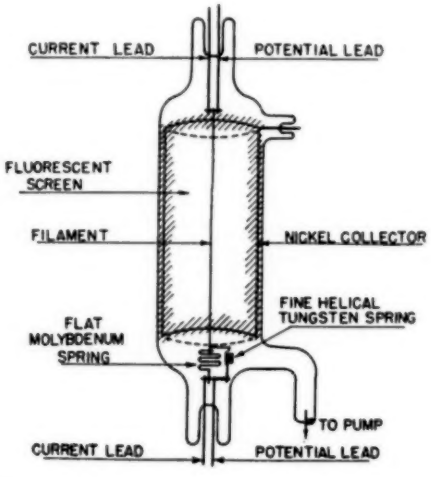

FIG. 2. One-dimensional electron projection tube.

FIG. 3. Photograph of the projection tube in which was mounted the single crystal wire used for the measurement of the thermionic constants reported in this paper. The two white marks set off the portion of the crystal upon which the measurements were taken.

Presumably a crystal seed with its (110) crystal axis coinciding with the axis of the wire now exists in the wire at the surface of the mercury in tube *A*. Tube *C* is then sealed off at the constriction *H* leaving tube *A* and tube *B* connected only by tube *D*. The pressure in tube *A* is reduced slightly thus insuring an "overlap" of the seed. The thin-walled tube *F* is then broken by the magnetic hammer *G*, thus connecting the capillary leak *L* and the mercury manometer *M*, which is across the capillary, to tube *B*. *A* Hyvac pump is connected to *J* through an adjustable leak, thereby maintaining the pressure difference across the capillary leak at any desired value under one atmosphere.

During the rest of the process, the wire is held at 2600°K. Since the wire is immersed in hydrogen, a very steep temperature gradient exists at the surface of the mercury. As the hydrogen is slowly removed from tube *B* through the capillary leak *L*, the mercury slowly falls in *A*, thereby moving the steep temperature gradient down the length of the wire and extending the crystal seed with it. A temperature of 2600°K and lowering speeds of 1 inch per hour down to $\frac{1}{8}$ inch

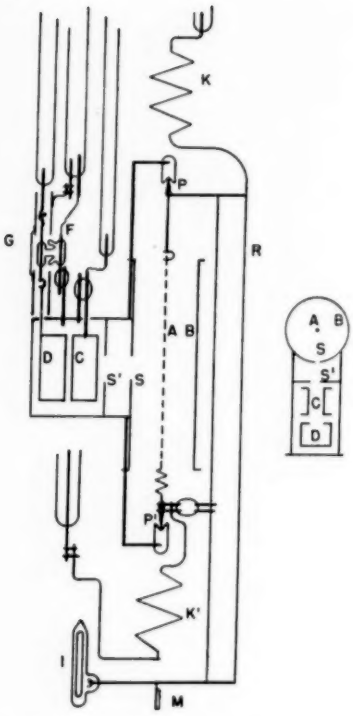

FIG. 4. Cross section and top view of tube used to measure the thermionic constants for the different crystal directions. This shows the single crystal wire *A* mounted in the rotor *R* so that it can be rotated in front of the slit *S* cut in the side of the cylindrical anode *B*.

per hour were found to give fairly satisfactory results.

After the mercury lowering process is completed, the wire must be heated for several hours in hydrogen at the advanced temperature of about 2950°K to absorb into the body crystal numerous small surface crystals.

After the completion of the heat treatment the wire is transferred to an electron projection tube. These tubes were developed by Johnson and Shockley[1] and later further by Nelson[2] and Martin.[3] Fig. 2 taken from Nelson's thesis shows a typical one-dimensional projection tube. The applied electric field between the filament and the fluorescent screen is radial, so that if a sufficiently high field is used, the thermal electrons emitted by the filament travel in straight lines radially to the screen. Thus, the illumination at any part of the screen is a qualitative measure of the emission of the portion of the filament having the same cylindrical coordinates of azimuth and distance along the wire axis provided, of course, that the filament is round.

A regular pattern on the fluorescent screen possessing the symmetry properties of a cubic crystal with one of its face diagonals along the axis of the screen (two reflection planes at right angles) indicates the presence of a single crystal in the corresponding position on the wire.

Figure 3 is a photograph of a projection tube in which was mounted the wire upon which the thermionic measurements set forth in the following section of this paper were made. The large single crystal is about 9 cm long. The two horizontal lines show the region of the wire from which the thermionic data were taken. Photomicrographs of the surface of the wire will be shown in the next section.

Precautions are necessary to obtain a smooth surface on the recrystallized wire. The hydrogen must be free from oxygen, water vapor, and hydrocarbon vapors because these active etching agents give a very rough surface to the wire. It is for these reasons that the crystal-growing apparatus was designed in the form set forth above, since in this form each step can be carried out with the requisite cleanliness and purity of materials.

Apparatus for Measuring the Thermionic Constants of Single Crystal Wire

The tube used to make the quantitative thermionic measurements was designed and constructed by Dr. R. B. Nelson but was rebuilt to incorporate certain refinements. The metallic parts of the tube are all of tantalum except for leads and springs. The envelope is of Pyrex.

Figure 4 is a schematic diagram of the metallic parts of the tube. A sufficiently high voltage is applied between the single crystal filament *A* and anode *B* to cause the thermal electrons from the filament to proceed radially in straight lines to the anode *B*. Those electrons whose trajectories are in line with the slit system *SS'* pass through to the collector *D* and are measured. The radial voltage gradient in the neighborhood of the wire *A* must be large compared to the local gradients set up by the differences of work function of the various crystal directions. Also, the voltage must be high enough to render insignificant the initial thermal velocities of the electrons. The lower voltage limit of the tube

turned out to be about 1000 volts. The upper limit set by field emission difficulties is about 3500 volts. Between these limits the tube showed no polarization or leakage difficulties. In this voltage range a negative potential of 800 volts relative to the anode B on the electrode C was found to eliminate slow secondary electrons from the slits SS' and to keep slow secondaries from leaving the collector D. A positive potential of 180 volts on the guard rings G keeps stray electrons from reaching the lead to the collector. The rotor frame R supports the wire A and is pivoted at the points PP' with tungsten pivots and glass bearings. Rotor R can be rotated about PP' from outside the tube by causing an electromagnet to attract the laminated soft iron rod I which is sealed in a Pyrex envelope, thus bringing the different crystal directions of the single crystal in A into alignment with the slit system SS'.

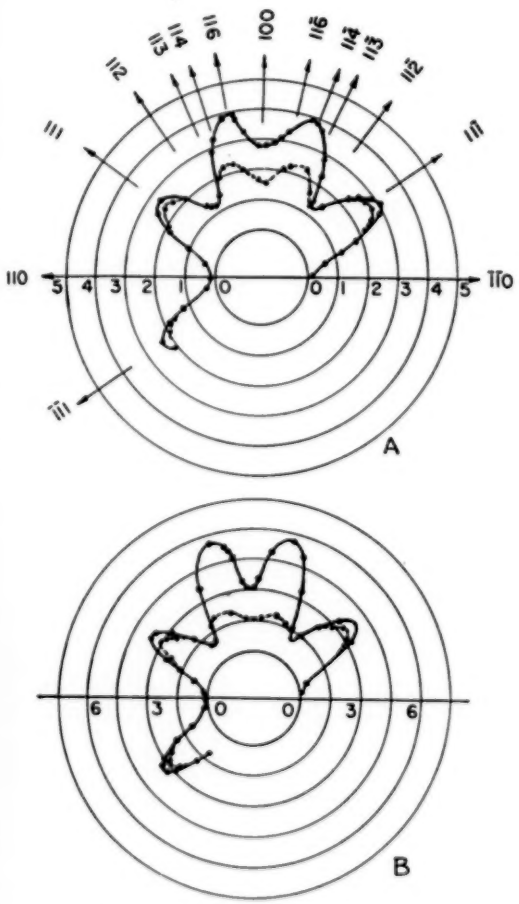

FIG. 5. A, emission *versus* angle at 1880°K; B, at 1480°K. Applied surface gradient 60,000 volts/cm.

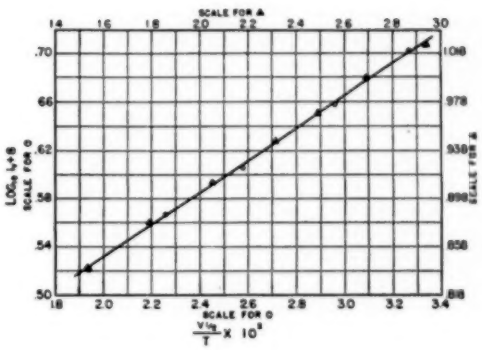

FIG. 6. Schottky plot for the (111) direction. Δ Data at 1890°K; o data at 1450°K.

The mirror M permits the measurement of the angles through which the crystal has been rotated. The tantalum spirals KK' serve to conduct the heating current through the wire and yet permit the free rotation of the rotor R. The glass insulator F which supports the collector system D is of special design.[5] The resolving power of the slit system and the optical system used to measure the angles through which the crystal is rotated is about three degrees.

The whole metallic system is suspended from a single tungsten-to-glass press; all the remaining leads, of which there are six, are flexible thus permitting the glass envelope to change its shape freely, as it does to a certain extent during the baking process, without throwing any of the parts out of alignment. The tube was gettered with barium-aluminum getter and sealed from the vacuum system before the measurements were taken. The technique used in the preparation of the structural parts for vacuum and the schedule of evacuation have been described by Nottingham.[6]

The direct current used to heat the filament A was supplied from storage batteries and accurately measured by use of a Leeds and Northrup type K potentiometer and a standard tenth-ohm resistor. The diameter of the wire, which must be accurately known, was measured by an interferometer and checked by weighing a measured length. From the value of the density of tungsten given by Jones and Langmuir,[7] these two methods agree to within two-tenths percent.

[5] W. B. Nottingham, Phys. Rev. **55**, 203 (1939).
[6] W. B. Nottingham, J. App. Phys. **8**, 762 (1937).
[7] H. A. Jones and I. Langmuir, Gen. Elec. Rev. **30**, 310, 354, 408, (1927).

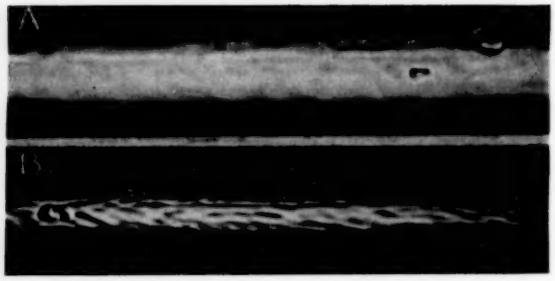

FIG. 7. A, photomicrograph of single crystal wire looking down the (001) direction; B, ten degrees off the (110) direction.

The Forsythe-Watson[8] temperature scale was used to determine the temperature of the middle section of the wire A. Over the range used, no end corrections were needed. The anode-to-filament voltage was supplied from a filtered kenotron rectifier and measured by use of the type K potentiometer and a precision voltage divider. The electrometer method used to measure the collector current over a range of 10^{-5} to 10^{-14} ampere is described by Nottingham.[5]

EXPERIMENTAL RESULTS

By rotating the single crystal wire to different positions in front of the slit system SS', the yield of thermal electrons from the different directions can be measured. The dependence of emission upon crystal direction is shown in Fig. 5A at 1880°K and in Fig. 5B at 1480°K. The emission before the wire was heated above 2500°K, after mounting in the final tube, is given by the combination of dotted and solid lines. For angles where the dotted lines do not show, the emission remained constant through further heat treatment. The solid lines show the values after heat treatment up to 2650°K. Little is known about the behavior of single-crystal surfaces undergoing heat treatment in a vacuum. Because of the possibility of an irreversible change in the surface structure at higher temperatures, a complete set of data was taken after the 2650°K flashing but before the wire was raised to higher temperatures. It is upon this set of data that the thermionic constants which are tabulated in the following are based. There was no need for repeating the measurements since the emission at any point did not change more than 5 percent even after an aggregate of 6 minutes at 2900°K and 2 minutes at 2960°K. The 30-second, 2900°K flashes were alternated with ten to twelve-hour heatings at 1800° to 2000°K.[9] The data collected here indicate, to the extent of the heat treatment given the wire during the measurement period, that no surface changes which affect the thermionic properties have taken place.

The polar emission diagrams show perfect symmetry of a cubic crystal with one of the face diagonals along the axis of the wire. The angles at which the various crystal directions cut the surface of the wire have been calculated and drawn into the polar diagram. To within the resolving power of the slit system and the optical system for measuring the angles (about 3°) these crystal directions agree with the maxima and minima found. This shows the presence of a nearly perfect crystal in a round wire. A back reflection Laue x-ray photograph down the (111) crystal axis of the wire was taken and checked the crystal orientation. This assignment of crystal directions is in perfect agreement with the results of Martin's[3] spherical system and Nelson's[2] cylindrical system, both sets of results having been corroborated by x-ray determination of the directions. Although the peaks of the two maxima on either side of the (001) direction occur very near the (116) directions, it is doubtful if they can be characteristic of any one given crystal direction because the (115), (117), etc.,

TABLE I. *Thermionic constants for the various crystal directions of tungsten. The estimated error in the determination of the φ_0 is about 0.5 percent. This means that the error in A^* is about ten percent.*

MILLER INDICES	φ_0	A^*	S
1 1 1	4.37	36	12.5
1 1 $\bar{1}$	4.35	41	11.5
$\bar{1}$ $\bar{1}$ $\bar{1}$	4.36	30	13.0
1 1 2	4.66	125	11.1
1 1 $\bar{2}$	4.66	125	11.2
1 1 6	4.35	56	11.7
1 1 $\bar{6}$	4.36	51	10.7
0 0 1	4.53	117	10.5
$\bar{1}$ $\bar{1}$ 0	4.65	15	9.6

[8] W. E. Forsythe and E. M. Watson, J. Opt. Soc. Am. **24**, 114 (1934).

[9] E. A. Coomes, Phys. Rev. **55**, 519 (1939).

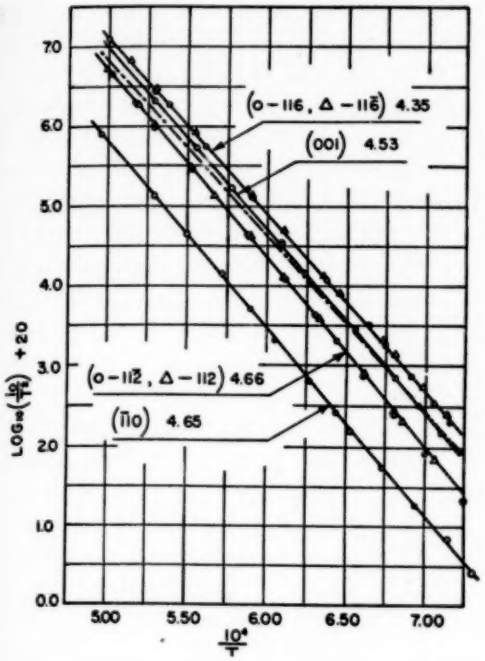

FIG. 8. Composite Richardson plot for the different crystal directions on the same scale. The broken line represents the emission from the (111) direction.

crystal directions come so close to them. Nevertheless, they will be labelled as (116).[10]

To enable the reduction of the high field emission values to "zero field" values, the dependence of the emission on the anode filament voltage for each maximum and for each minimum occurring on the polar plot was investigated for two different temperatures. Fig. 6 is a representative plot showing the voltage dependence of the emission in the (11$\bar{1}$) direction at 1890°K and 1450°K. The two sets of data are superimposed to show the agreement of slope. The data follow the well-known law derived from the Schottky mirror-image theory:

$$\log_{10} i_v = \log_{10} i_o + SV^{\frac{1}{2}}/T,$$

where i_v is the high field emission, i_o the "zero field" emission, and V the voltage. The constant S depends on the geometry of the emitter and collector system. For the system used here, assuming that the filament is perfectly round and smooth, the theoretical value of S is 10.5. Actual experimental values differ somewhat from this value presumably on account of surface irregularities of the wire. Surface projections will make for a larger S, whereas surface depressions of the order of magnitude of, or greater than, the resolving power of the collimating slits will make for a smaller S. The values of S as determined graphically from the Schottky plots for the various crystal directions are tabulated along with the other thermionic constants in Table I. These values of S were used to calculate the "zero field" emission i_o.

Figure 7A is a photomicrograph of the crystal wire looking down the (001) direction. This region of the wire is smooth and gives a value of S very nearly the theoretical value. Figure 7B is a photomicrograph taken ten degrees off the (110) direction and indicates a flat region normal to the (110) direction. This flatness explains the low S for this region. The furrowed surface on either side of the (110) direction extends nearly to the (111) direction. From an inspection of many specimens, it seems that this surface configuration is general for wire heat treated in the fashion set forth here.[2, 11] Until more is known about the surface structure of tungsten filaments, it is better to think of the thermionic data presented

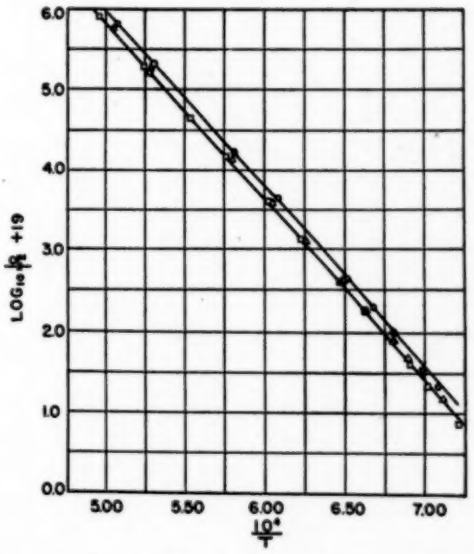

FIG. 9. Richardson plot for the three duplicate (111) directions. ○ data for (11$\bar{1}$) direction. □ data for (111) direction. Δ data for ($\bar{1}$11) direction.

[10] The work of Nelson, reference 2, and Martin, reference 3, did not point conclusively to the minimum in the (001) direction. However, Professor W. B. Nottingham has recently informed me that his projection tube data from aged crystals show a definite minimum in the (001) direction.

[11] R. P. Johnson, Phys. Rev. **54**, 459 (1938).

here as associated with different crystal directions rather than with the ideal crystal faces normal to these directions because one cannot as yet be sure that the actual surfaces normal to these directions are "pure," i.e., that an actual surface normal to a given crystal direction is made up solely of the ideal crystal face normal to this direction.

The temperature dependence of the emission from each maximum and each minimum was investigated. Using the values of S in Table I, the "zero field" emission can be calculated. These "zero field" values were fitted to the empirical formula

$$i_o = aA^*T^2 \exp\left[-e\varphi_0/kT\right],$$

where A^* and φ_0 are constants and a the area of the wire from which the emission comes. The value of a is calculated from the wire diameter and the dimensions of the slits. Fig. 8 is a composite plot of $\ln_{10} i_o/T^2$ *versus* $10^4/T$ for the various crystal directions showing the variation in slope and ordinates. Fig. 9 is a composite plot of the data from the three duplicated (111) directions. The two directions show good agreement, but the third, the $(11\bar{1})$ direction, exhibits higher ordinates but has the same slope as the other two. To within experimental error, the data for each direction lie on a straight line, φ_0 being determined from its slope. Knowing φ_0, $\log_{10} A^*$ is computed by selecting any one point exactly on the straight line. As seen from Table I, the variation in emission is accounted for by changes in both A^* and φ_0. For completeness it should be pointed out that Mendenhall and De Voe[12] under great experimental difficulties obtained the value of 4.35 electron volts for the photoelectric work function of a (310) crystal direction and 4.50 for a (112) direction.

Since there is a variation of 0.3 volt in the value of φ_0 over the various crystal directions, there will be relatively large tangential voltage gradients just outside the wire. For the case of the five-mil wire used here, the most rapid 0.3-volt change takes place in about twenty degrees, assuming each different crystal face is pure, giving tangential gradients of the order of 150 volts per centimeter. However, the data upon which the φ_{10} are based were taken with radial gradients of 60,000 volts per centimeter, so the effect of the tangential fields is negligible.

The Schottky mirror image theory of the voltage dependence of work function holds for pure polycrystalline tungsten surfaces from a surface gradient of about 2500 volts per cm[13] up to the order of a million volts per cm where field emission begins to set in. It is not unreasonable that the surface fields between the various crystal faces exposed cause the deviation of experiment from theory for gradients under 2500 volts per cm.[14] Certainly, from the very nature of the theory, the agreement for lower gradients should get better, if the surface is homogeneous in nature, i.e., a single crystal face. Making the reasonable assumption that the Schottky mirror image theory is correct, for a surface of all one crystal face, down to zero field, the i_o really represent zero field emission. By this method of measuring i_v at high field and using the Schottky theory to extrapolate to zero field emission i_o, the effect of the neighboring crystal faces on the behavior of electrons emitted from a given face has been eliminated.

Discussion

For a detailed interpretation of the empirical constants A^* and φ_0 the reader is referred to papers by Herzfeld,[15] Wigner,[16] and Becker and Brattain.[17] The values of φ_0 reported here closely represent the work required to remove an electron from the top of the Fermi band at zero degrees Kelvin to a distance outside of a homogeneous crystal face, this distance being large compared to the lattice constant but small compared to the dimensions of the crystal face. The differences between the φ_0 for the different crystal directions may be interpreted as being caused by differences in the nature of the double layers formed on the various crystal faces. The double layers are set up by the lack of symmetry of the electron distributions around the surface ions, and are such that they generate a constant potential inside the metal. However, the potential

[12] C. E. Mendenhall and C. F. De Voe, Phys. Rev. **51**, 346 (1937).

[13] W. B. Nottingham, Phys. Rev. **49**, 78 (1936).
[14] J. A. Becker, Rev. Mod. Phys. **7**, 95 (1935).
[15] K. F. Herzfeld, Phys. Rev. **35**, 248 (1930).
[16] E. Wigner, Phys. Rev. **49**, 696 (1936).
[17] J. A. Becker and W. H. Brattain, Phys. Rev. **45**, 694 (1934).

outside the metal is not constant but varies in such a way that the potential differences between the outer neighborhoods of different crystal faces are equal to the differences in the moments of their respective double layers.

As was mentioned before, the Schottky mirror-image theory of the voltage dependence of the work function does not hold for polycrystalline tungsten surfaces for surface gradients under about 2500 volts per centimeter.[13] Probably the most complete discussions of this deviation have been given by Becker[14] and Nottingham.[13] Becker found, if he assumed for a polycrystalline surface a checker board surface in which alternate checkers possessed different work functions, that the emission from such a surface would deviate from the Schottky theory in the same general way as actual polycrystalline surfaces have been found to deviate. In fact, if he chose the size of his checkers to correspond roughly to the grain size of polycrystalline tungsten wires (about 10^{-4} cm) and the difference in work function of adjacent checkers to be about 0.5 volt, he obtained good agreement with experiment for thoriated tungsten surfaces. Of course, the theory holds just the same for pure tungsten surfaces in which case it appears, from the data presented in Table I of this paper, that the differences in work function between the adjacent checkers should be of the order of several tenths of a volt. For a more detailed discussion the reader is referred to Becker's and Nottingham's papers; but it is perhaps not out of place to give a brief qualitative explanation of this deviation for pure polycrystalline tungsten on the basis of the data set forth in this paper.

Let x_0 be the distance from a plane homogeneous tungsten surface at which the image forces on the electron just equal the force of the externally applied electric field. Thus $x_0=\frac{1}{2}(e/E)^{\frac{1}{2}}$. For $E=1{,}000{,}000$ volts/cm, $x_0=19(10)^{-8}$ cm. For $E=60{,}000$ volts/cm (the surface gradient at which the Richardson data for this paper were taken) $x_0=76(10)^{-8}$ cm, and at $E=2500$ volts/cm, $x_0=380(10)^{-8}$ cm. The different crystal faces appearing in this polycrystalline surface will be roughly the same size as the grains. For the polycrystalline samples upon which thermionic measurements have been made, the grain size is known to be about 10^{-4} cm. Table I shows that the maximum difference in φ_0 between facets is at least 0.3 volt. On account of the difference in contact potential between neighboring facets, the potential for an electron just outside a facet of low work function will be lower than the potential outside a facet of high work function. Roughly speaking then, if x_0 is very small compared to the facet size (10^{-4} cm), that is for high field strengths, the emission from a given facet will be relatively uninfluenced by the neighboring facets of different work function. However, when x_0 approaches the same magnitude as the facet size, then the emission from a given facet will be influenced by the difference in contact potential between the given facet and the neighboring facets. Most of the emission comes from the facets of low work function. On account of the presence of the neighboring facets of higher work function the field strength on the facets of lower work function is actually lowered so that the field strength on these facets is lower than the experimenter thinks. As x_0 becomes very large ($E\rightarrow 0$), the work required to remove an electron from any crystal facet to a large distance becomes the same and the Schottky theory again holds. Therefore, the larger the facet size and the smaller the difference in work function the smaller become the surface fields at which the Schottky theory fails. Assuming the validity of an argument of this type, the deviation from the Schottky theory gives some idea of the nature of the surface of the emitter. For example, if the maximum difference in work function between neighboring facets is held constant, the smaller the size of the facets the higher will be the surface gradients for which the deviation from the Schottky theory sets in.

If the surface normal to a given crystal direction is not "pure," i.e., if it is made up of several different crystal faces, the φ_0 determined by the temperature dependence of its emission will be that of the crystal face of lowest φ_0 if the data give a straight Richardson line. Then the empirical A^* associated with this surface will be that associated with the crystal face of lowest φ_0 multiplied by the fraction of the surface area which is made up of the crystal face of lowest φ_0. Table I includes several low values of A^*, the lowest being that for the (110) direction. Fig. 7B shows the roughness of this surface and also the

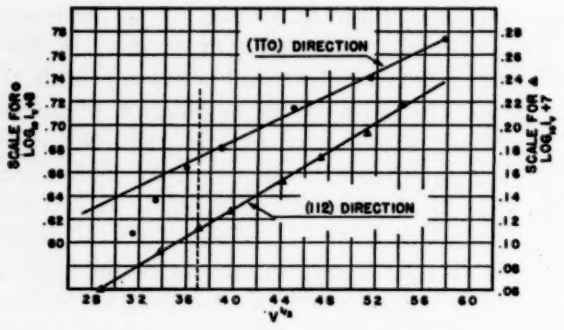

FIG. 10. Schottky plot for $(\bar{1}\bar{1}0)$ and (111) crystal directions.

roughness extending to the (111) directions. On account of this roughness these surfaces are presumably not pure. Fig. 10 is a Schottky plot for the (110) direction compared with that for the (112) direction which has a high A^* value. Microscopic examination (Fig. 7A) shows the surface normal the (112) direction to be smooth. The Schottky plot for the (110) direction deviates from the Schottky theory for a value of the surface gradient E of about 4.5×10^4 volts/cm ($x_0=90\times10^{-8}$ cm) whereas the Schottky plot for the (112) direction [as well as all other directions with the exception of the (110) direction] agrees with the theory down to much lower voltages.[18] This deviation for the (110) direction shows that there is a small scale "checkerboard effect" on the surface normal to the (110) direction. This evidence together with the roughness of the surface indicates that the surface normal to the (110) direction is not "pure" which may account for the low A^* value associated with this direction. On this basis one would expect on the surface normal to the (110) direction the existence in considerable proportion of crystal faces whose work function is higher than 4.65 volts. *Thus the values of A^* do not possess any unique physical significance but are strongly influenced by the lack of purity of the crystal surfaces as well as by inaccurate knowledge of the surface area,[14] temperature variation of the work function[13, 15, 16] and reflection effects.*[13]

As seen from Table I, a considerable part of the surface of the single crystal wire has values of φ_0 as low as 4.35 electron volts. The average φ_0 over the whole crystal wire as given by the temperature dependence of the emission from the whole wire would be only slightly larger than this value of 4.35. The accepted value of this average φ_0 for tungsten wire not treated in the special manner outlined here is about 4.50 ev. This seems to indicate that the special heat treatment starting from polished wire exposes crystal faces which do not occur in appreciable degree in the ordinary samples of wire. However, the φ_0 given in Table I for the (001) crystal direction nearly coincides with the average value for ordinary wire.[19] Furthermore, the empirical A^* for ordinary polycrystalline unpolished tungsten wire is around 60. The Schottky data[13] for this ordinary wire as well as the electron projection tube data[1] indicates the patchy nature of these surfaces showing that the value of 60 is really not characteristic of any of the pure crystal facets occurring in these samples.

Further work is under way to check the generality of the results reported here and to extend the measurements to thoriated and caesiated tungsten crystal surfaces.

I am indebted to many people who have given assistance in this work. In particular, I wish to thank Professor W. B. Nottingham, who directed this research, for his continued interest and many helpful suggestions. To Dr. R. B. Nelson, who constructed the tube used for the thermionic measurements in this work, I am grateful for valuable advice. Mr. Lawrence Ryan assisted in the glass blowing operations required in this problem. I am grateful to the Charles A. Coffin Foundation, established by the General Electric Company, for the Coffin Fellowship during the tenure of which this work was done.

[18] The surface gradients which exist even if the whole single crystal wire were made up of the pure crystal faces as well as the initial thermal velocities of the electrons spoil the "projection" properties of the tube for voltages under about 1000 volts.

[19] R. P. Johnson, Phys. Rev. **54**, 459 (1938) reports that under certain conditions tungsten filament surfaces tend to expose mainly faces normal to the (001) crystal directions.

Stationary States of Scalar and Vector Fields

H. SNYDER AND J. WEINBERG
University of California, Berkeley, California

(Received December 18, 1939)

In the presence of an electrostatic field (but not for a static world scalar or magnetostatic field) the stationary solutions of the quadratic relativistic wave equation for scalar particles do not form an orthonormal set. In spite of this they may in general be used to introduce normal coordinates for the quantum theory of this field. If the wave field and its canonical conjugate are expanded in terms of these stationary solutions, then the commutation laws for the amplitudes follow from the wave field commutators and the assumption of the integrability of the classical wave equation for arbitrary initial function and time derivative. Parallel considerations are applied to the vector field. An alternative method is described that involves the introduction of orthonormal functions and the construction of a "particle Hamiltonian."

I.

THE scalar and vector wave fields may be quantized according to Bose statistics by taking canonical commutation laws for the wave fields and their canonical conjugates. However, it has not been clear that the Hamiltonian can be brought to diagonal form by means of a unitary transformation when there is a static electric field present. When the electric field vanishes, and there are only static magnetic and gravitational fields present, the Hamiltonian is readily brought to diagonal form. One can easily understand why this is true. If we make a time Fourier analysis of the field we find: (*a*) all of the frequencies are real; (*b*) to every positive frequency there corresponds a negative frequency with equal magnitude, and the space dependence of the Fourier coefficients of the positive frequencies is the same as that of the corresponding negative frequencies; (*c*) the Fourier coefficients form a complete set of orthogonal functions in the space variables.

The situation is quite different when there is a static electric field present: (*a'*) the frequencies are not necessarily real, although there exist potentials for which they are; (*b'*) there is no direct correspondence between the positive and negative frequencies or their Fourier coefficients; (*c'*) the Fourier coefficients do not form a set of orthogonal functions. If the frequencies are real, Pauli[1] has shown, in spite of (*b'*) and (*c'*), that the total charge and energy take their canonical form in terms of the Fourier amplitudes of an unquantized field. Our principal task is to show that Bose quantization of these amplitudes is equivalent to the canonical commutation laws for the wave fields.

Furthermore, in the cases where (*a*,*b*,*c*) are true, it is possible to show that the frequencies and Fourier coefficients are the eigenvalue and eigenfunction, respectively, of a Hermitian operator, which may be interpreted as a "particle-Hamiltonian" for the individuals of an Einstein-Bose ensemble. In this paper we show how such a "particle-model" may be constructed in the case of the breakdown of (*b*,*c*), although not if any of the frequencies are complex.

II.

We will be concerned in this section only with electrostatic fields $\mathcal{E}=-\nabla V$. The Lagrangian for the scalar field then becomes:[2]

$$\mathfrak{L}=\left(\frac{\partial}{\partial t}-ieV\right)\psi^*\left(\frac{\partial}{\partial t}+ieV\right)\psi - \nabla\psi^*\cdot\nabla\psi-\psi^*\psi. \quad (1)$$

The momenta canonically conjugate to ψ and ψ^* are:

$$\pi=\partial\mathfrak{L}/\partial(\partial\psi/\partial t)=\psi^*-ieV\psi^*, \qquad \pi^*=\partial\mathfrak{L}/\partial(\partial\psi^*/\partial t)=\psi+ieV\psi. \quad (2)$$

The Hamiltonian for the system, obtained in the usual way, is:

$$H=\int U dv, \quad (3)$$

[1] W. Pauli, Princeton mimeographed notes (1935).

[2] W. Pauli and V. Weisskopf, Helv. Phys. Acta 7, 709 (1934).

with

$$U=\pi^*\pi+\nabla\psi^*\cdot\nabla\psi+\psi^*\psi+\rho V, \tag{4}$$

where the charge density ρ is given by

$$\rho=ie(\pi^*\psi^*-\pi\psi). \tag{5}$$

These expressions will be considered to be symmetrized whenever we use them quantum-mechanically.

From the Hamiltonian (3) we can immediately find the Hamiltonian equations of motion, which are, of course, equivalent to the Lagrangian equations.

$$\begin{aligned}\dot{\psi}&=\delta H/\delta\pi=\pi^*-ieV\psi,\\ \dot{\psi}^*&=\delta H/\delta\pi^*=\pi+ieV\psi^*,\end{aligned} \tag{6}$$

$$\begin{aligned}\dot{\pi}&=-\delta H/\delta\psi=\Delta\psi^*-\psi^*+ieV\pi,\\ \dot{\pi}^*&=-\delta H/\delta\psi^*=\Delta\psi-\psi-ieV\pi^*.\end{aligned} \tag{7}$$

The usual method of quantizing this Hamiltonian is to suppose that the ψ, ψ^*, π, and π^* satisfy the following commutation relations:

$$\begin{aligned}[\psi(x),\pi(x')]&=i\delta(x-x'),\\ [\psi^*(x),\pi^*(x')]&=i\delta(x-x'),\end{aligned} \tag{8}$$

and all other commutators zero. With these commutators it is easily shown that the time rate of change of any function $f(\psi,\psi^*,\pi,\pi^*)$ is given by:

$$i\dot{f}=[f,H] \tag{9}$$

In particular, the equations of motion for ψ, ψ^*, π, and π^* are (6) and (7).

One can also see that:

$$i\dot{q}=[q,H]=0, \tag{10}$$

where

$$q=\int\rho dv \tag{11}$$

is the total charge of the system.

Because of (10), both q and H should be simultaneously diagonalizable. It is, however, quite difficult to carry out the diagonalization explicitly using the commutation relations (8), because of the occurrence of V in the right-hand side of Eqs. (6). For this reason, we have carried out the quantization in a different manner, but we will show later that this quantization is equivalent to (8).

III.

If we substitute π^* from (6) into (7), treating ψ as a classical field, we find that ψ must satisfy a second-order partial differential equation, namely, the Klein-Gordon[3] equation

$$(\partial/\partial t+ieV)^2\psi=\Delta\psi-\psi, \tag{12}$$

with a similar equation for ψ^*.

"Any"[4] arbitrary function $\psi(x,t)$ may be written

$$\psi(x,t)=\int_{-\infty}^{\infty}dE_k e^{-iE_kt}\psi_k(x). \tag{13}$$

If $\psi(x,t)$ is to satisfy the K-G equation, then the $\psi_k(x)$ must satisfy:

$$(E_k-eV)^2\psi_k=\psi_k-\Delta\psi_k. \tag{14}$$

As a consequence of this, the general solution of (12) may be written:

$$\psi=\Sigma_k a_k\psi_k, \tag{15}$$

where the $\psi_k(x)$ are all of the solutions of (14) satisfying suitable boundary conditions, and where

$$\dot{a}_k=-iE_ka_k. \tag{16}$$

(For the present, E_k is assumed to be real.)

It should be noted that, in general, the functions ψ_k are not orthogonal to one another, but satisfy an orthogonality relation of the form:

$$\int\psi_k^*(E_k+E_l-2eV)\psi_l dv=0 \quad (k\neq l), \tag{17}$$

which has the weighting factor (E_k+E_l-2eV).

For all k, l,

$$\int\psi_k^*(E_k+E_l-2eV)\psi_l dv=\epsilon_k\delta_{kl}, \tag{18}$$

where ϵ_k is a number, which depending upon the particular ψ_k, may be either positive or negative. The case where some of the ϵ_k vanish will be treated separately; it is connected with the Klein paradox. This division of the ψ_k into states with positive and negative ϵ_k corresponds, as we shall see, to the division of the system into states of

[3] K-G will be used as an abbreviation for Klein-Gordon.

[4] The quotation marks mean that this is true for any function which is sufficiently regular and which remains bounded at positive and negative infinite times.

positive and negative charge. For the total charge is given by

$$q=ie\int(\pi^*\psi^*-\pi\psi)dv. \tag{19}$$

Because $\pi^*=\dot{\psi}+ieV\psi$, we find

$$\pi^*=-i\Sigma_k a_k(E_k-eV)\psi_k, \text{ etc.} \tag{20}$$

The total charge then becomes:

$$q=\Sigma_k a_k^* a_k\epsilon_k, \tag{21}$$

in which the division into states of positive and negative charge is evident.

A similar simple calculation gives the Hamiltonian its canonical form:

$$H=\Sigma_k a_k^* a_k E_k\epsilon_k. \tag{22}$$

Transition to q Numbers

Our procedure for quantizing this Hamiltonian, which up to this point has been treated classically, is to find commutation laws for the a_k and a_l^* so that for any function $f(a_k,a_l^*)$ we have $i\dot{f}=[f,H]$, or, in particular,

$$i\dot{a}_k=[a_k,H]=E_k a_k. \tag{23}$$

We suppose that $[a_k,a_l]=[a_k^*,a_l^*]=0$, and then

$$\begin{aligned} E_k a_k&=\Sigma_l\epsilon_l E_l[a_k a_l^* a_l-a_l^* a_l a_k],\\ E_k a_k&=\Sigma_l\epsilon_l E_l[a_k,a_l^*]a_l, \end{aligned} \tag{24}$$

from which we see that we must take:

$$[a_k,a_l^*]=\delta_{kl}/\epsilon_k. \tag{25}$$

The characteristic values of the symmetrized form of $a_k^* a_k$ are:

$$\tfrac{1}{2}[a_k^* a_k+a_k a_k^*]=(N_k+\tfrac{1}{2})/|\epsilon_k|\,; \qquad N_k=0,\,1,\,2,\,\cdots. \tag{26}$$

The total charge and energy then become:

$$q=e\Sigma_k(N_k+\tfrac{1}{2})\epsilon_k/|\epsilon_k|, \tag{27}$$

$$H=\Sigma_k E_k(N_k+\tfrac{1}{2})\epsilon_k/|\epsilon_k|, \tag{28}$$

where

$$\epsilon_k/|\epsilon_k|=\pm 1. \tag{29}$$

In order that the total charge vanish when there are no particles present, we must set the conditionally convergent series $\Sigma_k\epsilon_k/|\epsilon_k|$ equal to zero. This can be done even when electrostatic fields are present. Then the charge becomes:

$$q=e\Sigma_k N_k\epsilon_k/|\epsilon_k|. \tag{30}$$

IV.

We have given a quantum theory of this field by quantizing the normal coordinates a_k. We must show that this method of quantization is equivalent to taking the Einstein-Bose commutation laws (8) for ψ, ψ^*, π, and π^* and all other commutators zero.

We discover, using the commutation laws for the a_k and a_k^*, that:

$$[\psi(x),\psi^*(x')]=\Sigma_k\epsilon_k^{-1}\psi_k(x)\psi_k^*(x'), \tag{31}$$

$$[\psi(x),\pi(x')]=i\Sigma_k\epsilon_k^{-1}\psi_k(x)\psi_k^*(x')\times[E_k-eV(x')], \tag{32}$$

$$[\pi^*(x),\pi(x')]=\Sigma_k\epsilon_k^{-1}\psi_k(x)\psi_k^*(x')\times[E_k-eV(x)][E_k-eV(x')]. \tag{33}$$

All other commutators vanish, except the commutator of $\psi^*(x)$ and $\pi^*(x')$ which is the complex conjugate of (32).

If the commutation laws (31), (32), and (33) are to be the same as the usual ones, then the functions ψ_k must satisfy the following identities:

$$\Sigma_k\epsilon_k^{-1}\psi_k(x)\psi_k^*(x')=0, \tag{34}$$

$$\Sigma_k\epsilon_k^{-1}\psi_k(x)\psi_k^*(x')E_k=\delta(x-x'), \tag{35}$$

$$\Sigma_k\epsilon_k^{-1}\psi_k(x)\psi_k^*(x')E_k^2=2eV(x)\delta(x-x'). \tag{36}$$

The validity of these identities will be proven by constructing the Green's functions for the K-G equation. We observe that every solution of the K-G equation which remains bounded in time may be written:

$$\psi=\Sigma_k a_k^0 e^{-iE_k t}\psi_k(x), \tag{15a}$$

in which the a_k^0 are arbitrary numerical constants, and the time variation of ψ is written explicitly. Since ψ satisfies a second-order differential equation in time, we must specify not only the initial value of ψ but also its time derivative at the initial time, say $t=t'$, in order to calculate ψ at other times. This means that the values of a_k^0 depend not only upon the initial values of ψ, but also upon those of $\dot{\psi}$. Furthermore, because "every" solution ψ may be written in the form (15a), there must exist a_k^0 so that ψ

and $\dot{\psi}$ will take on arbitrary initial values at $t=t'$.

From the fact that the differential equation is linear in ψ and of second order in the time derivatives, there will exist two Green's functions $G(x,t;x',t')$ and $L(x,t;x',t')$ by means of which we can calculate the value of ψ at t from the values of ψ and $\dot{\psi}$ at t', namely:

$$\psi(x,t)=\int G(x,t;x',t')\dot{\psi}(x',t')dv' + \int L(x,t;x',t')\psi(x',t')dv'. \quad (37)$$

We will construct the functions G and L as bilinear forms in $\psi_k(x)$ and $\psi_k^*(x')$. We write for the initial values of ψ and $\dot{\psi}$ at $t=t'$:

$$\psi(x',t')=\Sigma_k a_k^0 e^{-iE_k t'}\psi_k(x'), \quad (38)$$

$$\dot{\psi}(x',t')=-i\Sigma_k a_k^0 E_k e^{-iE_k t'}\psi_k(x'), \quad (39)$$

knowing that a_k^0 exist which will give them any pre-assigned values.

If we multiply $\psi(x',t')$ by $e^{iE_l t'}\psi_l^*(x')\times[E_l-2eV(x')]$, and $\dot{\psi}(x',t')$ by $ie^{iE_l t'}\psi_l^*(x')$, add the two results and integrate over all space, we find:

$$\epsilon_l a_l^0=e^{iE_l t'}\int \psi_l^*(x')\times\{[E_l-2eV(x')]\psi(x',t')+i\dot{\psi}(x',t')\}dv', \quad (40)$$

or, since we are supposing all $\epsilon_k\neq 0$,

$$a_l^0=\epsilon_l^{-1}e^{iE_l t'}\int \psi_l^*(x')\times\{[E_l-2eV(x')]\psi(x',t')+i\dot{\psi}(x',t')\}dv'. \quad (41)$$

If we place this value of a_l^0 in Eq. (15a), we find the following expressions for G and L:

$$L(x,t;x't')=i\Sigma_k\epsilon_k^{-1}e^{iE_k(t'-t)}\psi_k(x)\psi_k^*(x'), \quad (42)$$

$$G(x,t;x't')=\Sigma_k\epsilon_k^{-1}e^{iE_k(t'-t)}\times\psi_k(x)\psi_k^*(x')[E_k-2eV(x')]. \quad (43)$$

These expressions (42) and (43) are the Green's functions for the K-G equation and give ψ and $\dot{\psi}$ their initial values (38) and (39) at $t=t'$. Since ψ and $\dot{\psi}$ are arbitrary at $t=t'$, we see from Eq. (37) that:

$$L(x,t';x',t')=i\Sigma_k\epsilon_k^{-1}\psi_k(x)\psi_k^*(x')=0, \quad (44)$$

$$G(x,t';x',t')=\Sigma_k\epsilon_k^{-1}\psi_k(x)\psi_k^*(x')\times[E_k-2eV(x')]=\delta(x-x'). \quad (45)$$

Equation (44) is the identity (34), and Eq. (45) is equivalent to identity (35). By differentiating Eq. (37) with respect to the time, one finds, for the same reasons, that:

$$dG(x,t;x't')/dt|_{t=t'}=-i\Sigma_k\epsilon_k^{-1}\psi_k(x)\times\psi_k^*(x')E_k[E_k-2eV(x')]=0, \quad (46)$$

which is equivalent to identity (36), since identity (35) is true. The differentiation of L in (35) with respect to time gives us a repetition of the proof of identity (35).

In this way we have proven that our method of quantizing the scalar field is equivalent to the usual method of quantization under the condition:

that for arbitrary initial ψ and $\dot{\psi}$, the K-G *equation may be integrated to give a ψ which remains bounded in time.* (47)

There exist potentials for which this condition will not be satisfied: if this happens it can be shown that the Hamiltonian and charge cannot be simultaneously diagonalized when the commutation relationships (8) are satisfied.

V.

The methods of Sections II to IV may be employed to extend the results there obtained for the Pauli-Weisskopf scalar field, to the case of the mesotron vector field. The mesotron Hamiltonian has been given by Yukawa and Sakata[5] in terms of the vector field-coordinates ψ, ψ^* and their respective canonically conjugate momenta π, π^*[6] as:

$$H=\int\{\pi\cdot\pi^*+(D^*\cdot\pi)(D\cdot\pi^*)+(D^*\times\psi^*)\cdot(D\times\psi)+\rho V+\psi^*\cdot\psi\}dv, \quad (48)$$

[5] H. Yukawa and S. Sakata, "The Interaction of Elementary Particles III," Proc. Physico-Math. Soc. Japan, Ser. 3, 20, 319 (1938).

[6] Vector signs will be omitted, for convenience, on the symbols like ψ, D, α, G. $(\cdot)$ and $[\times]$ have their usual meanings.

where A, V are the vector and scalar potentials of the electromagnetic field (assumed time-independent) and where we define

$$D=\nabla-ieA, \qquad D^*=\nabla+ieA, \tag{49}$$

and where the charge-density ρ is given by

$$\rho=ie(\pi^*\cdot\psi^*-\pi\cdot\psi). \tag{50}$$

Using Green's theorem, one may write (48) in the form

$$H=\int\{\pi\cdot[\pi^*-D(D\cdot\pi^*)-ieV\psi] +\psi^*\cdot[\psi+D\times(D\times\psi)+ieV\pi^*]\}dv. \tag{51}$$

By varying π and ψ^* and their complex conjugates, we may obtain the classical Hamiltonian equations of motion:

$$\dot{\pi}^*=-\delta H/\delta\psi^*=-D\times(D\times\psi)-\psi-ieV\pi^*, \tag{52}$$

$$\dot{\psi}=\delta H/\delta\pi=\pi^*-D(D\cdot\pi^*)-ieV\psi, \tag{53}$$

and conjugates. Under restrictions similar to those in (13), one may make a Fourier analysis of ψ and π^* with respect to the time:

$$\psi=\Sigma_k e^{-iE_kt}\psi_k, \quad \pi^*=\Sigma_k e^{-iE_kt}\pi_k^*. \tag{54}$$

In order, then, to satisfy (52) and (53), we must have:

$$i(E_k-eV)\pi_k^*=\psi_k+D\times(D\times\psi_k), \tag{55}$$

$$-i(E_k-eV)\psi_k=\pi_k^*-D(D\cdot\pi_k^*); \tag{56}$$

and, for the present, we shall assume E_k real. From (55) and (56) one easily obtains:

$$\int\{(E_k-eV)\psi_l^*\cdot\pi_k^*+(E_l-eV)\psi_k\cdot\pi_l\}dv=0, \tag{57}$$

$$\int\{(E_k-eV)\pi_l\cdot\psi_k+(E_l-eV)\pi_k^*\cdot\psi_l^*\}dv=0, \tag{58}$$

which may be combined to give the analog of (17):

$$(E_k-E_l)i\int\{\psi_l^*\cdot\pi_k^*-\psi_k\cdot\pi_l\}dv=0, \tag{59}$$

or

$$i\int\{\psi_l^*\cdot\pi_k^*-\psi_k\cdot\pi_l\}dv=\epsilon_k\delta_{kl}. \tag{60}$$

As before, the sign of ϵ_k will determine the sign of the charge of particles in the kth state, so that, for the moment, we shall exclude the possibility $\epsilon_k=0$, treated separately in the succeeding paper.

We may now proceed to the quantum theory by symmetrizing all bilinear expressions in π, ψ, π^*, ψ^*, and by redefining ψ, π^* in terms of a sequence of operators a_k independent of the space-variables but dependent on the time. We shall take:

$$\psi=\Sigma_k a_k\psi_k, \qquad \pi^*=\Sigma_k a_k\pi_k^*, \tag{61}$$

corresponding to the general classical solutions of (54). Applying (60) to (50) and (51), one finds

$$q=\int\rho dv=\Sigma_k(a_k^*a_k+a_ka_k^*)\epsilon_k/2, \tag{62}$$

$$H=\Sigma_kE_k(a_k^*a_k+a_ka_k^*)\epsilon_k/2, \tag{63}$$

for the total charge and energy, respectively. (This is comparable to (21) and (22) in the Pauli-Weisskopf case.) To obtain the quantum analog of the canonical equations, we must take

$$i\dot{a}_k=E_ka_k=[a_k,H], \tag{64}$$

which, in general, will require

$$[a_k,a_l^*]=\delta_{kl}/\epsilon_k, \quad [a_k,a_l]=[a_k^*,a_l^*]=0. \tag{65}$$

This, of course, results in Bose quantization of the states numbered by k, as shown by the results (26) to (30), which now follow exactly as before.

It is not clear, however, that these equations represent the quantization of the mesotron field, until one can demonstrate that ψ and π defined by (61) and (65) satisfy canonical commutation laws as in (8). For the vector-functions ψ, π, one must then be able to prove:

$$\begin{aligned}[\alpha\cdot\psi(x),\beta\cdot\pi(x')]&=i(\alpha\cdot\beta)\delta(x-x'),\\ [\alpha\cdot\psi^*(x),\beta\cdot\pi^*(x')]&=i(\alpha\cdot\beta)\delta(x-x'),\end{aligned} \tag{66}$$

all other commutators zero, for arbitrary constant vectors, α and β. By (65), we find, however:

$$\begin{aligned}[\alpha\cdot\psi(x),\beta\cdot\psi^*(x')]&=\Sigma_k\epsilon_k^{-1}\alpha\cdot\psi_k(x)\beta\cdot\psi_k^*(x'),\\ [\alpha\cdot\psi(x),\beta\cdot\pi(x')]&=\Sigma_k\epsilon_k^{-1}\alpha\cdot\psi_k(x)\beta\cdot\pi_k(x'),\\ [\alpha\cdot\pi^*(x),\beta\cdot\pi(x')]&=\Sigma_k\epsilon_k^{-1}\alpha\cdot\pi^*(x)\beta\cdot\pi(x'),\\ [\alpha\cdot\pi^*(x),\beta\cdot\psi^*(x')]&=\Sigma_k\epsilon_k^{-1}\alpha\cdot\pi^*(x)\beta\cdot\psi^*(x'),\end{aligned} \tag{67}$$

all other commutators zero. If these are to be equivalent to (66), the following identities must

then be shown to be valid:

$$\Sigma_k \epsilon_k^{-1} \alpha \cdot \psi_k(x) \beta \cdot \psi_k^*(x') = \Sigma_k \epsilon_k^{-1} \alpha \cdot \pi_k^*(x) \beta \cdot \pi_k(x') = 0, \quad (68)$$

$$\Sigma_k \epsilon_k^{-1} \alpha \cdot \psi_k(x) \beta \cdot \pi_k(x') = -\Sigma_k \epsilon_k^{-1} \alpha \cdot \pi_k^*(x) \beta \cdot \psi_k^*(x') = i(\alpha \cdot \beta) \delta(x-x'). \quad (69)$$

We may prove (68) and (69) by returning to the classical equations (52) and (53). If they exist, the following vector functions form a system of Green's functions for (52) and (53):

$$\begin{aligned} G(x,t;x',t') &= -i\Sigma_k \epsilon_k^{-1} e^{iE_k(t'-t)} \alpha \cdot \psi_k(x) \pi_k(x'), \\ L(x,t;x',t') &= i\Sigma_k \epsilon_k^{-1} e^{iE_k(t'-t)} \alpha \cdot \psi_k(x) \psi_k^*(x'), \\ \Gamma(x,t;x',t') &= -i\Sigma_k \epsilon_k^{-1} e^{iE_k(t'-t)} \alpha \cdot \pi_k^*(x) \pi_k(x'), \\ \Lambda(x,t;x',t') &= i\Sigma_k \epsilon_k^{-1} e^{iE_k(t'-t)} \alpha \cdot \pi_k^*(x) \psi_k^*(x'), \end{aligned} \quad (70)$$

in the sense that

$$\begin{aligned} \alpha \cdot \psi(x,t) &= \int G(x,t;x',t') \cdot \psi(x',t') dv' \\ &\quad + \int L(x,t;x',t') \cdot \pi^*(x',t') dv', \end{aligned} \quad (71)$$

$$\begin{aligned} \alpha \cdot \pi^*(x,t) &= \int \Gamma(x,t;x',t') \cdot \psi(x',t') dv' \\ &\quad + \int \Lambda(x,t;x',t') \cdot \pi^*(x',t') dv'. \end{aligned}$$

(71) may be verified by applying (54) and (60) to the general solution of (52) and (53).

Because the latter form a linear system containing only first derivatives in the time, it is assumed that we may assign initial values independently to $\psi(x,t)$, $\pi^*(x,t)$ for all values of x at some time $t=t'$, when ψ, π^* are expressible in the form (54). This is equivalent to the assumption in Section IV that ψ and $\dot{\psi}$ may be given arbitrary, independent, initial values. Choosing this pair of initial values as 0, $\beta\delta(x-x')$ at $t=t'$ in (71):

$$L(x,t';x',t') \cdot \beta = \Gamma(x,t';x',t') \cdot \beta = 0, \quad (72)$$

$$G(x,t';x',t') \cdot \beta = \Lambda(x,t';x',t') \cdot \beta = (\alpha \cdot \beta) \delta(x-x'). \quad (73)$$

Making use of the definitions (70) in (72) and (73), shows the latter to be identical with the desired relations (68) and (69); and hence the validity of (66) is proved.

In this way we have shown how to bring the energy of the mesotron field into diagonal form in the presence of static electromagnetic fields, subject to the restriction of (47).

VI.

In this section we deal with the problem of finding a transformation from canonical field coordinates $\psi(x)$, $\pi(x)$ to new field quantities $\phi_+(x)$, $\phi_-(x)$ in terms of which the charge q and energy H take their diagonal form:

$$q = e \int \{\phi_+^* \phi_+ - \phi_-^* \phi_-\} dv, \quad (74)$$

$$H = \int \{\phi_+^* \Omega_+ \phi_+ + \phi_-^* \Omega_- \phi_-\} dv, \quad (75)$$

where the products of ϕ's are to be taken symmetrized, and where $\Omega_\pm$ are Hermitian, linear, functional operators on the space-coordinates. We shall also require the commutation rules corresponding to the Einstein-Bose quantization to hold:

$$[\phi_+(x), \phi_+^*(x')] = [\phi_-(x), \phi_-^*(x')] = \delta(x-x'), \quad (76)$$

all other commutators zero.

If the ϕ's are expanded in terms of the orthonormal set of eigenfunctions of the corresponding $\Omega_\pm$, one obtains the canonical forms of Section III, (25), (27), (28). This means that $\Omega_\pm$ may be interpreted as a Hamiltonian for a single particle of charge $\pm e$; and the field may then (insofar as the total charge and energy are concerned) be interpreted as an Einstein-Bose assembly of such particles.

Pauli and Weisskopf[2] have shown how to construct a "particle Hamiltonian" of the scalar mesotron field when no external fields are present, by means of the transformation[7]

$$\psi = 2^{-\frac{1}{2}}(1-\Delta)^{-\frac{1}{4}}(\phi_+ + \phi_-^*); \quad \pi = i2^{-\frac{1}{2}}(1-\Delta)^{\frac{1}{4}}(\phi_+^* - \phi_-), \quad (77)$$

[7] The "square root of a Hermitian operator C", $C^{\frac{1}{2}}$, operating on any function f may be defined by expanding f in eigenfunctions γ_k of C.

$$C\gamma_k = c_k \gamma_k, \qquad f = \Sigma_k f_k \gamma_k$$

for then we may set

$$C^{\frac{1}{2}} f = \Sigma_k C_k^{\frac{1}{2}} f_k \gamma_k.$$

with $$\Omega_+=\Omega_-=(1-\Delta)^{\frac{1}{2}}. \tag{78}$$

One sees clearly how to modify the transformation when magnetostatic fields $\nabla\times A(x)$ or world-scalar fields $-\nabla K(x)$ are present:

$$\psi=(2\mathbf{O})^{-\frac{1}{2}}(\phi_+ +\phi_-{}^*),\quad \pi=i2^{-\frac{1}{2}}\mathbf{O}^{\frac{1}{2}}(\phi_+{}^*-\phi_-), \tag{79}$$

with $$\Omega_+=\Omega_-=\mathbf{O},\quad \mathbf{O}^2=K(x)-(\nabla-ieA)^2. \tag{80}$$

When electrostatic fields, $\mathcal{E}=-\nabla V$, are present, however, it is not at all easy to obtain such a transformation. The behavior of positive and negative charges in this field is essentially different; and $\Omega_\pm$ must be different operators which are interchanged by changing the sign of e. The difficulty also may be understood formally from the fact that the solutions of the K-G equation, in this case, are not properly orthogonal.

It may be shown that when it is possible to obtain $\phi_\pm$ by linear functional transformation on π and ψ, this may be done in the form:

$$\begin{aligned}\psi&=(\mathbf{O}+\mathbf{O}^\dagger)^{-\frac{1}{2}}(\phi_+ +\phi_-{}^*),\\ \pi&=i(\mathbf{O}+\mathbf{O}^\dagger)^{-\frac{1}{2}}(\mathbf{O}^\dagger\phi_+{}^*-\mathbf{O}\phi_-),\end{aligned} \tag{81}$$

where $\mathbf{O}$ is defined as a solution of

$$\mathbf{O}^2+e[\mathbf{O},V]=1-\Delta; \tag{82}$$

and $\mathbf{O}^\dagger$ is the operator complex-adjoint to $\mathbf{O}$, satisfying

$$(\mathbf{O}^\dagger)^2-e[\mathbf{O}^\dagger,V]=1-\Delta. \tag{83}$$

The energy operators are given by

$$\begin{aligned}\Omega_+&=(\mathbf{O}+\mathbf{O}^\dagger)^{\frac{1}{2}}(\mathbf{O}+eV)(\mathbf{O}+\mathbf{O}^\dagger)^{-\frac{1}{2}},\\ \Omega_-&=(\mathbf{O}+\mathbf{O}^\dagger)^{\frac{1}{2}}(\mathbf{O}^\dagger-eV)(\mathbf{O}+\mathbf{O}^\dagger)^{-\frac{1}{2}}.\end{aligned} \tag{84}$$

From the work of the preceding sections, it is not surprising that the characteristic values of $\Omega_\pm$ turn out to be $\pm E_k$, where E_k are the frequencies corresponding to the solutions ψ_k with $\epsilon_k/|\epsilon_k|=\pm1$ of the Klein-Gordon equation with the given potential V. The connection between the eigenfunctions $\phi_\pm{}^{(k)}$ of $\Omega_\pm$ and the corresponding solutions ψ_k of the Klein-Gordon equation is:

$$\phi_\pm{}^{(k)}=(\mathbf{O}+\mathbf{O}^\dagger)^{\frac{1}{2}}\psi_k,\qquad \epsilon_k/|\epsilon_k|=\pm1, \tag{85}$$

with $$\Omega_\pm\phi_\pm{}^{(k)}=\pm E_k\phi_\pm{}^{(k)}. \tag{86}$$

These last remarks make clear the limitations under which it turns out that one may construct a "particle-Hamiltonian" of the field with the aid of a linear functional transformation:

The Klein-Gordon equation must satisfy the restrictions of (47); and, in particular, the fields must not be so strong that there occur any Klein-Gordon solutions with $\epsilon_k=0$. In this formulation of the problem, complex frequencies E_k may not occur because of the Hermiticity of $\Omega_\pm$. These cases are discussed separately in the following paper. Thus, when the total Hamiltonian and charge may be diagonalized at all, the "particle-Hamiltonian" discussed here may be constructed.

When high Fourier-components of V are not present, one may neglect $|[\Delta,V]|\ll1$; and assuming that all momenta $p\ll1$, the equation defining $\mathbf{O}$ becomes

$$\mathbf{O}^2\backsimeq1-\Delta,\qquad \mathbf{O}^\dagger\backsimeq\mathbf{O}\backsimeq1-\tfrac{1}{2}\Delta. \tag{87}$$

In this nonrelativistic limit, we obtain the ordinary Hamiltonians for particles of charge $\pm e$.

$$\Omega_+\backsimeq1-\tfrac{1}{2}\Delta+eV,\quad \Omega_-\backsimeq1-\tfrac{1}{2}\Delta-eV,$$

$$\phi_+\backsimeq2^{-\frac{1}{2}}(\psi+i\pi^*), \tag{88}$$

$$\phi_-\backsimeq2^{-\frac{1}{2}}(\psi^*+i\pi), \tag{89}$$

where $$\pi^*=\psi+ieV\psi.$$

The $\mathbf{O}$ equation may be solved exactly in the simple case of a homogeneous electric field of infinite extent $eV=x/a$, $a>0$. Although the analogue of the Klein paradox is certainly present in this case, there are no solutions of the Klein-Gordon equation:

$$(1-\Delta)\psi_k=(E_k-x/a)^2\psi_k \tag{90}$$

with $\epsilon_k=0$. If we set $p=-i(d/dx)$, $[\mathbf{O},V]=-(i/a)\cdot(d\mathbf{O}/dp)$, and $\mathbf{O}$ is determined by

$$\mathbf{O}^2-(i/a)\cdot(d\mathbf{O}/dp)=1+p^2. \tag{91}$$

We may define $\omega(p)$ by

$$(-i/a)(d/dp\ \ln\omega)=\mathbf{O} \tag{92}$$

and then ω must satisfy the simple equation

$$(d^2/dp^2)\omega+a^2(1+p^2)\omega=0. \tag{93}$$

In this case, where $\mathbf{O}$ is a function of p alone, $[\mathbf{O},\mathbf{O}^\dagger]=0$, and we may write

$$(\mathbf{O}+\mathbf{O}^\dagger)^{-1}=\omega\omega^\dagger/W. \tag{94}$$

From (84) and (92),

$$\Omega_+=(-i/a)[d/dp \ln (\omega/\omega^\dagger)^{\frac{1}{2}}]+(i/a)d/dp,$$
$$\Omega_-=(-i/a)[d/dp \ln (\omega/\omega^\dagger)^{\frac{1}{2}}]-(i/a)d/dp, \quad (95)$$

where
$$W=(-i/a)\begin{vmatrix} d\omega/dp & \omega \\ d\omega^\dagger/dp & \omega^\dagger \end{vmatrix} \quad (96)$$

is a real, constant number, which should be taken positive to make $(\mathbf{O}+\mathbf{O}^\dagger)^{\frac{1}{2}}$ Hermitian.

The orthonormal eigenfunctions $\phi_\pm^{(k)}$ defined by (86) are given explicitly by (95) in the form

$$\phi_\pm^{(k)}(x)=a^{\frac{1}{2}}/2\pi\int_{-\infty}^{\infty}(\omega/\omega^\dagger)^{\pm\frac{1}{2}}e^{ip(x-aE_k)}dp. \quad (97)$$

One can easily verify that $\phi_\pm^{(k)}$ are orthonormal in the sense:

$$\int_{-\infty}^{\infty}\phi_\pm^{*(k)}\phi_\pm^{(l)}dx=\delta(E_k-E_l).$$

From (85), (94), (97) one obtains:

$$\psi_k(x)=(1/2\pi)(a/W)^{\frac{1}{2}}\int_{-\infty}^{+\infty}\omega(p)e^{ip(x-aE_k)}dp \quad (98)$$

for a state k corresponding to *positive* charge. By a brief calculation, one may verify that $\psi_k(x)$ actually satisfies the Klein-Gordon equation and the required relation (18):

$$\int_{-\infty}^{+\infty}\psi_k^*(E_k+E_l-2x/a)\psi_l dx=\delta(E_k-E_l).$$

Because of the covariance of the wave functions under translation of the origin of coordinates, there is some freedom of choice of ω, the only restrictions on solutions of (93) being that $W>0$ and that the integrals defining ψ_k and $\phi_\pm^{(k)}$, (97) and (98) must exist. Here we choose ω so that the asymptotic behavior of $\phi_\pm^{(k)}(x)$ for large values of $|x|$ is simply obtainable. For large values of $|p|$, we take

$$\omega(p)/\omega^\dagger(p)\sim e^{-(ia/2)(\ln p+p^2+\vartheta)}, \quad (99)$$

where ϑ is a real constant depending only on a.

Then:

$$\phi_+^{(k)}(x)\sim\phi_-^{(k)}(-x)$$
$$\sim(2\pi)^{\frac{1}{2}}e^{-a\pi/2+(ia/2)(\ln \xi_k-\xi_k^2+\vartheta+\pi/2a)},$$
$$\phi_+^{(k)}(-x)\sim\phi_-^{(k)}(x) \quad (100)$$
$$\sim(2\pi)^{\frac{1}{2}}e^{-(ia/2)(\ln \xi_k-\xi_k^2+\vartheta+\pi/2a)}$$

for large positive values of x and $\xi_k=(x-aE_k)/a$. The transmission coefficient $e^{-a\pi/2}$, analogous to that of Dirac's electron theory, appears in these results.

In a recent paper, Kemmer[8] has carried through a linearization of the Proca[9] and K-G equations with the aid of Duffin's[10] 5- and 10-rowed matrices. Although the energy appears in a form analogous to (75),

$$H=-i\int\Psi^\dagger\beta_4\mathfrak{IC}\Psi dv,$$

where $i\dot{\Psi}=\mathfrak{IC}\Psi$, one should observe that, in our units, $(\hbar=c=m_0=1)$,

$$\mathfrak{IC}=eV+\beta_4\times\Sigma_k[\beta_k,\beta_4]\frac{\partial}{\partial x_k}$$
$$+(e/2)\Sigma_k\mathcal{E}_k\{[\beta_k,\beta_4^2]+\beta_k\},$$

where β_k, β_4 are Hermitian matrices, and $\mathcal{E}_k=-\partial V/\partial x_k$, $(k=1, 2, 3)$ are the field-strengths of the external electrostatic field. Thus $\mathfrak{IC}$ is not Hermitian, but contains noncommuting Hermitian and skew Hermitian parts proportional to $\mathcal{E}_k$. This is intimately connected with the fact that the eigenfunctions of $\mathfrak{IC}$ (essentially the ψ_k's) are in general not orthogonal and that characteristic values of $\mathfrak{IC}$ may be complex. These limitations must be kept in mind in applying Kemmer's particle-Hamiltonian.

We should like to express our thanks to Professor J. R. Oppenheimer for his suggestion of the problem and for continual advice and encouragement during the course of its solution.

[8] H. Kemmer, Proc. Roy. Soc. **A173**, 91 (1939).
[9] A. Proca, J. de phys. et rad. [VII] **7**, 347 (1936).
[10] R. J. Duffin, Phys. Rev. **54**, 1114 (1938).

On The Existence of Stationary States of the Mesotron Field

L. I. SCHIFF, H. SNYDER, AND J. WEINBERG
University of California, Berkeley, California

(Received December 18, 1939)

For some electrostatic potentials, such as that represented by a sufficiently deep well, the Pauli-Weisskopf wave equation has complex frequencies. It is shown that when this happens the quantized field Hamiltonian can no longer be diagonalized. Some points of similarity and difference between this theory and the Dirac positron theory are discussed.

IT has been shown in the preceding paper[1] that the quantized field Hamiltonian of the Pauli-Weisskopf theory can be brought into diagonal form by a unitary transformation when

$$\epsilon_{kl} \equiv \int \psi_l^*(E_k + E_l^* - 2eV)\psi_k dv \qquad (1)$$

is diagonal. Here, the orthogonality relation between solutions ψ_k of the differential equation is $\epsilon_{kl}(E_k - E_l^*) = 0$. It is apparent that when any of the E_k become complex, ϵ_{kl} is no longer diagonal, $\epsilon_k = 0$, and the formalism of the preceding paper breaks down. In Section I of the present paper we show that complex frequencies actually can occur for a simple type of potential. In Section II it is shown that under these circumstances the Hamiltonian can no longer be diagonalized.

I.

The existence of complex frequencies of the Klein-Gordon differential equation is most readily demonstrated by solving the equation explicitly for a square well electrostatic potential. We take a potential that is attractive for a particle of charge e: $eV(r) = -V_0 < 0$ for $r < a$, and $eV(r) = 0$ for $r > a$; the character of the results obtained below for this potential do not depend on the discontinuity of $V(r)$ at $r = a$. The equation separates in spherical coordinates, and it is sufficient for our purposes to consider only the spherically symmetric part $\psi_0 \equiv u/r (l = 0)$. The regular solution for a bound state of frequency E, which we shall assume for the moment to be real, corresponds to $E^2 < 1$, $(E + V_0)^2 > 1$, and is:

$$\begin{aligned} u &= A \sin(\xi r/a), \qquad r < a, \\ u &= A \sin \xi \cdot \exp[-\eta(r/a - 1)], \qquad r > a. \end{aligned} \qquad (2)$$

Here, $\xi \equiv a[(E + V_0)^2 - 1]^{\frac{1}{2}}$, $\eta \equiv a(1 - E^2)^{\frac{1}{2}}$, and the boundary condition at $r = a$ gives:

$$\xi \cot \xi = -\eta. \qquad (3)$$

The solution of Eq. (3), giving E in terms of V_0, may be found by plotting $\xi \cot \xi$ and $-\eta$ against E for various values of V_0. It is found that there is no solution such that $E^2 < 1$ for small V_0; for $V_0 < 2$ but greater than a value V_1, there is just one root E_1 that decreases from $+1$ as V_0 increases. This state of affairs continues for V_0 somewhat greater than 2 but less than a value V_2, at which point a second root E_2 slightly greater than -1 appears. As V_0 increases further, E_1 continues to decrease while E_2 increases, until for a value V_3 of V_0 the two roots come together and the solutions become identical. For $V_0 > V_3$, the roots are complex and their solutions complex functions that are regular for all r. The pair of roots and the pair of solutions are then complex conjugates of each other. For sufficiently small a, V_1 can be greater than 2, while V_2 and V_3 are always greater than 2; all three decrease with increasing a.

We can readily evaluate ϵ from Eqs. (1) and (2):

$$\epsilon = 4\pi A^2 a[(E + V_0)(1 - \sin \xi \cos \xi/\xi) + E \sin^2 \xi/\eta],$$

from which it follows that

$$\epsilon = -(4\pi A^2 \sin^2 \xi/a)[(\partial/\partial E)(\xi \cot \xi) - (\partial/\partial E)(-\eta)].$$

By comparison with the slopes of the curves of

[1] H. Snyder and J. Weinberg, Phys. Rev., this issue; equations of this paper are referred to as I(34), for example. The units used in both papers are such that $c = \hbar = m_0 = 1$.

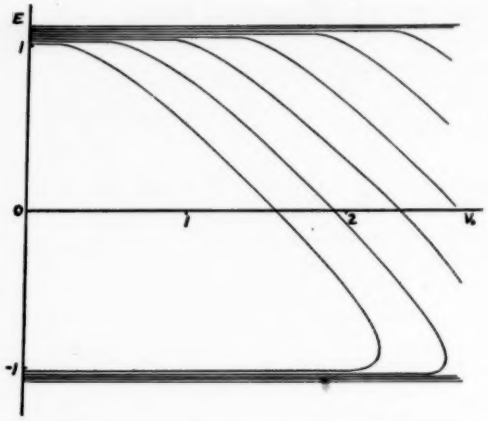

FIG. 1. The frequency E of the Klein-Gordon equation with a square well potential in a large box, as a function of the depth V_0 of the potential, for $l=0$.

$\xi \cot \xi$ and $-\eta$ against E, one sees that $\epsilon>0$ for the root E_1, $\epsilon<0$ for the root E_2, and $\epsilon=0$ for $E_1=E_2(V_0=V_3)$ since the two curves are tangent to each other at this point. This behavior of the lowest frequencies and their ϵ's is followed by the higher roots that arise from the other branches of the $\xi \cot \xi$ curve.

It is instructive to follow the behavior of the frequencies in the continuum as well as for $E^2<1$, in order to ascertain whether or not anything happens in the continuum to make up for the loss of pairs of real discrete eigenvalues. This can be accomplished by placing the potential well at the center of a spherical region of radius $R \gg a$, at which the current is made to vanish. The "continuum" ($E^2>1$) then consists of a set of closely spaced discrete states. The (unnormalized) regular solutions are properly joined pairs of the following:

$$\begin{aligned} &u=\sinh(\lambda r/a), \quad r<a, \quad (E+V_0)^2<1, \\ &u=\sin(\xi r/a), \quad r<a, \quad (E+V_0)^2>1; \end{aligned} \tag{4}$$

$$\begin{aligned} &u=\sinh[(\eta/a)(r-R)], \quad r>a, \quad E^2<1, \\ &u=\sin[(\mu/a)(r-R)], \quad r>a, \quad E^2>1; \end{aligned} \tag{5}$$

where $\lambda \equiv a[1-(E+V_0)^2]^{\frac{1}{2}}$, $\mu \equiv a(E^2-1)^{\frac{1}{2}}$. The positions of the roots are most readily found by plotting the logarithmic derivative of Eqs. (4) against $(E+V_0)$ and the logarithmic derivative of Eqs. (5) against E, superposing them on each other with the origin of the former curve shifted to the left by a variable amount V_0, and picking off the values of E for which intersections occur. The schematic curves of Fig. 1 were obtained in this way; they move to the left and crowd together as a increases. It is seen that the lowest level of the upper "continuum" ($E>1$) and the highest level of the lower "continuum" ($E<-1$) come together fist, then the second lowest of the upper and the second highest of the lower "continuum," etc. Thus the confluence of a pair of roots represents a genuine replacement of a pair of real frequencies by a conjugate complex pair of complex frequencies, accompanied by no other gain or loss of roots.

It must be remembered that the contribution of one of the real frequencies to the quantized field energy and charge is given by $NE\epsilon$ and $Ne\epsilon$, respectively, where N is the occupation number for the state in question. Thus the frequency E_1 represents (for $N=1$) a particle of charge e bound by an attractive potential, while the frequency E_2 represents a particle of charge $-e$ *bound by a repulsive potential* such that its energy is between 0 and 1. It should be remarked again that all of these results follow in qualitatively similar fashion for any sufficiently deep and broad potential well, and do not depend on the discontinuity of the above chosen $V(r)$ at $r=a$.

In view of the paradoxical result italicized above and the appearance of complex frequencies for sufficiently deep and broad potentials, it is of interest to see if similar results obtain in the case of a Dirac particle. Separating in spherical coordinates in the usual way[2] and considering only the pair of solutions of lowest angular momentum ($j=\frac{1}{2}$, $\kappa=\pm 1$), we obtain for the (unnormalized) solution corresponding to the first of Eqs. (5) and $\kappa=-1$:

$$\begin{aligned} rg&=\sinh[(\eta/a)(r-R)], \\ rf&=(1+E)^{-1}\{(\eta/a)\cosh[(\eta/a)(r-R)] \\ &\qquad -r^{-1}\sinh[(\eta/a)(r-R)]\}, \end{aligned}$$

with similar solutions for the other three cases. The same procedure for finding the frequencies may then be followed as in the Pauli-Weisskopf case, except that the boundary condition at $r=a$ is now that f/g be continuous.

The behavior of the roots is plotted schematically in Fig. 2; again the curves move to the left and crowd together as a increases. There is

[2] H. A. Bethe, *Handbuch der Physik* **24/1**, p. 312.

no crossing or disappearance of real roots; they simply move successively from the bottom of the upper to the top of the lower "continuum." If the vacuum is defined as that state of the system in which the total charge is equal to just that of the filled negative energy "continuum" for $V_0=0$ and the energy is a minimum, then one sees that there are no bound positron states, and the paradoxical result obtained above for the Pauli-Weisskopf case does not occur here. For sufficiently large V_0, however, the vacuum is not the lowest possible energy state of the system, but differs from it by a charge and energy that are both finite for finite V_0. The states for $\kappa=+1$ are obtained from the above by interchanging f and g and changing the signs of E and V_0; they behave qualitatively the same as, and are separate from, the states for $\kappa=-1$.

II.

We have now to see whether it is possible to extend the methods of the preceding paper to this case that the Klein-Gordon frequencies may be complex. From the example given above it is clear that as the potential V is deepened, a pair of ϵ_k, one positive and one negative, vanish and that their respective frequencies E_k^+ and E_k^- become equal: $E_k^+=E_k^-=E$. As the potential is further deepened complex frequencies appear. It is easy to see that quite generally the ϵ_k must vanish in pairs, since the identities I (34, 35, 36) must hold uniformly as the potential is gradually altered.

For the special case that the potential is just deep enough to make a pair of ϵ_k vanish, energy and charge take the form

$$H=(N_+-N_-)E+\sum{}'N_kE_k\epsilon_k/|\epsilon_k|,$$
$$q=(N_+-N_-)e+e\sum{}'N_k\epsilon_k/|\epsilon_k|,$$

where the prime on the summation excludes states of vanishing ϵ_k. Since only (N_+-N_-) occurs in these forms, N_+ and N_- cannot be determined by charge and energy alone, and the system is degenerate: an arbitrary number of pairs may appear without contributing to the energy. For this state charge and current density will in general be infinite. This situation is the extreme limit for which stationary states of the field may be defined.

When complex frequencies E_k occur, $\epsilon_k=0$ also; and we must restate the essential conclusions of the preceding paper. Defining:

$$\epsilon_{kl}\equiv\int\psi_l^*(E_k+E_l^*-2eV)\psi_k dv,$$

and

$$\sum_l\zeta_{nl}\epsilon_{lk}\equiv\delta_{nk},$$

we get:

$$\epsilon_{kl}(E_k-E_l^*)=0$$

—orthogonality relation;

$$q=e\sum_{kl}\tfrac{1}{2}(a_ka_l^*+a_l^*a_k)\epsilon_{kl}$$

—total charge;

$$H=\sum_{kl}\tfrac{1}{2}(a_ka_l^*+a_l^*a_k)\epsilon_{kl}E_k$$

—total energy;

$$L(x,t';x',t')=i\sum_{kl}\zeta_{kl}\psi_k(x)\psi_l^*(x')=0$$

—Green's function;

$$[\psi(x),\psi^*(x')]=\sum_{kl}[a_k,a_l^*]\psi_k(x)\psi_l^*(x')=0$$

—commutation law.

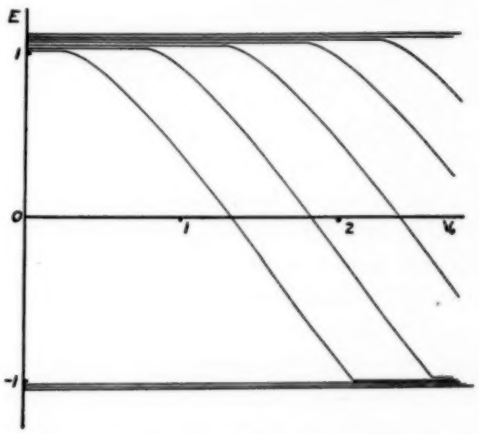

FIG. 2. The frequency E of the Dirac equation with potential as in Fig. 1, for $j=\frac{1}{2}$, $l=0$, $\kappa=-1$.

Either from the requirement $\dot{a}_k=-iEa_k=[a_k,H]$, or from the commutation laws I(8) taken together with the uniqueness theorem for the Green's function, we obtain the commutation rules:

$$[a_k,a_l^*]=\zeta_{kl},\qquad[a_l,a_k^*]=\zeta_{kl}^*,\qquad(6)$$

with all other commutators zero.

If one state has the complex frequency $E=U+iW$ corresponding to a wave-function ψ

and quantized amplitude a, then ψ^* will also be a solution of I(14), with frequency $E^*=U-iW$, to which we may assign a quantized amplitude b^*. Since a, b, a^*, b^* commute with all other a_k, a_k^*, we may consider separately the terms q_0, H_0 in q, H, due to the former alone:

$$q_0/e=\tfrac{1}{2}(ab+ba)\epsilon+\tfrac{1}{2}(a^*b^*+b^*a^*)\epsilon^*,$$
$$H_0=\tfrac{1}{2}(ab+ba)\epsilon E+\tfrac{1}{2}(a^*b^*+b^*a^*)\epsilon^*E^*,$$

where the complex number ϵ is defined by:

$$\epsilon\equiv 2\int\psi^2(E-eV)dv,$$

and where

$$[a,b]=\epsilon^{-1}, \qquad [b^*,a^*]=\epsilon^{*-1}, \tag{7}$$

with all other commutators zero. We next define two Hermitian operators N, M:

$$N\equiv\tfrac{1}{2}(ab+ba)\epsilon+\tfrac{1}{2}(a^*b^*+b^*a^*)\epsilon^*,$$
$$M\equiv(1/2i)(ab+ba)\epsilon-(1/2i)(a^*b^*+b^*a^*)\epsilon^*,$$

which satisfy $[M,N]=0$. In terms of these,

$$q_0=Ne, \qquad H_0=NU-MW.$$

Simple application of (7) shows:

$$\begin{matrix}[a,N]=a,\\ [a,M]=-ia;\end{matrix} \quad \text{and} \quad \begin{matrix}[b,N]=-b,\\ [b,M]=ib.\end{matrix} \tag{8}$$

It can then be shown that if a has one finite matrix element in the representation in which M is diagonal, then M has at least one complex eigenvalue. But M was defined to be Hermitian and cannot have complex eigenvalues. Hence if there exists a diagonal representation of H_0 (and therefore of M) when complex values of E occur in I(14), the charge and current densities will be everywhere infinite. Since in this case there are no physically admissible solutions, we say that M cannot be diagonalized.

The preceding discussion may be applied equally well to scalar or vector mesotron fields, since the generalized relations (6) hold in either case.

In spite of the fact the M cannot be diagonalized, it is easy to find Hermitian matrices of infinite rank which satisfy (8). The off-diagonal elements of M in the rth row are of order r, and the roots of the rth-order secular determinant for the characteristic values of M approach no limit as $r\to\infty$. The physical origin of this divergence lies in the fact that the emission of pairs into these degenerate states stimulates, because of the Einstein-Bose quantization, the further emission into these same states.

The arguments given here show then that there are certain types of electrostatic potential for which it is not possible to find stationary states for the scalar field. A situation somewhat analogous to this occurs in the Dirac electron theory, with a Coulomb field and with $Z>137$, in the present scalar theory with $Z>\frac{1}{2}\cdot 137$, or even in nonrelativistic wave mechanics, for potentials a/r^2, for $a<-\frac{1}{4}$; in all these cases the S-state eigenfunctions become singular, and the set of functions satisfying the regularity conditions is not complete: wherever this is so, the field Hamiltonian cannot be brought to diagonal form. The case we have here considered, however, is unique in that the potentials V involved are nowhere infinite, and solutions of the Pauli-Weisskopf field equations free of singularities exist.

In all these cases where the energy cannot be brought to diagonal form, we must take into account either existing deviations from the assumed potential, such as the breakdown of the Coulomb law at small distances, or the reaction of the pair field itself on the external field. In the simple case discussed in Section I, it is clear that no finite work can maintain the potential indefinitely, and the power necessary to maintain it for a finite time can be calculated from time dependent solutions of the field equations.

It is a pleasure to thank Professor J. R. Oppenheimer for suggesting this problem and for many helpful discussions concerning its solution.

Generalized Theory of Diffusion

E. J. HELLUND
University of Washington, Seattle, Washington
(Received September 21, 1939)

The theory of diffusion in mixtures with more than two components has been developed as an extension of the theory of Enskog for binary mixtures. In particular, the various coefficients have been evaluated as functions of the binary coefficients of diffusion. Attention has also been given to the theory of osmotic diffusion in connection with the Loschmidt experiment. The analysis has been carried through in such a manner as to be applicable to Einstein-Bose and Fermi-Dirac gases as well as the Maxwell-Boltzmann Type. The paper has been divided into two parts which deal with first, pressure diffusion and second, with thermal diffusion.

INTRODUCTION

THE phenomena of diffusion are divisible roughly speaking into two classes which may be characterized as effects of the first and second orders, respectively. One generally considers in the first class the effects of pressure and potential gradients and in the second the effect of temperature gradients. In the treatment by means of perturbation theory the first class is a function chiefly of the first approximation to the first-order variation of the distribution function, while the second necessitates the consideration of the second approximation.

Rigorous analysis of the problem of diffusion in mixtures of two gases has been given by Enskog and Chapman. The work of Enskog,[1] who first discovered thermal diffusion, allows with some modification the generalization to mixtures with three or more components. It is evident with even first consideration that the problem of diffusion in this case is not simply a repetition of the theory of binary diffusion, since one immediately perceives that the possibility exists for diffusion induced by streaming of one gas through the mixture. This streaming roughly may be thought of as producing forces which act on each component gas with different magnitudes by virtue of the different interactions which exist between the individual molecules of each component. It is evident that, in special cases only, is the theory of binary diffusion applicable to mixtures.

One encounters experimentally the condition of streaming by one component quite frequently. This state occurs for example when a source or sink exists for a given element. That is, whenever the removal or creation of an element (by such processes as the condensation and vaporization or combination and decomposition) is not uniform throughout the gas enclosure, pressure gradients are set up which then induce these currents in the mixture. The phenomena of electron winds and ion drift produced by electric fields and of polarizable particles in inhomogeneous fields, are likewise familiar. Seemingly somewhat removed, but still in the same category, one may consider the case of high temperature radiation through gas mixtures.

In addition to the case of streaming of one component into the mixture we must consider the problem of diffusion of one component. This leads to an analysis closely related to the diffusion previously mentioned. Experiments which would fall into this category are those for which diffusion of air and some other gas is observed. Data on the coefficients for oxygen, nitrogen, hydrogen, and carbon dioxide into air have been given with considerable accuracy.

Last one must consider the thermal diffusion in mixtures of three or more components. This phenomenon is like the case of ordinary diffusion complicated by the existence of several components with different interactions. The expression becomes there the more involved and is not expressible in terms of binary thermal diffusion coefficients with any degree of simplicity.

The plan followed is to proceed from the Boltzmann equation with the left member transformed

[1] D. Enskog, (a) "Kinetische Theorie der Vorgänge in Mässig Verdünnten Gasen," Dissertation, Upsala.

into derivatives of the pressures and potentials and temperature. In the work[2] cited below these equations were simplified at that point by the limitation to mixtures of two components only. All discussion up to this point is thus to be obtained in this work which will be referred to as H.U. for reference in the ensuing discussion.

Formal Expressions for the Mass Current

One proceeds then from the equations for a mixture of N gases which are the equations obtained from the Boltzmann equations by considering a solution to first orders alone.

$$\frac{f_j^{0_2}\exp(\tau_j^2)}{A_j}\left[\frac{\xi_{j\alpha}}{n_jkTc_j^{\frac{1}{2}}}\left(\frac{\rho_j}{\rho}\right)\left\{\frac{\partial p^q}{\partial\chi_\alpha}-\rho_qX_{q\alpha}\right\}\right]=\sum_{s=1}^{N}I_{js}(\chi^j+\chi^s),\quad j\neq q \tag{1}$$

$$\frac{f_q^{0_2}\exp(\tau_q^2)}{A_q}\left[\frac{\xi_{q\alpha}}{n_qkTc_q^{\frac{1}{2}}}\left(\frac{\rho_q-\rho}{\rho}\right)\left\{\frac{\partial p^q}{\partial\chi_\alpha}-\rho_qX_{q\alpha}\right\}\right]=\sum_{s=1}^{N}I_{qs}(\chi^q+\chi^s),\quad j=q \tag{2}$$

where f_j^0 is the distribution function for the jth component. The remaining symbolism is that given in H.U. (see also Appendix A). In addition, it must be noticed that only a perturbation by forces acting on the qth component is considered. There is, however, no loss of generality since the equations are linear. If one now assumes that the perturbation of the distribution functions is given by

$$\chi^s=\frac{\pi^{\frac{1}{2}}}{kT}L_q^s\left(\frac{\partial p^q}{\partial\chi_\alpha}-\rho_qX_{q\alpha}\right)\equiv\pi^{\frac{1}{2}}L_q^sZ^q/kT, \tag{3}$$

and the collision integrals are transformed by using the relation

$$d\varphi_q=n_qd\omega_q/\pi^{\frac{1}{2}}F_{\frac{1}{2}}(A_q). \tag{4}$$

The equations which result are then expressible in the following form

$$\frac{f_j^{0_2}\exp(\tau_j^2)}{A_jF_{\frac{1}{2}}(A_j)}\frac{\xi_{j\alpha}}{(m_j)^{\frac{1}{2}}}\left(\frac{\rho_j}{\rho}\right)=\sum_{s=1}^{N}n_jn_s\left(\frac{m_j+m_s}{m_jm_s}\right)^{\frac{1}{2}}I_{js}'\{L_q^j+L_q^s\},\quad j\neq q \tag{5}$$

$$\frac{f_q^{0_2}\exp(\tau_q^2)}{A_qF_{\frac{1}{2}}(A_q)}\frac{\xi_{q\alpha}}{(m_q)^{\frac{1}{2}}}\left(\frac{\rho_q-\rho}{\rho}\right)=\sum_{s=1}^{N}n_qn_s\left(\frac{m_q+m_s}{m_qm_s}\right)^{\frac{1}{2}}I_{qs}'\{L_q^q+L_q^s\}.\quad j=q. \tag{6}$$

The I_{js}' are the collision integrals defined with integration on $d\omega$ and substitution of the variable γ for g, the relative velocity, where

$$\gamma_{r,s}=g_{r,s}\left(\frac{m_rm_s}{2kT(m_r+m_s)}\right)^{\frac{1}{2}}. \tag{7}$$

In the following we shall have occasion to use the definition of the mixed bracket given by Enskog[3]

$$[L,L]_{j,s}=\int L^jI_{js}'\{L^j+L^s\}d\omega_j+\int L^sI_{sj}'\{L^s+L^j\}d\omega_s. \tag{8}$$

It is necessary now to extend the definition of the curly bracket, H.U. (Enskog[4]). The new form

[2] E. J. Hellund and E. A. Uehling, Phys. Rev. **56**, 818–835 (1939).
[3] Reference 1, p. 67.
[4] Reference 1, p. 68.

is to be taken as

$$\{L;N;L\}=\sum_{j\geq s}n_jn_s\left(\frac{m_j+m_s}{m_jm_s}\right)^{\frac{1}{2}}[L,L]_{j,s}. \tag{9}$$

In view of the properties of the mixed bracket $[F,G]_{j,s}$ there exist the same set for $\{F;N;G\}$,

$$\{F;N;G\}=\{G;N;F\}, \tag{10a}$$

$$\{F;N;G+H\}=\{F;N;G\}+\{F;N;H\}, \tag{10b}$$

$$\{F;N;cH\}=C\{F;N;H\}, \tag{10c}$$

$$\{F;N;F\}\geqslant 0. \tag{10d}$$

It may now be shown that the coefficient of mass diffusion is expressible in terms of this extended curly bracket, and that the solution of the perturbation problem resolves itself into a variational calculation.

It is desired to evaluate the difference of the velocity of streaming of the q component gas and the entire mixture. That is,

$$\begin{aligned}U_q-\sum_{s=1}^{N}\frac{U_s\rho_s}{\rho}&=U_q\left(\frac{\rho-\rho_q}{\rho}\right)-\sum_{s\neq q}^{N}\frac{U_s\rho_s}{\rho}\\&=\int\frac{f_q^{\circ}(1+\theta_qf_q^{\circ})\chi^qU}{n_q}d\varphi_q\left(\frac{\rho-\rho_q}{\rho}\right)-\sum_{s\neq q}\int\frac{f_s^{\circ}(1+\theta_sf_s^{\circ})\chi^sU}{n_s}d\varphi_s\left(\frac{\rho_s}{\rho}\right).\end{aligned} \tag{11}$$

By transformation of variable this becomes

$$-\left(\frac{2}{kT}\right)^{\frac{1}{2}}\left[\int\frac{f_q^{\circ 2}\exp(\tau_q^2)}{A_qF_1(A_q)}\frac{\xi_q}{(m_q)^{\frac{1}{2}}}dw_q\left(\frac{\rho_q-\rho}{\rho}\right)L_q{}^q+\sum_{s\neq q}\int\frac{f_s^{\circ 2}\exp(\tau_s^2)}{A_sF_1(A_s)}\frac{\xi_s}{(m_s)^{\frac{1}{2}}}dw_s\frac{\rho_s}{\rho}L_q{}^s\right]Z^q. \tag{12}$$

The last expression is then by virtue of Eqs. (5) and (6), just $\{L_q;N;L_q\}$, so that,

$$U_q-\sum_{s=1}^{N}\frac{U_s\rho_s}{\rho}=-\left(\frac{2}{kT}\right)^{\frac{1}{2}}\{L_q;N;L_q\}. \tag{13}$$

The mass current of component q is given by

$$J_p{}^q=-\left(\frac{2}{kT}\right)^{\frac{1}{2}}\{L_q;N;L_q\}\rho_qZ^q. \tag{14}$$

To demonstrate that the function L may be arrived at by a variational calculation one proceeds just as in the case of two components. That is, if,

$$\{L^*;N;L^*\}=\{L^*;N;L\}, \tag{15}$$

where L^* is an approximation to the exact solution which is to be made as good a solution as possible, by adjustment of the parameters on which it depends, then

$$\begin{aligned}0\leqslant\{L^*-L;N;L^*-L\}&=\{L^*;N;L^*\}+\{L;N;L\}-2\{L^*;N,L\}\\&=\{L;N;L\}-\{L^*;N;L^*\}.\end{aligned} \tag{16}$$

Thus L^* must be chosen so as to maximize the bracket.

If temperature variations are considered one also finds the perturbation of the distribution function to be determined in like manner. However for the present, thermal diffusion will not be considered, but will be treated after the analysis of pressure diffusion.

Explicit Determination of the Mass and Particle Currents

When the method of solution has been determined there remains only the consideration of the auxiliary conditions relating to the macroscopic description of the state of the gas for the perturbed and unperturbed case, (H.U.). To satisfy the auxiliary conditions the solution may be formulated in terms of $MN+N-1$ parameters as follows,

$$L^*=\sum_{j=1}^{M}\sum_{s=1}^{N}\beta_s{}^j h_s{}^j+\sum_{1=s}^{N}\beta_0{}^s\left(\frac{\xi^q}{n_q(m_q)^{\frac{1}{2}}}-\frac{\xi^s}{n_s(m_s)^{\frac{1}{2}}}\right). \tag{17}$$

In the following we shall write

$$H_s{}^q=\frac{\xi^q}{n_q(m_q)^{\frac{1}{2}}}-\frac{\xi^s}{n_s(m_s)^{\frac{1}{2}}}. \tag{18}$$

One then obtains the system of equations which are the result of the maximal property for the best solution to be obtained from a given number of parameters.

$$\begin{gathered}\{H_t{}^q;N;\sum_{s=1}^{N}\beta_0{}^s H_s{}^q+\sum_{1}^{M}\sum_{1}^{N}\beta_s{}^j h_s{}^j\}-\{H_t{}^q;N;L\}=0,\quad t=1\cdots N,\\ \{h_t{}^r;N;\sum_{1}^{N}\beta_0{}^s H_s{}^q+\sum_{1}^{M}\sum_{1}^{N}\beta_s{}^j h_s{}^j\}-\{h_t{}^r;N;L\}=0,\quad r=1\cdots M;\ t=1\cdots N,\\ \sum_{1}^{N}\beta_0{}^s H_s{}^q+\sum_{1}^{M}\sum_{1}^{N}\beta_s{}^j h_s{}^j-L^*=0.\end{gathered} \tag{19}$$

This yields for L^*,

$$L^*=-\frac{\begin{vmatrix}\{H_t{}^q;N;H_s{}^q\}, & \{H_t{}^q;N;h_s{}^j\}, & \{H_t{}^q;N;L\}\\ \{h_t{}^r;N;H_s{}^q\}, & \{h_t{}^r;N;h_s{}^j\}, & \{h_t{}^r;N;L\}\\ H_s{}^q, & h_s{}^j, & 0\end{vmatrix}}{\begin{vmatrix}\{H_t{}^q;N;H_s{}^q\}, & \{H_t{}^q;N;h_s{}^j\}\\ \{h_t{}^r;N;H_s{}^q\}, & \{h_t{}^r;N;h_s{}^j\}\end{vmatrix}}. \tag{20}$$

Consequently we have for the mass current

$$J_\rho{}^q=-\left(\frac{2}{kT}\right)^{\frac{1}{2}}\rho_q Z^q\{L_q{}^*;N;L_q{}^*\}=-\left(\frac{2}{kT}\right)^{\frac{1}{2}}\rho_q\{L_q{}^*;N;L_q\}Z^q, \tag{21}$$

$$=+\left(\frac{2}{kT}\right)^{\frac{1}{2}}\rho_q\frac{\begin{vmatrix}\{H_t{}^q;N;H_s{}^q\}, & \{H_t{}^q;N;h_s{}^j\}, & \{H_t{}^q;N;L\}\\ \{h_t{}^r;N;H_s{}^q\}, & \{h_t{}^r;N;h_s{}^j\}, & \{h_t{}^r;N;L\}\\ \{H_s{}^q;N;L\}, & \{h_s{}^j;N;L\}, & 0\end{vmatrix}}{\begin{vmatrix}\{H_t{}^q;N;H_s{}^q\}, & \{H_t{}^q;N;h_s{}^j\}\\ \{h_t{}^r;N;H_s{}^q\}, & \{h_t{}^r;N;h_s{}^j\}\end{vmatrix}}Z^q. \tag{22}$$

Excluding the composition dependence of the diffusion coefficient the result for the mass current is given with sufficient accuracy by the zero-order functions H_s^q. Consequently we evaluate the brackets $\{H_r^q; N; H_s^q\}$. For the case $r \neq s$ we have,

$$\{H_r^q; N; H_s^q\} = n_r n_s \left(\frac{m_r+m_s}{m_r m_s}\right)^{\frac{1}{2}} [H_r^q, H_s^q]_{r,s} + n_q n_s \left(\frac{m_q+m_s}{m_q m_s}\right)^{\frac{1}{2}} [H_r^q, H_s^q]_{q,s}$$

$$+ n_q n_r \left(\frac{m_q+m_r}{m_q m_r}\right)^{\frac{1}{2}} [H_r^q, H_s^q]_{q,r} + \sum_{t \neq s,r} n_q n_t \left(\frac{m_q+m_t}{m_q m_t}\right)^{\frac{1}{2}} [H_r^q, H_s^q]_{q,t}. \quad (23)$$

And for the case $r=s$,

$$\{H_t^q; N; H_r^q\} = \sum_{s=1}^{N} n_s n_r \left(\frac{m_s+m_r}{m_s m_r}\right)^{\frac{1}{2}} [H_r^q, H_r^q]_{r,s} + \sum_{t \neq r} n_t n \left(\frac{m_t+m_r}{m_q m_r}\right)^{\frac{1}{2}} [H_r^q, H_r^q]_{t,q}. \quad (24)$$

There exist the following relations which serve to evaluate the mixed brackets

$$[\xi_r, \xi_r]_{r,s} = \frac{8}{3}\pi^{7/2} \frac{m_s}{m_r+m_s} P_{q,s}^{1,5}(1), \quad (25)$$

$$[\xi_r, \xi_s]_{r,s} = -\frac{8}{3}\pi^{7/2} \frac{(m_r m_s)^{\frac{1}{2}}}{m_r+m_s} P_{r,s}^{1,5}(1), \quad (26)$$

where the definition of the function $P_{1,2}{}^{1,5}(1)$ is that of Enskog[5] with the modifications due to statistics noted in H.U.

Also we have

$$\{H_r^q; N; L_q\} = -\pi^{\frac{1}{2}}/2\rho_q. \quad (27)$$

It is to be noted that the statistical density dependence is ignored as well as the interference effect (H.U.) in the expression for the brackets. Only the effect in the cross section is included in the form given. One obtains for the mixed brackets the expression

$$\{H_r^q; N; H_s^q\}_{r \neq s} = -\frac{8}{3}\pi^{7/2} \frac{P_{r,s}^{1,5}(1)}{(m_r m_s (m_r+m_s))^{\frac{1}{2}}} + \frac{8}{3}\pi^{7/2} \left(\frac{\rho_s+\rho_q}{\rho_q}\right) \frac{P_{s,q}^{1,5}(1)}{[m_s m_q (m_s+m_q)]^{\frac{1}{2}}}$$

$$+ \frac{8}{3}\pi^{7/2} \left(\frac{\rho_r+\rho_q}{\rho_q}\right) \frac{P_{r,s}^{1,5}(1)}{[m_r m_q (m_r+m_q)]^{\frac{1}{2}}} + \frac{8}{3}\pi^{7/2} \sum_{t \neq s,r} \frac{\rho_t}{\rho_q} \frac{P_{t,q}^{1,5}(1)}{[m_t m_q (m_t+m_q)]^{\frac{1}{2}}}, \quad (28)$$

$$\{H_r^q; N; H_r^q\} = \frac{(\rho_q+\rho_r)^2}{\rho_q \rho_r} \frac{\frac{8}{3}\pi^{7/2} P_{q,r}^{1,5}(1)}{[m_q m_r (m_q+m_r)]^{\frac{1}{2}}} + \sum_{s \neq q,r} \frac{\frac{\rho_s}{\rho_r} \cdot \frac{8}{3}\pi^{7/2} P_{r,s}^{1,5}(1)}{[m_r m_s (m_r+m_s)]^{\frac{1}{2}}} + \sum_{t \neq r} \frac{\rho_t}{\rho_q} \frac{8}{3}\pi^{7/2} P_{t,q}^{1,5}(1). \quad (29)$$

It is to be noted here that the coefficient of mass diffusion for two gases is given by

$$D_{12} = \frac{3}{16}\left(\frac{kT}{2\pi}\right)^{\frac{1}{2}} \frac{[m_1 m_2 (m_1+m_2)]^{\frac{1}{2}}}{\rho_1+\rho_2} \cdot \frac{1}{P_{1,2}^{1,5}(1)}. \quad (30)$$

[5] Reference 1, p. 91.

One may therefore express the brackets in term of the binary diffusion coefficients as follows,

$$\{H_r^q; N; \underset{r\neq s}{H_s^q}\} = \frac{\pi^3}{2}\left(\frac{kT}{2}\right)^{\frac{1}{2}}\left[\frac{-1}{D_{r,s}(\rho_r+\rho_s)} + \frac{1}{\rho_q D_{q,s}} + \sum_{t\neq s,r}\frac{\rho_t}{\rho_q}\frac{1}{D_{t,q}(\rho_t+\rho_q)} + \frac{1}{\rho_q D_{q,r}}\right], \tag{31}$$

$$\{H_r^q; N; H_r^q\} = \frac{\pi^3}{2}\left(\frac{kT}{2}\right)^{\frac{1}{2}}\left[\frac{(\rho_q+\rho_r)}{\rho_q\rho_r}\cdot\frac{1}{D_{q,r}} + \sum_{s\neq q,r}\frac{\rho_s}{\rho_r}\cdot\frac{1}{D_{r,s}(\rho_r+\rho_s)} + \sum_{t\neq r}\frac{\rho_t}{\rho_q}\frac{1}{D_{t,q}(\rho_t+\rho_q)}\right]. \tag{32}$$

One therefore obtains for the mass current of the qth gas component into the mixture of which it is a member, the determinantal form,

$$J_p^q = (2kT)^{\frac{1}{2}}\rho_q \frac{\begin{vmatrix} \frac{\pi^3}{2}\left(\frac{kT}{2}\right)^{\frac{1}{2}}\left[\begin{matrix} -\frac{1}{D_{r,s}(\rho_r+\rho_s)} + \frac{1}{\rho_q D_{q,s}} + \frac{1}{\rho_q D_{q,r}} \\ + \sum_{t\neq s,r}\frac{\rho_t}{\rho_q}\frac{1}{D_{t,q}}(\rho_t+\rho_q)^{-1} \end{matrix}\right] & \cdot & \frac{-\pi^{\frac{3}{2}}}{2\rho_q} \\ \cdots\cdots\cdots\cdots & \cdot & \cdot \\ -\frac{\pi^{\frac{3}{2}}}{2\rho_q} \cdots\cdots\cdots\cdots & \cdot & 0 \end{vmatrix}}{\left|\frac{\pi^3}{2}\left(\frac{kT}{2}\right)^{\frac{1}{2}}\left[\begin{matrix} -\frac{1}{D_{r,s}(\rho_r+\rho_s)} + \frac{1}{\rho_q D_{q,s}} + \frac{1}{\rho_q D_{q,r}} \\ + \sum_{t\neq s,r}\frac{\rho_t}{\rho_q}\frac{1}{D_{t,q}(\rho_t+\rho_q)} \end{matrix}\right]\right|} \frac{\left(\frac{\partial p^q}{\partial x} - \rho_q X_{qx}\right)}{(kT)}. \tag{33}$$

In the above only the bracket form for $r\neq s$ has been used, but it must be remembered that the diagonal elements of the determinant require the expression (32). The diffusion coefficient itself is just the coefficient of $(\partial p^q/\partial x - \rho_q X_{qx})/kT$ in J_p^q. From the form it may be perceived that no explicit temperature dependence exists, since the determinant in the numerator has the last row and column free of temperature dependence. Likewise the factor π will cancel. Hence the coefficient of the gas q may be written,

$$D_{1,2,\cdots N}^{*p,q} = -\frac{\begin{vmatrix} \left[-\frac{1}{D_{r,s}(\rho_r+\rho_s)} + \frac{1}{\rho_q}\left(\frac{1}{D_{q,s}}+\frac{1}{D_{q,r}}\right) + \sum_{t\neq s,r}\frac{\rho_t}{\rho_q}\frac{1}{D_{t,q}(\rho_t+\rho_q)}\right] & -1 \\ -1 \cdots\cdots\cdots\cdots & 0 \end{vmatrix}}{\left|\left[-\frac{1}{D_{r,s}(\rho_r+\rho_s)} + \frac{1}{\rho_q}\left(\frac{1}{D_{q,s}}+\frac{1}{D_{q,r}}\right) + \sum_{t\neq s,r}\frac{\rho_t}{\rho_q}\frac{1}{D_{t,q}(\rho_t+\rho_q)}\right]\right|}. \tag{34}$$

For the case of three gases which is very nearly the case for experiments of diffusion of gases into air the result expanded is,

$$D_{1,2}^{*p,3} = \left(\frac{\rho_1+\rho_2}{\rho^2}\right)\left\{\frac{(\rho_1+\rho_2)(\rho_1+\rho_3)(\rho_2+\rho_3)D_{31}D_{32} + \rho_3\rho_2(\rho_3+\rho_2)D_{32}D_{12} + \rho_3\rho_1(\rho_3+\rho_1)D_{31}D_{12}}{\rho_3(\rho_1+\rho_2)D_{12} + \rho_2(\rho_1+\rho_3)D_{31} + \rho_1(\rho_3+\rho_2)D_{32}}\right\}. \tag{35}$$

The coefficient (35), just derived, as well as (34) is not the coefficient observed which corresponds to the binary diffusion coefficient, but must be changed by the factor,

$$D_{1,2}^{*p,3}\left(\frac{\rho}{\rho_1+\rho_2}\right) = D_{1,2}^{3,p}, \tag{36a}$$

and in general,

$$D_{1,2\cdots N}^{\rho,q} = D_{1,2\cdots N}^{*\rho,q}\left(\frac{\rho}{\rho-\rho_q}\right). \tag{36b}$$

It is essential to recognize here that the coefficients given are taken as giving the mass current when multiplied into the gradient of pressure or particle density, and not the mass density. Likewise these coefficients are not with respect to the velocity of the mixture, but the mass velocity. If a steady state of pressure is to be maintained in an experiment of the Loschmidt type, the total particle current is zero and hence the diffusion measured with respect to a stationary partition must be compared with the coefficient calculated with respect to the particle velocity. Thus what must be calculated is,

$$n_q\left\{U_q - \sum_{s=1}^{N}\frac{n_s U_s}{\sum_{t=1}^{N} n_t}\right\} = J_n{}^q. \tag{37}$$

This expression is readily evaluated since the function $L_q \equiv L_q', \cdots L_q{}^N$ has already been obtained. One obtains

$$J_n{}^q = n_q\left[\int \frac{f_q{}^\circ(1+\theta_q f_q{}^\circ)\chi^q U_q d\varphi_q}{n_q} - \sum_{s=1}^{N}\int \frac{f_s{}^\circ(1+\theta_s f_s{}^\circ)}{n_s}\chi^s U_s d\varphi_s \frac{n_s}{n}\right] \tag{38}$$

or

$$J_n{}^q = n_q\left[\int \frac{f_q{}^\circ(1+\theta_q f_q{}^\circ)}{F_{\frac{1}{2}}(A_q)}\frac{L^q\xi^q}{(m_q)^{\frac{1}{2}}}dw_q - \sum_{1}^{N}\frac{\int f_s{}^\circ(1+\theta_s f_s{}^\circ)}{F_{\frac{1}{2}}(A_s)}\frac{L^s\xi^s}{(m_s)^{\frac{1}{2}}}dw_s\frac{n_s}{n}\right]\left(\frac{2}{kT}\right)^{\frac{1}{2}} Z^q, \tag{39}$$

where

$$L^q = \sum_{s\neq q}\beta_0{}^s\frac{\xi^q}{n_q(m_q)^{\frac{1}{2}}} \tag{40a}$$

$$L^r = -\beta_0{}^r\frac{\xi^r}{n_r(m_r)^{\frac{1}{2}}}. \tag{40b}$$

One obtains

$$J_n{}^q = n_q\left[\sum\frac{\pi^{\frac{1}{2}}}{2\rho_q}\beta_0{}^r\frac{[\rho_r(n-n_q)+n_r\rho_q]}{n\rho_r}\right]. \tag{41}$$

To obtain the diffusion coefficient which corresponds to (34), one replaces in the numerator determinant the last row by the elements,

$$-\left\{\frac{\rho_r(n-n_q)+n_r\rho_q}{n\rho_r}\right\};\ r\neq q. \tag{42}$$

In deriving the expression for the diffusion with pressure gradients on all components, with constant total pressure, one may use the same basic set of functions $H_s{}^q$ to evaluate the perturbations. The expression for $\{H_s{}^q; N; L_s\}$ are changed in the determinant, but the remaining elements remain unchanged in form and hence the successive contributions to the diffusion are easily summable. The new brackets are,

$$\{H_r{}^q; N; L_s\} = 0; \quad r\neq s, \qquad \{H_s{}^q; N; L_s\} = \pi^{\frac{1}{2}}/2\rho_s. \tag{43}$$

Construction of the form $\{L_s; N; L_q\}$ then leads to the replacement of the last column in the numerator determinant of $-\pi^{\frac{1}{2}}Z^q/2\rho_q$ by,

$$-\frac{\pi^{\frac{1}{2}}}{2\rho_q}Z^q, \cdots \left(\frac{\pi^{\frac{1}{2}}}{2\rho_s}Z^s-\frac{\pi^{\frac{1}{2}}}{2\rho_q}Z^q\right), \frac{-\pi^{\frac{1}{2}}Z^q}{2\rho_q}, \cdots. \tag{44}$$

Summing for the last column and row, they appear as

$$\begin{vmatrix} & & & \frac{\pi^{\frac{1}{2}}}{2}\left[\frac{1}{\rho_1}Z^1-\frac{1}{\rho_q}Z^q\right] \\ & & & \frac{\pi^{\frac{1}{2}}}{2}\left[\frac{1}{\rho_2}Z^2-\frac{1}{\rho_q}Z^q\right] \\ & & & \vdots \\ & & & \frac{\pi^{\frac{1}{2}}}{2}\left[\frac{1}{\rho_{q-1}}Z^{q-1}-\frac{1}{\rho_q}Z^q\right] \\ & & & \frac{\pi^{\frac{1}{2}}}{2}\left[\frac{1}{\rho_{q+1}}Z^{q+1}-\frac{1}{\rho_q}Z^q\right] \\ & & & \vdots \\ & & & \frac{\pi^{\frac{1}{2}}}{2}\left[\frac{1}{\rho_N}Z^N-\frac{1}{\rho_q}Z^q\right] \\ -\frac{\pi^{\frac{1}{2}}}{2\rho_q}, & -\frac{\pi^{\frac{1}{2}}}{2\rho_q}, & \cdots\cdots\cdots\cdots & 0 \end{vmatrix} \tag{45}$$

For the case of 3 gases, if one assumes that $Z^1=-Z^3\rho_1/(\rho_1+\rho_2)$ and that $Z^2=-Z^3\rho_2/(\rho_1+\rho_2)$ one obtains the factor $\rho/(\rho-\rho_3)$ given in (36). The general factor follows from the same hypothesis for the various z_i. It would be necessary to justify the values given above in order to claim validity for the coefficients (36), for a given experiment. In general, however, the pressure variations are arbitrary, as well as the forces per unit mass for each component.

In (45) the elements of the last row replaced by (42) yield the expression desired to represent the number of particle which would diffuse through a stationary cross-sectional area in an enclosed vessel of the Loschmidt experiment, provided, with no external forces, we set

$$\sum_{s=1}^{N} Z^s=0.$$

For the case of three gases one may write

$$-kTJ_\rho{}^3=\left(\frac{1}{\rho_2}Z^2-\frac{1}{\rho_3}Z^3\right)\left\{-\frac{1}{\rho_1 D_{1,2}}-\frac{1}{\rho_1 D_{3,1}}+\frac{1}{(\rho-\rho_1)D_{3,2}}\right\}\Big/\Delta$$

$$+\left(\frac{1}{\rho_1}Z^1-\frac{1}{\rho_3}Z^3\right)\left\{\frac{-1}{\rho_2 D_{1,2}}+\frac{1}{(\rho-\rho_2)D_{3,1}}\frac{-1}{\rho_2 D_{3,2}}\right\}\Big/\Delta. \tag{46}$$

Also

$$-kTJ_n^3=\left(\frac{1}{\rho_2}Z^2-\frac{1}{\rho_3}Z^3\right)\left\{-\left(\frac{n_1+n_2}{n}\right)\frac{\rho}{\rho_1(\rho_1+\rho_2)}\cdot\frac{1}{D_{1,2}}+\frac{\rho}{n}\cdot\frac{n_1}{\rho_1}\cdot\frac{1}{(\rho_3+\rho_2)}\cdot\frac{1}{D_{3,2}}-\frac{1}{D_{3,1}}\cdot\frac{\rho n_2}{n\rho_2\rho_1}\right\}\Big/m_3\Delta$$

$$+\left(\frac{1}{\rho_1}Z^1-\frac{1}{\rho_3}Z^3\right)\left\{-\left(\frac{n_1+n_2}{n}\right)\frac{\rho}{\rho_2}\cdot\frac{1}{(\rho_1+\rho_2)}\cdot\frac{1}{D_{1,2}}-\frac{\rho}{n}\cdot\frac{n_1}{\rho_1\rho_2}\cdot\frac{1}{D_{3,2}}+\frac{\rho}{n}\cdot\frac{n_2}{\rho_2}\cdot\frac{1}{(\rho_3+\rho_1)}\cdot\frac{1}{D_{3,1}}\right\}\Big/m_3\Delta, \quad (47)$$

where

$$\Delta=\frac{1}{D_{3,1}D_{3,2}D_{1,2}}\frac{\rho^2}{\rho_1\rho_2\rho_3(\rho_3+\rho_1)(\rho_3+\rho_2)(\rho_1+\rho_2)}[\rho_3(\rho_1+\rho_2)D_{1,2}+\rho_2(\rho_3+\rho_1)D_{3,1}+\rho_1(\rho_3+\rho_2)D_{3,2}]. \quad (48)$$

It is perhaps of some interest to show that in an experiment of the Loschmidt type, diffusion may occur even when the gradient of density of the gas in question is zero. The effect, like thermal diffusion, is due to differences in mass and cross sections of the remaining components. This diffusion is the analog of the osmotic diffusion of liquids. To show this point, let us set, $Z^3=0$ and $Z^1=-Z^2$. Then

$$J_\rho^3=\frac{-D_{1,2}\dfrac{\rho_3(\rho_1+\rho_2)}{\rho}[D_{3,2}(\rho_3+\rho_2)-D_{3,1}(\rho_3+\rho_1)]\left(\dfrac{Z^1}{kT}\right)}{[\rho_3(\rho_1+\rho_2)D_{1,2}+\rho_2(\rho_3+\rho_1)D_{3,1}+\rho_1(\rho_3+\rho_2)D_{3,2}]} \quad (49)$$

and

$$J_n^3=\frac{-D_{1,2}\dfrac{\rho_3(\rho_1+\rho_2)}{nm_3}\left[\dfrac{D_{3,2}(\rho_3+\rho_2)}{m_2}-\dfrac{D_{3,1}(\rho_3+\rho_1)}{m_1}\right]\left(\dfrac{Z^1}{kT}\right)}{[\rho_3(\rho_1+\rho_2)D_{1,2}+\rho_2(\rho_3+\rho_1)D_{3,1}+\rho_1(\rho_3+\rho_2)D_{3,2}]}. \quad (50)$$

For the special case when $S_{1,2}\to 0$,

$$J_n^3=-\frac{\frac{3}{8}\left(\dfrac{kT}{2\pi}\right)^{\frac{1}{2}}(kT)}{P}\left\{\left(\frac{m_3+m_2}{m_3m_2}\right)^{\frac{1}{2}}S_{3,2}{}^{-2}-\left(\frac{m_3+m_1}{m_3m_1}\right)^{\frac{1}{2}}S_{3,1}{}^{-2}\right\}\left(\frac{Z^1}{kT}\right), \quad (51)$$

where P is the total pressure.

In (51) the binary coefficients have been given the classical values for elastic spheres. The diffusion initially set up, produces an opposing pressure gradient which then sets up a diffusion current in the opposite direction restoring the initial constant density of the third component. This would necessarily imply that the currents, one and two, would alternately exceed one another. The effect initially, would be large and decrease as the distributions of the first two components tended toward spatial uniformity.

In conclusion it may be emphasized that all measurements on mixtures of three or more components are dependent on the density ratios as well as the total densities, although the former dependence is not particularly strong. This dependence is quite apart from the composition dependence taken into account by the consideration of further terms in the approximation to the distribution function.

Appendix

In view of the fact that some change in notation between this paper and H.U. exists, the following equations are given from H.U. as numbered in that paper, and the changes noted.

$$\frac{f_i^{\circ 2}}{A_i\exp(-\tau_i^2)}\left[\frac{1}{c_i^{\frac{1}{2}}}\frac{1}{T}\xi_{i\alpha}\frac{\partial T}{\partial x_\alpha}\left(\tau_i^2-\frac{5}{2}\frac{p^i}{n_ikT}\right)+\left(\xi_{i\alpha}\xi_{i\beta}-\frac{\tau_i^2}{3}\delta_{\alpha\beta}\right)\left(\frac{\partial U_\alpha}{\partial x_\beta}+\frac{\partial U_\beta}{\partial x_\alpha}\right)\right.$$

$$\left.+\frac{2c_i^{\frac{1}{2}}}{\rho_i}\xi_{i\alpha}\left\{\left(\frac{\partial p^i}{\partial x_\alpha}-\rho_iX_{i\alpha}\right)-\frac{\rho_i}{\rho}\sum_{j=1}^{N}\left(\frac{\rho p_j}{\partial x_\alpha}-\rho_jX_{j\alpha}\right)\right\}\right]=-\sum_{j=1}^{N}I_{ij}(\chi). \quad (28)$$

In the present paper χ is represented by $\chi^i+\chi^j$. Also

$$I_{ij}(\chi)=G_j\left(\frac{m_j}{n}\right)^3\left(\frac{c_i+c_j}{c_ic_j}\right)^{\frac{1}{2}}c_j^{-\frac{1}{2}}F_i(A_i)F_i(A_j)J_{ij}(\chi), \tag{29}$$

$$J_{ij}(\chi)=F_i^{-1}(A_i)F_i^{-1}(A_j)\int dw_j\int\gamma_{ij}\omega_{ij}(\theta,\alpha)d\Omega\cdot f_i^{\circ\prime}f_j^{\circ\prime}\cdot(1+\theta_if_i^\circ)(1+\theta_jf_j^\circ)(\chi_i+\chi_j-\chi_i'-\chi_j'). \tag{30}$$

The following identity holds,

$$I_{ij}'(\chi^i+\chi^j)=J_{ij}(\chi).$$

Also, definition of the square brackets in H.U. is related to the present one by,

$$[F,G]_{ij}+[F,G]_{ji}]_{\text{H.U.}}\equiv[F,G]_{ij}.$$

FEBRUARY 15, 1940 PHYSICAL REVIEW VOLUME 57

Generalized Theory of Diffusion. II

E. J. HELLUND
University of Washington, Seattle, Washington

(Received November 16, 1939)

The theory of diffusion in ternary and higher order gas mixtures is completed with the discussion of thermal diffusion. The theory is carried to the point where assumptions about molecular interactions are necessary to obtain quantitative expression of the coefficients. In the special case of elastic spheres the formulae have been given in terms of the masses and cross sections, neglecting, however, the diffraction effects.

INTRODUCTION

THERMAL diffusion remains one of the few processes of diffusion which are difficult to analyze from elementary considerations, even for the case of binary mixtures. The coefficient is a function of differences in masses and force interactions and, in addition, respective particle concentrations and their ratios. No emphasis therefore need be given to the increased complication which the analysis of ternary and higher order mixtures introduces. It is nevertheless desirable to obtain formulae for the thermal coefficients in such cases in order to obtain additional insight into the processes involved as well as to check values obtained by direct experimentation.

In connection with the theory of isotope separation it is of interest to determine if the addition of new components has any optimum effect, and if so, to determine what the characteristics of these additional components must be in relation to the isotopes involved. It is also true that the isotopes occur frequently as groups of three or more so that from the point of view of application of theory to experiment, the binary analysis is inadequate for an actual description of results. These problems receive added interest and importance in light of the recent work of Furry, Jones and Onsager,[1] on isotope separation by thermal diffusion coupled with convective action.

The effect on the distribution function of the gas molecules by a temperature gradient is given by the equations which the first-order variations must satisfy (I APPENDIX (A))*

$$\frac{f_j^{\circ 2}}{A_j}\exp(\tau_j^2)\frac{1}{c_j^{\frac{1}{2}}}\cdot\frac{1}{T}\xi_j\frac{\partial T}{\partial x}\left(\tau_j^2-\frac{5}{2}\frac{p^j}{n_jkT}\right)=\sum_{s=1}^{N}I_{js}\{\chi^j+\chi^s\}, \tag{1}$$

where the symbolism is that of (I).

[1] Furry, Jones and Onsager, Phys. Rev. **55**, 1083 (1939).

* Reference to the first part will throughout be indicated by I.

If we take χ to be given by

$$\chi \equiv \frac{\pi^{\frac{1}{2}}}{kT} M \frac{\partial T}{\partial x},$$

one then obtains the following system of equations,

$$\frac{f_j^{\circ 2} \exp(\tau_j^2)}{A_j F_{\frac{1}{2}}(A_j)} \frac{\xi_{ja}}{(m_j)^{\frac{1}{2}}} \left(\tau_j^2 - \frac{5}{2} \frac{p^{(j)}}{n_j kT} \right) n_j k = -\sum_{s=1}^{N} n_j n_s \left(\frac{m_j + m_s}{m_j m_s} \right)^{\frac{1}{2}} I' \{ M^j + M^s \}. \tag{2}$$

And one obtains as in (I),

$$M = \frac{\begin{vmatrix} \cdots\cdots\cdots\cdots & \{H_s^q; N; M\} \\ H_s^q \cdots\cdots\cdots\cdots & 0 \end{vmatrix}}{|\{H_s^q; N; H_t^q\}|}. \tag{3}$$

As in I, attention has been focused on the qth component, and the basic set H_s^q of I employed in II. Eqs. (2), unlike the set in I, maintain symmetry with respect to all components. Since also the brackets $\{\xi_r; N; M\}$ vanish, it is necessary to include functions quadratic in τ. Thus, the simplest set sufficient to discuss thermal diffusion is,

$$H_s^q = \frac{\xi^q}{n_q (m_q)^{\frac{1}{2}}} - \frac{\xi^s}{n_s (m_s)^{\frac{1}{2}}}, \tag{4a}$$

$$h_s^1 = \xi^s \left[\tau_s^2 - \frac{5}{2} \frac{F_{3/2}(A_s)}{F_{1/2}(A_s)} \right]. \tag{4b}$$

Since the experiment to which we wish to apply the theory is one wherein a gas-filled vessel is in equilibrium under a certain temperature gradient, it is convenient to add the perturbations of the distribution functions due to pressure and temperature variations.

$$\chi_{P,T} = \frac{\pi^{\frac{1}{2}}}{kT} \frac{\begin{vmatrix} \cdots\cdots\cdots & \left\{ H_r^q; N; M \dfrac{\partial T}{\partial x} + \sum L_s Z^s \right\} \\ & \vdots \\ H_r^q \cdots\cdots\cdots\cdots & 0 \end{vmatrix}}{-\Delta}, \tag{5}$$

where Δ is the denominator in (3), and the term $\sum L_s Z^s$ is to be summed over all "s," (I). The conditions for equilibrium then demand that the particle current of any component calculated from (5) is zero, and that the total pressure be constant,

$$\left(\sum_{i=1}^{N} p^{(i)} = \text{const.} \right).$$

In analyzing the separations produced in a set of gases by thermal diffusion, one would then desire the values of all partial pressure gradients as well as the temperature gradient. From (5) it is possible to obtain $N-1$ independent equations by making the particle currents vanish. One additional equation is obtained from the condition that the sum of all the partial pressure gradients must vanish.

The relations which may now be used to simplify (5) are

$$\{H_s^q; N; M\partial T/\partial x\} = 0, \tag{6}$$

$$\{h_s'; N; \sum L_s Z^s\} = 0, \tag{7}$$

$$\{h_j'; N; M\partial T/\partial x\} = -\frac{2}{3}\frac{n_j k}{(m_j)^{\frac{1}{2}}}\frac{\Gamma(9/2)}{F_{\frac{1}{2}}(A_j)}\left[F_{5/2}(A_j) - \frac{5}{7}\frac{F_{3/2}(A_j)^2}{F_{1/2}(A_j)}\right]\left(\frac{\partial T}{\partial x}\right), \tag{8}$$

$$\{H_j^q; N; \sum L_s Z^s\} = \frac{\pi^{\frac{1}{2}}}{2}\left(\frac{1}{\rho_j}Z^j - \frac{1}{\rho_q}Z^q\right). \tag{9}$$

In computing the currents from (5), one finds that the contribution from the h's vanishes. Moreover, one finds, apart from a common factor, that the functions H_1^q, $H_2^q \cdots$ contribute to the current of particles of type "j," $j \neq q$, the amounts,

$$n_j\left(\frac{m_1 - m_q}{m_1}\right),\ n_j\left(\frac{m_2 - m_q}{m_2}\right),\ \cdots\ \frac{\rho_j - m_q(n_j - n)}{m_j} \tag{10}$$

and to the current of particles of type "q" the amounts,

$$\frac{m_1(n_q - n) - \rho_q}{m_1},\ \frac{m_2(n_q - n) - \rho_q}{m_2},\ \cdots. \tag{11}$$

If one replaces in (5) the values given (6), (7), (8), (9), (10), and (11), denoting the cofactors of the last column by A_r^s (where s denotes the particular current considered, and r the row), one finds the following set of equations to determine the various partial pressure gradients (where the classical values have been taken for the expressions (8)),

$$\sum A_j^s\left(\frac{1}{\rho_j}Z^j - \frac{1}{\rho_q}Z^q\right) - \sum_{v=N+1}^{2N} A_v^s \frac{5}{2}k\frac{n_{v-N}}{(m_{v-N})^{\frac{1}{2}}}\frac{\partial T}{\partial x} = 0, \tag{12a}$$

$$\sum_{v=1}^{N} Z^v = 0. \tag{12b}$$

It may be easily shown then, that

$$\frac{Z^j}{\rho_j} - \frac{Z^q}{\rho_q} = \frac{5}{2}k\frac{\begin{vmatrix} b_{j1}, & b_{j2}, & \cdots & \cdots & 0 \\ \cdots & \cdots & \cdots & \cdots & \dfrac{n_1}{(m_1)^{\frac{1}{2}}} \\ a_{r,s} & & & & \vdots \\ & & & & \dfrac{n_N}{(m_N)^{\frac{1}{2}}} \end{vmatrix}}{|a_{r,s}|}\cdot\frac{\partial T}{\partial x}, \tag{13}$$

where

$$b_{js} = \{H_j^q; N; h_s'\};\quad a_{r,s} = \{h_r'; N; h_s'\}.$$

To evaluate the determinants, it is necessary to calculate the $a_{r,s}$ and $b_{j,s}$.

$$\{H_r^q; N; H_s^q\} = \frac{-(8/3)\pi^{7/2}P_{r,s}^{1,5}}{[m_r m_s(m_r+m_s)]^{\frac{1}{2}}} + \sum\frac{[\rho_j + \rho_q(\delta_r^j + \delta_s^j)]}{\rho_q}\cdot\frac{(8/3)\pi^{7/2}P_{q,j}^{1,5}}{[m_q m_j(m_q+m_j)]^{\frac{1}{2}}}. \tag{14a}$$

$$\{H_r^q; N; H_r^q\} = \frac{(\rho_q+\rho_r)^2}{\rho_q\rho_r}\cdot\frac{(8/3)\pi^{7/2}P_{q,r}^{1,5}(1)}{[m_q m_r(m_q+m_r)]^{\frac{1}{2}}} + \sum_{i\neq r}\frac{\rho_j}{\rho_q}\cdot\frac{(8/3)\pi^{7/2}P_{q,j}^{1,5}(1)}{[m_j m_r(m_j+m_r)]^{\frac{1}{2}}}, \tag{14b}$$

$$\{H_r^q; N; h_s'\} = n_s\cdot\frac{8}{3}\pi^{7/2}\left[\frac{(m_r)^{\frac{1}{2}}}{(m_r+m_s)^{\frac{1}{2}}}\left\{P_{r,s}^{1,7}(1)-\frac{5}{2}P_{r,s}^{1,5}(1)\right\}-\frac{(m_s)^{\frac{1}{2}}}{(m_q+m_s)^{\frac{1}{2}}}\left\{P_{q,s}^{1,7}(1)-\frac{5}{2}P_{q,s}^{1,5}(1)\right\}\right], \tag{14c}$$

$$\{H_r^q; N; h_r'\} = -\frac{8}{3}\pi^{7/2}\left[n_r\frac{(m_q)^{\frac{1}{2}}}{(m_q+m_r)^{\frac{1}{2}}}\left\{P_{q,r}^{1,7}(1)-\frac{5}{2}P_{q,r}^{1,5}(1)\right\}\right.$$
$$\left.+\sum\frac{n_j}{m_r}\left(\frac{m_j}{m_j+m_r}\right)^{\frac{1}{2}}\left\{P_{j,r}^{1,7}(1)-\frac{5}{2}P_{j,r}^{1,5}(1)\right\}\right], \tag{14d}$$

$$\{h_r'; N; h_s'\} = \frac{-(8/3)\pi^{7/2}\rho_r\rho_s}{(m_r+m_s)^{5/2}}\left[\frac{55}{4}P_{r,s}^{1,5}(1)-5P_{r,s}^{1,7}(1)-\frac{4}{3}P_{r,s}^{2,7}(1)+P_{r,s}^{1,9}(1)\right], \tag{14e}$$

$$\{h_r'; N; h_r'\} = \frac{8}{3}\pi^{7/2}\sum_{s\neq r}n_r n_s\left(\frac{m_s}{m_r}\right)^{\frac{1}{2}}(m_r+m_s)^{-(5/2)}\cdot\left[\frac{5}{4}(6m_r^2+5m_s^2)P_{r,s}^{1,5}(1)-5m_s^2P_{r,s}^{1,7}(1)\right.$$
$$\left.+\frac{4}{3}m_r m_s P_{r,s}^{2,7}(1)+m_s^2P_{r,s}^{1,9}(1)\right]+\frac{8}{9}\pi^{7/2}n_r^2\left(\frac{2}{m_r}\right)^{\frac{1}{2}}P_{r,r}^{2,7}(1). \tag{14f}$$

With the values of the various brackets given in the group (14) the problem of the determination of the separations which can be produced in gas mixtures is halted until definite assumptions about the force interactions have been made. The simplest force law which can be used, which may be regarded as a first approximation to the actual law, is the elastic sphere model. In this case the various P functions have the following values,

$$P_{r,s}^{1,5}(1) = S^2_{r,s}/2, \tag{15a}$$

$$P_{r,s}^{1,7}(1) = 3S^2_{r,s}/2, \tag{15b}$$

$$P_{r,s}^{2,7}(1) = 3S^2_{r,s}/2, \tag{15c}$$

$$P_{r,s}^{1,9}(1) = 6S^2_{r,s}, \tag{15d}$$

where the $S_{r,s}$ are the elastic sphere diameters of interaction, equal to the average of the actual diameters of the two types of particles.

One has for then the case of three gases,

$$\frac{Z_2}{\rho_2}-\frac{Z_1}{\rho_1}=\frac{5}{2}k\frac{\begin{vmatrix} C_3^{12}, & -C_3^{21}, & f_3^2, & 0 \\ \cdots & \cdots & \cdots & 1 \\ & & & 1 \\ & B_{ij} & & 1 \end{vmatrix}}{|B_{ij}|}\cdot\frac{\partial T}{\partial x}, \tag{16}$$

$$\frac{Z_3}{\rho_3}-\frac{Z_1}{\rho_1}=\frac{5}{2}k\frac{\begin{vmatrix} C_2^{13}, & f_2^3, & -C_2^{21}, & 0 \\ \cdots & \cdots & \cdots & 1 \\ & & & 1 \\ & B_{ij} & & 1 \end{vmatrix}}{|B_{ij}|}\cdot\frac{\partial T}{\partial x}, \tag{17}$$

where
$$B_{jj}=-\frac{1}{3}\left[(2)^{5/2}S_{jj}^{2}n_j+\binom{m_j}{m_k}S_{jk}^{2}n_k+\binom{m_j}{m_l}S_{jl}^{2}n_l\right], \qquad j\neq k\neq l=1,2,3, \tag{18}$$

$$\binom{m_j}{m_k}=\left(\frac{m_k}{m_j+m_k}\right)^{\frac{1}{2}}\left\{\frac{30m_j^{2}+13m_k^{2}+16m_jm_k}{(m_j+m_k)^{2}}\right\}, \tag{19}$$

$$B_{jk}=-9\left[\frac{m_j^{3}m_k^{2}}{(m_j+m_k)^{5}}\right]^{\frac{1}{2}}S_{jk}^{2}n_k, \tag{20}$$

$$C_3^{12}=\frac{2}{3}\cdot\frac{1}{m_1}\left[\frac{(\rho_1+\rho_2)}{(m_1+m_2)}\left(\frac{m_2}{m_1+m_2}\right)^{\frac{1}{2}}S_{12}^{2}+\frac{\rho_3(m_3)^{\frac{1}{2}}}{(m_1+m_3)^{\frac{1}{2}}}S_{13}^{2}\right], \tag{21}$$

$$f_3^{2}=\frac{2}{3}n_3\left[\frac{(m_2)^{\frac{1}{2}}}{(m_2+m_3)^{\frac{1}{2}}}S_{23}^{2}-\frac{(m_3)^{\frac{1}{2}}}{(m_1+m_3)^{\frac{1}{2}}}S_{13}^{2}\right]. \tag{22}$$

An application of the preceding theory has been made with respect to a mixture of hydrogen, deuterium, and helium. The ratio of hydrogen to deuterium was taken as 5000 to 1 and the concentration of helium was taken as 0, 1/5, 2/5, 3/5, 4/5 and 1 with respect to the hydrogen number density. The collision diameter of deuterium was taken equal to that of hydrogen. This assumption appears to be sufficiently accurate in view of the experiments of Grew and Atkins[2] on thermal diffusion in deuterium mixtures.

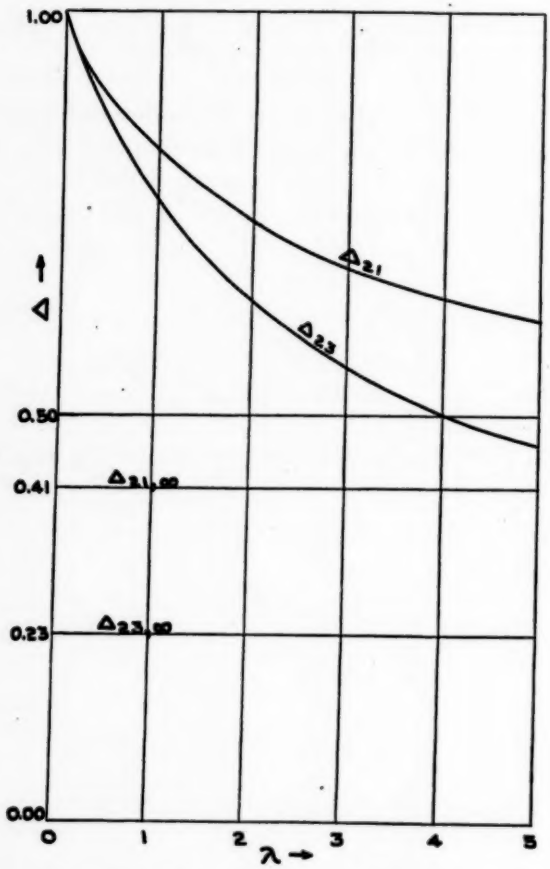

FIG. 1. Plot of the separation of deuterium and hydrogen, and of deuterium and helium against a variable helium concentration.

The results on the deuterium, hydrogen, helium mixture are of particular interest in view of the equality of masses of deuterium and helium. Any effect between the latter in a binary mixture depends solely on differences in cross sections. It is found that helium is much "harder" relatively, than deuterium. In the case chosen for application it may be expected from the mass effect that the result of addition of helium is to increase the separation of hydrogen and deuterium, provided the separations are dependent mainly on the mass ratios. Similarly from the mass effect it may be expected that the addition of an element intermediate in mass will tend to increase the separation of any pair of elements. The character and extent of such separation will of course be influenced by the remaining variables, which describe the mixture (cross sections and concentrations). For particular mass ratios it is apparent that the latter variables may be most important.

[2] K. E. Grew and B. E. Atkins, Proc. Phys. Soc. 48, 415–420 (1936).

If hydrogen, deuterium, and helium are numbered successively 1, 2, and 3, then we find,

$$\frac{\partial p^{(1)}}{\partial x} = -\frac{5}{2}k\frac{\rho_1}{\rho}\{\rho_2\delta_1+\rho_3\delta_2\}\frac{\partial T}{\partial x}, \tag{23}$$

$$\frac{\partial p^{(2)}}{\partial x} = +\frac{5}{2}k\frac{\rho_2}{\rho}\{\rho_1\delta_1+\rho_3(\delta_1-\delta_2)\}\frac{\partial T}{\partial x}, \tag{24}$$

$$\frac{\partial p^{(1)}}{\partial x}+\frac{\partial p^{(2)}}{\partial x}+\frac{\partial p^{(3)}}{\partial x}=0, \tag{25}$$

where

$$\delta_1=\frac{89\lambda^3+2{,}065\lambda^2+14{,}057\lambda+30{,}764}{344\lambda^3+7{,}090\lambda^2+50{,}637\lambda+98680}, \tag{26}$$

$$\delta_2=\frac{73\lambda^3+1{,}664\lambda^2+11{,}070\lambda+21{,}906}{344\lambda^3+7{,}090\lambda^2+50{,}637\lambda+98{,}680}, \tag{27}$$

$$\frac{n_3}{n_2}=1000\lambda, \quad \frac{n_1}{n_2}=5000, \quad \frac{m_3}{m_1}=\frac{m_2}{m_1}=2. \tag{28}$$

From (23) and (24) one readily obtains

$$\frac{\partial}{\partial x}\left(\log\frac{n_2}{n_1}\right)=\frac{5}{2}\frac{\partial}{\partial x}(\log T)\left\{\frac{[m_2(\rho_1+\rho_3)+\rho_2 m_1]\delta_1}{\rho}+\frac{(m_1-m_2)}{\rho}\rho_3\delta_2\right\}. \tag{29}$$

Let us define the coefficient Δ as

$$\Delta_{21}=\frac{\partial(\log n_2/n_1)/\partial x}{[\partial(\log n_2/n_1)/\partial x]_{n_3=0}}. \tag{30}$$

It is this coefficient which will be used as a measure of the separations to be produced in a mixture, and in Fig. 1 has been plotted for deuterium-hydrogen and for deuterium-helium, against an increasing helium concentration.

It will be observed from Fig. 1 that in both cases the separation becomes less as the helium concentration increases. No experimental data appears to be available as a check on this behavior and thus no check on the effect of the elastic sphere approximation can be made. Both hydrogen and deuterium, admittedly are not symmetric molecules and deviations are likely to be found from the curves in Fig. 1, since the phenomenon of thermal diffusion is so dependent on the type of force interaction between molecules.

LETTERS TO THE EDITOR

Prompt publication of brief reports of important discoveries in physics may be secured by addressing them to this department. Closing dates for this department are, for the first issue of the month, the eighteenth of the preceding month, for the second issue, the third of the month. Because of the late closing dates for the section no proof can be shown to authors. The Board of Editors does not hold itself responsible for the opinions expressed by the correspondents.

Communications should not in general exceed 600 words in length.

Secondary Neutrons from Uranium

Halban, Joliot, Kowarski and Perrin[1] report new experiments on the secondary neutrons which are produced in the fission of uranium. The purpose of this present note is to point out that these newer experiments lead to nearly the same value of the number of secondary neutrons per fission as do the considerably different older ones of Halban, Joliot, and Kowarski[2] and indicate that an explosive chain reaction cannot occur for any mixture of hydrogen and ordinary uranium. For the sake of brevity it is assumed that this note will be read in conjunction with the paper of Halban, Joliot, Kowarski and Perrin so that a resumé of the latter is omitted.

The rate of production of secondary neutrons by fission is $Q_{\text{int}}w\nu$, ν being the number of secondary neutrons per fission. This must equal the total number of neutrons slowed per second, $Q_{\text{int}}/(1-p)+Q_{\text{ext}}$ minus the rate of production of primary neutrons, 1. From this one gets

$$\nu=\frac{1}{w}\left[\frac{Q_{\text{int}}/(1-p)+Q_{\text{ext}}-1}{Q_{\text{int}}}\right]. \tag{1}$$

Using the experimental results of Halban, Joliot, Kowarski and Perrin, the same nuclear cross sections and their value of p for the $3H$ experiment, the values of ν given in the next to the last column of Table I have been obtained. The values of p for the $2H$ and $1H$ experiments have been calculated from that for $3H$ on the crude assumption that the rate of change of p with the logarithm of the concentration of H is the same as in the range from $65H$ to $30H$. (This same assumption would give $p=0.38$ for $3H$.) The agreement of the three values is most satisfactory and probably would not be seriously modified by use of some more exact calculation of the change of p with changing concentration of hydrogen. The common value of 3.1 cannot be considered as accurate because of the great extrapolation involved in the estimate of p. A lower value of p would give a lower value of ν in nearly the same proportion. Recalculation of the results of the older experiments[3] gives a value of 2.6 ± 0.6 for ν. In them the H/U ratio was 64 : 1, so that capture by hydrogen predominated. In the newer ones capture by H is unimportant. Also, the values of p are very different. The agreement of the results of the two experiments is excellent in view of these great differences.

TABLE I. *Number of secondary neutrons per fission ν calculated from the experimental results of Halban, Joliot, Kowarski and Perrin. The condition for any explosive chain reaction is that $P_e[=w\nu(1-p)]>1$.*

Amt. of H_2O	τ_{INT}	Q_{INT}	Q_{EXT}	w	p	ν	P_e
$1H$	0.49	0.76	0.61	0.61	0.59	3.1	0.79
$2H$	0.46	1.24	0.47	0.57	0.53	3.0	0.80
$3H$	0.43	1.67	0.45	0.54	0.50	3.1	0.84

The condition for a divergent, explosive chain is $w\nu(1-p)>1$. Setting this critical product equal to P_e and inserting the above expression for ν gives an equation which reduces to $P_e=1-(1-p)(1-Q_{\text{ext}})/Q_{\text{int}}$. Since $1-p$ and Q_{int} are both positive the condition $P_e>1$ is satisfied if $Q_{\text{ext}}>1$. For all three sets of the newer experiments $Q_{\text{ext}}<1$ so $P_e<1$, and no explosive chain could be produced in such wet uranium oxide of any amount. It is important that this conclusion is entirely independent of the numerical value of p, the most uncertain of the quantities involved. The calculated values of P_e are given in the last column of Table I. The apparent rise of P_e with increasing content of H is probably not significant since the value of P_e for the older experiments is 0.23. It appears that the slow increase of P_e with additional hydrogen is more than compensated by the reduction of w by capture of neutrons by hydrogen. Dividing P_e by $1-p$ gives 1.7 for the value of $w\nu$ for the $3H$ mixture. It must be still higher for pure uranium. The value determined by Anderson, Fermi and Szilard[4] by another method is 1.5 so that this newer result merely strengthens the evidence for the conclusion already reached by them that the chain reaction could be maintained in a system which would slow down the neutrons without absorbing them.

LOUIS A. TURNER

Palmer Physical Laboratory,
Princeton, New Jersey,
January 25, 1940.

[1] Halban, Joliot, Kowarski and Perrin, J. de phys. et rad. **10**, 428 (1939).

[2] Halban, Joliot and Kowarski, Nature **143**, 470, 680, 939 (1939).

[3] In this calculation the same σ's have been used as in reference 1, plus $\sigma_{\text{cap }N}=1.3\times10^{-24}$ cm² and $\sigma_{\text{cap }O}=0.0\times10^{-24}$ cm² from Frisch, Halban and Koch, Kgl. Danske Vid. Selsk Math. Phys. Med. **15**, No. 10 (1937). $\Sigma A=34.5$ assuming that the 1.6 molar solution contains 128 g of NH_4NO_3 and 921 g of H_2O per liter at 20°C, as determined by interpolation in the data of the Int. Crit. Tab. In like manner $\Sigma A'=37.1$, the 1.6 molar solution of $UO_2(NO_3)_2$ containing 630 g of the anhydrous salt and 866 g of H_2O per liter at 20°C. The revised value $p=0.14$ has been used. Eq. (2) on page 25 of Turner, Rev. Mod. Phys. **12**, 1 (1940) is in error. ΣA outside of the bracket should be changed to $\Sigma A'$ with corresponding changes above, since the probability that a neutron will produce fission is $A_f/\Sigma A'$, not $A_f/\Sigma A$.

[4] Anderson, Fermi and Szilard, Phys. Rev. **56**, 284 (1939).

Simultaneous Penetrating Rays from the Atmosphere

It has been suggested by Nordheim and Hebb[1] and others that mesotrons may be produced by multiple processes in atmosphere. The following experiment was performed in order to test this hypothesis. A similar experiment has been reported recently by Wataghin, de Souza Santos and Pompeia.[2] However, the following data give further information on the regions in which these rays are produced.

Quadruple-coincidence counts were made with the four counters arranged, as shown in Fig. 1, so as to form two

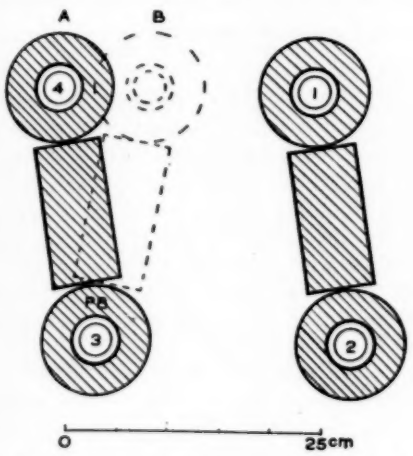

FIG. 1. Arrangement of coincidence telescopes.

double-counter telescopes inclined at about 10° to the vertical. The apparatus was set up near sea level about three meters under a thin wooden roof covered with sheet copper. With the telescopes in the parallel position (*A*, Fig. 1) quadruple coincidence could be produced by two penetrating rays from a shower arising in that portion of the roof in the range of both telescopes or in the atmosphere at any height above a few meters. Similarly, with the telescopes in the oblique position (*B*, Fig. 1) quadruple coincidence could be produced by two simultaneous penetrating rays arising in a part of the roof or in the atmosphere near the apparatus. Also coincidence could be produced in either case by three or more simultaneous penetrating rays originating at any distance from the apparatus or in the lead shield. It was assumed that the contribution to the counting rate by the last-mentioned process would be slightly greater for the more compact, oblique arrangement of the counters and shields. The triple coincidence data in Table I support this to some extent.

The expected random-coincidence frequency was calculated by means of Auger's formula[3] from the data given in Table I.

Table II gives a summary of the observations with the double telescope.

Since the coincidence rates are about 100 times the expected random rate, these results confirm previous observations of simultaneous penetrating rays. Most of the previously-observed penetrating showers have originated in dense materials. Because the oblique arrangement is more sensitive for all showers arising in the immediate vicinity of the counters, it is thought that the small excess rate with the parallel arrangement is very favorable to the hypothesis that penetrating rays are produced simultaneously in the atmosphere. Moreover, the high counting rate with the oblique arrangement indicates that many of these rays are produced near-by, and most of the coincidences observed with the parallel arrangement must have a similar origin. Thus, only a small fraction, in the latter case, can be due to simultaneous rays arising at the great heights at which most mesotrons are thought to be produced.

TABLE I. *Data used to estimate accidental coincidence frequency, etc.*

Recovery time estimated by using two tubes	0.9×10^{-3} sec.
Counting rate of an individual telescope	55 hr.$^{-1}$
Counting rate of an individual tube	60 min.$^{-1}$
Random coincidence rate between telescopes	0.75×10^{-3} hr.$^{-1}$
Total random fourfold coincidence rate	0.85×10^{-3} hr.$^{-1}$
Triple coincidence rate, counters 1, 2 and 3, Position *A*	0.30 ± 0.01 hr.$^{-1}$
Position *B*	0.32 ± 0.01 hr.$^{-1}$

TABLE II. *Comparison of counting rates of parallel and oblique telescopes.*

ARRANGEMENT	NO. RUNS	TOTAL TIME IN HR.	QUADRUPLE COINCIDENCES	COUNTING RATE HR.$^{-1}$
A	8	1128	103	$0.091_3 \pm 0.006_1$
B	7	861	67	$0.077_8 \pm 0.006_4$
Excess rate with arrangement *A*				$0.013_5 \pm 0.008_8$
Weighted mean excess for consecutive runs				$0.014_9 \pm 0.009_2$

VERNAL JOSEPHSON
DAROL K. FROMAN

Macdonald Physics Laboratory,
McGill University,
Montreal, Canada,

J. C. STEARNS

Department of Physics,
University of Denver,
Denver, Colorado,
January 30, 1940.

[1] L. W. Nordheim and M. H. Hebb, Phys. Rev. **56**, 494 (1939).
[2] Wataghin, de Souza Santos and Pompeia, Phys. Rev. **57**, 61 (1940).
[3] P. Auger, Rev. Mod. Phys. **11**, 288 (1939).

Positive Ion Emission from Nickel

A study of positive ion emission from nickel when heated to temperatures at which appreciable vaporization occurs has been made, using a modified Dempster type mass spectrograph. Ions were obtained having relative masses of 58 and 60 corresponding to the two most abundant isotopes of nickel. Ni^+ ions were observed from five separate filaments. It was found helpful to heat the filaments at moderate temperatures for sufficient time to insure thorough outgassing.

A similar attempt has been made to observe positive ion emission from iron and cobalt filaments but so far no ions have been observed.

G. A. JARVIS

Department of Physics,
University of Wisconsin,
Madison, Wisconsin,
January 24, 1940.

Correlation Between Cosmic-Ray Intensity and Upper Air Pressures and Temperatures

In the studies of the relation between cosmic-ray intensity and atmospheric temperature heretofore reported, the temperatures used have been those observed at the ground level. If, however, the correlation is of physical significance, it would seem that the average temperature over a wide range of altitude should be considered. A correlation study has accordingly been made between the cosmic-ray intensity at Cheltenham and the upper air pressures and temperatures as observed by the U. S. Weather Bureau at Washington. The study covers a period of one year from June, 1938, to June, 1939, the data being averaged over seven-day intervals. The cosmic-ray data used were the averages of the sea-level readings of the Type C meter running at Cheltenham reduced by 1.11[1] times the readings from a similar meter at Huancayo, Peru, in order to eliminate the effect of world-wide changes in intensity. The temperatures and pressures of the upper air were observed by radiosonde balloons sent up by the Weather Bureau nearly every day during the year. From day to day the maximum height of the observations varied up to a limit of 23,000 meters (reached only once). Above 14,000 meters, too few data were available to make the calculations quite trustworthy.

The customary correlation coefficients were computed between the seven-day averages of the cosmic-ray intensities (at the surface) and the corresponding seven-day averages of both temperature and pressure at each of a number of different elevations. These are shown labeled "pressure" and "temperature" in the diagram. It is found that up to a height of 10 km the changes in air temperature follow so closely those at the ground that neither the correlation nor the temperature coefficient is greatly

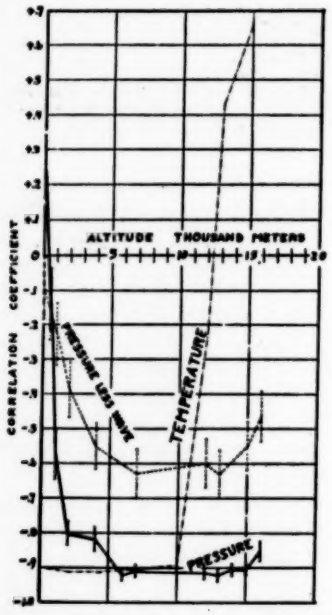

FIG. 1. Correlation coefficients between cosmic-ray intensities and temperature and pressure at different elevations.

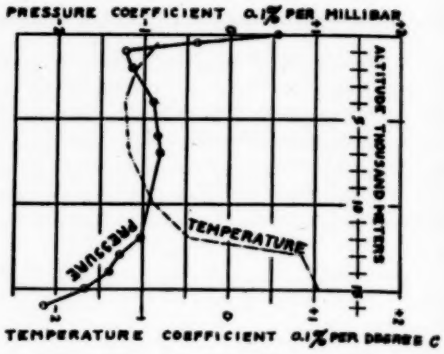

FIG. 2. Pressure and temperature coefficients of cosmic-ray intensity as functions of elevation.

different from that based on surface temperatures. Temperatures in the lower stratosphere (10 to 15 km), however, are not closely correlated with cosmic-ray intensity. On the other hand, changes in pressure which measures the integrated expansion of the air at lower levels remain closely correlated with the cosmic-ray changes up to 15 km.

The temperature, pressure and cosmic-ray intensity each pass through an annual wave during the year. Above about 1000 meters, the minimum of the pressure wave corresponds roughly with the maximum of the cosmic-ray intensity wave (negative correlation). Below the 1000 meters, the amplitude of the pressure wave passes through a minimum, the phase changes rapidly with decreasing elevation and all correlation with cosmic-ray intensity seems to vanish. The slight positive correlation found at the surface for data already corrected for the barometer is probably only accidental although the correlation coefficient used at Cheltenham (0.180 percent/mm Hg) may not have been best for this particular time and method of averaging.

In order to test whether there was anything more to the pressure *vs.* cosmic-ray intensity correlation than that resulting from a common annual wave, the best annual sine wave was fitted to the cosmic data and also to the pressure data. Then each seven-day average was measured from the corresponding annual wave and again correlation coefficients computed. While this process reduced the numerical value of the correlations, they still remained many times their probable error.

The annual wave of temperature goes through a minimum of amplitude and a rapid change of phase in the neighborhood of 12,000 meters ($t \sim -55°C$, boundary of the stratosphere). Below this and extending down to the surface the phase of minimum temperature is also early in February and there is a high negative correlation with the cosmic-ray intensity. However, when temperature differences from the annual wave of temperature are compared with the variation of cosmic-ray intensity from its annual wave, the correlation is quite small—at least for higher levels—and hence has not been included inthe diagram.

In addition to the correlation coefficients, the pressure coefficients (0.1 percent per millibar) and the temperature coefficients (0.1 percent per degree C) were computed and are given in Figs. 1 and 2.

I wish to thank Professor A. H. Compton for discussing this with me, Dr. John A. Fleming of the Department of Terrestrial Magnetism for making available the Cheltenham and Huancayo data, and Mr. D. M. Little, Principal Meterologist in charge of the Aerological Division of the U. S. Weather Bureau for supplying me with the air data for these calculations.

NIEL F. BEARDSLEY

University of Chicago,
Chicago, Illinois,
January 31, 1940.

[1] S. E. Forbush, Phys. Rev. **54**, 983 (1938).

Structure and Ferromagnetism of Cold-Worked Copper Containing Iron

Copper containing small amounts of iron in solid solution is not ferromagnetic even if cold worked. On heat treatment iron precipitates very rapidly from solid solution in a relatively stable nonferromagnetic form, sometimes even in particles sufficiently large to be visible under the microscope. Cold working immediately transforms this nonmagnetic iron to the magnetic condition. The idea has been proposed[1] that the first precipitate of iron is face-centered cubic in structure and is possibly still continuous with the copper lattice. There have been no direct experimental determinations of the structure of the precipitate in either the nonmagnetic or magnetic form.

At the writer's request Dr. A. B. Greninger of the Laboratory of Physical Metallurgy, Harvard University kindly undertook a study of some samples by x-ray methods. Wire, 0.06 inch diameter, containing 2.3 percent iron was quenched after 3 hours at 1050°C. It was then very slightly ferromagnetic. Reheating at 650°C for 3 hours diminished the attraction of a strong electromagnet, but if the reheated wire were cold drawn to a reduction of area of 24 percent it became strongly ferromagnetic. Diffraction patterns were obtained with a Debye camera of 5.7 cm radius using unfiltered cobalt radiation and a 7-hour exposure (normal exposure times to show structure are about 1 hour). The wires were all of large grain size and hence it was difficult to obtain satisfactory patterns. No trace of body-centered cubic lines was observed. A filing sample taken from the reheated cold-drawn wire gave a pattern which, with a 12-hour exposure, showed two unmistakable lines corresponding to the strongest of the body-centered cubic alpha-iron pattern. The iron lines were no stronger after subsequent heat treatment for 3 minutes at 650°C. Similar filings again annealed *in vacuum* for 3 hours at 1050°C, quenched and reheated 3 hours at 650°C showed no trace of the iron lines.

These experiments show that there is little body-centered cubic iron (probably none) in copper-iron alloys containing the nonmagnetic precipitate but that it becomes detectable after cold working, coincident with the appearance of ferromagnetic properties.

CYRIL STANLEY SMITH

Research Metallurgist,
American Brass Company,
Waterbury, Connecticut,
January 29, 1940.

[1] R. B. Gordon and M. Cohen, "Age hardening of copper-cobalt and copper-iron alloys," Am. Soc. for Metals, Preprint No. 39, October, 1939. See particularly the discussion of the present writer on this paper. F. Bitter and A. R. Kaufman, Phys. Rev. **56**, 1044 (1939).

Cloud-Chamber Photographs of Cosmic Rays up to an Altitude of 29,300 Feet

On December 21 Mr. Wiston Bostick and I made an airplane flight up to 29,300 feet for the purpose of taking cloud-chamber photographs of cosmic rays. A Wilson chamber of 15 cm diameter was placed between the pole pieces of a large permanent magnet which gave a magnetic field of 700 gauss. Expansions could be made either at random or controlled by counters. Stereoscopic pictures were taken.

Two hundred thirty pictures were taken in which there were more than 25 tracks of such a density and momentum as to practically exclude the possibility of their being produced by either electrons or protons. In Fig. 1 a typical

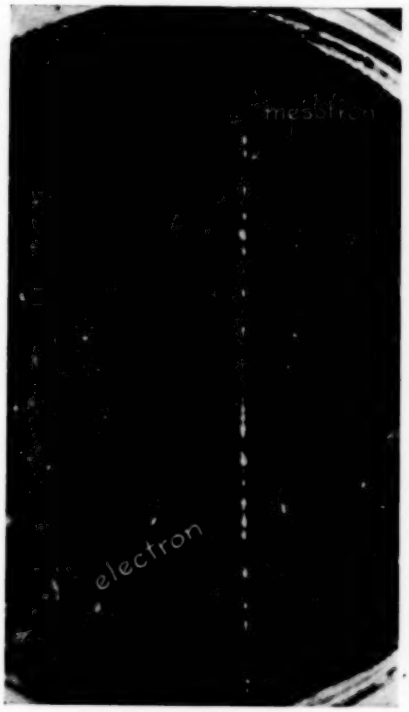

FIG. 1. Typical photograph showing both an electron ($H\rho = 4.2 \times 10^4$) and a mesotron ($H\rho = 1.4 \times 10^5$).

photograph is reproduced which shows for the same expansion the occurrence of an electron of $H\rho = 4.2 \times 10^4$ as a thin track and a mesotron with $H\rho = 1.4 \times 10^5$ for which the ionization is much greater. All the heavy tracks occurred only in the 110 photographs which were taken above 20,000 feet.

The pictures reveal further some much stronger ionizing particles which one may associate with either protons, α-particles or still heavier nuclei.

Though a full report of this work will soon appear, it has seemed worth while to call prompt attention to the surprisingly frequent occurrence of slow mesotrons at the altitudes reached in this experiment.

GERHARD HERZOG

Ryerson Physical Laboratory,
University of Chicago,
Chicago, Illinois,
February 1, 1940.

The Coefficient of Thermal Diffusion of Neon and Its Variation with Temperature

If a mixture of two gases is contained in a vessel consisting of two bulbs fastened together by means of a connecting tube, then as a result of the existence of thermal diffusion the relative concentrations of the two constituents will be slightly different in the two bulbs if these are at different temperatures. This effect was predicted theoretically by Enskog[1] and Chapman[2] and has been amply verified experimentally.

In the case of isotopic molecules the difference in concentration ΔC can be expressed in a particularly simple form:

$$\Delta C = \alpha C_1 C_2 \log T_1/T_0. \quad (1)$$

C_1, C_2 are the relative concentrations of the two types of molecules, $C_1+C_2=1$; T_0, T_1, are the temperatures of the two bulbs, and α is known as the coefficient of thermal diffusion. The nature of the phenomenon is such that in general the relative concentration of the heavier molecule is greater in the cooler bulb.

An experimental determination of α for methane[3] was recently made. The study has now been extended to neon for several temperature ranges. In Table I are recorded the results found.

The relative abundances of the isotopes were measured with a mass spectrometer and the general method used in computing α was similar to that employed in reference 3. The bulb system used was essentially as before. In this case the time allowed for a run was at least five times the relaxation time of the system. In making the computations corrections were made for the volume of gas in the tube connecting the two bulbs. The consistency of the isotope abundance readings and considerations of other possible errors lead one to believe that the final computed α's are accurate within about five percent.

As a first approximation for elastic spheres Enskog's results give in this case

$$\alpha = (105/118)(M_2-M_1)(M_2+M_1), \quad (2)$$

where the M's are the relative masses of the two types of molecules. In the case of Ne^{20} and Ne^{22} this gives $\alpha=0.0424$. In the last column of Table I is recorded R_T (the ratio of the experimentally found α to that computed by (2)).

The increase of α with temperature is to be expected as the atoms at higher temperature behave more nearly like perfect elastic spheres. In the highest temperature range studied the R_T has a value 0.71 as compared with a value 0.3 found previously for methane for approximately the same temperature range. Neon atoms are thus considerably "harder" than methane molecules. As α for neon varies rapidly with temperature the values given in Table I can only be considered as "average" values for the temperature intervals.

TABLE I. *Values of the coefficient of thermal diffusion α of neon in three temperature ranges and the ratio R_T of these values to those computed for elastic spheres.*

T_0	T_1	$\Delta\frac{Ne^{22}}{Ne^{20}}$	"AVERAGE" α IN TEMPERATURE RANGE	R_T
10°C	344°C	(6.6±0.1)%[a]	0.0302	0.71
−183	21	(6.1±0.1)%[b]	0.0188	0.44
−183	−78	(3.9±0.3)%[c]	0.0165	0.39

[a] This represents the percentage decrease of Ne^{22}/Ne^{20} ratio in hot bulb after five repeated runs. The number given is the average of a total of seven different determinations on three different samples. The error is the mean deviation in the seven readings.
[b] Percentage decrease after four repeated runs. The number given is the average of a total of four determinations on two different samples.
[c] Percentage decrease after five repeated runs. The number given is the average of a total of six determinations on two different samples.

Atkins, Bastick and Ibbs[4] recently measured the coefficients of thermal separation for all of the binary mixtures of helium, neon, argon, krypton and xenon in the temperature range 15°C to 100°C. The value of R_T calculated here for neon fits in well with the R_T's computed for the binary mixtures. This would seem to indicate that there is no great difference in the nature of collision processes between two isotopic gases or a mixture of two nonisotopic gases.

As neon has a relatively high α the thermal diffusion column method should be very effective in separating the isotopes.

ALFRED O. NIER

Department of Physics,
University of Minnesota,
Minneapolis, Minnesota,
January 30, 1940.

[1] D. Enskog, Physik. Zeits. **12**, 56, 533 (1911).
[2] S. Chapman, Phil. Trans. **A217**, 115 (1917).
[3] A. O. Nier, Phys. Rev. **56**, 1009 (1939).
[4] B. E. Atkins, R. E. Bastick and T. L. Ibbs, Proc. Roy. Soc. **A172**, 142 (1939).

Nuclear Excitation of Lead by X-Rays

The only case of nuclear excitation by x-rays[1,2] which has been reported is In^{115}, in spite of the fact that the authors, and probably others, have made attempts to find other examples of this process. The theory of metastable states,[3-5] however, predicts that, for a given spin change, the lower the excitation energy of the metastable state the longer will be its half-life. Thus states with periods long enough to be observable are more likely to come from low lying levels. This suggests the possibility that metastable states may have been excited but not observed due to the absorption of the low energy internally converted electrons by the counter walls. Accordingly, counters were constructed with the metal under investigation forming the cylindrical cathode.

The counters were irradiated by placing them directly behind a lead target which was bombarded with electrons from the electrostatic generator. After four minutes irradiation with 35 μa of 1.5-Mev electrons, a lead counter showed an activity of 40 counts per minute above background with a 1.6±0.2-minute period. Three different lead counters were used, one of which had a C.P. lead cylinder. All gave consistent results. An excitation curve for this activity was obtained and gave a threshold of 0.65±0.02 Mev corresponding to the lowest activation level.

No activity was observed when a lead foil was irradiated as above and wrapped around a thin wall counter. If the radiation emitted is mainly internally converted electrons, the upper limit of the energy can be placed at 250 kv.

In order to estimate the lower limit, a copper foil, 0.034 gram/cm², was placed inside the lead electrode. This reduced the intensity of the activity to about one-half. The lower limit is thus estimated at about 150 kv.

It is interesting to note that the spin of lead in the ground state is either 0 or ½ depending upon the isotope, whereas the spins of the three previously known nuclei (In^{113}, In^{115}, Sr^{87}) in which metastable states have been excited are all 9/2. Also In^{113}, In^{115}, and Sr^{87} are each members of isobaric pairs, which is not the case with any of the known lead isotopes.

Three other elements, copper, bismuth, and mercury, were used as G-M tube cathodes and irradiated. No activity was observed with any of these metals. Periods between 20 seconds and 5 hours could have been detected.

BERNARD WALDMAN
GEORGE B. COLLINS

University of Notre Dame,
Notre Dame, Indiana,
January 30, 1940.

[1] B. Pontecorvo and A. Lazard, Comptes rendus **208**, 99 (1939).
[2] Collins, Waldman, Stubblefield and Goldhaber, Phys. Rev. **55**, 507 (1939); Phys. Rev. **55**, 1129 (1939).
[3] C. F. Weizsäcker, Naturwiss. **24**, 813 (1936).
[4] H. A. Bethe, Rev. Mod. Phys. **9**, 226 (1937).
[5] M. H. Hebb and G. E. Uhlenbeck, Physica **5**, 605 (1938).

Simultaneous Penetrating Particles in the Cosmic Radiation. II.

In a previous paper[1] we described some experiments which indicated the existence of showers containing at least two particles capable of penetrating about 17 cm of lead. Further measurements were made to obtain evidence on the size of showers and the number of penetrating particles.

We increased the distance between the two telescopes of arrangement I to 120 cm and found that the coincidence rate decreased to 6×10^{-4} min.$^{-1}$ (Fig. 1) [12 coincidences in 18,800 min. with an error of $\pm2\times10^{-4}$ min.$^{-1}$].

A further measurement (III) was made with a fivefold coincidence set. The fifth counter was located between the two telescopes of arrangement I at the depth of 23 cm of lead (Fig. 2). The resolving power was carefully controlled, and the frequency of the random fivefold coincidences was of the order of 10^{-7} min.$^{-1}$ (one coincidence in 20 years). As a preliminary result of the observation during

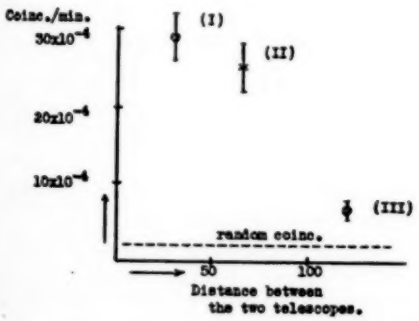

FIG. 1. Coincidence rates as a function of the distance between cosmic-ray telescopes.

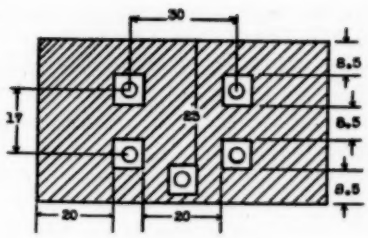

FIG. 2. Arrangement of tubes in a fivefold coincidence set.

17,000 min. we obtained nine fivefold coincidences, that is a frequency of the order of 5×10^{-4} min.$^{-1}$. This indicates the existence of showers containing at least three particles.

From Fig. 1 we deduce that the penetrating particles in the observed showers are spread over a surface of the order of 1 m², and from the comparison of the results of the fivefold coincidences with those of the arrangement I we can determine that the frequency of fivefold coincidences is about 15 percent of the frequency of fourfold coincidences. Thus we conclude that a considerable part of the showers, in which fourfold coincidences are observed, contains so many particles that in about 15 percent of the showers registered in arrangement I (fourfold coincidences) the fifth counter should respond. The ratio of area of the fifth counter to the area of the whole shower is only 0.01. This suggests that the average number of particles in the observed showers is of the order of 15.

A more detailed report on these measurements and others which are now in progress will be published elsewhere.

G. WATAGHIN
M. D. DE SOUZA SANTOS
P. A. POMPEIA

Department of Physics,
São Paulo University,
São Paulo, Brazil,
January 30, 1940.

[1] G. Wataghin, M. D. de Souza Santos and P. A. Pompeia, Phys. Rev. **57**, 61 (1940).

Nuclear Electron Showers

Although some of the light particles constituting the penetrating part of the large air showers can go through more than 15 cm of lead the evidence seems to be that they are electrons of high energy, ranging from 10^{13} to about 10^{15} ev, and obey the Bhabha-Heitler cascade theory of shower production. However, Auger[1] has observed the presence of a considerable number of heavy particles (protons) in the penetrating part of the large air showers, and this fact prompts one to investigate whether there is evidence which would indicate the presence of a phenomenon other than that of the cascade process.

In an article by Street[2] there are four photographs (the fifth I believe to be a meson shower) showing the presence of showers, but also containing tracks of heavy particles among the shower particles. This type of shower is rare compared to the usual type of cascade shower found at sea level, which contains tracks of electrons only. Street is therefore of the opinion that this type of shower may be

different from the usual cascade type, and may be ascribed to some separate and less frequent process.

The writer desires to point out that this infrequent type of shower observed by Fussell and described in Street's article is somewhat similar to the penetrating part of the large air showers, and both may be evidence of nuclear electron showers. The nuclear electron showers may be caused by a close interaction either of a high energy electron ($\sim 10^{10}$ ev) or a neutral meson with the nucleus, and are the subsequent production in one elementary act of a large number of electron pairs. For electrons of high energy ($\sim 10^{10}$ ev) the probability for nuclear electron shower production becomes of the same order as the probability for the radiative process. For lower energies neutral mesons would have to be invoked as the principal shower-producing agent. The probability of a strong interaction between neutral mesons and the nucleus is suggested by a paper of Bethe.[3] The presence of the heavy particles in this type of shower is evidence of the participation of the nucleus in this phenomenon. If the electrons produced in these showers have energies less than 10^{10} ev, they are likely to initiate showers of the ordinary cascade type. But, if the nuclear electron showers indicate a breakdown in theory, the emphasis should be not only on an energy cut-off but also on some limiting value of the order of e^2/mc^2 for the range of interaction. Such a breakdown in theory would not influence either the scattering or the radiative processes, inasmuch as they are due to longer range interactions.

Direct experimental evidence for pair emission from the nucleus is afforded by the recent work of Fowler and Lauritsen[4] who have observed the emission of electron pairs by fluorine when under proton bombardment. Although this is not multiple pair emission, it serves to suggest the possibility of a direct nonelectromagnetic interaction between electrons-positrons and the nucleus. In this connection it may be of interest to cite the recent careful experimental work of Sizoo and Barendregt[5] who have verified the anomalously large cross section of the order of 10^{-22} cm for the production of pairs by beta-electrons, first observed by Skobeltzyn and Stepanowa.[6] This large cross section cannot be reconciled with the theoretical formula of quantum electrodynamics, and suggests a breakdown in theory. At these low energies (1 to 10 mc^2) the probability for the radiative process is not much greater than the probability for the occurrence of the shorter range interactions as manifested by nuclear pair production and the anomalous scattering of beta-particles. As emphasized above it is these short range interactions which are the cause of the breakdown of the theory. The applicability of existing theory to the higher energy ranges is evidently due to the fact that for higher energies forces of longer range than e^2/mc^2 predominate.

ALEXANDER W. STERN

Brooklyn, New York,
December 8, 1939.

[1] Auger, Maze, Ehrenfest and Freon, J. de phys. et rad. 10, 39 (1939); Auger and Pluvinage, Comptes rendus 209, 481 (1939).
[2] J. C. Street, J. Frank. Inst. 227, 765 (1939).
[3] H. A. Bethe, Phys. Rev. 55, 1261 (1939).
[4] W. A. Fowler and C. C. Lauritsen, Phys. Rev. 56, 840 (1939).
[5] G. Sizoo and F. Barendregt, Physica 6, 1085 (1939).
[6] D. Skobeltzyn and E. Stepanowa, J. de phys. et rad. 6, 1 (1935).

Positive Point-to-Plane Corona in Pure A, H_2 and N_2

The positive point-to-plane corona studies of Trichel and Kip have been extended to very pure mercury-free A, N_2 and H_2 gases at pressures ranging from 380 mm to 760 mm in baked-out Pyrex tubes with outgassed electrodes. The gap length was 2.5 cm, and the point was a hemispherically capped cylinder of 0.4 mm diameter. Experiments over a more extended pressure range are now under way. The pre-onset phenomena, starting potentials for burst pulses, streamers and self-sustaining corona were studied with oscillograph, current and potential measurements as well as observations with telemicroscope. The oscillograph was attached across a 3-megohm resistor in series with the plate using capacity pick-up. This arrangement recorded chiefly inductive kicks, but steady current produced corresponding shifts in the zero. For A and H_2, a one-stage pre-amplifier consisting of a 57 tube was required. The potentials for onset for the various phenomena in the different gases are shown in Table I. In A, pre-onset phenomena consisted of random individual pulses corresponding to externally produced ionization. These were due to individual avalanches produced at lower fields by electrons from γ-ray ionization and at higher potentials by single electrons appearing in the gap. At higher potentials the pulses increased in amplitude and somewhat in frequency. Eventually a point is reached where photo-ionization of these avalanches suffices to give a succession of avalanches close together forming intermittent burst pulses. These are at first choked off by statistical fluctuations and later by accumulated space charge. At still higher potentials, the individual fluctuations in the burst pulses became larger in amplitude and occur with somewhat *greater* intervals of time between them. When the burst pulse corona becomes self-sustaining, increased current and potential cause the fluctuations to decrease in amplitude and increase greatly in frequency, as observed by Trichel. No streamers were observed, but the potentials were not carried to sparking for fear of contamination. In all the phenomena the amplitude of fluctuations was of the order of 10^{-2} to 10^{-4} of

TABLE I. *Data on the different pre-onset phenomena.*

	ARGON	H_2	N_2
Single Avalanche Pulses:			
Potential	1460 volts	2150	3600
Current	$<10^{-10}$ amp.	$<10^{-10}$	$<10^{-10}$
Oscill. Amplitude	1···3 cm	1···3 cm	1···3 cm
Amplification in % of total	Full Amplification = 100%		
Burst Pulses:			
Potential	1600 volts	2200	3750
Current	$<10^{-9}$ amp.	$<10^{-9}$	$\leq 10^{-9}$
Oscill. Amplitude	3···5 cm	3···5 cm	3···5 cm
Amplification	100%	35%	10%···20%
Streamers:			
Potential			3800 volts
Current			$2\cdots 5\times 10^{-6}$ amp.
Oscill. Amplitude			5 cm
Amplification			~1%···5%
Corona-Onset:			
Potential	1720 volts	2300	4000
Current	5×10^{-7} amp.	1×10^{-6}	1×10^{-6}
Oscill. Amplitude	1 cm	1 cm	2 cm
Amplification	30%	20%	10%

those in air or N_2. This comes from the low values of the fields at which ionization by collision sets in which reduces effective ionization about points. With the self-sustaining corona, the glow adheres to the point and is of a reddish purple color. At two to three mm from the point a *very faint* bluish white glow is observed. It is probable that this is due to the excitation phenomena associated with change of charge and inelastic impacts of the second class as the positive argon ions slow down.

In H_2 the sequence of the phenomena is essentially the same. The only notable difference is that the amplitude of the fluctuations observed in H_2 are two to five times as great and that owing to inelastic electron impacts the potentials are all higher. In N_2 the potentials required are still greater. Here the amplitudes of the avalanches and pulses are less than in air but 100 times greater than in argon. It is thus not surprising to see streamer formation occurring at about burst pulse potentials. The streamers differ from those observed by Kip in two respects: 1. They are far more infrequent and occur in a more limited potential region. 2. The streamers cross the gap at *onset* but cause no breakdown. The infrequency must be ascribed to the absence of negative ions. The photoelectrons from the plate in air cross the gap as *negative ions* and reach the anode in time to start a new streamer as the positive ion space charge has cleared. In pure N_2, *electrons* cross the gap before the positive space charge from the last streamer or burst pulse clears and only an occasional electron or ion starts a streamer. That streamers cross the gap at onset for the short gaps used is natural; they also do in shorter air gaps. In pure N_2 the mobility of ions is twice that in air, and hence space charges are less so that crossing occurs for longer gaps. That the few streamers crossing at onset do not cause spark breakdown is in part due to the smaller streamer intensity in N_2. Photon absorption and photoelectric ionization density are less in pure N_2 so that the efficiency of the streamers in creating a cathode spot and an effective channel for the return spark is less. In N_2 streamers again occur just before breakdown. In argon breakdown appears to occur as a sort of a glow which is not preceded by streamer action. Further, more quantitative studies are being carried on.

GERHARD L. WEISSLER

Department of Physics,
University of California,
Berkeley, California,
January 15, 1940.

Bremsstrahlung of RaE

In a previous paper,[1] we described a method for distinguishing between the respective intensities of the "inner" and of the "outer bremsstrahlung" in the gamma-radiation of RaE.

It should be remembered that this was obtained by measuring the whole of the radiation for different radiators, and extrapolating the results of the measurements to the case of a hypothetical radiator of atomic number zero, in which case the outer bremsstrahlung would be zero and the radiation exclusively composed of inner bremsstrahlung.

It must be added that repeating the measurements with a series of lead screens of various thicknesses also gives us information as to the quality of the radiation.

The chief aim of our work was to investigate the problem of the inner bremsstrahlung; but the experimental data also provide us with the same indications for the outer bremsstrahlung (by subtracting the inner bremsstrahlung from the whole); and consequently enable us also to check the validity of the radiation quantum theory, in the range of 150–1000 kev.

We restrict ourselves to the case of a platinum radiator; here, the gamma-radiation is composed chiefly of the outer bremsstrahlung. The inner bremsstrahlung contributes only a few percent so that the errors of determination in the inner bremsstrahlung do not affect the results for the outer bremsstrahlung very much.

In order to determine by way of calculus the intensity and the quality of the outer bremsstrahlung of RaE, from its beta-spectrum, one should consider simultaneously: (1) the cross section of any electron of the absorbing platinum for the bremsstrahlung phenomenon; (2) the loss of energy of the beta-rays, almost exclusively due to collisions (ionization); (3) the number of beta-rays capable of giving rise to the phenomenon of bremsstrahlung.

(1) Let us calculate in the case of platinum the cross section per electron for a photon with an energy between k and $k+dk$ to be emitted, by the action of a beta-ray whose energy is E. It should be a function of E and k, which we may call: $F(E,k)dk$; the function is known theoretically (see e.g. Heitler[2]).

(2) We may assume that the value of F does not change in an interval dE; the number Ndx of electrons which a beta-ray can approach while its energy remains between E and $E-dE$ is given by the theory of the loss of energy by collisions (see again Heitler, reference 2, p. 219, formula 5).

$$-dE/dx = NG(E),$$
$$Ndx = -dE/G(E)$$

(N is the number of electrons per cm^3).

(3) Let us call $P(E)dE$ the probability of a beta-ray of RaE having an initial energy between E and $E+dE$; the function $P(E)$ is known from the experimental research on the beta-spectrum of RaE. (See e.g. Flammersfeld.[3]) The average number of beta-rays capable of giving rise to the phenomenon is the probability of a beta-ray having an initial energy greater than E. This probability is:

$$S(E) = \int_E^{E_{max}} P(E)dE.$$

The product of these three quantities: Fdk; Ndx; $S(E)$; (only the latter to be found experimentally) will be of the form:

$$H(E,k)dEdk.$$

It represents the probability for a quantum with an energy between k and $k+dk$ to be emitted by the action of a beta-ray of RaE, when the beta-ray has an energy between E and $E-dE$.

The integral

$$R(k)dk = dk\int_k^{E_{max}} H(E,k)dE$$

should represent the probability for a quantum with an

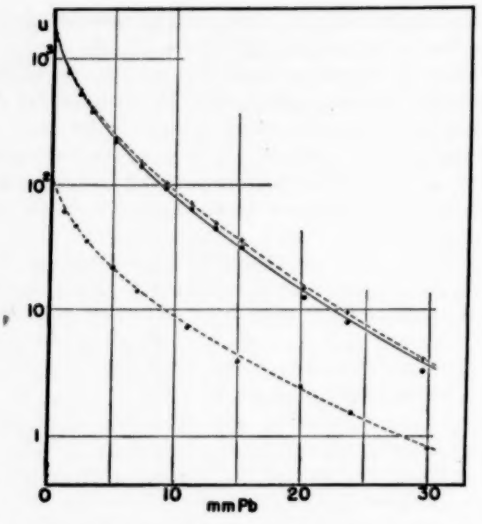

FIG. 1. Absorption curve of the outer bremsstrahlung. The dotted curve above is the experimental absorption curve of the radiation of RaE, when surrounded with a platinum radiator. The results of actual measurements are marked by crosses. The other dotted curve is the experimental absorption curve of the inner bremsstrahlung. The black circles represent the difference between the measurements marked by crosses and the corresponding values of the inner bremsstrahlung absorption curve. Accordingly, the black circles represent the experimental measurements of the absorption of the outer bremsstrahlung in lead, while the *theoretical* curve is the full curve on the figure.

energy between k and $k+dk$ to be emitted by the action of any beta-ray of RaE, at any time of its run.

Now having the spectral distribution of the outer bremsstrahlung for a platinum radiator, we can easily determine quantitatively the absorption curve of that radiation in lead, as we did for the inner bremsstrahlung.

The comparison with the experimental data is made in Fig. 1. *The agreement is good, within the limits of an admitted error of a few percent.*

It should be emphasized again that the comparison is here, as previously, both qualitative and quantitative.

E. STAHEL
J. GUILLISSEN

Université Libre de Bruxelles,
Brussels, Belgium,
December 15, 1939.

[1] E. Stahel and J. Guillissen, J. de phy. et rad. (in press).
[2] W. Heitler, *Quantum Theory of Radiation* (Oxford, 1936), p. 165, formula 16.
[3] F. Flammersfeld, Physik. Zeits. **38**, 973 (1937).

New High Pressures Reached with Multiple Apparatus

It has been suggested a number of times that hydrostatic pressures of any magnitude could be obtained with a nest of pressure vessels, one within the other, exposed to progressively higher pressures. The practical complications of such a scheme are, however, obviously great. By the partial use of such a scheme, in which the most vulnerable part of the pressure vessel receives external support, I have been able to extend useful measurements to 50,000 kg/cm².[1] This note reports a more complete application of the idea, which has made it possible to reach pressures considerably higher.

The gain in doubling the pressure apparatus may be considerably more than double because of the increase in intrinsic strength under high hydrostatic pressure. This was clearly foreshadowed by the experiments of Griggs,[2] who found that the crushing strength along the c axis of a single quartz crystal was increased from 22,000 to about 120,000 kg/cm² by a confining pressure of 20,000 kg/cm². I have now applied to a Carboloy piston without fracture a compressive stress of between 200,000 and 250,000 kg/cm². The crushing strength of Carboloy under normal conditions is not more than 70,000 kg/cm². The confining pressure was afforded by bismuth undergoing transition, so that the confining pressure was automatically kept at about 25,000 kg/cm². Under ordinary conditions Carboloy is highly brittle, and breaks with practically no plastic deformation, but under a confining pressure of this magnitude the Carboloy piston was plastically and permanently shortened by 5.5 percent, and considerably bent, with no perceptible cracks or other obvious damage. Glass-hard steel under the same confining pressure similarly shows an increase of compressive strength and very considerable plastic deformation, and also an appreciable increase of compressive strength at atmospheric pressure after the cold working afforded by the plastic deformation while supported. I have verified Griggs' observation of the great increase of the strength of quartz single crystal under a confining pressure of 25,000, applying without fracture compressive stresses of the order of 150,000. The strength in the c direction is greater than at right angles, as was also found by Griggs. The effective Young's modulus appears to be increased at this stress by something of the order of 25 percent. Quartz glass has its strength increased by something of the same order as the crystal. Quartz glass compressed in this way ruptures on release of pressure into characteristic disks perpendicular to the axis of compression, and Mr. Griggs finds that optical anisotropy has been developed, indicating some permanent plastic flow. He finds no optical anisotropy in any fragments of quartz crystals ruptured at high pressures.

A "one sided" compressive stress in a piston may be converted into an approximately equal hydrostatic pressure in a thin disk of softer material compressed by the end of the piston, lateral extrusion of the soft material being prevented by friction. In this way I have applied a hydrostatic pressure of between 200,000 and 250,000 kg/cm² to a thin plate of single crystal graphite at room temperature with no conversion to diamond. This extends the negative result beyond the pressure of 100,000 kg/cm² which I have already reported.[3] Since the pressure of thermodynamically reversible transition is according to the most recent thermodynamic evidence not far from 20,000, it is probable that no pressure, however high, will accomplish the conversion at room temperature. This is suggested by the theory of Tammann, according to which the speed of formation of nuclei of a new phase at first increases as pressure is increased beyond the thermodynamically

reversible transition point, but then passes through a maximum and drops again.

The experiments just described were mostly performed in my apparatus for 50,000 kg/cm², support being usually afforded by bismuth in transition, but sometimes by lead. My apparatus for 30,000 affords opportunity for support by a true liquid, for experiments on a somewhat larger scale, and for measurements of greater precision and complication. In this apparatus several exploratory measurements have been made on materials confined in a small cylinder of $\frac{1}{16}$ inch bore and $\frac{7}{16}$ inch outside diameter, compressed by a $\frac{1}{16}$-inch Carboloy piston. The cylinder of the 30,000 apparatus contains in addition to the transmitting liquid (iso-pentane) and a manganin gauge for measuring pressure a large block of bismuth, the function of which is to maintain pressure in the supporting liquid at 25,000 during the transition, during which the motion of the main piston, 0.5 inch in diameter, is approximately 0.1 inch. The initial quantity of liquid is so chosen, after preliminary trial, that the 0.5-inch piston makes up on the $\frac{1}{16}$-inch piston at the moment that the transition pressure of bismuth is reached. The pressure on the $\frac{1}{16}$-inch piston is then given roughly by the excess pressure on the 0.5-inch piston. In this way I have observed at pressures estimated to be between 125,000 and 150,000 kg/cm² an elastic volume compression in NaCl of something over 20 percent. The compression at 50,000 is known to be 13 percent,[5] and the relation deviates markedly from linearity. It is therefore probable that NaCl has no transition with important volume change to the CsCl type of structure, unlike the rubidium and potassium salts, and as predicted by Jacobs[6] on theoretical grounds. Sulfur has also been compressed to approximately the same pressure with about 30 percent loss of volume, and no irreversible change to a more metallic form, which is to be looked for in analogy with black phosphorus. Incidentally the possibility of reaching pressures so high in a cylinder of the above dimensions means an increase in strength of the cylinder for internal pressure (that is, in tension) markedly greater than would be accounted for merely by the additive effect of the supporting pressure of 25,000.

Finally, preliminary exploration shows the feasibility of using inside the 30,000 apparatus and supported by uniform hydrostatic pressure, a miniature double container, supported by an external cone in the same manner as now employed in my 50,000 apparatus, with resulting further increase in the range of controllable and measurable hydrostatic pressure.

P. W. BRIDGMAN

Physics Laboratories,
Harvard University,
Cambridge, Massachusetts,
January 18, 1940.

[1] P. W. Bridgman, Phys. Rev. **48**, 893–906 (1935) and Phys. Rev. **57**, 237 (1940).
[2] D. Griggs and J. B. Bell, Bull. Geol. Soc. Am. **49**, 1723–1746 (1938).
[3] P. W. Bridgman, Phys. Rev. **48**, 832 (1935).
[4] F. D. Rossini and R. S. Jessup, Nat. Bur. Stand. J. Research **21**, 491–514 (1938).
[5] Second reference under (1).
[6] R. B. Jacobs, Phys. Rev. **54**, 468–474 (1938).

Proceedings of the American Physical Society

Minutes of the Columbus, Ohio, Meeting, December 28–30, 1939

THE 41st Annual Meeting (the 232nd regular meeting) of the American Physical Society was held at Columbus, Ohio, on Thursday, Friday and Saturday, December 28, 29 and 30, 1939, in affiliation with Section B—Physics of the American Association for the Advancement of Science. All sessions of the meetings were held at The Ohio State University. The presiding officers were Professor John Zeleny, Vice President of the Society, Dr. W. E. Forsythe, Professor R. C. Gibbs, Professor Elmer Hutchisson and Dean Alpheus W. Smith.

On Friday afternoon, December 29, at two-thirty o'clock the Society held a joint session with Section B of the American Association for the Advancement of Science and with the American Association of Physics Teachers. Dr. Herbert E. Ives of the Bell Telephone Laboratories delivered an address entitled "The Measurement of Velocity and Atomic Clocks." Professor I. I. Rabi of Columbia University addressed the session on the subject "Radio-frequency Spectra of Atoms and Molecules." The presiding officer was Dr. Karl K. Darrow of the Bell Telephone Laboratories.

On Friday evening, December 29, the Society held a joint dinner with the American Association of Physics Teachers at the Deshler-Wallick Hotel. The attendance was approximately two hundred. Dr. Karl K. Darrow presided.

Annual Business Meeting. The regular Annual Business Meeting of the American Physical Society was held on Friday afternoon, December 29, 1939 at two o'clock, Vice President Zeleny presiding. Dr. W. H. Brattain reported for the tellers that the following had been elected as officers for the year 1940:

President, John Zeleny; *Vice President*, George B. Pegram; *Secretary*, W. L. Severinghaus; *Treasurer*, George B. Pegram; *Members of the Council*, F. G. Brickwedde and Henry D. Smyth; *Members of the Board of Editors*, Samuel K. Allison, Philip M. Morse and John A. Wheeler.

The Secretary reported that during the year 221 persons had accepted election to membership. He reported the deaths of 14 members, that 40 members had resigned and 51 members had been dropped. The membership as of December 26, 1939 was as follows: Fellows: 788; Members: 2772; Honorary Members: 5; Total Membership: 3565.

The Treasurer presented a summary of the financial condition of the Society. The Treasurer's financial report will be audited, printed and distributed to the members.

Dr. J. W. Buchta, the Assistant Editor, made a brief report on the general status of the publications of the Society and stated that a detailed and audited financial report for 1939 would be printed and distributed to the members.

The meeting adjourned at two-twenty P.M.

Meeting of the Council. At the meeting of the Council held on Thursday morning, December 28, 1939, eighteen candidates were elected to fellowship and thirty-four candidates were elected to membership. *Elected to fellowship:* Allen V. Astin, C. Hawley Cartwright, Jacob Clay, Gioacchino Failla, James B. Fisk, William W. Hansen, Serge A. Korff, Henry M. O'Bryan, Arthur L. Patterson, Franco Rasetti, Lynn H. Rumbaugh, Leonard I. Schiff, Theodore E. Sterne, Arthur von Hippel, Milton G. White, Howell J. Williams, John H. Williams, and E. Bright Wilson, Jr. *Elected to membership:* Thomas C. Bagg, F. Meade Bailey, Clifford Beck, Sister Bernarda, Maurice A. Biot, William W. Beeman, Harvey Brooks, Allan L. Burton, Jr., George W. Charles, Vinton C. Fishel, Herbert Friedman, William Garten, Jr., Herbert Goldstein, Roy Goslin, Eugene M. Grabbe, Theodore Jorgensen, Jr., Mother Marion Kent, Kenneth E. Keyes, J. Stewart Marshall, Ralph W. Mann, Karl Martinez, Boyce D. McDaniel, James O. McNally, Eugene McNatt, Park H. Miller, Jr.,

Wilford E. Morris, Jacob Neufeld, H. F. Newhall, E. W. Richmeyer, Charles F. Robinson, Richard Scheib, Jr., Wave H. Shaffer, Erwin F. Shrader, and William Widmaier.

The regular scientific program of the Society consisted of seventy-five contributed papers of which six, numbers 22, 37, 53, 54, 61 and 72, were read by title. The abstracts of the contributed papers are given in the following pages. An Author Index will be found at the end.

W. L. SEVERINGHAUS, *Secretary*

ABSTRACTS

1. Effect of Hyperfine Structure upon the Magnetic Rotation of the Plane of Maximum Polarization of Resonance Radiation. BERTRUND J. MILLER, *St. Ambrose College.*—An equation has been developed for the polarization, and the angle of maximum polarization of resonance radiation as observed along a magnetic field perpendicular to the electric vector and the direction of propagation of the incident beam. Explicit application has been made to the polarization and the angle for the line $^1S_0-{}^1P_1$ for various values of the ratio of the hyperfine separation constant to the natural breadth of the levels, for a nuclear moment of $\frac{1}{2}$. It was noted here that the form of the curves might differ widely from that to be expected from classical considerations. The polarization, and the angle of maximum polarization for the D lines, for several values of the same ratio, were computed and compared with experimental observations. Thus a range of possible values of A was determined, which is not in disagreement with previous figures, and a value for τ established which agrees well with that calculated from optical dispersion data.

2. The Excitation of High Stages of Ionization in Gases. HARRY D. POLSTER AND FRED W. PAUL, *Ohio State University. (Introduced by Harold P. Knauss.)*—Various methods have been employed in an attempt to produce high stages of ionization in gases to make possible the spectroscopic investigation of highly ionized rare gas atoms. Of these the most successful have been the use of a condensed discharge in a quartz or Pyrex capillary and in a Geissler tube. Banks of condensers having capacitances of 0.1 μf, 0.3 μf, and 0.9 μf have been charged with voltages as high as 25 kv and then discharged through the gases. The resulting light is very brilliant and bluish-white in color. The spectra have been recorded with a 3-meter grazing incidence vacuum spectrograph. In testing the set-up oxygen has been used and the spectra of O III, O IV, and O V have been brought out quite strongly. Preliminary observations in the spectra of neon have permitted the identification of a few lines of Ne V.

3. The Spectra of Cb V and Cb VII. GEORGE W. CHARLES AND FRED W. PAUL, *Ohio State University. (Introduced by Harold P. Knauss.)*—Condensed sparks in a high vacuum chamber between electrodes of columbium metal have been used as a source of light on a 3-meter grazing incidence vacuum spectrograph. The resulting spectrograms have been measured and the data have been partially analyzed. Tentative identifications have been made in the spectra of Cb V and Cb VII with the aid of isoelectronic sequence data. The brightness of these spectra and the fact that they can account for only a small part of the lines observed lead to the hope that some identifications may be made in the spectra of Cb VI and Cb VIII.

4. The Zeeman Effect in Krypton. J. B. GREEN, D. W. BOWMAN AND E. H. HURLBURT, *Ohio State University.*—The spectrum of krypton emitted in a magnetic field of about 36,000 gauss has been measured, using a high frequency electrodeless capillary discharge. Preliminary measurements indicate that a revision of Pogány's measurements[1] is necessary, especially for $4p^55s$ ($1s_2$ and $1s_4$) which are found by us to have values much closer to the theoretical values than Pogány's, which seem to be inverted. A much closer agreement with theory is also found for the $4p^55p$ configuration. Rasmussen's[2] reclassifications of some of the levels are checked, and a few further reclassifications suggested.

[1] B. Pogány, Zeits. f. Physik **93**, 364 (1934–5).
[2] E. Rasmussen, Zeits. f. Physik **73**, 779 (1931–2).

5. Sommerfeld's Fine Structure Constant. ALFRED LANDÉ, *Ohio State University.*—The *suggestion*[1] of obtaining the electronic density amplitude $\psi(r)$ and Sommerfeld's constant α from a homogeneous integral equation, which was transformed into a consistent *theory* by M. Born[2] through his idea of a phase retardation inside the electron, is revised by a reciprocal treatment of (p, E) and the distances $(\Delta r, \Delta t)$. The equation $(c\Delta t)^2-(\Delta r)^2=-a^2$ determines the time Δt of a signal traveling Δr. Then $\Delta t=0$ for $\Delta r=a$ means *particles of diameter a*, similar to *Dirac's* theory of the classical electron,[3] with $a=\gamma e^2/mc^2$ and $\gamma=2/3$. If $R=r/a$ we obtain the integral equation

$$\psi(R)=(\gamma\alpha/2\pi)^2\int\psi(R')K(\gamma\alpha,\,|R-R'|)dV',$$

where dV' is the noninvariant volume element divided by a^3, and K is the symmetric kernel

$$K=\int_0^\infty dP 4\pi P^2\times\sin(AP)/(AP)\times\sin[iB(P^2+1)^{\frac{1}{2}}]/[B(P^2+1)^{\frac{1}{2}}],$$

$$A=\gamma\alpha|R-R'|,\quad B=\gamma\alpha(|R-R'|^2-1)^{\frac{1}{2}}.$$

$1/\alpha$ is calculated to be 136.08.

[1] A. Landé, J. Frank. Inst. **228**, 495 (1939).
[2] M. Born, Proc. Roy. Soc. Edinburgh **49**, 219 (1939).
[3] P. A. M. Dirac, Proc. Roy. Soc. **A167**, 148 (1939).

6. Spectroscopic Comparison of Strengths of Hydrogen Bonds Between CH_3OD and Certain Solvents.* WALTER GORDY, *Mary Hardin-Baylor College*, AND SPENCER C. STANFORD, *The College of Wooster*.—Forty-two different organic liquids are rated according to their proton-attracting power by comparing the strengths of the hydrogen bonds which they form with heavy methyl alcohol. The classes of liquids studied are: aldehydes, ketones, esters, ethers and amines. The amount of perturbation which the different solvents produce in the OD vibrational band of the CH_3OD is taken as a measure of the strength of the deuterium bridges formed with the CH_3OD. The study is a continuation of a previous work in which 26 similar liquids were observed, and the results agree with those of the former study in showing that the proton-attracting power of the different classes of liquids rises in the order: esters<aldehydes and ketones <ethers<amines. From the data gathered it is possible to observe the effects of unsaturation, substitution and other structural variations on the electron donor power of the O or N atom to which the OD group forms a bond. It is shown that the strength of the deuterium bonds formed with CH_3OD bears a close relation to the basicities of the solvents to their reactivities with certain other compounds, and to their solubilities for other proton donor solutes. There appears to be no correlation between the dipole moments of the solvents and the strengths of the bonds formed with the CH_3OD.

* The observations reported here were made in the Mendenhall Laboratory of Physics, Ohio State University.

7. New Measurements on the Vibration-Rotation Bands of Water Vapor. HARALD H. NIELSEN, *Ohio State University*.—The five bands ν_2(1595 cm^{-1}), $2\nu_2$(3152 cm^{-1}), ν_3(3756 cm^{-1}), $\nu_2+\nu_3$(15,332 cm^{-1}) and $\nu_1+\nu_3$(7253 cm^{-1}), using Dennison's notation, have been remeasured under high dispersion. By enclosing the optical parts of the spectrometer with an air-tight box it has been possible almost completely to resolve these bands. Much more detail in the rotational structure is discernible than is possible in the earlier absorption curves,[1] and many separations between lines have been recorded of 0.5 cm^{-1} or less. While the lines observed have not been completely classified, some modifications of the analysis by Mecke[2] appear necessary. This is especially true of $2\nu_2$ where an additional line, not earlier recorded, has been found near the center so that the interval between the two most intense lines nearest the center is reduced to about 40 cm^{-1} as is the case for the fundamental ν_2. Measurements on the spectra of the "heavy" waters are also in progress. High dispersion data on the frequency ν_3 have been completed and the band is almost completely resolved.

[1] Phys. Rev. **37**, 1493 (1931); **39**, 77 (1932).
[2] R. Mecke, Zeits. f. Physik **81**, 313 (1933).

8. The Infra-Red Absorption Spectrum of the Deutero-Acetylenes. ALVIN H. NIELSEN,* *Ohio State University*.—The spectrum of the deutero-acetylenes has been re-investigated from 2.0μ to 10.0μ, using prism and grating spectrometers. The gas was made by allowing high purity D_2O to react with calcium carbide which had been thoroughly baked out. No bands of C_2H_2 were observed. The prism curve revealed the following bands for C_2DH: ν_2 at 3340 cm^{-1}, ν_3 at 2560 cm^{-1}, $2\nu_4$ at 1340 cm^{-1}, and $\nu_4+\nu_5$ at 1202 cm^{-1}. In C_2D_2 the bands observed were ν_3 at 2414 cm^{-1} and $\nu_4+\nu_5$ at 1043 cm^{-1}. By means of a grating having 4800 lines per inch, ν_2 in C_2DH was resolved giving a rotational $\Delta\nu$ of 1.98 cm^{-1}. The rotational $\Delta\nu$ for $2\nu_4$ and $\nu_4+\nu_5$ in C_2DH, determined by means of a grating having 2000 lines per inch, are 1.98 cm^{-1} and 1.96 cm^{-1}, respectively. The moment of inertia calculated from the average of these spacings is 28.0×10^{-40} g cm^2 in agreement with the value 27.9×10^{-40} g cm^2 of Herzberg, Patat and Spinks[2] determined from photographs of near infra-red overtone bands. The lines in $2\nu_4$ and $\nu_4+\nu_5$ appear complex. This may be because of superposition of corresponding bands in $H-C^{12}-C^{12}-D$, $H-C^{12}-C^{13}-D$, $H-C^{13}-C^{12}-D$, and $H-C^{13}-C^{13}-D$. The remaining unresolved bands are being measured and will be reported at a later time.

* University of Tennessee.
[1] E. F. Barker and H. M. Randall, Phys. Rev. **45**, 124(A) (1934); W. F. Colby, Phys. Rev. **47**, 388 (1935).
[2] Herzberg, Patat and Spinks, Zeits. f. Physik **92**, 87 (1934).

9. Infra-Red Absorption Spectrum of Methylphenylacetylene. FORREST F. CLEVELAND AND M. J. MURRAY, *Armour Institute of Technology*.—The infra-red absorption spectrum of methylphenylacetylene ($C_6H_5C\equiv CCH_3$) between 500 and 2300 cm^{-1} has been obtained with a prism spectrometer. The results are compared with the Raman spectrum, previously measured by the authors,[1] and are found to be inconclusive as regards the assignment of the fundamental whose overtone, according to Badger's hypothesis,[2] is responsible for the resonance doubling of the frequency near 2230 cm^{-1}. The frequency near 1100 cm^{-1} which most nearly satisfies the frequency condition for resonance is a weak one at 1095 cm^{-1}. The first overtone of this frequency, 2190 cm^{-1}, has a value even less than that of the smaller frequency of the doublet, 2214, 2254. The second overtone of the 756 cm^{-1} frequency, 2268 cm^{-1}, on the other hand, is greater than the larger frequency of the doublet. The authors wish to express their appreciation to Professor H. M. Randall for the use of his laboratory at the University of Michigan and to Mr. Robert A. Oetjen for his assistance in obtaining the experimental record.

[1] M. J. Murray and Forrest F. Cleveland, J. Am. Chem. Soc. in press.
[2] R. M. Badger, J. Chem. Phys. **5**, 178 (1937).

10. The Absorption Spectra of α, β, γ, δ-Tetraphenylporphine and a Series of Its Metal Complex Salts. V. M. ALBERS AND H. V. KNORR, *Antioch College*.—The absorption spectra of α, β, γ, δ-tetraphenylporphine and the Cd, Ag, Zn, Pb, Ni, Co, FeCl, MnCl and $SnCl_2$ complex salts have been studied over the region from 900 mμ to 370 mμ in benzene solution, using a recording spectroradiometer previously described.[1] No absorption bands were observed for any of these substances between 900 mμ and 700 mμ. They all, however, show characteristic absorption in the visible region. Absorption curves, showing molecular absorption coefficients as a function of wave-length, have

been determined for all of these substances from 700 mμ to 370 mμ.

[1] V. M. Albers and H. V. Knorr, J. Opt. Soc. Am. **28**, 121–123 (1938)

11. The Fluorescence Spectra of α, β, γ, δ-Tetraphenylporphine and Some of Its Metal Complex Salts. H. V. KNORR AND V. M. ALBERS, *Antioch College.*—The fluorescence spectrum of α, β, γ, δ-tetraphenylporphine in anhydrous benzene and under an atmosphere of N_2, has been photographed by a method previously described.[1] The spectra of the Ni, FeCl, and Ag complex salts have also been photographed under similar conditions. A fluorescence band is observed with its maximum at 655 mμ, for each of these substances. This same band was also observed for tetraphenylporphine under an atmosphere of CO_2. Two additional bands have been observed in the near infra-red portion of the spectrum for the tetraphenylporphine.

[1] H. V. Knorr and V. M. Albers, Cold Spring Harbor Symposia on Quantitative Biology **3**, 98–107 (1935).

12. A Constant Current Network for Supplying Power to a Cyclotron Oscillator. A. J. ALLEN, *University of Pittsburgh,* AND R. G. FRANKLIN, *Biochemical Research Foundation of the Franklin Institute.*—A constant current network using 3 phase-4100 v from the power distribution system and supplying from 0.6 to 3.6 amperes up to 12 kv to the plates of a cyclotron oscillator has been developed. The network makes use of a simple resonant circuit for transforming constant voltage to constant current.[1] The capacitors are made variable in steps and the inductor continuously variable to give the desired power output. The voltage, current, and protection requirements for the various parts are given. The network tends to eliminate power surges, provides a convenient method for regulating the power input into the cyclotron, and eliminates the use of transformers for the plate supply.

[1] Elec. Eng. **54**, 102 (1935).

13. The Ohio State University Cyclotron. ALPHEUS W. SMITH AND M. L. POOL, *Ohio State University.*—A brief introduction to the cyclotron here under construction will be made. The salient features to be discussed include the magnet frame, glass-insulated and water-cooled magnet coils, vacuum chamber and system, radiofrequency oscillator system and quarter wave-length transmission line. The relation of the cyclotron to other departments in the University will be pointed out.

14. Performance of Westinghouse Electrostatic Generator up to 3.7 mv. W. H. WELLS, R. O. HAXBY,* W. E. SHOUPP* AND W. E. STEPHENS,* *Westinghouse Research Laboratories.*—The voltages attained as a function of pressure up to 80 pounds per sq. in. are limited with the present belt arrangement by sparking, mainly along the surfaces of the belts. Voltages are measured with a generating voltmeter which has been calibrated against gamma-ray resonance values determined at the University of Wisconsin. Molecular hydrogen ions of masses two and three are used to determine the linearity and calibration constant of the voltmeter when used as a null instrument. Voltages in the region of 3 mv are constant for observing times of several minutes to less than 0.5 percent and can be read during these time intervals to 0.2 percent.

* Westinghouse Research Fellow.

15. Coincidence Measurements in As^{76}. L. M. LANGER, A. C. G. MITCHELL AND P. W. MCDANIEL, *Indiana University.*—Using a strongly activated source of As^{76} (26 hours), prepared by irradiation of As by slow neutrons from the Berkeley cyclotron, gamma-gamma and beta-gamma coincidences have been investigated. The maximum energy of the beta-rays was measured by absorption in Al, using a single counter. The end point was found to be 3.24 mv. The number of gamma-gamma coincidences was found to be 0.28 ± 0.02 per thousand gamma-rays detected. Beta-gamma coincidences were measured as a function of the thickness of aluminum absorber placed between the source and the beta-ray counter. The number of beta-gamma coincidences per thousand beta-rays detected was found to vary with the energy of the beta-rays. The shape of the curve suggests that there are at least two groups of beta-rays present, both of which go to an excited state of Se^{76}.

16. Investigation of Beta- and Gamma-Rays from Sb^{122} and Sb^{124}. A. C. G. MITCHELL, L. M. LANGER AND P. W. MCDANIEL, *Indiana University.*—The beta- and gamma-rays emitted by Sb, irradiated by slow neutrons, have been studied by the method described in the previous abstract. In Sb both beta-rays and gamma-rays were observed to be associated with each of the two periods of 70 hours and 60 days. The energy of the gamma-rays was measured by the coincident method of absorption of Compton electrons. The radiation was found to be inhomogeneous. The highest energy gamma-ray, which is associated with the long period, has an energy of 1.7 mv as determined from the range of the Compton recoils. Gamma-gamma coincidences decay with the long period, indicating more than one gamma-ray associated with this period. Absence of gamma-gamma coincidences with the short period indicates that only one gamma-ray of measurable intensity is associated with it. The maximum energy of the beta-rays of the long period was found, by absorption in Al, to be 1.53 mv. That of the short period is not greater than and probably equal to the same value. Beta-gamma coincidences, measured as a function of the energy of the beta-rays, show that there is only one group of beta-rays associated with the long period and this leads to an excited state of Te.

17. The Disintegration of N^{14} and N^{15} by Deuterons. M. G. HOLLOWAY, *Cornell University.* (*Introduced by R. F. Bacher.*)—The study of the disintegration of N^{14} and N^{15} has been continued using a gas mixture having much higher concentration (70 percent) of N^{15}. A search has been made for alpha-particle and proton groups in the region between 7 cm and 3 cm range. A new alpha-group of 3.48 cm range

was found at the end of the very intense distribution of alphas below 3.2 cm. This 3.48-cm alpha-group is attributed to the $N^{14}(d\alpha)C^{12}$ reaction in which the C^{12} is left in an excited state at 7.78 Mev. There is some indication of a proton group of about 3.5 cm range, which would arise from the $N^{15}(dp)N^{16}$ reaction.

18. Lithium and Carbon (p,n) Thresholds. R. O. HAXBY,* W. E. SHOUPP,* W. E. STEPHENS* AND W. H. WELLS, *Westinghouse Research Laboratories.*—Using high energy protons from the Westinghouse pressure electrostatic generator,[1] we have bombarded targets of lithium hydroxide and graphite and measured the thresholds for the production of neutrons. The neutrons were detected by a boron trifluoride ionization chamber surrounded with paraffin and connected to a linear amplifier and counter. The linearity and constant of the generating voltmeter was determined by measuring the 0.862-Mev gamma-ray resonance[2] from $F(p,\gamma)$ at 1.724 Mev and 2.586 Mev using H_2^+ and H_3^+. Hence our voltages depend on the Wisconsin voltage calibration of the fluorine resonances. The $Li^7(p,n)Be^7-Q_1$ threshold occurred at a proton energy $Ep=1.86\pm0.02$ Mev. This gives $Q_1=1.62\pm0.02$ Mev and $Be^7-Li^7=0.86\pm0.03$ Mev. This difference is somewhat lower than the estimate of 1.0 Mev made by Rumbaugh, Roberts and Hafstad[3] from the fraction of K-electron captures accompanied by gamma-rays, but is within their limits of error. This threshold is also smaller than that measured by Hill and Valley[4] due, perhaps, to our use of a more sensitive neutron detector. The $C^{13}(p,n)N^{13}-Q_2$ threshold was measured at $Ep=3.20\pm0.03$ Mev giving $Q_2=2.97\pm0.03$ Mev and $N^{13}-C^{13}=2.21\pm0.03$ Mev. So $N^{13}=C^{13}+e_+ +\mu+1.19\pm0.03$ Mev. This agrees well with Lyman's observed value of the maximum energy of these positrons $=1.198\pm0.006$ Mev.[5]

* Westinghouse Research Fellow.
[1] W. H. Wells, Phys. Rev. 55, 599(A) (1939); J. App. Phys. 9, 677 (1938).
[2] Bernet, Herb and Parkinson, Phys. Rev. 54, 398 (1938).
[3] Rumbaugh, Roberts and Hafstad, Phys. Rev. 54, 657 (1938).
[4] J. E. Hill and G. E. Valley, Phys. Rev. 55, 678(A) (1939).
[5] E. M. Lyman, Phys. Rev. 55, 234 (1938).

19. Radioactive Isotopes of Sr, Y and Zr. L. A. DUBRIDGE AND JOHN MARSHALL, *University of Rochester.*—Bombardment of Rb, Sr and Y with protons, deuterons and neutrons produces eleven radioactivities whose assignments, periods, properties and methods of formation are as follows:

Sr^{85}: isomers, 60 min. and 65 days, x-rays and gamma-rays only, 0.8 Mev γ-ray accompanying long period; $Rb^{85}(p,n)$.

Sr^{87*}: 2.7-hr. isomeric state, 0.37 Mev γ-ray internally converted;[1] $Rb^{87}(p,n)$, $Sr^{87}(n,n)$ and $Y^{87}(85\text{ hr.})+e_k^-$. Cross section for $Sr^{87}(n,n)Sr^{87*}$ is of the same order of magnitude as for $In^{115}(n,n)In^{115*}$.

Sr^{89}: 55 days, e^-, $Sr^{88}(d,p)$[2].

Y^{88}: 15 days, K capture, $Sr^{84}(d,n)$.

Y^{86}: 80 days, K capture, 2 Mev γ-ray, $Sr^{86}(p,n)$.

Y^{87}: isomers, 85 hr. and 14 hr. 85-hr. activity, but not the 14-hr., decays by K capture to Sr^{87*}(2.7 hr.). Over 95 percent of the equilibrium activity of this period is due to conversion electrons of Sr^{87*}. Both periods formed by $Sr^{87}(p,n)$ and $Sr^{86}(d,n)$.[2]

Y^{88}: 2 hr., e^+, $Sr^{88}(p,n)$ and $Sr^{87}(d,n)$.[2]

Zr^{89}: isomers, 4 min. and 70 hr. Short period emits only x-rays and gamma-rays in isomeric transition, 70-hr. period emits 1-Mev positrons. $Y^{89}(p,n)$.

[1] L. A. DuBridge and J. Marshall, Phys. Rev. 56, 706 (1939).
[2] Reported also by D. W. Stewart, Phys. Rev. 56, 629 (1939).

20. The Production of Radium E and Radium F from Bismuth. J. M. CORK, J. HALPERN AND H. TATEL, *University of Michigan.*—It was shown by J. Livingood that on bombarding bismuth with 22-cm deuterons, neutron capture resulted in the formation of radium E. When the energy of the incident deuterons is increased it is now shown that both radium E and radium F (polonium) are made during bombardment. The latter process is associated with a proton capture. By observing the subsequent alpha-activity, making use of a linear amplifier and cloud chamber, data are obtained showing the yield of each product at varying excitation energies. At 10 Mev about four atoms of radium E are formed for each one of polonium. An apparent threshold energy for radium F exists at about 6.8 Mev. The atomic cross sections at 10 Mev are 9×10^{-29} cm^2 and 4×10^{-28} cm^2 for the formation of radium F and radium E, respectively.

21. Nuclear Excitation by Charged Particles Which Do Not Penetrate the Potential Barrier. EUGENE FEENBERG, *Washington Square College, New York University.*—A charged particle passing near a nucleus may lose some of its kinetic energy without actually penetrating the potential barrier.[1] The mechanism for the energy transfer is the Coulomb interaction between the particle and the protons in the nucleus. In the inhomogeneous and rapidly changing Coulomb field of the particle, the nucleus is subjected to forces which tend to produce distortion without change in volume. The momentary distortion resolves itself into a superposition of surface vibrations which persist until the excitation energy is lost in radiation or transferred to other types of motion in the nucleus. The coupling energy between a charged particle and the surface vibrations of a uniformly charged liquid drop has been determined and applied to compute the cross section for inelastic collision. In contrast to the more general formula given by Weisskopf, the expression for the cross section obtained from the liquid-drop model contains no undetermined nuclear matrix elements. Most of the cross section arises from the excitation of the surface wave with two units of orbital angular momentum. In very heavy nuclei this type of surface vibration has an excitation energy of about 0.8 Mev.[2] For particle energies greater than 3 Mev the cross section varies as the square of the momentum of the incident particle and in the case of 6-Mev alpha-particles on lead has a value greater than 10^{-26} cm^2.

[1] V. F. Weisskopf, Phys. Rev. 53, 1018 (1938).
[2] N. Bohr and J. A. Wheeler, Phys. Rev. 56, 426 (1939).

22. Scattering and Polarization of Electrons. M. E. Rose,* *Yale University.*—The possibility of accounting for the observed small polarization of electrons in double scattering[1] and the anomalously small scattering of fast electrons ($E \lesssim 500$ kv) in heavy elements[2] by assuming non-Coulomb forces near the nucleus is examined. Without any assumptions as to the nature of the forces it is found that due to the small range, *in general* either $s_{\frac{1}{2}}$ or $p_{\frac{1}{2}}$ waves can be scattered but not both. With the correct polarization the scattering of $s_{\frac{1}{2}}$ waves yields too small an intensity at low energies ($E \lesssim 300$ kv). Scattering of $p_{\frac{1}{2}}$ waves results in a correct polarization and scattering at low energies but the scattering at high energies cannot be made less than 70 percent Coulombian whereas about 15 percent Coulombian scattering is required. Under special conditions both $s_{\frac{1}{2}}$ and $p_{\frac{1}{2}}$ waves may be scattered. A necessary condition for this is that the logarithmic derivatives of both inside wave functions at the boundary be nearly equal to $-(1+(1-\alpha^2Z^2)^{\frac{1}{2}})/\text{range}$. This requires a very large interaction at small distances. The sufficient conditions for correct polarization and scattering are found in the form of a special energy dependence of the logarithmic derivatives of the inside wave functions at the boundary.

* Sterling Fellow.
[1] For example, E. G. Dymond, Proc. Roy. Soc. **A145**, 657 (1934).
[2] A. Barber and F. C. Champion, Proc. Roy. Soc. **A168**, 159 (1938).

23. The Crystalline Electric Field in $CuSO_4 : 5H_2O$. O. M. Jordahl, *Northwestern University.*—With the publication of data on the principal magnetic susceptibilities of $CuSO_4 : 5H_2O$,[1] it becomes possible to study in detail the symmetry and magnitude of the crystalline electric field around the cupric ion. According to the analysis by Krishnan and Mookherji,[1] both for the crystal as a whole and for the single ion in the crystal, two of the principal magnetic susceptibilities should be the same. The value of the third principal susceptibility is less than the other values by about 20 percent in the crystal but is greater by about 40 percent in the case of a single ion. Using methods previously employed[2] we assume a predominant crystalline electric field of cubic symmetry and superpose a smaller field of tetragonal symmetry suitably oriented. The very large asymmetry in the magnetic susceptibilities means that the departure from cubic symmetry is considerable. Nevertheless it is the cubic field (fourth degree term) which primarily determines the mean magnetic susceptibility. The potential term in the Hamiltonian is

$$V = D(x^4+y^4+z^4)+A(x'^2-2y'^2+z^2) \text{ where } D>A.$$

Excellent agreement is secured between the computed and "observed" values of the principal magnetic susceptibility of the cupric ion if the $x'y'$ axes of the tetragonal field make angles of 45° with the x,y axes of cubic field and the splittings of the energy levels produced by the cubic and tetragonal fields are, respectively, 18,300 cm^{-1} and 2550 cm^{-1}. A tetragonal component whose axes coincide with the cubic field axes is unsatisfactory. The relation between this assumed field and the crystal structure of $CuSO_4 : 5H_2O$ [3] will be discussed.

[1] K. S. Krishnan and A. Mookherji, Phys. Rev. **50**, 860 (1936); **54**, 533 and 841 (1938).
[2] O. M. Jordahl, Phys. Rev. **45**, 87 (1934).
[3] C. A. Beevers and H. Lipson, Proc. Roy. Soc. **A146**, 570 (1934).

24. Interaction of Electrons with Nuclei. E. Guth, *University of Notre Dame.*—The deviations from theory of observed fine structure of H_α and D_α, isotope displacements and electron scattering by nuclei can be explained by assuming that Coulomb's law for the interaction between electrons and nuclei breaks down at a certain distance r_0. The experimental results indicate that inside the nucleus there exists either a small negative potential ($\sim Ze^2/r_0$) with a large nuclear radius, or a big positive potential with a small radius ($\sim e^2/mc^2$). The effect of such deviations from Coulomb's law on the scattering of electrons is calculated, and it is shown that observable effects may result for electron energies of about 1.5 Mev and higher. Scattering experiments might distinguish between the two types of nuclear potentials mentioned. An interpretation of isotope displacement data over the whole periodic system is made by using a two-parameter nuclear potential. The displacements can be interpreted partly as the outcome of an additional electron-proton (and electron-neutron) interaction. The specific effects expected to result from such deviations from Coulomb's law will be discussed for various phenomena e.g. polarization of electrons in double scattering etc.

25. Calculation of Transmission Coefficients and Explanation of the Periodic Deviations from the Schottky Line. Charles J. Mullin and E. Guth, *University of Notre Dame.*—In order to calculate transmission coefficients by the W.K.B. method for certain potential barriers, especially for those with sharp boundaries, approximations higher than the first (hitherto not used) are considered. The necessary formulae are developed. Former calculations using the first W.K.B. approximation are shown to be inconsistent. Interference effects in the transmission coefficient can explain the recently discovered periodic deviations from the Schottky line.[1] Both exact and W.K.B. calculations for simplified potential barriers account fairly well for the observed deviations.[2]

[1] D. Turnbull, *et al.*, Phys. Rev. **56**, 652, 663 (1939).
[2] Cf. also H. M. Mott-Smith, Phys. Rev. **56**, 668 (1939). However, with the special fields that he considered, he did not show this effect.

26. Some Properties of Retarded and Advanced Potentials. Boris Podolsky and Kaiser S. Kunz, *University of Cincinnati.*—The general solution of inhomogeneous wave equations of the type $\nabla^2\varphi-(1/c^2)\partial^2\varphi/\partial t^2 = -4\pi\rho$, for the case of a charged particle moving in an external field, with the total field assumed known at the time $t=0$, can be written in either of the two forms: $\varphi=\text{retarded potential}+\psi_1$, or $\varphi=\text{advanced potential}+\psi_2$, where ψ_1 and ψ_2 are suitably chosen complementary functions. To study the properties of the complementary functions, and to obtain physical interpretations, space-time is divided into three regions: (1) the absolute past of the particle at $t=0$, (2) the absolute future of the same, and (3) the remaining region. It is then found that: first, in region (3) φ is independent of the shape of the world line of the particle; second, in region (1) ψ_2 is independent of the shape of the world line; third, in region (2) ψ_1 is independent of the shape of the world line. Application of this result leads to the conclusion that the retarded

potential gives the field produced by the particle, while ψ_1 gives the effects of the external field. The corresponding statement cannot be made for the advanced potential and ψ_2.

27. Magnetic Forces. F. W. WARBURTON, *University of Kentucky.*—The force of one electron on another developed from Riemann's potential is attractive because of its symmetry, action-reaction and propagation. The induced e.m.f., computed from the force of protons and electrons in a primary circuit acting on electrons in the secondary circuit, contains explicitly the relative velocity of the secondary element and the field-producing apparatus and the acceleration of the primary electrons. It satisfies the unipolar induction experiments with a rotating solenoid, the acceleration term canceling the motional term. However, when applied to the orbital electrons in the magnet acting on electrons in the secondary wire the results are not so favorable. This force and other similar symmetrical expressions, as well as the nonsymmetrical conventional magnetic force, obey constancy of field momentum plus mechanical momentum.

28. Analysis of B_2H_6 with a Mass Spectrometer. JOHN A. HIPPLE, JR.,* *Westinghouse Research Laboratories.*—A mass-spectrometer of the magnetic analyzer type has been constructed by platinizing the inside of a glass tube bent in the form of a semicircle. This is simpler and more convenient than the customary method of inserting a curved metal shielding tube inside the glass, and appears to function as well. The tube may be baked out in the same manner as before. A sample of B_2H_6 has been analyzed using 90-volt electrons. As this has the same structure as C_2H_6, a comparison of the relative intensities of the corresponding products is given in the following table (corrected for the isotope effect in B_2H_6):

	X_2H_6	X_2H_5	X_2H_4	X_2H_3	X_2H_2	X_2H	X_2	XH	X
B	0	100	44.8	21.7	63.7	2.9	2.2	0	40
C	100	76	360	105	62	12	2.5	2.5	1

Peaks at the mass numbers 11.5, 12 and 13 with intensities relative to B_2H_6 of 4.9, 12.6, and 17.7, respectively, were not included in the table because the interpretation is not clear due to the effects of the isotopes and doubly charged ions. The most striking feature of the analysis is the absence of the ion corresponding to the simple ionization of the parent molecule. There was a small peak at mass 28, but it seems likely that this is a slight N_2 impurity. In any case, B_2H_6 is less than 1/1000 of B_2H_5.

* Research Fellow.

29. Collisions of Negative Atomic Ions with Molecules. PAUL F. DARBY AND WILLARD H. BENNETT,* *Ohio State University.*—A method for the analysis of the particles derived from the collisions of negative atomic ions with molecules has been developed. The ions are produced in a glow discharge and formed into a beam in high vacuum by electron lenses. A narrow velocity range is selected by passing the beam through a magnetic field. It is then focused into a collision chamber where it passes through a unidirectional beam of molecules proceeding at right angles to the ion beam. The ions thus formed are collected into a beam and separated by a magnetic field in the same manner as the initial ion beam. This procedure makes for clear cut results and easier handling of the colliding ions although the resolving power of the system is not great. Details of design and experimental results will be given.

* Now with Electronic Research Corporation.

30. Electrical Discharge on Liquid Surfaces. L. B. SNODDY, HUGH F. HENRY AND J. W. BEAMS, *University of Virginia.*—The study of electrical discharges on surfaces of conducting liquids previously reported[1] has been extended to include surfaces of soap bubbles, bubbles of air in liquids, and the surface of water covered with oil. The discharges in each case are produced by a high potential impulse from a Marx circuit (maximum potential about 80 kv). The soap bubbles were formed between two metal pipes which formed the discharge electrodes. The discharge path follows the surface of the bubbles, although this distance is approximately 1.5 times the straight sparkover distance. This occurs with the bubble filled with H_2, air, or illuminating gas and does not seem to depend appreciably on the film thickness. The same results are obtained for bubbles passing between two electrodes in the interior of a viscous slightly conducting liquid. The discharge in most cases follows the surface of the air cavity. In the case of water covered with oil, the discharge follows the water oil interface.

[1] L. B. Snoddy and J. W. Beams, Phys. Rev. **55**, 663 (1939).

31. Progressive Breakdown in a Long Discharge Tube. F. H. MITCHELL, *University of Virginia.* (*Introduced by L. B. Snoddy.*)—Negative impulsive potentials were applied to an electrode in one end of a glass discharge tube 12 meters long and 14 cm in diameter, containing dry air. By means of a high speed cathode-ray oscillograph, a family of curves was obtained expressing the average speed of the discharge between two electrodes 6.4 meters apart as a function of applied potential (25 to 115 kv) and pressure (0.006 to 8.0 mm Hg). With increasing potential and pressure the speed reached a maximum, which varied from 3×10^9 cm/sec. (at 0.3 mm and 25 kv) to 1.0×10^{10} cm/sec. (at 1.5 mm and 115 kv). At higher pressures the speed for all potentials decreased approximately exponentially, with increasing pressure, becoming 1×10^9 cm/sec. at values ranging from 1.0 mm and 25 kv to 8 mm and 115 kv. The luminous column completely filled the tube at all pressures used, in contrast to the previously noted[1] contraction when positive potential was applied.

[1] Dietrich, Snoddy and Beams, Phys. Rev. **53**, 923 (1938).

32. Dielectric Properties of the Rutile Crystalline Modification of TiO_2. L. J. BERBERICH AND M. E. BELL, *Westinghouse Electric and Manufacturing Company.*—Most materials have dielectric constants in the range 1–10. Notable among the exceptions is rutile, the crystalline modification of TiO_2 which is stable at high temperatures. Three samples of this material have been investigated in the form of disks pressed from powdered crystals, then

sintered. Curves of dielectric constant against frequency show a rise at very low frequencies, probably attributable to interfacial polarization, with a uniformly high value of approximately 100 extending through the highest radio-frequencies, falling off only in the infra-red region. With increasing temperature the dielectric constant decreases with an average coefficient of 8.2×10^{-4}/°C in the temperature range of 20 to 120°C. Only a very few of the materials investigated so far, including TlCl, TlBr and rutile, show this negative coefficient of dielectric constant. The conductivity of rutile is well represented in the high temperature region by a straight line on the semi-log plot against the reciprocal of the absolute temperature. The dielectric constant of typical mixtures of rutile with low dielectric constant materials shows agreement with the empirical logarithmic mixture formula,

$$\ln \epsilon_m = x_1 \ln \epsilon_1 + x_2 \ln \epsilon_2.$$

A qualitative explanation of the high dielectric constant and negative temperature coefficient can be made in the light of published work on weakly ionic crystals, assuming that the degree of ionic binding varies with the distance between titanium and oxygen atoms, resulting in a large electric moment being formed for a relatively small movement of the mass points.

33. Nonlinear Resistance Elements in Circuit Networks. PETER I. WOLD, *Union College.*—Graphical methods for treating circuit networks containing nonlinear resistance elements are found to be particularly powerful, and application of such methods to vacuum tube circuits has proved highly effective. If linear resistance loads are used in the latter, the form of the I_p-E_g curve, is set by the characteristics of the tube; and the voltage curve taken over the output load, will be of the same form. By using properly chosen nonlinear elements in the load, there arises the possibility of modifying the I_p-E_g characteristic in a desired manner. In this case also, the output voltage curve will, in general, be of a different form from the output current curve. Nonlinearity of the output curves, because of the tube nonlinearity, can be reduced very substantially.

34. Another Criterion in the Identification and Prediction of Half-Lives. G. DICKSON, P. W. MCDANIEL AND E. J. KONOPINSKI, *Indiana University.*—By taking care to eliminate the effects of fast neutrons, we have minimized the intensity of the 4-min. V^{52} activity usually produced strongly when chromium is bombarded by Ra-Be neutrons and have obtained evidence for a weak activity of 2.27 hours half-life. This we identified chemically as due to chromium and assign to Cr^{55}. This finding is of interest as a confirmation of a method of predicting and identifying half-lives based on the treatment of nuclei differing by an alpha-particle as analogous. The logarithms of known half-lives of such analogous nuclei were plotted as a function of atomic number. For most series with odd isotopic number fairly smooth behavior is thus obtained. There is a continuous rise up to the stable isotopes of each series and a subsequent falling off. The 2.27-hour half-life we found fitted in well with the series for Cr^{55} (we had predicted 3 hours) whereas Cr^{51} should have a half-life longer than 10 years. Other assignments heretofore made on questionable grounds can now be made more definitely; for example, the 2.5-hr. Ni activity is thus Ni^{66} rather than Ni^{63}. A total of about 80 predictions of yet unknown half-lives with varying degrees of reliability have been listed by us on the basis of this method.

35. Positron Energy Distribution of Si^{27}. R. L. MCCREARY, G. KUERTI AND S. N. VANVOORHIS, *University of Rochester.*—An induced radioactivity produced by the bombardment of aluminum with protons has previously been reported.[1] The half-life of this activity was found to be 3.7 seconds and the observed threshold 6.0 ± 0.1 Mev, giving a value for the minimum reaction energy of 5.8 ± 0.1 Mev. The assignment was made to Si^{27} by the reaction, $Al^{27}(p,n)Si^{27}$, since no other reaction could account for the large yield. Further experiments have been made with a cloud chamber in a uniform magnetic field to check the sign of the emitted particles and to measure their energy distribution. Because of the short half-life, the sample was mounted on the end of an arm which could be moved alternately into the proton beam and in front of a window in the side of the cloud chamber. At the same time switches attached to the arm turned on the cyclotron filament in the first position and set off the cloud chamber expansion in the second. The bombardment of the sample lasted 3 seconds and the time between the end of bombardment and the expansion of the cloud chamber was 1½ seconds. The tracks produced in the cloud chamber were those of high energy positrons and over 1000 of these tracks have been measured. By inspection the upper energy limit of the distribution is found to be 3.74 Mev. A Fermi plot, following the method of Kurie *et al.*,[2] yields the same value. This is smaller than the value of 4.0 ± 0.1 Mev expected from the reaction energy and larger than the value 3.4 Mev calculated on the basis of the Coulomb energy.[3]

[1] G. Kuerti and S. N. Van Voorhis, Phys. Rev. **56**, 614 (1939).
[2] F. N. D. Kurie, J. R. Richardson and H. C. Paxton, Phys. Rev. **49**, 368 (1936).
[3] M. G. White, L. A. Delsasso, J. G. Fox and E. C. Creutz, Phys. Rev. **56**, 512 (1939).

36. Experiments with Mono-Energetic Slow Neutrons. C. P. BAKER AND R. F. BACHER, *Cornell University.*—The arc ion source employed in the cyclotron has been operated at 400 cycles with thyratron control which gave an on-time of 50 to 150 microseconds. It has been found that the deuteron beam starts and stops in a few microseconds and thus gives rise to well-defined bursts of neutrons from the beryllium target. Control of an amplifier used with BF_3 ionization chamber by a method different from that used by Alvarez,[1] made possible the detection of those neutrons which had a predetermined time of flight from the source.[1, 2] Preliminary results indicate that the work can be carried to energies well above the Cd cut-off which has been found to occur at approximately 0.15 ev. Present evidence also indicates that the Cd resonance is resolved from the absorption which occurs at lower energies and that the maximum resonance absorption occurs at 0.1 ev.

[1] L. W. Alvarez, Phys. Rev. **54**, 609 (1938).
[2] Fertel, Moon, Thomson and Wynn-Williams, Nature **142**, 829 (1938).

37. The Scattering of Resonance Neutrons in Paraffin. V. W. COHEN, H. H. GOLDSMITH, *Columbia University*, AND M. HAMERMESH, *New York University*.—In view of the importance of the neutron-proton scattering cross section, we have extended our previously reported work[1] by measuring the scattering in paraffin of Ag and In neutrons. These have the advantage of a smaller $\Delta E/E$ value than the Rh resonance neutrons. Ag has the additional advantage of having a larger resonance energy. The result for both Ag and In neutrons is $\sigma = 20 \pm 2(10^{-24})$ cm^2, agreeing with the value obtained by us for Rh. Simons[2] has recently reported a value of 14.8 ± 5 percent for the scattering of Ag and I neutrons in water. However, due to the poor geometrical arrangement he employed, the corrections in Simons' experiment are both large and difficult to evaluate. Until he has stated what corrections he made we cannot consider his value in disagreement with ours.

[1] Cohen, Goldsmith and Schwinger, Phys. Rev. 55, 106 (1939).
[2] L. Simons, Phys. Rev. 55, 792 (1939).

38. The Elastic Scattering of Fast Neutrons. R. F. BACHER, *Cornell University*.—Experiments[1] with the neutrons from the $Be^9(d,n)B^{10}$ reaction as detected by the fast neutron reaction $Al^{27}(n,p)Mg^{27}$ have been continued and extended to C and Cu as scatterers. The accuracy of the experiments has been somewhat increased and is believed to be about 5 percent. Surrounding detector and source with carbon gave no increase in activity while the similar experiment for copper gave a 6 percent increase which may just possibly be real. There is no evidence of appreciable "elastic" scattering. Since the above experiment is most affected by large angle scattering, a further experiment has been carried out with and without a hollow cylinder of the scattering material between source and detector and with the detector at greater distance (12 cm) from the source. Increases of activity in the detector of 15, 30 and 36 percent for C, Cu and Pb, respectively, were observed indicating definite evidence of "elastic" scattering at small angles.

[1] R. F. Bacher, Phys. Rev. 55, 679 (1939).

39. The Magnetic Moment of the Neutron. LUIS W. ALVAREZ, *University of California*, AND F. BLOCH, *Stanford University*.—The magnetic resonance method of determining nuclear magnetic moments in molecular beams, recently described by Rabi and his collaborators, has been extended to allow the determination of the neutron moment. In place of deflection by inhomogeneous magnetic fields, magnetic scattering is used to produce and analyze the polarized beam of neutrons. Partial depolarization of the neutron beam is observed when the Larmor precessional frequency of the neutrons in a strong field is in resonance with a weak oscillating magnetic field normal to the strong field. A knowledge of the frequency and field when the resonance is observed, plus the assumption that the neutron spin is $\frac{1}{2}$, yields the moment directly. A new method is described which permits the magnetic moment of any nucleus to be determined directly in absolute nuclear magnetons merely by a measurement of the *ratio* of two magnetic fields, (1) that at which resonance occurs in a Rabi type experiment for a certain frequency, and (2) that at which protons are accelerated in a cyclotron operated on the nth harmonic of that frequency. The final result of a long series of experiments during which 200 million neutrons were counted is that $\mu_n = 1.93_8 \pm 0.03$ absolute nuclear magnetons.

40. The Radiofrequency Spectra of Atoms. P. KUSCH, S. MILLMAN AND I. I. RABI, *Columbia University*.—The ground states of many atoms possess hyperfine structures whose intervals range from about 0.005 to 0.4 cm^{-1}. The usual optical methods are limited in precision and resolution by line widths and instrumental factors. For many questions it is of interest to possess more precise measurements of these intervals, whether large or small, than exist in the literature. We utilize the absorption and stimulated emission of electromagnetic waves of appropriate frequency (several hundred megacycles) by atoms in an atomic beam. The lines represent transitions within a hyperfine structure multiplet. The transitions are observed by the effect on the atom rather than on the radiation. The resonance lines are so narrow that they exhibit clearly resolved Zeeman patterns in a field of only 0.2 gauss. Some lines are 10^{-6} cm^{-1} wide. The precision of frequency measurement in this region is very high and an accuracy of 0.01 percent was obtained with little difficulty. The hyperfine structure of the ground states of Li^6 and Li^7 was measured with the purpose of comparing the resultant ratio of nuclear moments with the moment ratio obtained directly, and to see how well hyperfine structure can be explained by the effect of nuclear magnetic moment alone. The results agree to one part in 2000. It is possible to utilize this method even when the available electromagnetic frequencies are only a portion of the hyperfine structure interval by observations on the Zeeman pattern at high magnetic fields.

41. The Problem of the Scattering of Fast Electrons. JOHN A. WHEELER, *Princeton University*.—Recent electron deflection experiments of Fowler and Oppenheimer and Oleson, Chao, Halpern and Crane have given results which disagree quite strikingly with theoretical predictions, such as those of Williams, based on present theory. The investigation whose results are reported here shows that the discrepancy can be accounted for on the theoretical side neither by possible uncertainties in the screening of the atomic field, nor by the influence of the polarization of the electron spin, nor by any fault in Williams' method of treating multiple scattering, nor by any first-order effect of interference of the scattered electron waves coming from different atoms. However, for crystals above a critical size t_c given by $n\lambda\sigma^{\frac{1}{2}}t_c \sim 1$ (n atoms per unit volume, λ de Broglie wave-length, σ scattering cross section), higher order interference effects become important (as in the Darwin-Ewald x-ray theory) and reduce the predicted scattering to a value which is, within the probable limits of error, in accord with the observations cited. We thus have no reason based on *these* experiments to

doubt that we can represent the interaction between electrons and nuclei in a collision process in terms of simple electrostatic forces.

42. On the Applicability of Quantum Theory to Mesotron Collisions. J. R. OPPENHEIMER, *University of California.*—The application of quantum mechanics to Yukawa's theory of mesotrons gives a cross section for mesotron-electron collisions which agrees with the classical result for energy transfers under 10^{10} v.; for higher energies the probability of a given fractional energy transfer becomes independent of mesotron energy; these anomalous terms in the cross section correspond to the sesquipole moment of the mesotron spin. The complete result agrees quantitatively with the magnitude and variation with material and filtration of the soft component of cosmic radiation, with the dependence of shower and burst production on shower size, and with the absolute probability of burst production. Parallel calculations for nuclear collisions and for *bremsstrahlung* give cross sections too large to be reconciled with experiment. In all cases momentum transfers large compared to μc (μ the mesotron mass) occur; only for the electron collisions is the coupling energy small compared to the proper energy of the fields (and then only for energies under 10^{13} v.). This condition, and not the smallness of the momentum transfer, would thus seem to limit the applicability of present theory.

43. A Simple Calculation of Disintegration by Mesons. J. F. CARLSON, *Purdue University.*—The collision of a meson with a nucleus in which the meson is absorbed by one of the nuclear particles should give rise to energetic protons or neutrons. For any but the simplest nuclei this process is quite complicated. For the simplest nucleus, a deuteron, the calculations have been carried out and the dependence of the cross section of this collision on the meson energy and the binding energy of the deuteron has been obtained. Both the scalar and vector models of the meson have been used. The cross sections for meson energies are found to be quite sensitive to the model used. The cross section for the scalar model goes to zero directly as the velocity of the meson, while for the vector model this dependence is as the cube of the meson velocity. In both cases the dependence on the binding of the particles is as the square root of their binding energy.

44. Calcite Diffraction Patterns and X-Ray Line Widths. LEONARD T. POCKMAN, *Cornell University.*—Probably our most direct knowledge of the calcite diffraction pattern comes from Miller's[1] recent calculations based on double spectrometer work of L. G. Parratt. Some important assumptions demanded in Miller's calculations are not required in a similar calculation based on curves obtained with a single spectrometer of high geometrical resolving power. This is a preliminary report of work undertaken to obtain such curves. A secondary objective is to obtain further evidence bearing on the large discrepancy between line widths measured with the double spectrometer and with the focusing spectrograph. Two adjustable slits of novel design have been constructed. The jaws of each slit are of lead glass, optically flat on faces (1 cm×0.7 cm) forming the slit. Parallelism, secured by forcing the movable jaw against the stationary jaw and retained by frictional forces, was found good with slit width of 10^{-3} cm by an optical method and 10^{-4} cm by x-rays. The zero reading of the slit micrometer is determined photographically with x-rays. For the present work the total reflection from the faces causes no complication. Preliminary photographic width measurements of Mo $K\alpha_1$, with a spectrometrically good calcite, give uncorrected results only a few percent wider than the narrowest (1, +1) widths reported with the double spectrometer.

[1] F. Miller, Phys. Rev. **56**, 757 (1939).

45. *K* Emission and Absorption: Fine Structure of Copper. S. T. STEPHENSON, *State College of Washington.*—The Kronig type fine structure in the absorption spectrum of many elements is well known. Several authors have also reported emission structure lying as much as a hundred volts on the short wave-length side of various $K\beta_{2,5}$ lines. This structure might be (1) Kronig type absorption in the target of the emitter or it might be (2) real emission due to lattice electrons in permitted energy zones of the target returning to vacant K levels. For (2) to be possible one would have to have: first, vacant K levels caused by electron bombardment of the copper target; second, electrons in the higher permitted energy zones of the copper crystal due again to the continual electron bombardment of the copper target; and third, transition probabilities which allow this type of transition. A careful study of the positions of the emission bands from copper as compared with the absorption structure appears to decide, contrary to some preliminary results,[1] against this latter hypothesis. Absorption in the target is the source of most if not of all the emission structure observed in these experiments for copper. A similar study is carried out for some other elements.

[1] S. T. Stephenson, Phys. Rev. **56**, 856 (1939).

46. *K*-Absorption Edges of Kr (36) and Br (35).* C. H. SHAW AND T. M. SNYDER, *Johns Hopkins University.*—The K-absorption edges of krypton and bromine have been measured with a double crystal spectrometer. An argon-alcohol Geiger counter was used to measure the x-ray intensities. The absorption edge of krypton is practically without structure, due to the relatively great width of the K level. A rough estimate of the width of the K level may be made and is 2.6 volts. For bromine the structure is confined to a single intense region of transmission on the high frequency side of the absorption edge in agreement with the results of Cioffari.[1] The present results indicate that any other structure in the curve is less than 2 percent of the intensity of the first absorption minimum. The structure for bromine to be expected from theory was calculated in a manner similar to that used by Petersen for his calculations on chlorine.[2] The scattering phases were determined by extrapolating from those for krypton as calculated by Faxén and Holtsmark.[3] The theoretical results agree with experiment in predicting a region of transmission at the observed position. The predicted dis-

tance of the absorption minimum from the edge is 5.4 volts, while the observed distance is 5.6 volts. The theory, however, indicates that there is more than one maximum, in disagreement with the experimental results. It was thought possible that predicted structure farther from the edge than the observed minimum is washed out by the varying interatomic separation due to molecular vibrations. Present calculations indicate, however, that such is not the case.

* This research was supported by a grant-in-aid made to Professor J. A. Bearden from the Penrose Fund of the American Philosophical Society.
[1] B. Cioffari, Phys. Rev. **51**, 630 (1937).
[2] H. Petersen, Zeits. f. Physik **80**, 258 (1933).
[3] Faxén and Holtsmark, Zeits. f. Physik **45**, 307 (1927).

47. Secondary X-Ray Diffraction Maxima From Tobacco Mosaic Virus. I. FANKUCHEN,* *Birbeck College, University of London.*—A preliminary account[1, 2] has been given by Bernal and the writer of x-ray studies of tobacco mosaic virus. Briefly the x-ray patterns from oriented specimens consist of two quite distinct parts. The small angle scattering varies with the virus concentration while the large angle scattering is quite independent of it. These parts are termed the inter- and intramolecular patterns, respectively. The reflections forming the intramolecular pattern of an unusually well oriented solution of virus could be measured accurately. The unit cell dimension (68A) along the particle length could be determined directly from the layer line separation. The cell dimensions at right angles presented difficulties in their determination. The diameter of the particles (152A) was known from intermolecular patterns[1] and the observed reflections could all be explained only by assuming a unit cell within the particle of greater size than the known particle diameter itself. This difficulty is removed however if the reflections are indexed on the basis of an hexagonal unit cell, $a=88$A, $c=68$A. Some reflections cannot then be given integral indices and are attributed to secondary maxima which occur because of the small number (3) of unit cells within the individual particle. If this explanation is correct, it is interesting as being the first occasion on which secondary maxima have been observed for x-rays.

* Now National Research Council Fellow in Protein Chemistry, Physics Department, Massachusetts Institute of Technology.
[1] J. D. Bernal and I. Fankuchen, Nature **138**, 1051 (1936).
[2] J. D. Bernal and I. Frankuchen, Nature **139**, 923 (1937).

48. A Study of the Changes Produced in Metals by Hammering. RAYMOND G. SPENCER AND J. WALLACE MARSHALL, *Albion College.*—A small cylinder, fitted with two accurately ground solid pistons, was used to hold the specimens while they were hammered. X-ray diffraction patterns show the crystallites in malleable iron are first markedly strained and then broken up into fine fragments and, in so doing, are partially relieved of strain. When a major portion of the crystallites are powdered, the sample has very little strength. This is in agreement with one of the conclusions drawn by Spencer[1] from his studies of fatiguing. The diffraction patterns of aluminum can be explained by assuming that some of the crystallites are strained and then broken up after which another portion is strained and broken up. In the case of Dow metal, some of the lines are displaced, some increase in intensity, some decrease in intensity and some completely disappear. In order to explain this, it seems necessary to assume that the hammering has partially relieved the original strain in some sets of planes in the crystallites, has introduced strain in other sets of planes and has caused gliding of others.

[1] R. G. Spencer, Phys. Rev. **55**, 991 (1939).

49. Emission and Absorption Processes Involving the 3*d* and 4*s* Bands of Copper and Nickel.* H. FRIEDMAN AND W. W. BEEMAN, *Johns Hopkins University.* (*Introduced by J. A. Bearden.*)—Neither the shapes nor the wave-length positions of the K-absorption edges of copper and nickel are changed when these elements are alloyed together. This indicates either that the constituents of the alloy do not share a common band system or that the ionization of the K shell of the absorbing atom so perturbs its outer levels that they do not mix with the levels of adjacent atoms. The $K\beta_{2,5}$ lines which arise from transitions of conduction electrons into the K shell have been measured for these alloys and considerable evidence has been found for a shared band system. Structure on the high frequency side of the Cu $K\beta_{2,5}$ line, which has been interpreted[1] as emission from the 4*s* band of Cu, disappears in the low percentage copper alloys. In such alloys the 4*s* electron of copper is shared with the nickel.

* This work was supported by a grant made to Professor J. A. Bearden from the Penrose Fund by the American Philosophical Society.
[1] W. W. Beeman and H. Friedman, Phys. Rev. **56**, 392 (1939).

50. Order in the Copper-Gold Alloy System.[1] L. H. GERMER AND F. E. HAWORTH, *Bell Telephone Laboratories.*—A high temperature electron diffraction camera has been developed in which diffraction patterns of alloy films have been obtained by the transmission method. Studies have been made of copper-gold alloys containing 25, 50 and 75 atomic percent copper. Results of many of the experiments are in approximate agreement with those of x-ray investigations upon quenched alloys. For example, films of the alloy containing 25 atomic percent copper have been found to have a face-centered cubic structure in which ordering is not developed by any heat treatment; films of 50 atomic percent copper develop a simple tetragonal structure upon heating to temperatures below 375°C, above this temperature the structure is face-centered cubic and disordered, and in films which have been slowly cooled from temperatures above 375°C crystals have been discovered which have a complex orthorhombic structure together with other crystals which are tetragonal;[2] films of 75 atomic percent copper develop the well-known cubic superstructure. In the course of the investigation many observations have been made regarding atomic diffusion in these alloys and regarding the corrosion of the alloys at various elevated temperatures.

[1] Continuing work reported in Phys. Rev. **56**, 212 (1939).
[2] See C. H. Johansson and J. O. Linde, Ann. d. Physik **25**, 1–48 (1936).

51. Astigmatism, Aberration and Coma of Concave Gratings. H. BEUTLER, *University of Chicago.*—For 15,000 lines/inch gratings of six to twenty feet curvature, the effects of higher order terms in the grating formula are

masked by the graininess of the photographic plate. These effects were revealed in adjusting some large 30,000 lines/inch gratings on a 67"-circle and on a 30-foot circle. The grating theory has been developed for the extension of slit, of rulings and of images perpendicular to the Rowland plane. The general results are represented by a set of graphs, which show for any angle of incidence and of reflection: (1) the wave-length and the dispersion; (2) the astigmatism in (a) the length of the spectral lines from a point source on the slit and (b) the slit length necessary for giving the optimum intensity on the plate; (3) the allowed grating width (limited by aberration), restricting the attainable resolving power and brightness of the spectrum; (4) the coma arising from the extension of the rulings and of the slit, limiting the length of the rulings for a permissible loss in resolving power. From these diagrams, it is possible to determine, for any desired wave-length range, the angles at which the optimum brightness and resolving power are obtained, provided the grating considered has a uniform reflectivity, as is true for most 30,000 line gratings.

52. A High Power Tungsten Light Source. N. METROPOLIS AND H. BEUTLER, *University of Chicago.*—The usual type of tungsten ribbon lamp (carrying about 16 amp.) proved too weak for absorption spectra under high dispersion (0.4–0.2A/mm); the same difficulty arose with the conventional hydrogen discharge tube (especially with an astigmatic grating). Some attempts were made with graphite rods electrically heated in argon at atmospheric pressure, but graphite evaporates too rapidly at 3000°C. In the present form, we use a tungsten ribbon $3'' \times \frac{1}{8}''$ $\times 0.02''$ carrying 150 amp. a.c. in argon at atmospheric pressure. The tungsten ribbon is clamped to monel leads, which screw into two concentric, water-cooled brass cylinders. They form with an insulating layer a compact unit that is sealed with Picein into a three-liter Pyrex bulb. The lamp has an additional quartz window diametrically opposite to facilitate alignment. The tungsten temperature is kept near its melting point (3600°K). The lifetime is limited to about 50 hr. by the evaporation. The deposit of *W* on the exit window is rendered negligible by interposing a double slit system. At λ3000A the brilliancy of *W* at 3600°K is 80 times greater than that of a commercial ribbon lamp kept at 2600°K; at λ5000A the gain is twenty-fold.

53. Spectral Transmission of Glucose Glass in the Near Infra-Red. WILLI M. COHN, *El Cerrito-Berkeley, California.*—The transmission of samples of glucose glass varying in thermal history was previously investigated.[1] This work covered the visible part of the spectrum. Transmission data in the near infra-red are presented now as far as could be obtained photographically (12,000A). No limit of absorption was found at long wave-lengths as far as tested. The possible use of organic glass for investigations in the near infra-red is discussed.

[1] Willi M. Cohn, "A Spectral Investigation of Glucose Glass," J. Chem. Phys. 6, 65–67 (1938).

54. Radio-Phosphorus in Soil Studies. STANLEY S. BALLARD AND L. A. DEAN, *University of Hawaii.*—The use of radioactive phosphorus has been found to have certain advantages over the conventional chemical methods ordinarily employed in soil studies. Among the problems that have been investigated are measurements of the rate of sorption of phosphorus by soils, fertilizer placement studies, and measurements of the movement of applied phosphorus through a soil. A satisfactory technic has been developed for making quantitative measurements with a Lauritsen electroscope of the radioactive strength of soils, plant materials, and solutions such as soil extracts. The average deviation from the mean of several determinations was approximately 1 percent when either soils or solutions were being tested, indicating that the technic is sufficiently accurate for such use. A description of the technic and some applications has been submitted to the *Journal of Applied Physics*. In progress is a study using radio phosphorus for measuring the phosphate fixation of different soil types, in terms of the phosphate uptake of tomato plants. Grateful acknowledgment is made to the Radiation Laboratory of the University of California for the gift of several samples of radio phosphorus.

55. Activation of Indium by Alpha-Particles. J. R. RISSER, K. LARK-HOROVITZ AND R. N. SMITH, *Purdue University.*—The activation of indium by alpha-particles as recently[1] described leads to a capture process with formation of radioactive Sb^{118} and the excitation of In^{115}. By using very short activation periods, the capture process alone can be observed, leading to a lifetime of 3.6 min. for the end product. The cross section of this process is of the order 10^{-26} cm². The excitation of indium has been studied with different energies of alpha-particles and can be observed from 16 Mev down to about 11 Mev, at energies about 5 Mev smaller than the potential barrier. At 16 Mev the cross section of the excitation process is about 3×10^{-25} cm². This cross section is higher by a factor of about 10 than the one observed for the excitation of In^{115} with protons,[2] but is much smaller than the corresponding capture cross section, again analogous to the results obtained in the proton activation[3] of indium. The cross section is smaller by a factor of 1/1000 than the one predicted from the theory of excitation of nuclei by electric fields,[3] but much higher than the theoretically predicted excitation of In^{115} by inelastic *collision.**

[1] Lark-Horovitz, Risser and Smith, Phys. Rev. 55, 878 (1939)
[2] S. W. Barnes, Phys. Rev. 56, 414 (1939).
[3] V. F. Weisskopf, Phys. Rev. 53, 1018 (1938).
* Private communication of V. F. Weisskopf.

56. Absorption Measurements of Beta-Rays. B. L. MOORE, *Cornell University.* (*Introduced by R. F. Bacher.*)—The comparison method developed by Sargent[1] has been applied to the beta-ray spectra of C^{11}, N^{13}, Na^{24}, Mg^{27}, P^{32} and the isomers of Rh^{104}. The absorption end points are found by comparing the upper region of the spectrum with that of RaE. Energy end points are then found using Sargent's range energy relation which was obtained from the extrapolated end points of the absorption curves for homogeneous high energy electrons. The measurements were made with an argon-filled ionization chamber and Edelmann electrometer. End points in Mev so obtained are: $C^{11}(e^+)1.03 \pm 0.03$; $N^{13}(e^+)1.24 \pm 0.03$; $Na^{24}(e^-)1.36$

± 0.05; $Mg^{27}(\epsilon^-)1.74\pm0.05$; $P^{32}(\epsilon^-)1.72\pm0.03$; $Rh^{104}(\epsilon^-)$ (both the 42 sec. and the 4.3 min. periods) 2.46 ± 0.10. For N^{13}, Na^{24} and P^{32} a comparison with more accurate values from magnetic spectrograph measurements indicates agreement within the estimated errors except for N^{13} for which Lyman[2] found 1.198 ± 0.006 Mev. Uncertainties in the end points by absorption appear to be considerably reduced by the use of the comparison method. The main advantages of this method are that strong sources are not necessary and the end points may be obtained with a relatively small amount of work.

[1] B. W. Sargent, Can. J. Research **A17**, 82–102 (1939).
[2] E. M. Lyman, Phys. Rev. **55**, 234 (1939).

57. Energy Spectra of Radioactive Indium. J. L. Lawson and J. M. Cork, *University of Michigan.*—The energy spectra of several of the indium isotopes have been obtained by means of a magnetic spectrometer. It was originally reported by Cork and Lawson[1] that a 0.39-Mev gamma-ray was associated with the 1.73-Mev beta-radiation ascribed to In^{117} because of their rather similar half-lives of about two hours. Barnes,[2] however, showed that this gamma-ray was present in indium separated from long-lived radioactive tin, and was therefore probably due to In^{113}. It is now shown that this gamma-radiation is not associated with the 1.73-Mev beta-radiation. The half-lives of these activities have been determined in the spectrometer to be 104 ± 2 min. and 117 ± 3 min., respectively, for the 0.39-Mev gamma-ray and the 1.73-Mev beta-ray. The spectrum of the 0.336-Mev gamma-ray ascribed to In^{115*} has been more precisely determined, and its half-life as obtained in the spectrometer is 272 ± 3 min. The long-lived indium shows two activities, one of 65-hours half-life and the other of approximately 50-days half-life. The spectra of both of these activities have been obtained in the spectrometer. The 65-hour activity apparently consists only of two internally converted gamma-rays of energies 172 ± 2 kev and 247 ± 2 kev, respectively. The very long-lived radioactive indium displays a continuous beta-ray spectrum whose upper limit is 1.98 ± 0.03 Mev, and an internally converted gamma-ray of energy 0.192 ± 0.002 Mev.

[1] J. M. Cork and J. L. Lawson, Phys. Rev. **56**, 291 (1939).
[2] S. W. Barnes, Phys. Rev. **56**, 414 (1939).

58. Some Improvements in Geiger-Müller Counter Systems. Harold McMaster and M. L. Pool, *Ohio State University.*—A complete scale-of-sixteen Geiger-Müller counter with a maximum speed of 140,000 random counts per minute has been constructed. A fast choked multivibrator vacuum tube relay drives the Cenco recorder. A 0.01-mf mica condenser placed between the control grid of the high voltage regulator tube and ground reduced the sixty-cycle ripple to 0.1 volt without further filtering. The interpolation meter of the scale-of-sixteen is coupled directly to one tube in each scale-of-two. The direct coupling eliminates one tube per scale-of-two previously used to actuate the meter.[1] A direct-current coupled multivibrator quenching circuit is used which has most of the desirable features of both the Neber-Harper and alternating-current coupled multivibrator. The quenching circuit is set to deliver a maximum of 140,000 random counts per minute to the scaling and recording circuits in which there are no losses at this speed. Corrections for losses due to randomness need be applied only to the quenching unit, and correction charts reliable up to speeds of 25,000 random counts per minute have been prepared.

[1] Harold Lifschutz, Rev. Sci. Inst. **10**, 21 (1939).

59. Positive Excess and Electron Component in the Cosmic-Ray Spectrum. Donald J. Hughes, *University of Chicago.* (*Introduced by Arthur H. Compton.*)—In obtaining the energy distribution of mesotrons, H. Jones found an excess of positive particles throughout the energy spectrum, the ratio of positives to negatives amounting to 1.29. This work has been continued to determine whether this positive excess occurs in the particles striking the apparatus or is caused by a greater absorption of the negative particles in the 10-cm lead filter. Care has been taken to reduce any instrumental asymmetry by careful temperature control and frequent reversals of the magnetic field. A total of 1339 tracks was measured. With the lead filter the positive-negative ratio is 1.21 ± 0.083 (standard error), while with no lead the value is 1.18 ± 0.083. This confirms Jones' finding and further indicates a real positive excess in the incident particles. The lead absorbs 11 percent of the cosmic rays that traverse the magnetic field. Comparison of the spectra taken with and without lead shows that this absorption is entirely in the energy range $2\times10^8 - 10^9$ ev, where 26 percent of the rays are absorbed. This shows that there are very few absorbable particles (electrons) of energy greater than 10^9 ev but a considerable number in the range $2\times10^8 - 10^9$ ev.

60. Time Variations in Cosmic-Ray Intensity at High Altitudes. William P. Jesse, *University of Chicago.*—During the past year twelve balloon flights with a recording ionization chamber have been carried out at Chicago to observe any possible time changes in cosmic-ray intensity at high altitudes. The same apparatus was carried in ten of the flights. In each flight a height was attained sufficient to define clearly the maximum of the cosmic-ray intensity curve. The minimum pressure recorded was 1.6 cm. During the period of observation, time changes in the peak value of the cosmic-ray intensity curve of over 14 percent have been observed. These changes have a distinct correlation with the intensity variations observed at the mountain station of the Carnegie Institution at Huancayo, Peru. The variations at this station correspond to the "world-wide" variations observed by Forbush. When the high altitude values are somewhat arbitrarily corrected for such "world-wide" variations on the basis of the Huancayo data, a residual variation remains with a maximum in the early spring and a minimum in the late summer. Further measurements will be necessary to determine whether this represents a true seasonal effect.

61. Collision Energy Loss of Low Energy Cosmic-Ray Electrons. J. K. Boggild, I. C. Kuo, S. H. Neddermeyer and C. D. Anderson, *California Institute of Technology.*—The direct energy loss measurements of cosmic-ray electrons have heretofore been made largely in heavy elements where radiation accounts for the major part of the loss in

energy, and the results have been found in approximate agreement with theory. In order to study the energy loss of electrons due to direct inelastic atomic collisions, 5000 cloud-chamber photographs were taken in which a carbon plate of 4 mm thickness was placed across the chamber. For this purpose only electrons of low energy (20 Mev to 60 Mev) are suitable. These occur infrequently and only 36 cases suitable for accurate measurement were found. In the table the observed average values of energy loss in Mev/cm are compared with the theoretical average values.

Energy range in Mev	Average energy in Mev	Observed total energy loss	Calculated collision loss	Calculated radiation loss	Calculated total energy loss
10–20	16.8	4.3	4.3	0.5	4.8
20–40	30.3	5.0	4.6	1.1	5.7
40–60	47.8	6.7	4.8	1.9	6.7

These preliminary experiments show that in the energy range studied the theoretical formulae for energy loss of electrons (no heavy tracks were included) by direct collisions are in approximate agreement with observation. An experimental test of these formulae is important since they have been assumed correct in the mass estimates of the mesotron which have been made so far.

62. A Device for Viewing of Slow Rotary Motions. RICHARD M. SUTTON, *Haverford College.*—Stroboscopes and rotascopes which permit intermittent observation of rotating systems for periodic short elements of time are ideal for "stopping" motions at speeds greater than 20 r.p.s.; but, because of flicker, they are not suitable for lower speeds. An optical mechanism is designed for the steady observation of bodies in rotation. It consists of a reversing prism arranged to rotate about a longitudinal axis at one-half the speed of the observed rotation, in which case the observer sees what is essentially a stationary mirror image of the rotating object. In order to see the object in the correct relationship in all respects, a second reversing prism is mounted axially beyond the first but is not revolved, and the eye-prism is revolved at half the speed of the motion but in the opposite sense. The observer then has the point of view of a person revolving with the motion but unaware of his own rotation, in which case stationary objects appear to revolve in an opposite sense. The motion must be observed along the axis of rotation; the field of view is limited by the solid angle subtended by the far end of the second prism.

63. The Lubrication of Plane Sliders. F. MORGAN, M. MUSKAT, AND D. W. REED, *Gulf Research & Development Company.*—A machine has been designed and built for measuring the friction torque between plane sliders or thrust bearings and a rotating table. It provides means for variations in lubricant viscosity, bearing load, and slider speed. It also permits the study not only of sliders of various shapes, but also of such as have fixed wedge angles, or which are pivoted and self-aligning. Experiments performed in the thick film region with both fixed angle and self-aligning sliders have confirmed recent extensions of the hydrodynamic theory of such lubrication systems. The machine also permits a study of the thin film region of lubrication under carefully controlled conditions.

64. The Vapor Pressure of Bismuth between 603° and 638°C. ALFRED H. WEBER, *Saint Louis University.*—The vapor pressure of liquid bismuth at temperatures between 603° and 638°C has been measured by the molecular effusion method used by Rudberg[1,2] and others. The masses of the evaporated bismuth deposits were obtained by direct weighing with a microbalance. Seven values of the vapor pressure obtained fall fairly well on the straight line plot ($\log_{10} p$ *vs.* $1/T$) of the empirical equation

$$\log_{10} p(\text{in mm}) = -52.23(205)/T + 9.03. \qquad (1)$$

This equation is in very good agreement with the expression[3]

$$\log_{10} p(\text{in mm}) = -52.23(200)/T + 8.876, \qquad (2)$$

which is stated to apply in the range 1210–1420°C. Apparently expression (2) has not been tested hitherto in the temperature range of the present experiments. The author acknowledges the assistance of S. C. Kirsch, S.J., of St. Joseph's College, Philadelphia, who calibrated the Kovar-tungsten thermocouple used in these experiments. He also expresses his thanks to the Physics Department of the University of Pennsylvania for the loan of the microbalance used in the weighings.

[1] E. Rudberg, Phys. Rev. **46**, 763 (1934).
[2] E. Rudberg and J. Lempert, J. Chem. Phys. **3**, 627 (1935).
[3] *International Critical Tables*, Vol. III (1926), p. 205.

65. Vitrification of Water. B. J. LUYET, *St. Louis University.*—The author reported previously that by the sudden immersion in liquid air of small quantities of aqueous solutions of various inorganic or organic substances he obtained these solutions in the vitreous state. Vitrification was impossible when the concentration was not higher than about 20 percent, that is, when the proportion of water exceeded considerably that of the other component. This impossibility was attributed to the high rate of formation of crystalline nuclei in subcooled water, to the high velocity of growth of the crystals of ice, and to the enormous quantity of heat produced by the growing crystallization centers in freezing water, which kept the local temperature from dropping. A cooling velocity sufficient to vitrify pure water was finally obtained in the following manner. A fine stream of water, falling vertically from a pipette, was flattened between two metal disks previously cooled in liquid air, one of which was fastened behind the stream while the other was thrown against the stream and against the first disk by the propelling action of the spring of a toy pistol. The thin layers of solid water so obtained, transported to a cooled polarizing microscope, stayed dark between crossed Nicols until the temperature was high enough for devitrification to occur.

66. An Anomalous Effect in the Viscosity of Glass. W. B. PIETENPOL AND D. E. BILLINGS, *University of Colorado.*—A method for determining the surface tension of molten glass, by which under static conditions the pressure difference between the inside and outside of a bubble is balanced by the surface tension of the liquid, has been previously published.[1] Later the theory for the viscous forces present when the bubble is expanding was deduced.[2]

This theory has now been applied to the experimental determination of the viscosity of glass throughout a limited temperature range above the softening point. Contrary to all previous results a rapid increase in viscosity with increase in temperature is found slightly above the softening region. For example, the viscosity of a typical lime glass increases from approximately 2.5 to 6×10^8 poises with an increase in temperature from 678° to 686°C. This should not be interpreted as the previously suggested "transformation temperature" which "corresponds to a viscosity of from 10^{13} to 10^{14} poises." The expanding bubble is very sensitive to temperature equilibrium conditions of the glass. The significance of this change in viscosity in the annealing of glass is pointed out and it is suggested that it may have an important bearing on the theory of glass structure.

[1] W. B. Pietenpol, Physics 7, 26 (1936).
[2] E. C. Westerfield and W. B. Pietenpol, Phys. Rev. 55, 306 (1939).

67. The Hardness of Rubber and Other Highly Elastic Materials. LEWIS LARRICK, *The B. F. Goodrich Co.*—The penetration of vulcanized rubber by spherical indentors follows the laws of classical elasticity for indents as large as 10 percent of the diameter of the indentor, and at depths of penetration as great as 30 percent the deviation is not great. This makes possible a new, convenient method for measuring the elastic moduli of such materials. Values of Young's modulus so obtained range from about 200 pounds per square inch for soft rubber compounds to over 1000 pounds per square inch for heavily pigmented compounds. Since hardness is customarily defined as resistance to penetration, the elastic modulus can be used as a measure of hardness. The laws of penetration are derived from the conventional problem of the contact of two elastic spheres. Inasmuch as vulcanized rubber is generally treated as an incompressible material (Poisson's ratio is $\frac{1}{2}$), the equation for the penetration of a rectangular block of rubber by a rigid sphere reduces to: $d=(K/E^{\frac{1}{3}})L^{\frac{1}{3}}D^{\frac{1}{3}}$ (where K is a geometric constant, E Young's modulus, L the load, and D the diameter of the indentor). Criteria for: (1) Similar test conditions (relative depth of indent), (2) Minimium size of face of sample, (3) Minimum thickness of sample, follow from the general theory. The values of the principal stresses are easily derived in certain special cases.

68. The Variation of the Principal Elastic Moduli of Cu_3Au with Temperature. SIDNEY SIEGEL,* *Westinghouse Research Laboratories.*—Single crystal rods of the copper-gold alloy Cu_3Au were prepared in a vacuum furnace. The specimens were annealed according to the procedure described by Sykes and Evans[1] to produce the best possible degree of order at room temperature. A dynamical method —that of the composite piezoelectric oscillator—was used to measure Young's and the rigidity moduli of several crystals of different orientation. Measurements were made over the temperature range 20° to 450°C, and the principal moduli S_{11}, S_{12}, and S_{44} calculated over this interval. All three moduli increase linearly with temperature up to about 250°. From 250° to 388° the slope becomes increasingly large, and at the order-disorder transformation temperature T_c, 388°, each modulus undergoes an abrupt change. The increase in S_{11} at T_c amounts to about 15 percent of its value there, 1.8×10^{-12} cm²/dn. The increase in S_{12} is also about 15 percent of its value there, -0.8×10^{-12} cm²/dn. The increase in S_{44} is about 3 percent of its value at T_c, 1.75×10^{-12} cm²/dn. The elastic constants of such initially well ordered crystals were found to be single-valued functions of the temperature, except very close to T_c, where steady final values were obtained only after 50 hours at constant temperature.

* Westinghouse Research Fellow.
[1] Sykes and Evans, J. Inst. Metals 58, 255 (1936).

69. Camera Lenses with Low Reflecting Films. C. HAWLEY CARTWRIGHT, *Massachusetts Institute of Technology.*—Several fast camera lenses were treated with evaporated metallic fluoride films to reduce the reflection from the air-glass surfaces. Two results were produced by diminishing the reflection in fast lenses: (1) the ghost images that normally occurred under adverse lighting conditions were entirely eliminated and (2) the effective speed of a lens was about doubled. The first result is due to ghost and flare being caused by at least two internal reflections (thus, reducing the reflectance of each surface ten times results in ghost images and flare being reduced a hundred-fold). The second result is somewhat subjective because the increase in exposure due to the added transmission of the lens is accompanied by more contrast, due to the absence of flare, and also an observable increase in detail.

70. Optical and Magnetic Properties of a Magnetite Suspension. C. W. HEAPS, *The Rice Institute.*—A suspension of magnetite powder in oil acts in a limited way as a light shutter. When a magnetic field is parallel to the light direction more light is transmitted than when the light is transverse. Microscopic examination shows that the particles form elongated groups. Each particle probably consists of relatively few magnetic domains, magnetized to saturation, and hence it attracts neighboring particles. The theory of the phenomenon, assuming the groups to be uniform and cylindrical, gives for the fraction of the incident light transmitted, $I/I_0=1-A(2L/a)^{\frac{1}{2}}+BL$, where A and B are structure constants, L is the Langevin function of a, and a is $\mu H/(kT)$ with the usual meaning for the symbols. If we assume the groups to behave like the molecules of a paramagnetic gas in the standard Langevin theory the function L is equal to I/I_0, where I is the intensity of magnetization of the suspension and I_0 is the saturated intensity. Thus the magnetization curve of the suspension may be determined by measurements of light intensities made in various fields. Experimental tests indicate that the theory is satisfactory provided the groups are not all assumed to be identical in shape.

71. The Concentration of Carbon 13 by Thermal Diffusion. ALFRED O. NIER, *University of Minnesota.*—A Clusius and Dickel[1] thermal diffusion column employing methane gas has been constructed for the purpose of concentrating C^{13}. The length of the column was 730 cm, the separation of the hot and cold walls 0.71 cm, and the mean circumference of the annular gas space 13.2 cm. For a

temperature difference of 300°C between walls and the outer wall water-cooled, the power consumption was 2750 watts. When the column was used without reservoirs at pressures of 21.7, 40.0 and 65.6 cm, the separation factors were 2.25, 6.25, and 4.25, respectively. These results are in *quantitative* agreement with the theory of Furry, Jones and Onsager[2] provided one: (a) employs the experimentally determined value of D_T/D for methane[3] rather than the arbitrary value assumed by Furry, Jones and Onsager, and (b) assumes the existence of a convection loss term, such as is given by Eq. (70) in reference 2, having a numerical value of approximately 0.6. When a reservoir having a volume of 20 liters was connected to the top it was possible to produce methane having a concentration of over 4 times the normal amount of $C^{13}H_4$. The pressure in this case was 46 cm, the value corresponding to greatest separation factor. With an infinite reservoir the concentration would have been over 6 times.

[1] K. Clusius and G. Dickel, Naturwiss. **26**, 546 (1938).
[2] W. Furry, R. C. Jones, L. Onsager, Phys. Rev. **55**, 1083 (1939).
[3] A. O. Nier, Phys. Rev. **56**, 1009 (1939).

72. Concentration of Isotopes by Thermal Diffusion: Rate of Approach to Equilibrium. J. BARDEEN, *University of Minnesota*.—The time-dependent partial differential equation involved in the theory[1] of the operation of a Clusius thermal diffusion column[2] is solved for various assumed boundary conditions at the ends of the column. The solutions give the concentration of molecules of a given species at any point in the column as a function of time. Among the cases treated are: (1) both ends of the column closed, (2) reservoir at the upper end, lower end closed, and (3) reservoir connected to upper end by a tube along which a concentration gradient can exist. Numerical calculations made for several cases are compared with experimental results of Nier,[3] who studied the operation of a column containing methane gas. (The column is to be used for the separation of the carbon isotopes.) In the calculation, use is made of the value of the thermal diffusion coefficient for methane obtained by a direct experiment,[4] and of the empirical values of the equilibrium separation factor. The theoretical curves giving the rate of approach to equilibrium agree well with the experimental.

[1] W. H. Furry, R. C. Jones, and L. Onsager, Phys. Rev. **55**, 1083 (1939).
[2] K. Clusius and G. Dickel, Naturwiss. **26**, 546 (1938).
[3] See preceding abstract.
[4] A. O. Nier, Phys. Rev. **56**, 1009 (1939).

73. Thermal Separation of Gases and Isotopes. ARTHUR BRAMLEY, *Swarthmore, Pa.*—The thermal method for the separation of gases and isotopes[1] depends for its success on the simultaneous action of a number of different processes. These can be divided conveniently into three groups: (a) A difference in the thermal behavior of the gases or isotopes depending on their difference in mass, e.g. thermal or initial diffusion. (b) A mass motion of the gas, such as a convection current up a hot wall and down a cold wall or in tubes with larger wall clearance turbulence or swirls, either of which plays an important part in transferring the heat across the intervening gas space. (c) A slight concentration of one of the components over the others exists in the Langmuir film[2] surrounding wires heated directly or indirectly. There is a definite motion of the gas in this film along the wire which arises from the swirling motion of the gas outside this film. An interchange of molecules occurs between the swirls themselves and between them and the Langmuir film on account of process (a).

[1] Bramley and Brewer, Science **90**, 165 (1939). Bramley and Brewer, J. Chem. Phys. **7**, 553 (1939). Brewer and Bramley, J. Chem. Phys. **7**, 972 (1939).
[2] Brody and Kőrösy, J. App. Phys. **10**, 584 (1939).

74. Concentration of Chlorine Isotopes by Centrifuging at Dry Ice Temperature.* F. C. ARMISTEAD AND J. W. BEAMS, *University of Virginia*.—The concentration of the chlorine isotopes obtained experimentally at room temperature (300°A) by the evaporative centrifuge method has been shown previously to be in accord with the theory of Lindemann and Aston and Mulliken. In the present paper the same theory has been checked at dry ice temperature (approximately 200°A). The centrifuge was of the air-driven vacuum type. The hollow rotor (8 cm effective I.D.) was spun inside an evacuated enclosure maintained at dry ice temperature. The tubular shaft (gauge 15) was 15″ long and made of stainless steel to increase heat insulation. Standing vibrations in the shaft were prevented by guides mounted in Bakelite. After placing 10 cc of liquid ethyl chloride in the rotor, it was spun to 1240 r.p.s. and evacuated through the shaft. The ethyl chloride vapor was drawn off very slowly through the shaft and a glass capillary, so that approximate equilibrium could exist in the rotor, and was collected in 2 cc (liquid) samples in traps cooled by liquid air. The isotopic ratio measured by the mass spectrometer in the first and in the last samples differed by 12 percent, which is in fair accord with the theory.

* Supported by a grant from the Research Corporation.

75. Interparticle Separations for Tobacco Mosaic Virus at Varying Concentrations, *p*H, and Ionic Concentrations. I. FANKUCHEN,† *Birkbeck College, University of London*.—In a preceding paper, a brief description of the x-ray patterns obtained from tobacco mosaic virus has been given. The intermolecular patterns obtained from all oriented specimens permit the direct computation of the interparticle distances. These distances have been determined for virus preparations (a) of varying water content, (b) gels at varying *p*H, (c) gels in solutions of varying ionic concentration. From (a), it is shown that as the water content increases the particles are displaced only in a direction at right angles to their lengths, maintaining their hexagonal arrangement in cross-section. The interparticle distance in A can be expressed by $\text{I.P.D.} = 1700/\sqrt{C}$ where C is concentration in grams of vacuum dried virus in 100 cc of specimen. For (b), it is found that the I.P.D. is a minimum at the isoelectric point. From (c), it is found that as the ionic concentration increases I.P.D. steadily decreases, reaching a stationary value for the stronger concentrations. It is believed that measurements of this character may help the arrival of a more quantitative theory of colloids than now exists.

† Now National Research Council Fellow in Protein Chemistry, Physics Dept., Massachusetts Institute of Technology.

Author Index to Abstracts of the Columbus, Ohio Meeting

Albers, V. M. and H. V. Knorr—No. 10
Albers, V. M.—see Knorr, H. V.
Allen, A. J. and R. G. Franklin—No. 12
Alvarez, Luis W. and F. Bloch—No. 39
Anderson, C. D.—see Boggild, J. K.
Armistead, F. C. and J. W. Beams—No. 74

Bacher, R. F.—No. 38
—— see Baker, C. P.
Baker, C. P. and R. F. Bacher—No. 36
Ballard, Stanley S. and L. A. Dean—No. 54
Bardeen, J.—No. 72
Beams, J. W.—see Armistead, F. C.
—— see Snoddy, L. B.
Beeman, W. W.—see Friedman, H.
Bell, M. E.—see Berberich, L. J.
Bennett, Willard H.—see Darby, Paul F.
Berberich, L. J. and M. E. Bell—No. 32
Beutler, H.—No. 51
—— see Metropolis, N.
Billings, D. E.—see Pietenpol, W. B.
Bloch, F.—see Alvarez, Luis W.
Boggild, J. K., I. C. Kuo, S. H. Neddermeyer and C. D. Anderson—No. 61
Bowman, D. W.—see Green, J. B.
Bramley, Arthur—No. 73

Carlson, J. F.—No. 43
Cartwright, C. Hawley—No. 69
Charles, George W. and Fred W. Paul—No. 3
Cleveland, Forrest F. and M. J. Murray—No. 9
Cohen, V. W., H. H. Goldsmith and M. Hamermesh—No. 37
Cohn, Willi M.—No. 53
Cork, J. M., J. Halpern and H. Tatel—No. 20
—— see Lawson, J. L.

Darby, Paul F. and Willard H. Bennett—No. 29
Dean, L. A.—see Ballard, Stanley S.
Dickson, G., P. W. McDaniel and E. J. Konopinski—No. 34
DuBridge, L. A. and John Marshall—No. 19

Fankuchen, I.—Nos. 47 and 75
Feenberg, Eugene—No. 21
Franklin, R. G.—see Allen, A. J.
Friedman, H. and W. W. Beeman—No. 49

Germer, L. H. and F. E. Haworth—No. 50
Goldsmith, H. H.—see Cohen, V. W.
Gordy, Walter and Spencer C. Stanford—No. 6
Green, J. B., D. W. Bowman and E. H. Hurlburt—No. 4
Guth, E.—No. 24
—— see Mullin, Charles J.

Halpern, J.—see Cork, J. M.
Hamermesh, M.—see Cohen, V. W.
Haworth, F. E.—see Germer, L. H.
Haxby, R. O., W. E. Shoupp, W. E. Stephens and W. H. Wells—No. 18
—— see Wells, W. H.
Heaps, C. W.—No. 70
Henry, Hugh F.—see Snoddy, L. B.
Hipple, John A., Jr.—No. 28
Holloway, M. G.—No. 17
Hughes, Donald J.—No. 59
Hurlburt, E. H.—see Green, J. B.

Jesse, William P.—No. 60
Jordahl, O. M.—No. 23

Knorr, H. V. and V. M. Albers—No. 11
—— see Albers, V. M.
Konopinski, E. J.—see Dickson, G.
Kuerti, G.—see McCreary, R. L.
Kunz, Kaiser S.—see Podolsky, Boris
Kuo, I. C.—see Boggild, J. K.
Kusch, P., S. Millman and I. I. Rabi—No. 40

Landé, Alfred—No. 5
Langer, L. M., A. C. G. Mitchell and P. W. McDaniel—No. 15
—— see Mitchell, A. C. G.
Lark-Horovitz, K.—see Risser, J. R.
Larrick, Lewis—No. 67
Lawson, J. L. and J. M. Cork—No. 57
Luyet, B. J.—No. 65

McCreary, R. L., G. Kuerti and S. N. VanVoorhis—No. 35
McDaniel, P. W.—see Dickson, G.
—— see Langer, L. M.
—— see Mitchell, A. C. G.
McMaster, Harold and M. L. Pool—No. 58
Marshall, John—see DuBridge, L. A.
Marshall, J. Wallace—see Spencer, Raymond G.
Metropolis, N. and H. Beutler—No. 52
Miller, Bertrund J.—No. 1
Millman, S.—see Kusch, P.
Mitchell, A. C. G., L. M. Langer and P. W. McDaniel—No. 16
—— see Langer, L. M.
Mitchell, F. H.—No. 31
Moore, B. L.—No. 56
Morgan, F., M. Muskat and D. W. Reed—No. 63
Mullin, Charles J. and E. Guth—No. 25
Murray, M. J.—see Cleveland, Forrest F.
Muskat, M.—see Morgan, F.

Neddermeyer, S. H.—see Boggild, J. K.
Nielsen, Alvin H.—No. 8
Nielsen, Harald H.—No. 7
Nier, Alfred O.—No. 71

Oppenheimer, J. R.—No. 42

Paul, Fred W.—see Charles, George W.
—— see Polster, Harry D.
Pietenpol, W. B. and D. E. Billings—No. 66
Pockman, Leonard T.—No. 44
Podolsky, Boris and Kaiser S. Kunz—No. 26
Polster, Harry D. and Fred W. Paul—No. 2
Pool, M. L.—see McMaster, Harold
—— see Smith, Alpheus W.

Rabi, I. I.—see Kusch, P.
Reed, D. W.—see Morgan, F.
Risser, J. R., K. Lark-Horovitz and R. N. Smith—No. 55
Rose, M. E.—No. 22

Shaw, C. H. and T. M. Snyder—No. 46
Shoupp, W. E.—see Haxby, R. O.
—— see Wells, W. H.
Siegel, Sidney—No. 68
Smith, Alpheus W. and M. L. Pool—No. 13
Smith, R. N.—see Risser, J. R.
Snoddy, L. B., Hugh F. Henry and J. W. Beams—No. 30
Snyder, T. M.—see Shaw, C. H.
Spencer, Raymond G. and J. Wallace Marshall—No. 48
Stanford, Spencer C.—see Gordy, Walter
Stephens, W. E.—see Haxby, R. O.
—— see Wells, W. H.
Stephenson, S. T.—No. 45
Sutton, Richard M.—No. 62

Tatel, H.—see Cork, J. M.

VanVoorhis, S. N.—see McCreary, R. L.

Warburton, F. W.—No. 27
Weber, Alfred H.—No. 64
Wells, W. H., R. O. Haxby, W. E. Shoupp and W. E. Stephens—No. 14
—— see Haxby, R. O.
Wheeler, John A.—No. 41
Wold, Peter I.—No. 33